

# Power Systems

---

Grzegorz Benysek

---

# **Improvement in the Quality of Delivery of Electrical Energy using Power Electronics Systems**

Grzegorz Benysek, PhD  
University of Zielona Góra  
Faculty of Electrical Engineering, Computer Science  
and Telecommunications  
Institute of Electrical Engineering  
Podgórska 50 street  
65-246 Zielona Góra  
Poland

British Library Cataloguing in Publication Data

Benysek, Grzegorz

Improvement in the quality of delivery of electrical energy  
using power electronics systems. - (Power systems)

1. Power electronics 2. Electric power systems - Control

I. Title

621.3'17

ISBN-13: 9781846286483

ISBN-10: 1846286484

Library of Congress Control Number: 2006936885

Power Systems Series ISSN 1612-1287

ISBN 978-1-84628-648-3

e-ISBN 978-1-84628-649-0

Printed on acid-free paper

© Springer-Verlag London Limited 2007

Apart from any fair dealing for the purposes of research or private study, or criticism or review, as permitted under the Copyright, Designs and Patents Act 1988, this publication may only be reproduced, stored or transmitted, in any form or by any means, with the prior permission in writing of the publishers, or in the case of reprographic reproduction in accordance with the terms of licences issued by the Copyright Licensing Agency. Enquiries concerning reproduction outside those terms should be sent to the publishers.

The use of registered names, trademarks, etc. in this publication does not imply, even in the absence of a specific statement, that such names are exempt from the relevant laws and regulations and therefore free for general use.

The publisher makes no representation, express or implied, with regard to the accuracy of the information contained in this book and cannot accept any legal responsibility or liability for any errors or omissions that may be made.

9 8 7 6 5 4 3 2 1

Springer Science+Business Media  
[springer.com](http://springer.com)

The author thanks all Institute of Electrical Engineering members for their help and technical advice on this thesis.

**Special thanks go to Prof. Ryszard Strzelecki.**

---

## **Foreword**

This book of the author G. Benysek is an important work for the development of the electric transmission system towards a more flexible technical system. Power transmission in electrical networks is essential for industrial and private consumers. The permanent reliability and stability of energy delivery is an obvious issue in all industrialised countries. Technical handling of the transmission system follows up to now well-tested approaches.

Requirements for the adaptation of the power system result from the change of the energy supply itself. Due to increasing efforts for environmental protection at one hand and limited hydrocarbon resources on the other hand, conventional power plants with fossil fuels will be reduced significantly in future. The energy delivery is then realised by a remaining distributed generation from fossil fuels and increasing power shares of renewable power plants. Hence, the management of the energy transmission has to be adapted to the new situation. Several power flows will occur independently from the demand side. Different characteristics of the energy sources and distributed responsibilities of energy conversion will take place on the supplier side. Nevertheless customers expect the same quality of delivery as known from decades with only small changes in the transmission system. The safety and the power quality of the energy delivery have the highest priority in the industrialised world.

This contrary requirements demand a solution, which can be delivered by power electronics.

Power electronics grows rapidly due to better isolation properties of the material and reduced switching losses. Improved reliability and device developments with higher power ranges and blocking voltages allow the use of power electronic circuits for delivery and control of energy.

This book introduces in seven chapters to the technical possibilities of using power electronics for improvement of the power quality. This means a combination of the technical developments in the fast-living power electronics with the requirements of a safety and high reliable energy supply. Therefore most of the presented solutions make the use of combined phrases necessary, this results in a wide choice of abbreviations. The Flexible AC Transmission System (FACTS) is a generic term for the presented ideas.

In the book chapters the practical applications of the different possibilities using power electronics for the improvement of energy supply are detailed explained. It is a merit of the author that this complex information is presented in an understandable manner despite its high scientific value. The use of the described circuits for the improvement of the quality of energy supply is one of the most important tasks towards a flexible and safety transmission system in future.

Prof. Detlef Schulz  
Helmut Schmidt University  
University of the Federal Armed Forces Hamburg

---

# Contents

<b>1</b>	<b>Introduction.....</b>	<b>1</b>
<b>2</b>	<b>Quality of Delivery.....</b>	<b>9</b>
2.1	Limitations of the Transmission Systems .....	9
2.1.1	FACTS to Enhance Limitations of the Transmission Systems ....	10
2.2	Power Quality .....	11
2.2.1	Equipment Used to Enhance PQ.....	14
<b>3</b>	<b>Traditional Power Electronics Systems for Transmission Control .....</b>	<b>17</b>
3.1	Power Flow Control.....	17
3.2	Converter Based FACTS .....	25
3.2.1	Series Devices .....	26
3.2.2	Shunt Devices .....	33
3.2.3	Combined Devices.....	40
3.2.4	HVDC.....	46
<b>4</b>	<b>Modern Power Electronics Systems for Transmission Control .....</b>	<b>53</b>
4.1	SSSC Based Interline Power Flow Controllers.....	53
4.2	Combined Interline Power Flow Controllers .....	64
<b>5</b>	<b>Probabilistic Dimensioning of the Systems for Transmission Control.....</b>	<b>71</b>
5.1	Interline Power Flow Controllers – Probabilistic Dimensioning .....	71
5.1.1	IPFC Theoretical Investigations .....	74
5.1.2	IPFC Experimental Investigations .....	78
5.2	STATCOM – Probabilistic Dimensioning.....	81
5.3	Summary.....	86
<b>6</b>	<b>Energy End-use Power Electronics Systems .....</b>	<b>89</b>
6.1	Converters Suitable for Custom Power Systems .....	89
6.1.1	Single Phase Converters .....	89
6.1.2	Three Phase Converters .....	90
6.1.3	Matrix Converters.....	91

6.1.4	Multilevel Converters .....	92
6.2	Compensating Type Custom Power Systems .....	97
6.2.1	Single Phase UPQC.....	101
6.2.2	Three Phase UPQC.....	104
6.3	Voltage Source Custom Power Systems.....	117
6.3.1	Voltage Active Power Filter .....	118
6.3.2	Symmetrical Voltage Active Power Filter.....	131
6.4	Compensating and Voltage Source Custom Power Systems – Comparison of Properties .....	142
<b>7</b>	<b>Conclusions.....</b>	<b>147</b>
7.1	Summary of Results.....	147
7.2	Future Work.....	149
<b>Appendices .....</b>		<b>157</b>
<b>Acronyms and Symbols.....</b>		<b>169</b>
<b>References .....</b>		<b>173</b>
<b>About the Author.....</b>		<b>187</b>
<b>Index.....</b>		<b>189</b>

# 1

---

## Introduction

Electricity is a very useful and popular energy form which plays an increasing role in our modern industrialized society. Scarcer natural resources and the ubiquitous presence of electrical power make it desirable and continuously increases demand, causing power systems to operate close to their stability and thermal ratings. All the latter mentioned reasons together with the high penetration of Distributed Resources (DR) and higher than ever interest in the quality of delivered energy are the driving forces responsible for extraordinary changes taking place in the electricity supply industry worldwide.

Against this background of rapid changes, the expansion programmes for many utilities are being thwarted by a variety of environmental and regulatory pressures that prevent the building of new transmission lines and electricity generating plants, the construction of which is becoming increasingly difficult.

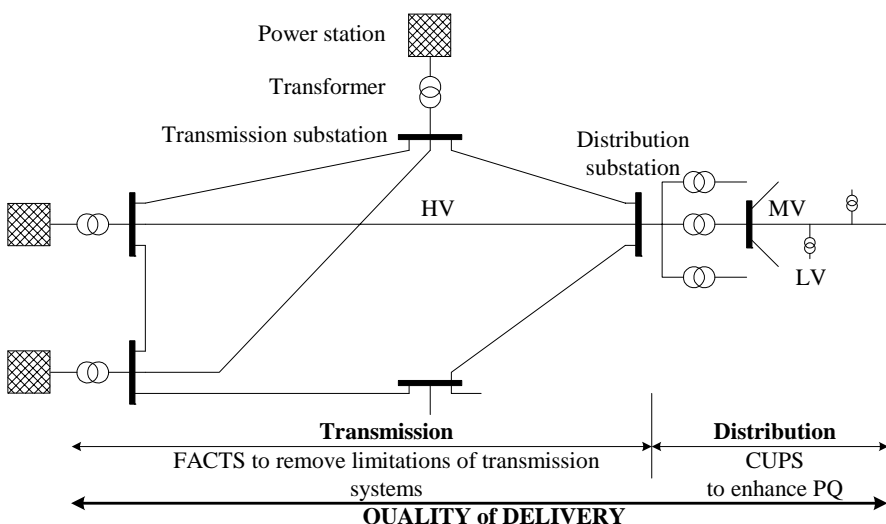


**Figure 1.1.** A simplified one-line diagram of the power system

The one-line diagram shown in Figure 1.1 illustrates the Electrical Power System (EPS) and its major components: generation, transmission and distribution systems. Electric power is generated at power stations predominantly by synchronous generators that are mostly driven by steam or hydro turbines. Hence, the electric power generated at any such station usually has to be transmitted over a great distance, through the transmission systems, to the distribution systems. The distribution networks distribute the energy from the transmission grid or small/local DR to customers.

The term quality of delivery, which appears in the title of this thesis, refers to the ability of the various components – generation, transmission, and distribution – to deliver the product (electric power) to any point of consumption in the amount and at the quality demanded by the customer.

The three components – generation, transmission and distribution – have different influences, individual and sometimes common, on the level of the quality of delivery. There are many issues involved, such as the maintenance of power apparatus and system, the stability of the operation system, faults, distortions, loads nonlinearities *etc.*, One must understand the potential impact of failure within one component on the performance of the whole. For example, a failure in the generation component may lead to failure in the transmission system and in consequent loss of load in the distribution system, while a failure in the transmission component may lead to failure in the generation component and subsequent loss of customer load in distribution. A failure in the distribution system rarely leads to failure in the other two components and causes very minimal, local, losses of customer load.

Some of these problems are related to power transmission systems and some of them to power distribution systems but all are fundamental from the point of view of quality of delivered power.

From the top in the EPS hierarchy, it has to be noted that a well designed power station which works without any failures (failures will not be considered in this thesis) is not a source of any difficulties in supplying quality because the generated system voltages are almost perfectly sinusoidal. Therefore the term quality of delivery will be treated in this thesis as a matter of two issues, related to limitations of the transmission systems as well as to Power Quality (PQ) problems of the distribution systems, *q.v.*, Figure 1.1.

As noted earlier, transmission systems are being pushed ever closer to their stability and thermal limits. The limitations of the transmission system can take many forms and may include one or more of the following characteristics [1-4]:

- voltage magnitude;
- thermal limits;
- transient stability;
- dynamic stability

The above mentioned limitations will be treated in this thesis as the only influences of the transmission systems on the level of quality of delivery.

It is to be noted that even if PQ is mainly a distribution system problem, the power transmission system may also have an impact on the PQ issues resulting, for example, in low system damping, because of a low resistance to the reactance ratio.

The PQ, at distribution level, broadly refers to maintaining a near sinusoidal power distribution bus voltage at a rated magnitude and frequency. In addition, the energy supplied to a customer must be uninterrupted. There are two different categories of causes for the deterioration in PQ, which is influenced not just by power delivery systems, but also by end-user equipment and facilities [2, 4]. The first category concerns natural causes, such as:

- faults or lightning strikes on distribution feeders;
- equipment failure

The second category concerns load or feeder line operation:

- power electronics based loads such as Uninterrupted Power Supply (UPS) or Adjustable Speed Drives (ASD);
- switching on/off large loads

This thesis builds on the assumption that interruptions and quality problems are often caused by the same phenomena, and therefore closely related to each other; sudden and large load changes, transients, faults and loss of generation often result in the disconnection of a part of the system (reliability), while at the same time other parts experience voltage sags and short interruptions (quality problems).

Therefore, the term Power Quality includes two aspects of power supply, namely Voltage Quality and Supply Reliability [5]. The Voltage Quality side includes various disturbances, such as, rapid changes, harmonics, interharmonics, flicker, imbalance and transients, whereas the reliability side involves phenomena with a longer duration, such as interruptions, voltage dips and sags, over and under voltages and frequency deviations.

An in-depth analysis of the options available for maximizing existing transmission and distribution resources, with high levels of stability and PQ, points in the direction of power electronics [6-15]. There is general agreement that novel power electronics equipment is a potential substitute for conventional solutions, which are normally based on electromechanical technologies that have slow response times and high maintenance costs [1].

Two kinds of power electronics applications gaining importance in power systems are already well defined: active and reactive power control and power quality improvement. The first application area is for arrangements known as Flexible Alternating Current Transmission System (FACTS), where the latest power electronic devices and methods are used to control the transmission side of the network [11, 16-18]. The second application area is for devices known as Custom Power System (CUPS), which focus on the distribution system supplying the energy end-uses and is a technology created in response to reports of poor power quality of supply affecting factories, offices, and homes [2, 13, 19-33].

### *Transmission Systems*

The character of a given power system changes with time, due to higher utilization of the transmission network and to increased generation capacity. If the transmission facilities are not suitably upgraded the power system becomes vulnerable to steady-state and transient stability problems [34, 35]. In such environments, transmission capacity becomes a virtue, therefore during the last few

years interest in the possibilities for controlling the power flows in transmission systems has increased significantly. There are a number of reasons for this: loss of system stability, power flow loops, high transmission losses, voltage limit violations and lack of ability to utilize transmission line capability up to the thermal limit. Speaking generally, these limits define the maximum electrical power which can be transmitted without causing damage to transmission lines and electrical equipment.

Traditional solutions for upgrading the electrical transmission system infrastructure have been primarily in the form of new power plants, new transmission lines, substations, and associated equipment. However, as experience has proven, the process of authorizing, locating, and constructing new transmission lines has become extremely difficult, expensive and time-consuming. It is envisaged that alternatively, FACTS controllers can enable the same objectives to be met with no major alterations to system layout.

The potential benefits of employing FACTS controllers include reduction of operation and transmission investment costs and implementation time compared to the construction of new transmission lines, increased system security and reliability, increased power transfer capabilities, and an overall enhancement of the quality of the electric energy delivered to customers [5, 12].

The application of power electronics devices to power transmission has a long tradition. It started with High Voltage Direct Current (HVDC) transmission systems. Thyristor-based HVDC installations provided a means for interconnecting power systems with different operating frequencies – *e.g.*, 50/60 Hz, for interconnecting power systems separated by the sea and for interconnecting weak and strong power systems [36, 37]. The most recent development in HVDC technology is the HVDC system based on solid-state voltage source converters, which enables independent, fast control of active and reactive powers [38, 39].

In addition to the above mentioned, there are other power electronics controllers that are members of the FACTS family. One such device is the Thyristor Controlled Braking Resistor (TCBR) which allows a quantity of real power to be dissipated in the resistor during the fault and therefore restricts the machine acceleration and increases the system stability. A Thyristor Controlled Phase Angle Regulator (TCPAR) injects voltage in quadrature with the line voltage. Therefore, by adjusting the magnitude of the injected voltage, the phase angle between the sending and receiving end voltages can be adjusted, thus increasing the stability limit allowing the system to operate at a higher power angle, provided the thermal limit is not reached.

With respect to FACTS equipment, Voltage Source Converter (VSC) technology, –which utilizes self-commutated thyristors/transistors, such as Gate Turn Off (GTO), Integrated Gate Commutated Thyristor (IGCT), and Insulated Gate Bipolar Transistor (IGBT)– has been successfully applied in a number of installations world-wide for Static Synchronous Compensators (STATCOM) [40-44], of there are several recently completed in the U.S., [45] – as well as for Unified Power Flow Controllers (UPFC) [18, 46, 47].

The above mentioned transmission system installations are in addition to the earlier generation of power electronics systems that utilize line-commutated thyristor technology for Static Var Compensators (SVC) [48-51], Thyristor

Switched Series Capacitor (TSSC) and Thyristor Controlled Series Compensators (TCSC) [52-55].

The newest member of the FACTS family is an Interline Power Flow Controller (IPFC) proposed for providing flexible power flow control in a multi-line power system [56-63]. In an IPFC, two or more parallel lines are compensated by Static Synchronous Series Compensators (SSSC) which are connected to a common Direct Current (*DC*) link. Thus the SSSCs can provide series compensation to the line to which they are connected. In addition, they can also transfer real power between the compensated lines. This capability makes it possible to equalize both real and reactive power between lines, to transfer power from an overloaded line to an underloaded and to damp out system oscillations resulting from a disturbance.

It can be concluded that the flexible Alternating Current (*AC*) transmission technology allows a greater control of power flow. Since these devices provide very fast power swing damping, the power transmission lines can be securely loaded up to their thermal limits.

### *Distribution Systems*

With the emergence of computers, sensitive loads and modern communications, a reliable electricity supply with high quality voltage has become a necessity.

A few years back, the main concern of consumers of electricity was reliability of supply *per se*. It is however not only simple supply reliability that consumers want today, they want an ideal *AC* line supply, that is, a pure sine wave of fundamental frequency and, in addition, a rated peak voltage value. Unfortunately the actual *AC* line supply that we receive differs from this ideal. There are many ways in which the lack of quality power affects customers.

Voltage sags and dips can cause loss of production in automated processes, and can also force a computer system or data processing system to crash. To prevent such events a UPS is often used, which in turn may generate harmonics. A consumer that is connected to the same bus that supplies a large motor load may have to face a critical dip in supply voltage every time the motor load is switched on. This may be quite unacceptable to many consumers. There are also very sensitive loads, such as hospitals, air traffic control and financial institutions that require clean and uninterrupted power.

A sustained overvoltage can cause damage to household appliances. An undervoltage has the same effect as that of voltage sag. Voltage imbalance can cause temperature rises in motors. Harmonics, *DC* offset, can cause waveform distortions. Unwanted harmonics currents flowing across the distribution network can cause losses and heating in transformers and Electromagnetic Interference (EMI) [64-66]. Interharmonics voltages can upset the operation of fluorescent lamps and television receivers. They can also produce acoustic noise.

It can be concluded that the lack of quality power can cause loss of production, and damage to equipment. It is therefore crucial that a high standard of PQ has to be maintained.

As with FACTS devices in transmission systems, power electronics devices can be applied to the power distribution systems to increase the reliability and the quality of power supplied to the customers – to increase the PQ [67-69]. The

devices applied to the power distribution systems for the benefit of customers (end-users) are called Custom Power Systems. Through this technology the reliability and quality of the power delivered can be improved in terms of reduced interruptions and reduced voltage and current variations and distortions. The proper use of this technology will benefit all industrial, commercial and domestic customers.

Custom power devices are basically a compensating type, used for active filtering, load balancing, power factor correction and voltage regulation. Active filtering, which predominantly is responsible for elimination of harmonic currents and voltages, can be both shunt and series. Some CUPS devices with active filtering functions are used as load compensators, in which mode they correct the imbalance and distortions in the load currents, such that compensated load draws a balanced sinusoidal current from the AC system. Some other devices are operated to provide balanced, harmonic free voltage to the customers. Below are described the selected devices that are members of the CUPS family.

A Parallel Active Power Filter (PAPF) [70-84], called also Distribution Static Synchronous Compensators (STATCOM) [2], is a device that can complete current compensation, *i.e.*, power factor correction, harmonic filtering, load balancing and which can also perform voltage regulation. Series Active Power Filter (SAPF), called also Dynamic Voltage Restorer (DVR) [2, 33], is a device that can provide voltage based compensation and therefore can protect the sensitive loads from sags/swells and interruptions in the supply side. Still, when there is distortion in the source voltage, SAPF provides harmonic free voltage to the customers. A Unified Power Quality Conditioner (UPQC) [24, 25, 27, 85-93] has the same structure as that of a UPFC [94-98] and can complete both current and voltage compensation at the same time.

Both Voltage Active Power Filters (VAPF) [99-118] and Symmetrical Voltage Active Power Filters (SVAPF) [109, 119] present a different way for power quality improvement. In a VAPF the PQ improvement is possible because the parallel connected VSC acts as a sinusoidal voltage source with fundamental frequency, additionally the SVAPF device possess the extra current source, therefore both conditioners are suited to fulfil a wide range of different tasks:

- to prevent “dirty” loads from polluting the electrical distribution network;
- to protect sensitive loads from line disturbances as voltage sags and distortions

### *Objectives*

On the basis of the above discussion it can now be stated that **the major purpose of this thesis is to present the possibilities, detailed features, as well as selected solutions and applications of the power electronics arrangements useful to the improvement in quality of delivery of the electric energy in Electric Power Systems.**

The aim is to introduce the power delivery problems and to discuss the solutions of some of these technical difficulties using power electronics based devices. To achieve this goal, generally in the first part of this book there will be a discussion on the limitations of the transmissions systems as well as PQ problems

of the distribution systems and their impact on the users. In the second part, the power electronics devices for transmission control will be introduced. Special attention will be paid to the newest and most promising members of the FACTS family to the Interline Power Flow Controllers. Their principle of operation, basic properties and controls will be presented. This part of the thesis deals also with a method for probabilistic dimensioning of the devices for transmission control. In the third part, the custom power solutions to some of the power quality problems of the distribution systems will be introduced. As is the case earlier special attention will be paid to three devices, UPQC, VAPF and SVAPF, where in the author's opinion, the third one is the most promising because of its variety. Finally the forth part shows directions for some future investigations.

Looked at in detail , this thesis is organized in six chapters.

Chapter 1 introduces the concept of quality of delivery and elucidates the subject matter of this thesis.

Chapter 2 starts with a discussion on the quality of delivery terms and their definitions. Attention is also given to: impact of poor quality of delivery on the EPS users; and power electronics based equipment to eliminate those limitations.

Chapter 3 presents the idea of FACTS devices, appropriate for overcoming limitations in transmission systems. The first section deals with power flow control issues. Next there is a presentation of the principle of operation, basic properties and capabilities for transient and dynamic stability improvement of the following systems: SSSC, STATCOM, UPFC and HVDC.

In Chapter 4 the major attention is paid to the IPFC, which is the newest and most powerful member of the FACTS family. In both above Chapters the transient stability issues are explained there on the basis of the equal-area criterion. The detailed description of methods for estimation of EPS stability, *e.g.*, Phillips-Heffron model, is beyond the scope of this thesis.

Chapter 5 introduces a method for probabilistic dimensioning devices suitable for transmission control. Special attention is paid to two arrangements: IPFC and STATCOM. The suggested method arises from the fact that processes which happen in EPS have a probabilistic nature (active and reactive power quantities, voltages *etc.*) and thus the power ratings of devices for transmission control can be considerably decreased.

Chapter 6 presents properties of the power electronics arrangements suitable for solving the power quality problems in the distribution systems. The first part deals with structures of the power electronics converters fitting the requirements of the CUPS. Special attention is paid to the multilevel converters, their operating principles and problems of balancing the DC voltages. Next, the principle of operation and basic properties of the following compensating devices are presented: PAPF, SAPF, hybrid Active Power Filter, UPQC, VAPF and SVAPF. A comparison of the energetic properties of the PAPF and VAPF will finish this chapter.

The book concludes with Chapter 7 in which a summary of the results and some future directions and opportunities in quality of delivery enhancements are provided.

## Quality of Delivery

The term quality of delivery refers to the ability of the various components – generation, transmission, and distribution – to deliver the electric power to all points of consumption in the amount and quality demanded by the customer. Because a power station which works without any failures is not a source of any trouble in supplying quality, the generated system voltages are almost perfectly sinusoidal, therefore for the purposes of this thesis the term *quality of delivery* will be treated as a matter of two issues, related to limitations of the transmission systems as well as to PQ problems of the distribution systems.

### 2.1 Limitations of the Transmission Systems

The limitations of the transmission system can take many forms and may include one or more of the following characteristics [2].

*Voltage magnitude.* On an AC power system, voltage is controlled by changing production and absorption of reactive power. There are a few reasons why it is necessary to handle reactive power and to control voltage. First, both customer and EPS equipment are designed to operate within a range of voltages. At low voltages, many types of equipment perform poorly; induction motors can overheat and be damaged, and some electronic equipment will not operate at all. High voltages can damage equipment and shorten its working life. Second, to maximize the amount of real power that can be transferred across a transmission system, reactive power flows must be minimized. Third, reactive power on the transmission system causes real-power losses. Both capacity and energy must be supplied to replace these losses. Voltage control is complicated by two additional factors. First, the transmission system itself is a nonlinear consumer of reactive power, depending on system loading. At very low levels of system load, transmission lines act as capacitors and increase voltages (the system consumes reactive power that must be generated). At high load levels, transmission lines absorb reactive power and thereby lower voltages (the system consumes a large amount of reactive power that must be replaced). The system's reactive power requirements also depend on the

generation and transmission configuration. Consequently, system reactive requirements vary in time as load levels and load and generation patterns change.

The EPS operator has several devices available that can be used to control voltages. For example generators which inject reactive power into the power system, tending to raise system voltage, or which absorb reactive power, tending to lower system voltage. Additionally transformer tap changers can be used for voltage control. These arrangements can force voltage up (or down) on one side of a transformer, but it is at the expense of reducing (or raising) the voltage on the other side. The reactive power required to raise (or lower) voltage on a bus is forced to flow through the transformer from the bus on the other side. Fixed or variable taps often provide  $\pm 10\%$  voltage selection.

*Thermal limits.* If the transmission line has not been loaded to its thermal limit (the thermal rating of normally designed transmission lines depends mainly on the voltage level at which they operate and the reactance) the power transfer capability can be increased by the use of, *e.g.*, switchable capacitors and controlled reactors. Such devices can supply or absorb reactive power, respectively raising or lowering the voltage of the transmission line. Also series compensation is used to increase the capability of power transfer by reducing the reactance of the transmission line.

*Transient and dynamic stability.* Transient stability refers to the ability of the power system to survive after a major disturbance, while dynamic stability refers to sustained or growing power swing oscillations between generators or a group of generators initiated by a disturbance (fault, major load changes *etc.*).

The mitigation of these oscillations is commonly performed with Power System Stabilizers (PSSs), sometimes additionally in conjunction with Automatic Voltage Regulators (AVRs).

### 2.1.1 FACTS to Enhance Limitations of the Transmission Systems

Most transmission system equipment (*e.g.*, capacitors, inductors, and tap changing transformers) is relatively static and can respond only slowly and in discrete steps, in contrast to FACTS devices which provide very fast response. Generally, FACTS devices can be divided into three major categories: series, shunt or combined devices.

The series devices impact the driving voltage and hence the current and power flow directly. Therefore, if the purpose of the application is to control the current/power flow and to damp oscillations, the series controllers are several times more powerful than the shunt devices. The SSSC or TSSC are the exemplary series devices of the FACTS family.

The shunt devices draw from or inject current into the line, thus they are applied to control voltage at and around the point of connection through injection of reactive current. The STATCOM or SVC are the exemplary shunt devices of the FACTS family.

This does not mean that the series controllers cannot be used for voltage control. Because the voltage fluctuations are largely a consequence of the voltage drop in series impedances of lines, inserting a series compensator might be the

**Table 2.1.** FACTS to enhance limitations of the transmission systems

Subject	Problem	Corrective action	Advisable FACTS
Voltage limits	Low voltage at heavy load	Supply reactive power	SVC, STATCOM
		Reduce line reactance	TCSC
	High voltage at low load	Absorb reactive power	SVC, STATCOM
	High voltage following an outage	Absorb reactive power, prevent overload	SVC, STATCOM
	Low voltage following an outage	Supply reactive power, prevent overload	SVC, STATCOM
Thermal limits	Transmission circuit overload	Increase transmission capacity	TCSC, SSSC, UPFC, IPFC
Stability	Limited transmission power	Decrease line reactance	TCSC, SSSC, UPFC, IPFC
Load flow	Power distribution on parallel lines	Adjust line reactances	TCSC, SSSC, UPFC, IPFC
		Adjust phase angle	UPFC, SSSC, IPFC

most cost-effective way of improving the voltage profile. Nevertheless, shunt devices are much more effective in maintaining a required voltage profile at a substation bus.

From the above consideration it follows that a combination of the series and shunt controllers can provide the best of both, *i.e.*, an effective power/current flow and line voltage control. The UPFC or IPFC are the exemplary combined devices of the FACTS family [18, 46, 47, 120].

The application of these above mentioned devices depends on the problem which has to be solved. Thus Table 2.1 presents an overview of problems occurring in the transmission system and which FACTS to use to solve these problems.

## 2.2 Power Quality

The term Power Quality has arisen in trying to clarify responsibilities of utilities and customers in respect to each other, but unfortunately is still an area of disagreement between power engineers. Many PQ related standards are at present in existence and are under constant revision. The definition of power quality given in the Institute of Electrical and Electronic Engineers (IEEE) dictionary [121] is as follows: “*Power quality is the concept of powering and grounding sensitive equipment in a matter that is suitable to the operation of that equipment*”.

The IEEE Working Group on Power Quality Definitions of SCC22 states: “*A point of view of an equipment designer or manufacturer might be that power quality is a perfect sinusoidal wave, with no variations in the voltage, and no noise present on the grounding system. A point of view of an electrical utility engineer might be that power quality is simply voltage availability or outage minutes. Finally, a point of view of an end-user is that power quality or “quality power” is simply the power that works for whatever equipment the end-user is applying. While each hypothetical point of view has a clear difference, it is clear that none is properly focused.*”

The International Electrotechnical Commission (IEC) does not use the term Power Quality in standards, but electromagnetic compatibility and the following definition of power quality is given [122]: “*The characteristics of the electricity at a given point on an electrical system, evaluated against a set of reference technical parameters - Note: These parameters might, in some cases, relate to the compatibility between electricity supplied on a network and the loads connected to that network*”.

A Union of the Electricity Industry (EURELECTRIC) report [123] on Power Quality in European networks states: “*The quality of the electricity supply is a function of its suitability as an energy source for the electrical equipment designed to be connected to the supply network. The two primary components of supply quality are:*

- *continuity (freedom from interruption): the degree to which the user can rely on its availability at all times;*
- *voltage level: the degree to which the voltage is maintained at all times within a specified range“*

[...]

“*The term ‘power quality’ is frequently used to describe these special characteristics of the supply voltage, particularly in developed countries where discontinuity and ordinary voltage variation have largely been eliminated as matters of frequent concern. The principal phenomena concerned in power quality are:*

- *harmonics and other departures from the intended frequency of the alternating supply voltage;*
- *voltage fluctuations, especially those causing flicker;*
- *voltage dips and short interruptions;*
- *unbalanced voltages on three-phase systems;*
- *transient overvoltages, having some of the characteristics of high-frequency phenomena*

*Power quality can be defined as the degree of any deviation from the nominal values of the abovementioned characteristics. It can be also defined as the degree to which both the utilization and delivery of electric power affects the performance of electrical equipment.”*

**Table 2.2.** The PQ issues [67]

Category	Typical characteristics		
	Spectrum	Duration	Magnitude
1.0 Transients			
1.1 Impulsive		50 ns - 1ms	< 6 kV
1.2 Oscillatory		5μs - 0.3 ms	0 - 4 p.u.
2.0 Short duration variations			
2.1 Interruptions		10 ms - 3 min.	< 1 %
2.2 Sag		10 ms - 1 min.	1 - 90 %
2.3 Swell		10 ms - 1 min.	110 - 180 %
2.4 Rapid voltage changes		not defined	> ±5 %
3.0 Long duration variations		stationary	< 106 % > 90 %
3.1 Under voltages		> 1 min.	80 - 90 %
3.2 Over voltages		> 1 min.	106 - 120 %
4.0 Voltage unbalance		stationary	0.5 - 2 %
5.0 Curve distortion			
5.1 DC offset	n=0	stationary	0 - 0.1 %
5.2 Harmonics	n=2 - 40	stationary	0 - 20 %
5.3 Interharmonics	0 - 6 kHz	stationary	0 - 2 %
5.4 Notches		stationary	
5.5 Noise	Broadband	stationary	0 - 1 %
5.6 Signal transmission	< 148 kHz	stationary	0.09
6.0 Voltage fluctuations	< 25 Hz	intermittent	0.2 - 7%
7.0 Net frequency variations	50 Hz	< 10 s	1 %

A report of the Council of European Energy Regulators (CEER) Working Group on Quality of Electricity Supply [124] states: “*The main parameters of voltage quality are frequency, voltage magnitude and its variation, voltage dips, temporary or transient overvoltages and harmonic distortion. European Standard EN 50160 lists the main voltage characteristics in low and medium voltage networks, under normal operating conditions*”.

From all these definitions, it can be stressed that the Power Quality is usually considered to include two aspects of power supply, namely Voltage Quality and Supply Reliability. The Voltage Quality part includes different disturbances, such as rapid changes, harmonics, interharmonics, flicker, unbalance and transients; whereas the reliability part involves phenomena with a longer duration, such as interruptions, voltage dips and sags, over and under voltages and frequency deviations. According to [3] and [67] the PQ issues may be classified as in Table 2.2.

The above issues are important in describing the actual phenomena which may cause the PQ problem. Another way to categorize the different disturbances is to look at possible causes for each kind of disturbance and to look at the consequences they might give. They are summarized in Table 2.3. [5]

It may also be advisable to take the reactive power into consideration as a PQ parameter, since the magnitude of the losses in the network and the sizes of transformers may be increased, due to the reactive power in the network. However since the voltage is chosen here as the PQ parameter the effect of the reactive power must be considered under the term voltage fluctuation, and the effect of reactive power must then be compensated with regard to this term.

### **2.2.1 Equipment Used to Enhance PQ**

Just as FACTS controllers improve transmission systems, the equipment used to enhance the quality of power that is delivered to customers is called CUPS.

There are many different types of devices, which may be used to enhance the PQ, and these may be generally divided into two groups: stepwise devices and compensating type devices. Stepwise devices may regulate the voltage by use of an electronically controlled voltage tap changer, or by the use of stepwise-coupled capacitors. Such apparatus may also be used for compensation of reactive power. However, the analysis of these devices will not be performed in this thesis.

Compensating type devices usually include VSCs controlled by various control strategies, which, depending on the topology, may be divided into three major types: current, voltage and combined compensation.

The typical current compensation device may be considered the PAPF, which can operate in two modes: i) current - acts as active filter, power factor corrector, load balancer *etc.*; ii) voltage - regulates a bus voltage against any distortion, sag/swell, unbalance and even short duration interruptions.

Voltage based compensation is classified as voltage harmonics filtration, voltage regulation and balancing, and removing voltage sags and dips and in general is carried out by using, *e.g.*, SAPF.

**Table 2.3.** Voltage disturbances [5]

Disturbance		Origin	Consequences
Voltage sag, undervoltage 2.2		Short circuits in the network grid. Start up of large motors.	Disconnection of sensitive loads. Fail functions.
Voltage swells. Overvoltages 2.3		Earth fault on another phase. Shut down of large loads. Lightning strike on network structure. Incorrect setting in substations.	Disconnection of equipment may harm equipment with inadequate design margins.
Harmonic distortion 5.2-5.3		Nonlinear loads. Resonance phenomena. Transformer saturation.	Extended heating. Fail function of electronic equipment.
Transients 1.1-1.2		Lightning strike. Switching event.	Insulation failure. Reduced lifetime of transformers, motors etc.
Voltage fluctuations, flicker 6.0		Arc furnaces. Wind turbines. Start up of large motors.	Ageing of insulation. Fail functions. Flicker.
Short duration interruptions 2.1		Direct short circuit. Disconnection. False tripping. Load shedding.	Disconnection.
Unbalanced 4.0		One phase loads. Weak connections in the network.	Voltage quality for overloaded phase. Overload and noise from 3-phase equipment.

Current and voltage compensation may also be combined. This combination is referred to as the UPQC. The conditioning functions of the UPQC are shared by the SAPF and PAPF. The SPAF performs harmonic isolation between supply and load, voltage regulation and voltage flicker/imbalance compensation, however the PAPF performs harmonic current filtering and negative sequence balancing as well as regulation of the *DC* link voltage.

VAPF [103-110, 125] and SVAPF [111, 119] offer a different way of PQ improvement. Generally in VAPF the PQ improvement is possible because the parallel connected VSC acts as a sinusoidal voltage source, with fundamental frequency ( $50Hz$ ). A quite similar way of improving power quality is possible using the SVAPF device which additionally possesses an extra current source.

---

## Traditional Power Electronics Systems for Transmission Control

### 3.1 Power Flow Control

During the last several years interest in the control of (active) power flows in transmission systems has increased significantly. There are a number of reasons for this:

- thermal issues are generally related to thermal limits caused, for example, by a change in the network configuration. Additionally, in a meshed power system, there can occur a situation where a low impedance line carries much more power than originally designed for, while parallel paths are underutilized, see Figure 3.1. With power flow control, the stressed line can be relieved, resulting in a better overall utilization of the network;

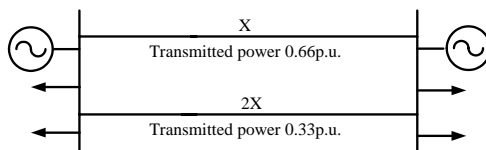


**Figure 3.1.** Power flow through parallel paths

- in the future when, among others, private companies will operate transmission lines and sell energy to interested parties, the load flow will have to be controlled. One possibility is to use HVDC lines; another possibility is load flow control using FACTS devices in an AC network see Figure 3.2;
- voltage and reactive power control issues: Low voltage at heavily loaded transmission lines as well high voltage at lightly loaded lines are undesirable occurrences in the transmission lines. The first one can be a limiting factor responsible for reduced value of the transmitted power and the second one can cause equipment damage. Both low voltage as well as

high voltage can exceed the voltage limits, therefore corrective actions have to be taken. The corrective actions with utilization of selected FACTS devices include correcting the power factor and compensating reactive losses in lines by supplying reactive power;

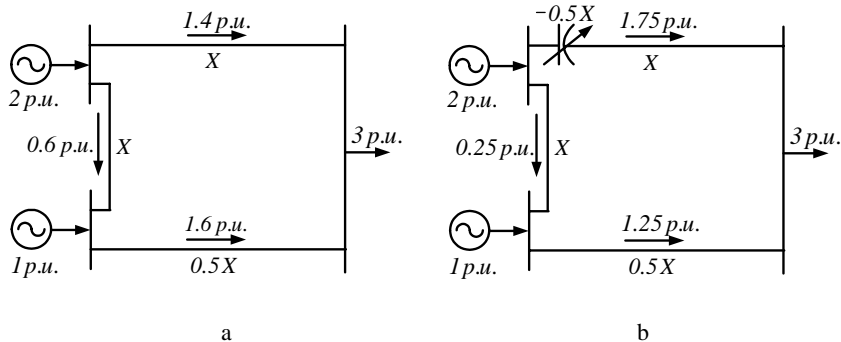


**Figure 3.2.** Power flow control in a meshed system: a. power flows; b. power flows with TCSC device

- loss reduction: Generally, total losses in a system cannot be reduced to such an extent that the installation of power flow controllers is justified. Easily avoidable are only the losses due to reactive power flow, which usually are quite small. A reduction of the losses due to active power flow would require a decrease of the line resistances. However, loss reduction in a particular area of the system is a relevant issue. Power transfers from one point to another will physically flow on a number of parallel paths and thereby impel losses on lines that might belong to another utility, thus causing increased costs for that company. If the latter utility cannot accept these losses, power flow control can be a solution;
- transient and dynamic stability control issues: Transient stability describes the ability of the power system to survive after a major disturbance; while dynamic stability describes sustained or growing power swing oscillations between generators or a group of generators initiated by a disturbance (fault, major load changes etc.). The first phenomenon can be improved by synchronizing power flow between sending and receiving ends. A solution for the second phenomenon lies in the use of equipment that permits dynamic damping of such oscillations. In the first as well as in the second situation active power flow control can be a solution

Summarizing, power flow control technologies have the abilities to solve both steady-state (better utilization of the transmission assets, minimization of losses; limit flows to contract paths etc.) and dynamic issues (dynamic damping of the oscillations) of the transmission systems.

Above, reasons for load flow control have been given. Consider the circuit in Figure 3.3, which shows a simplified case of power flow on an AC transmission

line. Sending as well as receiving end buses could be any transmission substations connected by a transmission line. Substations additionally may have loads, generations or may be interconnecting points on the further transmission system.  $V_1$  and  $V_2$  are the magnitudes of the bus voltages with an  $\delta$  angle between them. The line is assumed to have inductive impedance  $X$ , and ignored resistance and as well as capacitances.

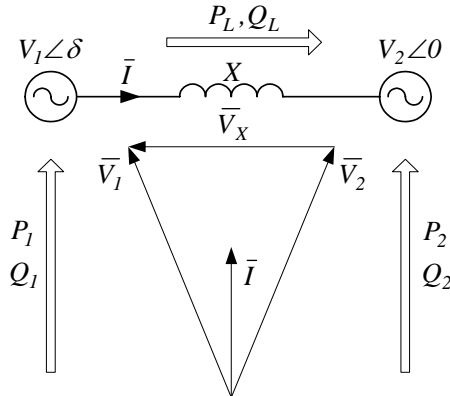


**Figure 3.3.** Transmission line

The active and reactive powers, like those shown in Figure 3.3, are, neglecting losses, given by the equations [1]

$$P_L = P_1 = -P_2 = \frac{V_1 \cdot V_2}{X} \sin(\delta) \quad (3.1)$$

$$Q_L = Q_1 + Q_2 = \frac{V_1^2 + V_2^2}{X} - 2 \frac{V_1 \cdot V_2}{X} \cos(\delta) \quad (3.2)$$

$$Q_1 = \frac{V_1^2}{X} - \frac{V_1 \cdot V_2}{X} \cos(\delta) \quad (3.3)$$

$$Q_2 = \frac{V_2^2}{X} - \frac{V_1 \cdot V_2}{X} \cos(\delta) \quad (3.4)$$

The above equations are basic to an understanding of the control of power flows on an AC transmission line. As one can see parameters that influence the most desirable active power flow through a transmission line are:

- $V_1$ , the voltage at the sending end;
- $V_2$ , the voltage at the receiving end;
- $X$ , the line's reactance;
- $\delta$ , the angle between the sending and receiving end voltages

It is easy to understand that, without control of any of the above mentioned parameters, the transmission line can be utilized only to a level well below that corresponding to  $\pi/2$ , with reference to the curve of active power vs. angle control, see Figure 3.4. This limitation is necessary, for example in order to keep an adequate margin needed for transient and dynamic stability.

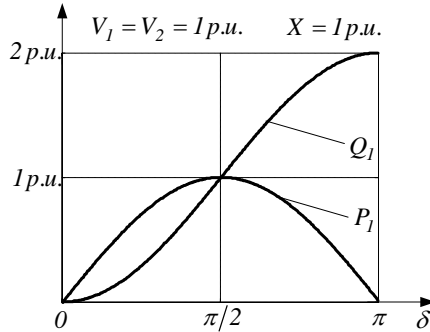


**Figure 3.4.** Power transmission vs. angle control

With reference to the above, let us discuss a few basic rules regarding the possibilities of power flow control. Control of the line impedance  $X$  (*e.g.*, with TSSC) can provide a powerful means of current control and therefore control of active power. Respectively, an increase or decrease of the value  $X$  will increase and decrease the height of the active power course [10]. Control of angle (*e.g.*, with Phase Angle Regulator) provides a powerful means of controlling the active power flow [1, 10].

Power flow can also be changed by injecting voltage in series with the transmission line. When injected voltage is perpendicular to the current, see Figure 3.5.a (*e.g.*, with SSSC), this means injection of reactive power in series (series reactive compensation) [56, 126]; this influences significantly the magnitude of the current flow and hence the active power flow. The voltage injected in series can be a phasor with variable magnitude and phase, see Figure 3.5.b (*e.g.*, with UPFC and IPFC). Varying the amplitude and phase angle of the series injected voltage can control the magnitude and the phase of the line current, this requires injection of both active and reactive power in series (series active and series reactive compensation). This means that voltage with adjustable magnitude and phase injected in series can provide control of both active and reactive power flows [10].

Power flow can also be controlled by changing the magnitude of the voltages at the sending and receiving end buses, see Figure 3.5.c. For this kind of control the shunt control devices (*e.g.*, SVC, STATCOM) [127-129] are responsible (by supplying or absorbing reactive current – current injection). Shunt devices basically impact the voltage at the point of connection and help maintain the system voltage when transferred power is varied. For example shunt reactors are used to compensate for the reactive power surplus in case of reduced power transfer or open transmission lines. In case of long transmission lines, some of the

shunt reactors are permanently connected to the system to give maximum security against overvoltages. The conventional shunt capacitor compensation provides the most economical reactive power source for voltage control when additional voltage support is needed. Conventional shunt control devices and modern shunt current injection devices (*e.g.*, STATCOM) can also control power flow in a limited range by supplying or absorbing reactive current at the point of connection to the transmission system. However such regulation has much more influence over the reactive power flow than the active power [1, 10].

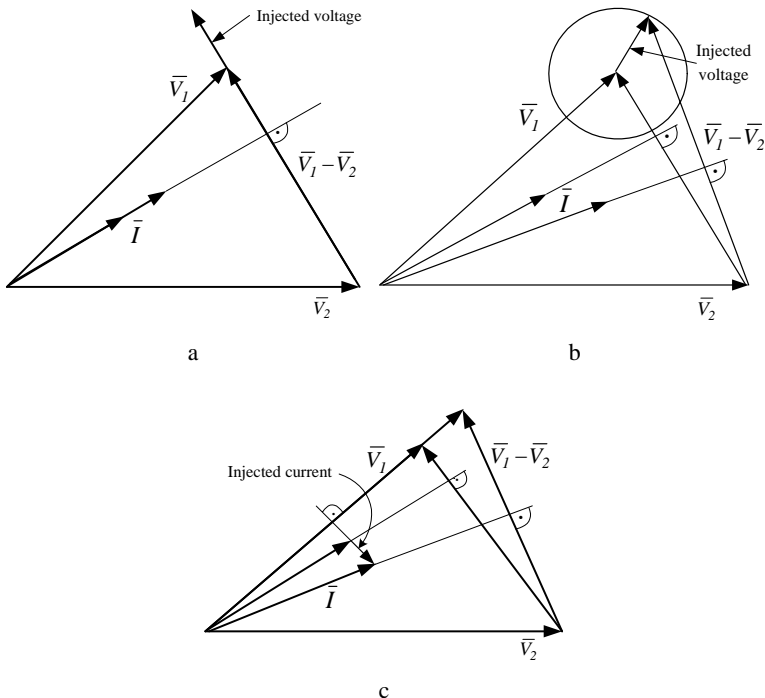


**Figure 3.5.** Power flow control- a. voltage perpendicular to the current; b. voltage with variable magnitude and phase; c. voltage control

Voltage and current injection methods are the most important and will be discussed in detail in the following chapters.

Another option to control power flow is HVDC [37]. HVDC devices convert *AC* to *DC*, transport it over a *DC* line and then convert *DC* back to *AC*. This has several advantages over the *AC* transmission:

- the distance of transmission has no influence on the power transfer in a *DC* line;
- even if converter stations require reactive power the *DC* line itself does not;
- in *DC* lines compensation to overcome the problems of line charging and stability limitations is unnecessary;

- only with the use of *DC* links is the asynchronous interconnection of two power systems possible

The converters are a major part of the HVDC, perform *AC/DC* and *DC/AC* conversion and provide the possibility to control the power flow through the HVDC link. The basic module of an HVDC converter is the three-phase, full-wave bridge circuit. In Figure 3.6 such a circuit is given. To simplify the considerations, the commutation reactances, at the *AC* side, are neglected and *DC* side current  $I_{dc}$  is constant.

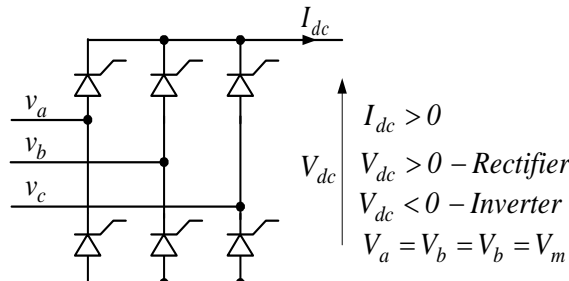


**Figure 3.6.** Three-phase full-wave bridge converter

The direct voltage  $V_{dc}$  across the bridge is composed of  $60^\circ$  segments of the line-to-line voltages. Therefore, the average direct voltage  $V_{dc0}$  is

$$V_{dc0} = 1.65 \cdot V_m \quad (3.5)$$

The gate control can be used to delay the ignition of the valves and therefore to control the voltage, respectively the power on the *DC* line. At control angles between  $0^\circ$  and  $90^\circ$  the converter operates as rectifier and therefore its thyristors are connected so that the power is positive flowing into the *DC* link. At control angles between  $90^\circ$  and  $180^\circ$  the converter operates as inverter and therefore its thyristors are connected in such a way that the power is positive flowing out of the *DC* line. With the firing delay angle  $\alpha$  the average direct voltage  $V_{dc}$  is given as

$$V_{dc} = V_{dc0} \cdot \cos(\alpha) \quad (3.6)$$

As one can see, there is only one major parameter that influences the active power flow through the *DC* tie. However, simplicity in definition of parameters responsible for power flow control goes hand in hand with limitations of the *DC* transmission systems:

- high cost of conversion equipment (need for dimensioning converters on the full transmitted power);
- generation of harmonics;
- requirement of reactive power (thyristor-based HVDC);
- complexity of controls

Because of the above mentioned restrictions the number of *DC* lines in a power grid is very small compared to number of *AC* lines. This indicates that *DC* transmission is justified only in specific applications and it is not anticipated that in the nearest future the *AC* lines will be replaced by a *DC* power grid.

Earlier in this chapter it is said that power flow control can significantly improve the transient and dynamic stability of the EPS. To recognize this relation let us take a close look at both phenomena.

Recovery from a sudden large disturbance is referred to transient stability. Typically, the disturbances are short circuits of different types which occur on the transmission lines. Under these conditions, the equal-area criterion will be used directly for the analysis. Figure 3.7.a shows the two line system [10] where a short circuit occurred (it is assumed that pre- and post-fault systems are the same), additionally the equivalent  $P_L$  vs.  $\delta$  curve illustrating the uncompensated system is presented in Figure 3.7.b.

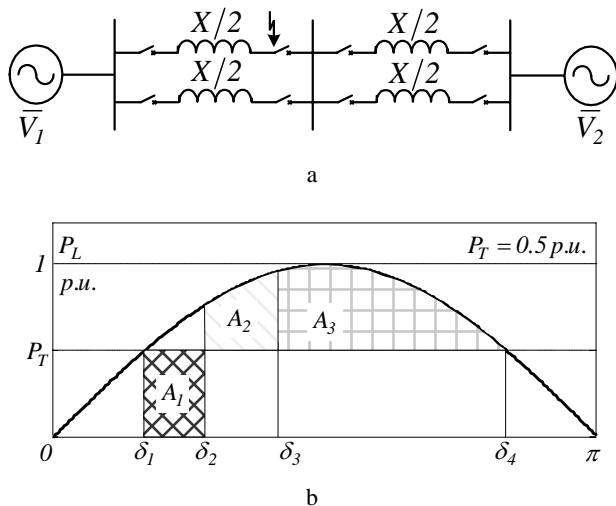


**Figure 3.7.** a. two line system; b. corresponding  $P_L$  vs.  $\delta$  curves to illustrate the dynamic behavior; where  $X=1$ p.u.,  $V_1=V_2=1$ p.u.

During the normal operating state, the line transmits  $P_T$  active power at angle  $\delta_1$ , (for given data that will be  $\delta_1=0.52$ p.u.). After the short circuit occurs, the sending end generator accelerates because the mechanical power produced remains unchanged while the electric power transmitted through the line becomes zero. Next, after the fault is cleared, at angle  $\delta_2=0.78$ p.u. (for purpose of this example as well as later considerations it is assumed that fault clearing occurs when angle increases by 50% and additionally after fault clearing all line segments are “present”), the sending end generator decelerates because the transmitted electric power exceeds the input mechanical. However the accumulated kinetic energy increases until equilibrium between the accelerating  $A_1$  and decelerating  $A_2$

energies, is reached at angle  $\delta_3$ . For the given transmission line in Figure 3.7,  $A_1$  can be determined on the base of a very simple dependency

$$A_1 = \int_{\delta_1}^{\delta_2} P_T \partial \delta = 0.26 \text{ p.u.} \quad (3.7)$$

Next, from dependency on decelerating energy

$$A_2 = \int_{\delta_2}^{\delta_3} P_L \partial \delta - \int_{\delta_2}^{\delta_3} P_T \partial \delta \quad (3.8)$$

using the principle  $A_1 = A_2$ , it is possible, after rather complicated computations, to determine that angle  $\delta_3 = 1.18 \text{ p.u.}$ , that angle  $\delta_4 = 2.61 \text{ p.u.}$  ( $P_L(\delta_4) = P_T$ ), and finally the available decelerating energy  $A_3$ ,

$$A_3 = \int_{\delta_3}^{\delta_4} P_L \partial \delta - \int_{\delta_3}^{\delta_4} P_T \partial \delta = 0.52 \text{ p.u.} \quad (3.9)$$

On the basis of the above discussion one can say that the given transmission system is able to absorb twice as much as the decelerating energy. However one must keep in mind that transmission lines usually operate closer to their thermal limits, in consequence the margin of transient stability  $A_3$  is smaller. Probably the most important issue, the practical limit for transmittable power through a line with resistance  $R$  (neglected here) before even the thermal limit is reached, may be imposed by relatively low ( $X/R < 5$ ) [10]. With reference to above mentioned, it is necessary to search for solutions which contrary to thermal or  $X/R$  ratio limitations allow an increase in the margin of transient stability. These technologies should influence the parameters determining the value of transmitted power.

A stable EPS is one in which the generators, when perturbed, return to their original. The perturbation may cause an oscillatory transient, but, with a stable system, the oscillation will be damped. Therefore the dynamic stability is the ability of the power system to maintain synchronism despite the occurrence of small disturbances.

Let us now consider transmission line equipped with two generators at both ends. In steady state the two generators will be operating at base frequency but any load imposed on the system will affect the frequency of both generators and in consequence will lead to deviations in  $\delta$  angle between voltages at both ends of the transmission line, see Figure 3.8. As a result, power transmitted through the line will oscillate around the operating point. A solution to the phenomenon lies in equipment that permits dynamic damping of such oscillations. The appropriate arrangement should increase the transmitted electric power to compensate for the surplus mechanical power produced by the accelerating generator ("+" region in

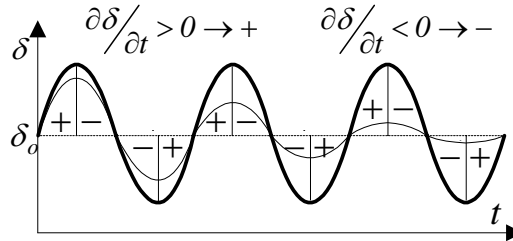


**Figure 3.8.** Deviations in  $\delta$  angle; where  $\delta_o$  operating point angle

Figure 3.8). Inversely when a generator decelerates (“-” region in Figure 3.8) the transmitted electric power must be decelerated. With reference to the above mentioned, it is necessary to search for arrangements influencing the parameters determining the value of transmitted power.

## 3.2 Converter Based FACTS

The purpose of this section is to briefly describe and define various converter based FACTS devices (voltage and current injection systems). It is worthy of mention here that for converter based devices there are two principal types of converters, these are Voltage Source Converters and Current Source Converters. However the first one seems to be more favored from an overall point of view and therefore will form the basis for presentation of the entire converter based FACTS devices. Generally, FACTS devices can be divided into three major categories:

- series devices;
- shunt devices;
- combined devices

As a series device a variable impedance (capacitor, reactor *etc.*) or power electronics based variable source which injects voltage in series with the line, could be utilized. When injected voltage is in phase quadrature with the line current, the series source exchanges (supplies or consumes) only reactive power and thus predominantly affects the active power in the line. From the other side if injected voltage is in phase with the line current, the series source handles (supplies or consumes) active power but predominantly affects the reactive power in the line. However in the last case an external source of the active power is needed (it could be an Energy Storage System (ESS) or shunt connected variable source).

As a shunt device the variable impedance (capacitor, reactor *etc.*) or variable source which injects current into the system at the point of common coupling may be utilized. As in the case of series devices, if injected current is in phase quadrature with the line voltage, the shunt device exchanges only reactive power with the line. Other phase relationships will also cause active power exchange. But this time there is no need for an extra source, because a shunt connected source can produce active power itself.

As a combined device unified series and shunt variable sources may be utilized (UPFC). In this type of device current is injected into the system with the shunt part, and voltage with the series part. Because both parts are unified, there can be a real power exchange between parts through the power link. As combined devices also unified series-series and unified series-series-shunt variable sources which are connected to a multilane transmission system could be utilized (IPFC). In these configurations it is possible to balance both real and reactive power flows in the lines.

However, the FACTS family is very extensive, and in this part of the book the major attention will be paid to the converter based arrangements that represent the basic approaches to overcome the transmission system limitations by series (SSSC), shunt (STATCOM) and combined (UPFC) compensation. To gain a wide view of the transmission control arrangements, this chapter ends with the mature technology of HVDC systems.

### 3.2.1 Series Devices

The SSSC is a series device of the FACTS family. For the purpose of steady-state operation, the SSSC injects, independently of the line current, controllable voltage in series with the transmission line (without an external electric energy source, injected voltage can be only perpendicular to the line current – series reactive compensation) for the purpose of increasing or decreasing the overall reactive voltage drop across the line and thereby controlling the transmitted electric power and improving dynamic limitations of the transmission systems. The variation of injected voltage is performed by means of a Voltage Source Converter connected on the secondary side of a coupling transformer. The VSC uses forced-commutated power electronic devices (GTOs, IGBTs or IGCTs) to synthesize a voltage  $\bar{V}_{VSC}$  from a *DC* voltage source. A capacitor connected on the *DC* side of the VSC acts as a *DC* voltage source. A low active power is drawn from the line to keep the capacitor charged and to meet transformer and VSC losses, so that the injected voltage  $\bar{V}_{SSSC}$  is practically 90 degrees out of phase with current  $\bar{I}$ . Two VSC technologies can be used:

- VSC using GTO-based square-wave converters and special interconnection transformers [130, 131]. Typically four three-level converters are used to build a *48-step* voltage waveform. Special interconnection transformers are used to neutralize harmonics contained in the square waves generated by individual converters. In this type of VSC, the fundamental component of voltage  $\bar{V}_{VSC}$  is proportional to the voltage  $V_{dc}$ . Therefore  $V_{dc}$  has to be varied for controlling the injected voltage;
- VSC using IGBT-based Pulse Width Modulation (PWM) converters. This type of converter uses PWM technique to synthesize a sinusoidal waveform from a *DC* voltage with a typical chopping frequency of a few kilohertz. Harmonics are cancelled by connecting filters at the *AC* side of the VSC.

This type of VSC uses a fixed DC voltage  $V_{dc}$ . Voltage  $\bar{V}_{SSSC}$  is varied by changing the modulation index of the PWM modulator

The principle of a SSSC is shown in Figure 3.9.

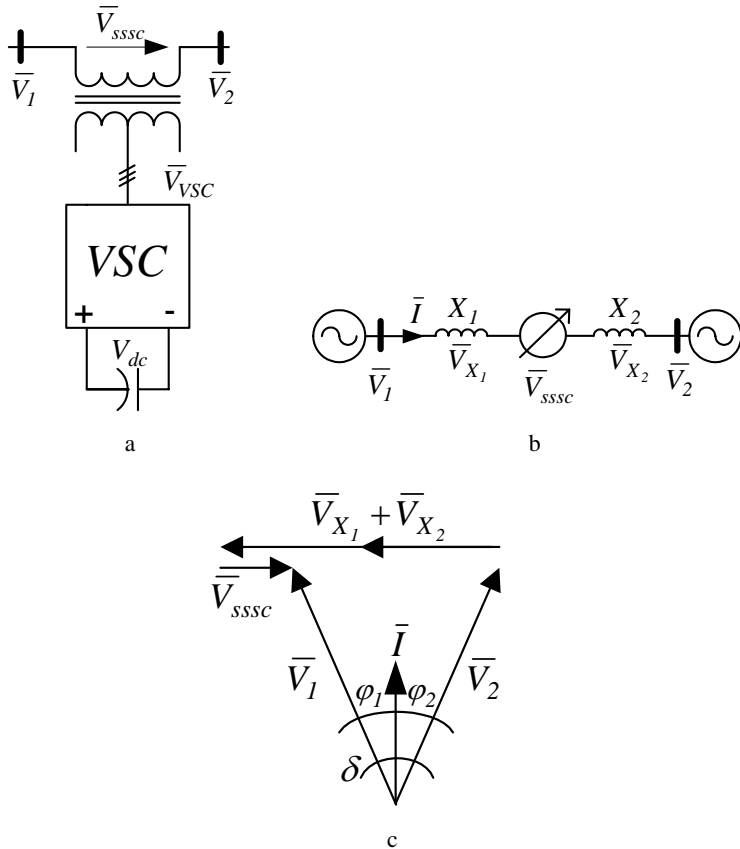


**Figure 3.9.** SSSC: a. its equivalent circuit; b. two machine system equipped with SSSC; c. vector diagram

The phasor diagram shows that the SSSC increases the magnitude of the voltage across the line, and therefore also increases the magnitude of the current  $\bar{I}$  resulting in an increase in the power flow. This corresponds to the effect of a capacitor placed in series. However, with a VSC it is possible to maintain a constant compensating voltage in the presence of variable line current because the voltage can be controlled independently of the current, *i.e.*, the VSC can also decrease the voltage across the line inductance, having the same effect as if the reactive line impedance were increased. Thus, the SSSC can decrease as well as increase the power flow to the same degree, simply by reversing the polarity of the injected voltage.

On the basis of above discussion we can define the dependency on the current flowing through the line

$$\bar{I} = \frac{\bar{V}_1 - \bar{V}_2 - \bar{V}_{sssc}}{jX_1 + jX_2} \quad (3.10)$$

Choosing  $\bar{I}$  as reference phasor, the following voltage phasors can be determined

$$\bar{V}_1 = V_1(\cos \varphi_1 + j \sin \varphi_1) \quad (3.11)$$

$$\bar{V}_2 = V_2(\cos \varphi_2 - j \sin \varphi_2) \quad (3.12)$$

$$\bar{V}_{sssc} = V_{sssc\_p} + jV_{sssc\_q} = V_{sssc}(\cos \varphi_c + j \sin \varphi_c) \quad (3.13)$$

where  $\varphi_c \angle (\bar{V}_{sssc}; \bar{I})$ .

Assuming a loss-free transmission system, the apparent powers respectively at the sending  $\bar{S}_1$  and receiving  $\bar{S}_2$  ends can be defined as

$$\bar{S}_1 = \bar{S}_2 = \bar{V}_1 \cdot \bar{I}^* = \bar{V}_2 \cdot \bar{I}^* \quad (3.14)$$

After a little algebra it is not hard to calculate the final formula on active and reactive powers transmitted through a line equipped with a series compensator [63]

$$\begin{aligned} P_{sssc} &= \frac{V_1 V_2}{X_1 + X_2} \underbrace{(\cos \varphi_2 \sin \varphi_1 + \cos \varphi_1 \sin \varphi_2)}_{\sin \delta} + \\ &+ \frac{V_2 V_{sssc}}{X_1 + X_2} \cos \varphi_2 \sin \varphi_c + \frac{V_2 V_{sssc}}{X_1 + X_2} \sin \varphi_2 \cos \varphi_c = \\ &= \frac{V_1 V_2}{X_1 + X_2} \sin \delta + \frac{V_2 V_{sssc\_q}}{X_1 + X_2} \cos \varphi_2 + \frac{V_2 V_{sssc\_p}}{X_1 + X_2} \sin \varphi_2 \end{aligned} \quad (3.15)$$

$$\begin{aligned} Q_{sssc} &= \frac{V_1 V_2}{X_1 + X_2} \underbrace{(\cos \varphi_2 \cos \varphi_1 - \sin \varphi_2 \sin \varphi_1)}_{\cos \delta} - \frac{V_2^2}{X_1 + X_2} + \\ &+ \frac{V_2 V_{sssc}}{X_1 + X_2} \cos \varphi_2 \cos \varphi_c - \frac{V_2 V_{sssc}}{X_1 + X_2} \sin \varphi_2 \sin \varphi_c = \\ &= \frac{V_1 V_2}{X_1 + X_2} \cos \delta - \frac{V_2^2}{X_1 + X_2} + \frac{V_2 V_{sssc\_p}}{X_1 + X_2} \cos \varphi_2 - \frac{V_2 V_{sssc\_q}}{X_1 + X_2} \sin \varphi_2 \end{aligned} \quad (3.16)$$

Because a loss-free SSSC device without an external energy source exchanges with the transmission line only reactive power, the injected voltage possess only

one component, perpendicular to the line current  $V_{sssc\_q}=V_{sssc}$ ;  $V_{sssc\_p}=0$ . Assuming equal voltage magnitudes at the both ends of the line  $V_1=V_2=V$  one can write that  $\varphi_1=\varphi_2=\delta/2$ , thus Equations 3.15 and 3.16 results respectively in [63]

$$P_{sssc} = \frac{V^2}{X_1 + X_2} \sin \delta + \frac{VV_{sssc}}{X_1 + X_2} \cos(\delta/2) \quad (3.17)$$

$$Q_{sssc} = \frac{V^2}{X_1 + X_2} \cos \delta - \frac{V^2}{X_1 + X_2} - \frac{VV_{sssc}}{X_1 + X_2} \sin(\delta/2) \quad (3.18)$$

On the basis of Equation 3.17 the transmitted active powers versus transmission angle characteristics are given in Figure 3.10. To show the power flow capabilities of the thyristor based series FACTS devices, the transmission characteristics of a TSSC device are presented additionally in Figure 3.10.

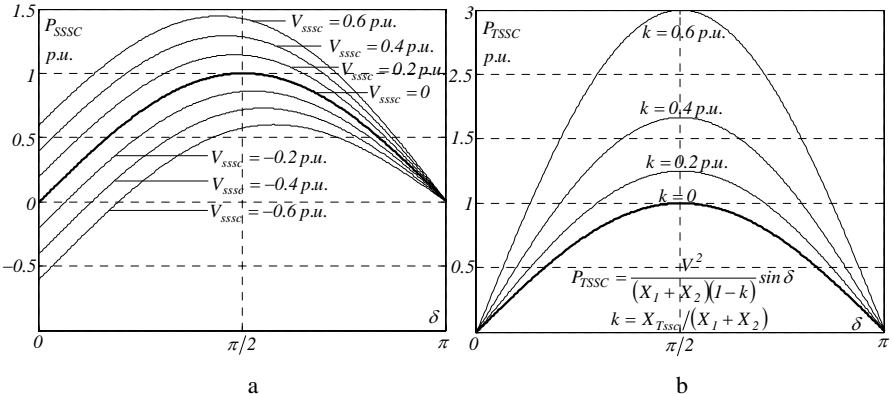


**Figure 3.10.** Basic transmission characteristics obtained for: a. SSSC; b. TSSC; where  $X_1+X_2=1$  p.u.,  $V=1$  p.u.

Comparison of the characteristics shows that at a given  $\delta$  the TSSC increases the transmitted active power by a fixed percentage of that transmitted by the uncompensated line. The SSSC can increase it by a fixed portion of the maximum transmitted power independent of  $\delta$  in the following range  $0 \leq \delta \leq \pi/2$ . One of the major disadvantages of both arrangements is fact that they cannot exchange active power with the transmission line (in SSSC this is possible but only with external energy storage). As a result independent control of the active and reactive transmitted powers is not possible and thus one must take into account that active power flow control can cause undesirable reactive power changes and related issues, e.g. reactive power loss.

As mentioned above, in an SSSC device instead of a DC capacitor a battery can be used as DC energy. In this case the converter can control both reactive and

active power exchange with the AC system. The capability of controlling active as well as reactive power exchange is a significant feature which can be used effectively in applications requiring power oscillation damping and to level peak power demand.

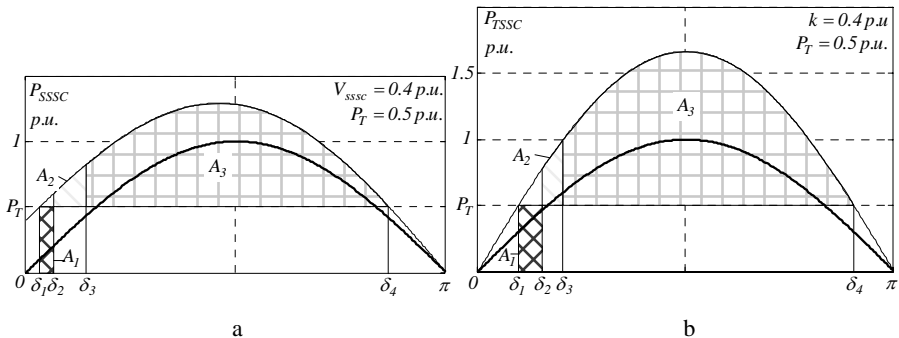


**Figure 3.11.**  $P$  vs.  $\delta$  curves to illustrate the dynamic behaviour for a two generator system with series compensators; for: a. SSSC; b. TSSC; where  $X_1+X_2=1$  p.u.,  $V=1$  p.u.

The above presented capabilities of the series compensators of controlling the transmitted power can be utilized to increase the transient stability limit as well to improve the dynamic stability. Once again let us consider the simple two generator system, introduced in Chapter 3.1 in Figure 3.7a, but this time equipped with series compensator (SSSC or TSSC). It is assumed that pre- and post-fault systems are the same; fault clearing occurs when angle increases by 50% and with or without the series compensation system carries the same power  $P_T$ . Curves presented in Figure 3.11 and data available in the Table 3.1 (obtained in the same way as in Chapter 3.1) show that series compensation can significantly increase the transient stability limit  $A_3$ . This is possible to achieve by limited cancellation of the impedance of the transmission line. The comparatively large stability limit achievable by TSSC arrangement results from accepted large level of the series compensation, which often is limited to less than 0.3 p.u.[10].

**Table 3.1.** Parameters describing dynamic behaviour; in parentheses  $A_3$  values related to transient stability limit of the uncompensated line

Device	$\delta_1$	$\delta_2$	$\delta_3$	$\delta_4$	$A_1=A_2$	$A_3$
TSSC	0.30 p.u.	0.45 p.u.	0.65 p.u.	2.83 p.u.	0.07 p.u.	1.81 p.u (3.4)
SSSC	0.10 p.u.	0.15 p.u.	0.33 p.u.	2.71 p.u.	0.02 p.u.	1.31 p.u. (2.5)

In the sense of improvement of the transient stability the SSSC and TSSC controllable parameters (respectively  $V_{sssc}$  and  $k$ ) should be determined to achieve maximum impact on transmission characteristics. Therefore the optimal parameters could be determined from the following equations:  $\partial P_{SSSC}/\partial V_{sssc}=0$ ;  $\partial P_{TSSC}/\partial k=0$ . However because neither of the equations has a solution, the maximum impact is

achieved if both  $V_{SSSC}$  and  $k$  are set to their maximum values, determined by the device rating.

Series compensation can also be useful to damp power oscillations. The above curves in Figure 3.12 show (from above) oscillations of the  $\delta$  angle, oscillations of the transmitted power and degree of the series compensation. As one can see the level of series compensation should be maximum (capacitive) when generator accelerates - to maximize the transmittable electric power, and minimum (inductive) when generator decelerates - to minimize the transmittable electric power.

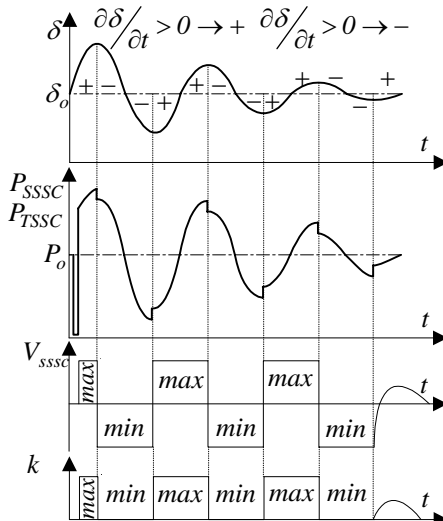


**Figure 3.12.** Power oscillations dumping by SSSC and TSSC

Except power flow capabilities and dynamic problems there are other issues related to the FACTS devices - their location and cross-couplings. From Equations 3.17 and 3.18 it is obvious that location of a SSSC does not affect transmission characteristics only in the line where it is installed but also in other lines, therefore the ratio between  $X_1$  and  $X_2$  is arbitrary their sum. The dependency defining reactance ratio,  $\partial P_{SSSC} / \partial (X_1/X_2) = 0$ , does not have a solution. However since the active power has to be transferred through a number of paths, any change of active power flow in one line will be complemented by changes in other lines (power flow control in line with SSSC will affect transmission characteristics in other lines). Therefore strong cross-coupling between controllable components and lines is to be expected. Additionally it is not quite obvious which line in a given meshed system will provide an optimal installation of a FACTS device. In addition FACTS placement or cross-coupling analysis may be done with regard to one of the following objectives:

- maximum impact on transmission characteristic;
- reduction of the real power loss of a particular line;

- reduction of the total system real power loss;
- reduction of the total system reactive power loss;
- impact on system stability

For the above mentioned objectives, methods based on the sensitivity approach may be used. The sensitivity of an output variable to a control variable can be defined [132]

$$\text{Sensitivity}_h^g = \frac{\partial h}{\partial g} \quad (3.19)$$

For example, when investigating the sensitivities of active power flows in line  $k$  to series capacities in line  $l$  (in other words influence of a controllable series capacitor in line  $l$  on active power flow in line  $k$ ), the following definition can be used

$$\text{Sensitivity}_{P_{kl}} = \frac{\partial P_k}{\partial X_l} \quad (3.20)$$

where  $P_k$  - active power flow through a line  $k$ .

Using the above definition, the investigation can include the simplest case, that is, the placement of one device in the system. However this method can be used in more sophisticated cases like “optimal” placement of many FACTS devices in a given meshed system with regard to the above mentioned objectives or the cross-couplings, that is, the effect that a device in one line (level of compensation, e.g., for a SSSC that will be  $V_{sssc}$  value) has on the active power flow (or other phenomena) in other lines. The sensitivity matrix can be used as a tool for investigating these effects for different FACTS devices.

For example, in given line  $k$ , to determine the sensitivities of SSSC controllable parameter  $V_{sssc-k}$  on effective Transient Stability (TS) enhancement, the following definition can be used

$$TS_{kk} = \frac{\partial P_{sssc-k}}{\partial V_{sssc-k}} \quad (3.21)$$

In the above definition, a dependency on active power transmitted through the line  $k$  equipped with SSSC was used because it is common knowledge that the most effective transient stability enhancement is possible to achieve through maximum impact on transmission characteristics. Therefore the smallest positive sensitivity index  $TS_{kk}$  should be selected. Calculations have shown that Equation 3.21 does not have a solution and that maximum impact on transmission characteristics is achieved if  $V_{sssc-k}$  is set to the maximum value determined by the SSSC device rating.

Let us have another look, but this time at influence of the control variable of the SSSC device on total system reactive power loss  $Q_L$ . For the SSSC device placed between buses  $k$  and  $l$ , it is considered that the voltage  $V_{sssc-kl}$  will be the control parameter. The Reactive Power Loss Sensitivity Factors (RPL) with respect to the control variable may be then given as follows

$$RPL_{kl} = \frac{\partial Q_L}{\partial V_{sssc-kl}} \quad (3.22)$$

The total reactive power loss in line between buses  $k$  and  $l$  can be defined with reference to Equation 3.18 as follows

$$\begin{aligned} Q_L &= Q_{sssc\_kl} + Q_{sssc\_lk} = \frac{2V_k V_l}{X_1 + X_2} \cos \delta - \frac{2V_k V_l}{X_1 + X_2} - \\ &- \frac{2V_l V_{sssc-kl}}{X_1 + X_2} \sin(\delta/2) \end{aligned} \quad (3.23)$$

Considering a line equipped with a SSSC device, connected between buses  $k$  and  $l$  and having equal voltage magnitudes at the both ends of the line  $V_k = V_l = V$  and total impedance  $X$ , the loss sensitivity with respect to  $V_{sssc-kl}$  can be computed as

$$RPL_{kl} = \frac{\partial Q_L}{\partial V_{sssc-kl}} = -\frac{2V \sin(\delta/2)}{X} \quad (3.24)$$

Using the loss sensitivities, the criteria for deciding device location might be stated as follows: SSSC must be placed in the line having the most positive loss sensitivity index  $RPL_{kl}$ .

### 3.2.2 Shunt Devices

The STATCOM is a technology that has gone through some evolution. Its precursor, the Static Var Compensator [48-51], has been widely used by utilities since the mid-1970's. SVC is capable of providing voltage support at its terminals by controlling the amount of reactive power injected into or absorbed from the power system. When system voltage is low, the SVC generates reactive power (SVC capacitive). When system voltage is high, it absorbs reactive power (SVC inductive). The variation of reactive power is performed by switching three phase capacitor banks and inductor banks connected on the secondary side of a coupling transformer. Because SVCs use capacitors, they suffer from the same degradation in reactive capability as voltage drops. Additionally SVC applications usually require harmonic filters to reduce the amount of harmonics injected into the power system.

Rather than using conventional capacitors and inductors combined with fast switches, the STATCOM uses power electronics to synthesize the reactive power output. A STATCOM is a controlled reactive power source and provides voltage support, which is its primary duty, by generating or absorbing reactive power at the point of common coupling without the need of large external reactors or capacitor banks [40-44, 133]. When system voltage is low, the STATCOM generates reactive power (STATCOM capacitive). When system voltage is high, it absorbs reactive power (STATCOM inductive).

The STATCOM basically consists of a step down transformer  $T_r$ , reactance  $L_F$ , a three phase GTO or IGBT based multipulse VSC, and a *DC* capacitor.

The VSC is the building block of a STATCOM and its major objective is to produce a sinusoidal *AC* voltage with minimal harmonic. Two basic techniques are used for reducing harmonics in the converter output voltage. Harmonic neutralization using magnetic coupling (multipulse converter configurations) and harmonic reduction using PWM:

- multipulse operation is achieved by connecting identical three-phase bridges to transformers which have outputs that are phase-displaced with respect to one another. Star and delta connected windings have a relative  $30^\circ$  phase shift and a *6-pulse* converter bridge connected to each transformer will give an overall *12-pulse* operation eliminating *5th* and *7th* harmonics. This principle can be extended to *24-* and *48-pulse* operation summing at the primary windings the transformed outputs of several *6-pulse* converters (*4* for *24-pulse* and *8* for *48-pulse* operation). The harmonic cancellation is carried over into the transformer secondary windings. The basic issue in structuring a high-power, multipulse converter is the complexity of the magnetic structure that is needed. The converter operation is carried out applying low frequency (usually line frequency) firing pulse to the power switches. Due to the low switching frequency, only about one third of the converter losses are due to the switching losses, the remaining two thirds are due to the magnetic interface (conduction losses);
- in multipulse there is only one turn-on, turn-off per device per cycle. Another approach is to have multiple pulses per half-cycle, and then vary the width of the pulses to vary the amplitude of the *AC* voltage, as is the case in PWM. With the PWM technique it is possible to generate high quality output waveforms, however it requires a considerable increase in the number switch operations (high switching frequency), which thereby generally increases the switching losses of the converter [134]

The VSC based STATCOM scheme together with vector diagrams clarifying principle of operation are shown in Figure 3.13.

The charged capacitor  $C$  provides a *DC* voltage to the converter, which produces a set of controllable three phase output voltages with the frequency of the *AC* power system. By varying the amplitude of the output voltage  $\bar{V}_C$ , the reactive power exchange between the converter and the *AC* system can be controlled. If the amplitude of the output voltage  $\bar{V}_C$  is increased above that of the *AC* system  $\bar{V}_T$ , a

leading current is produced, *i.e.*, the STATCOM is seen as a conductor by the AC system and reactive power is generated. Decreasing the amplitude of the output voltage below that of the AC system, a lagging current results and the STATCOM is seen as an inductor. In this case reactive power is absorbed. If the amplitudes are equal no power exchange takes place.

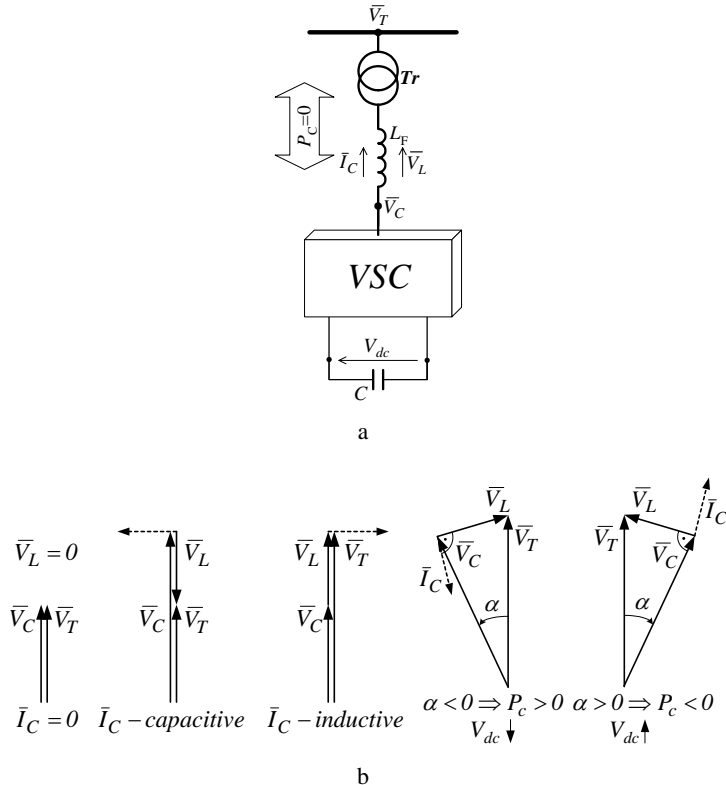


**Figure 3.13.** STATCOM: a. simplified circuit; b. vector diagrams clarifying principle of operation

A practical converter is not lossless. In the case of the DC capacitor, the energy stored in this capacitor would be consumed by the internal losses of the converter. By making the output voltages of the converter lag or lead the AC system voltages by a small angle, the converter respectively absorbs or leads a small amount of active power from the AC system to balance the losses in the converter.

Instead of a capacitor also a battery can be used as DC energy [135, 136]. In this case the converter can control both reactive and active power exchange with the AC system. The capability of controlling active as well as reactive power exchange is a significant feature which can be used effectively in applications requiring power oscillation damping, to level peak power demand, and to provide uninterrupted power for critical load.

The STATCOM can be operated in two different modes:

- in voltage regulation mode (the voltage is regulated within limits);
- in Var control mode (the STATCOM reactive power output is kept constant)

Typical applications of STATCOM are:

- effective voltage regulation and control;
- reduction of temporary overvoltages;
- improvement of steady-state power transfer capacity;
- improvement of transient stability margin;
- damping of power system oscillations

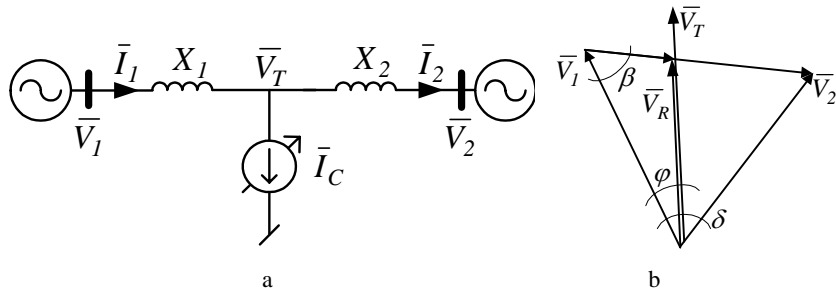


**Figure 3.14.** a. Two machine system equipped with STATCOM; b. vector diagram

In accordance to the network scheme presented in Figure 3.14 the following equations can be written

$$\bar{V}_T = \bar{V}_1 - j\bar{I}_1 X_1 \quad (3.25)$$

$$\bar{I}_2 = \bar{I}_1 - \bar{I}_C = \frac{\bar{V}_T - \bar{V}_2}{jX_2} \quad (3.26)$$

$$\bar{I}_1 = \frac{\bar{V}_1 - \bar{V}_2}{j(X_1 + X_2)} + \bar{I}_C \frac{X_2}{X_1 + X_2} \quad (3.27)$$

After some algebraic calculations, the final formula on the active power transmitted through the line equipped with shunt compensator is obtained [10]

$$P_s = \frac{V_1 \cdot V_2}{(X_1 + X_2)} \sin(\delta) \left( 1 + \frac{I_C}{V_R} \frac{X_1 \cdot X_2}{(X_1 + X_2)} \right) \quad (3.28)$$

where  $V_R = \sqrt{V_1^2 X_2^2 + V_2^2 X_1^2 + 2V_1 V_2 X_1 X_2 \cos(\delta)}$  / (  $X_1 + X_2$  ) - terminal voltage in situation when the STATCOM is out of operation.

The resulting characteristics of the transmitted power versus transmission angle are given in Figure 3.15. Additionally to show the power flow capabilities of the thyristor based shunt FACTS devices, the transmission characteristics of a SVC device are presented in Figure 3.15.

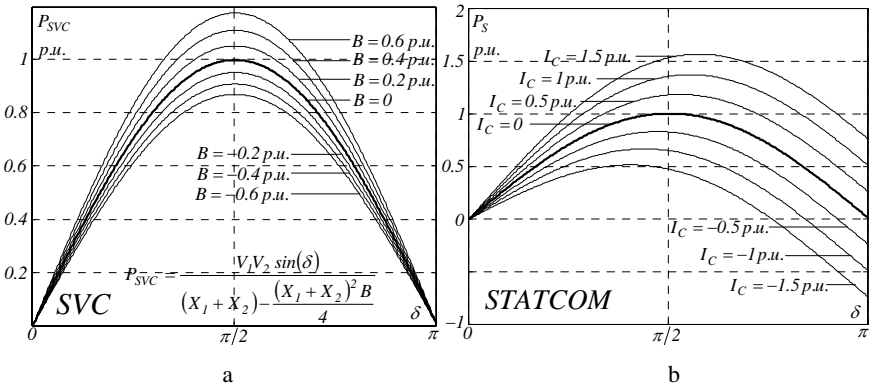


**Figure 3.15.** Transmission characteristics obtained for: a. SVC; b. STATCOM; where  $V_1 = V_2 = 1$  p.u.;  $X_1 + X_2 = 1$  p.u.;  $X_1 = X_2$

Comparison of the characteristics presented in Figure 3.15 shows that at a given  $\delta$  the SVC increases the transmitted active power by a fixed percentage of that transmitted by the uncompensated line. The STATCOM can increase it by a fixed portion of the maximum transmitted power independent of  $\delta$  in the following range  $\pi/2 \leq \delta \leq \pi$ .

The question still to be answered is where in the transmission line is the optimal placement to for the STATCOM, to maximize its impact on transmission characteristics (maximize transmitted power). For this purpose let us define the ratio between reactances  $X_1$  and  $X_2$

$$X_1 + X_2 = X ; \frac{X_1}{X_2} = X_{RATIO} \quad (3.29)$$

On the basis of above definition one can write

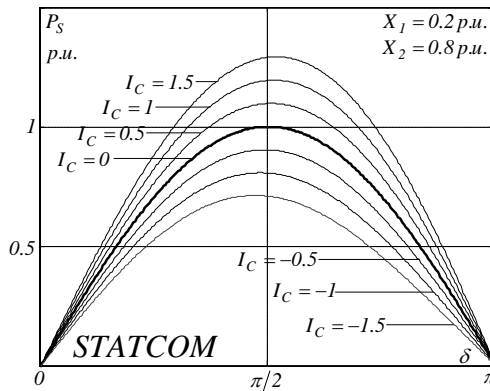
$$X_1 = \frac{X \cdot X_{RATIO}}{1 + X_{RATIO}} ; X_2 = \frac{X}{1 + X_{RATIO}} \quad (3.30)$$

To maximize STATCOM impact on transmitted power,  $X_{RATIO}$  should be selected so as to maximize the expression on active power transmitted through the line, Equation 3.28

$$\frac{\partial P_S}{\partial X_{RATIO}} = \frac{-I_C V_1 V_2 (-1 + X_{RATIO}) \sin(\delta)}{U_R (1 + X_{RATIO})^3} = 0 \Rightarrow X_{RATIO} \rightarrow 1 \quad (3.31)$$

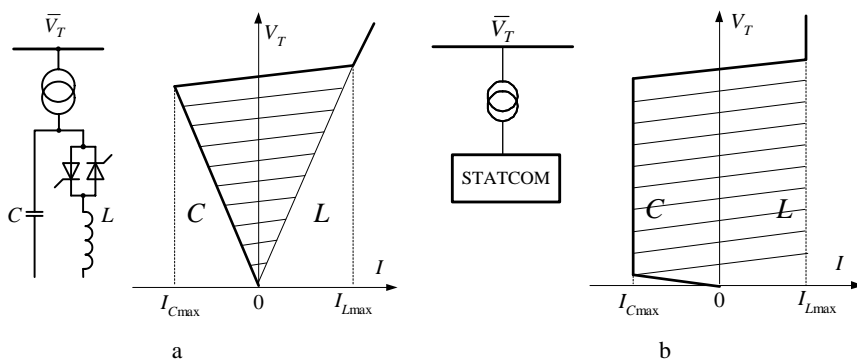
According to the above expression  $X_{RATIO}$  should be 1. This means that to maximize STATCOM impact on transmitted power it should be located at the middle of the line.

Figure 3.16 illustrates how the transmission line impedance ratio affects the transmission characteristic. As one can see, the major impact is in the part of the transmission characteristic for angles larger than  $\pi/2$ . In consequence the area representing the improvement in stability margin  $\dot{P}_s d\delta$  could be decreased.



**Figure 3.16.** Impact of the reactance ratio on transmission characteristics; where  $V_1 = V_2 = 1 \text{ p.u.}$

The V-I characteristics of the STATCOM and SVC are shown in Figure 3.17. In the linear operating range the compensation capability of the STATCOM and the SVC are similar. Concerning the nonlinear operating range, the STATCOM is able to control its output current over the rated maximum capacitive or inductive range



**Figure 3.17.** V-I characteristics of the: a. SVC; b. STATCOM

independently of AC system voltage, whereas the maximum possible compensating current of the SVC decreases linearly with AC voltage. Thus, the STATCOM is

more effective than the SVC in providing voltage support under large system disturbances during which the voltage excursions would be well outside of the linear operating range of the compensator.

The ability of the STATCOM to maintain full capacitive output current at low system voltage also makes it more effective than the SVC in improving the transient stability. In addition, the STATCOM will normally exhibit a faster response than the SVC because, with the VSC, the STATCOM has no delay associated with the thyristor.

The above presented capabilities of the shunt compensators to control the transmitted power can be utilized to increase the transient stability limit as well to improve the dynamic stability. Once again let us consider the simple two generator system, introduced in Chapter 3.1 in Figure 3.7.a, but this time equipped with shunt compensator (STATCOM or SVC). It is assumed that pre- and post-fault systems are the same; fault clearing occurs when the angle increases by 50% and with or without the shunt compensation system carries the same power  $P_T$ . The curves presented in Figure 3.18 and the data available in the Table 3.2 (obtained in the same way as in Chapter 3.1) show that shunt compensation can significantly increase the transient stability limit  $A_3$ . It is possible to achieve this *via* increasing transmission line voltage. However it is necessary to remember that the reactive power demand increases with increasing voltage. Therefore the practical shunt compensator can perform as long as the reactive power demand does not exceed its rating.

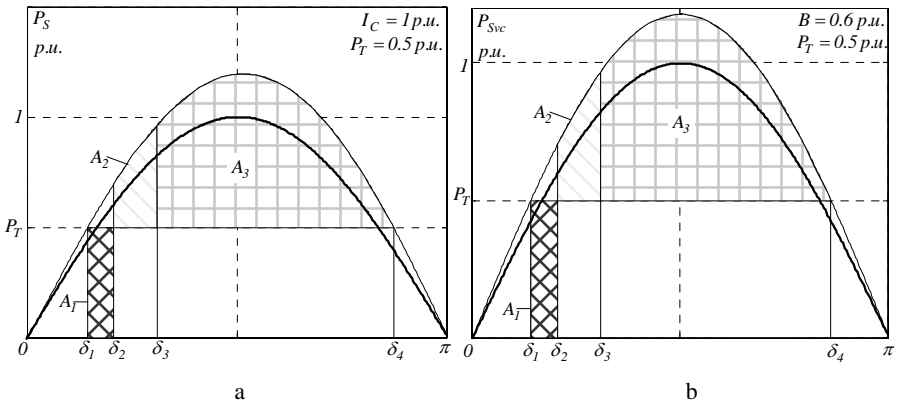


**Figure 3.18.**  $P$  vs.  $\delta$  curves to illustrate the dynamic behavior for a two generator system with shunt compensators: a. STATCOM for  $X_1=0.2$ p.u.,  $X_2=0.8$ p.u.; b. SVC for  $X_1=X_2$

In the sense of improvement of the transient stability the STATCOM and SVC controllable parameters (respectively  $I_c$  and  $B$ ) should be determined to achieve maximum impact on transmission characteristics. Therefore the optimal parameters can be determined from the following equations:  $\partial P_S / \partial I_c = 0$ ;  $\partial P_{SVC} / \partial B = 0$ . However, because neither equation has a solution the maximum impact is thus

achieved if both  $I_c$  and  $B$  are set to their maximum values, determined by the device rating.

**Table 3.2.** Parameters describing dynamic behavior; in parentheses  $A_3$  values related to transient stability limit of the uncompensated line

Device	$\delta_1$	$\delta_2$	$\delta_3$	$\delta_4$	$A_1=A_2$	$A_3$
$V_1=V_2=1p.u., X_1+X_2=1p.u., X_1=X_2$						
STATCOM	0.41 p.u.	0.61 p.u.	0.89 p.u.	3.14 p.u.	0.10 p.u.	1.40 p.u. (2.6)
	$V_1=V_2=1p.u., X_1+X_2=1p.u., X_1=0.2p.u., X_2=0.8p.u.$					
SVC	0.44 p.u.	0.66 p.u.	0.98 p.u.	2.73 p.u.	0.11 p.u.	0.90 p.u. (1.7)
	$V_1=V_2=1p.u., X_1+X_2=1p.u., X_1=X_2$					
0.43 p.u.    0.65 p.u.    0.97 p.u.    2.70 p.u.    0.11 p.u.    0.86 p.u. (1.6)						

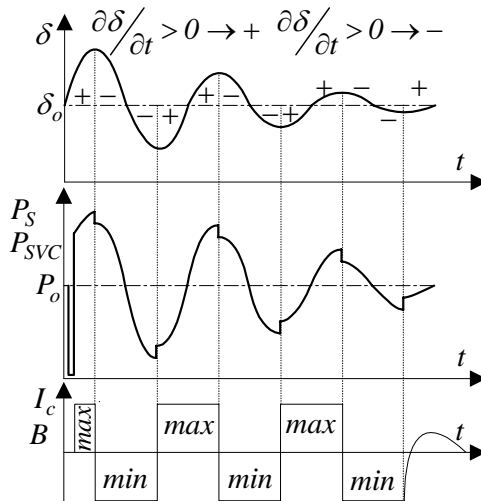


**Figure 3.19.** Power oscillation dumping by SVC and STATCOM

The shunt compensation can also be useful to damp power oscillations. The above curves in Figure 3.19 show oscillations of the  $\delta$  angle, oscillations of the transmitted power and degree of the shunt compensation. As one can see, the level of shunt compensation should be maximum-capacitive when generator accelerates – to maximize the transmittable electric power – and minimum-inductive when generator decelerates – to minimize the transmittable electric power.

### 3.2.3 Combined Devices

The Unified Power Flow Controller is one of the most versatile members of the Flexible AC Transmission Systems family using power electronics to control all parameters that affect power flow on a transmission line [94, 95]. The UPFC uses a

combination of a shunt controller (STATCOM) and a series controller (SSSC) interconnected through a common *DC* bus as shown in the Figure 3.20.

This FACTS topology provides much more flexibility than the SSSC for controlling the line active and reactive power because active power can now be transferred from the shunt converter to the series converter, through the *DC* bus. Contrary to the SSSC where the injected voltage  $\bar{V}_{SSSC}$  is forced to stay in quadrature with line current  $\bar{I}$ , the UPFC device injected voltage  $\bar{V}_{UPFC}$  can now have any angle with respect to line current. This means that series controller exchanges active and reactive powers with the line, where the reactive power is electronically provided by the series converter; next the demanded active power is drawn by the shunt converter from the *AC* network and supplied through the *DC* link. If the magnitude of injected voltage  $\bar{V}_{UPFC}$  is kept constant and if its phase angle  $\sigma$  with respect to  $\bar{V}_l$  is varied from 0 to 360 degrees, the locus described by the end of vector is a circle as shown on the phasor diagram in Figure 3.20. When injected voltage varies with its maximum achievable rms value  $V_{UPFCmax}$ , determined by the device rating, the circle defines maximum controllable area. As  $\sigma$  is varying, the phase shift  $\delta$  between voltages  $\bar{V}_l$  and  $\bar{V}_2$  at the two line ends also varies. It follows that both the active power  $P_{UPFC}$  and the reactive power  $Q_{UPFC}$  transmitted at one line end can be controlled.

In addition to allow control of the line active and reactive power, the UPFC provides an additional degree of freedom. As explained earlier the shunt converter is operating in such a way as to keep the voltage across the storage capacitor  $V_{dc}$  constant. So, the net real power absorbed from the line by the UPFC is equal only to the losses of the two converters and their transformers. The remaining capacity of the shunt converter can be used to exchange reactive power with the line so to provide a voltage  $\bar{V}_l$  regulation at the connection point.

The two VSCs can work independently of each other by separating the *DC* side. Thus in this case, the shunt converter is operating as a STATCOM that generates or absorbs reactive power to regulate the voltage magnitude at the connection point. Instead, the series converter is operating as SSSC that generates or absorbs reactive power to regulate the current flow.

Both the series and shunt converters use a Voltage Sourced Converter connected on the secondary side of a coupling transformer. The VSCs use forced commutated power electronic devices (GTOs, IGBTs or IGCTs) to synthesize a voltage from a *DC* voltage source. The common capacitor connected on the *DC* side of the VSCs acts as a *DC* voltage source. Two VSC technologies can be used for the VSCs:

- VSC using GTO-based square wave converters and special interconnection transformers – typically four three level converters are used to build a 48-step voltage waveform. Special interconnection transformers are used to neutralize harmonics contained in the square waves generated by individual converters. In this type of VSC, the fundamental component of voltage is proportional to the voltage  $V_{dc}$ . Therefore  $V_{dc}$  has to be varied for controlling the injected voltage;

- VSC using IGBT-based PWM converters – this type of converter uses PWM technique to synthesize a sinusoidal waveform from a *DC* voltage with a typical chopping frequency of a few kilohertz. Harmonics are cancelled by connecting filters at the *AC* side of the VSC. This type of VSC uses a fixed *DC* voltage  $V_{dc}$ . Voltage is varied by changing the modulation index of the PWM modulator

During investigations it will be assumed that UPFC device is positioned at the system terminals. Therefore the current  $\bar{I}_R$  absorbed from the sending end bus by the shunt converter doesn't affect the line current  $\bar{I}$  and in consequence location of a UPFC does not affect transmission characteristics in the line where it is installed. Therefore the ratio between  $X_1$  and  $X_2$  is their sum  $X$ . However, if a UPFC is positioned at another place other than system terminal, then in addition the  $\bar{I}_R$  current affects the transmission characteristics as if a STATCOM were present. From the previous section it is known that optimal STATCOM placement is in the middle of the line, therefore in this situation the optimal UPFC location is in the middle of the line.

The UPFC equivalent circuit shown in Figure 3.20 consists of a shunt connected voltage source, a series connected voltage source, and an active power constraint, which links the two voltage sources. The two voltage sources are connected to the AC system through the VSC transformers.

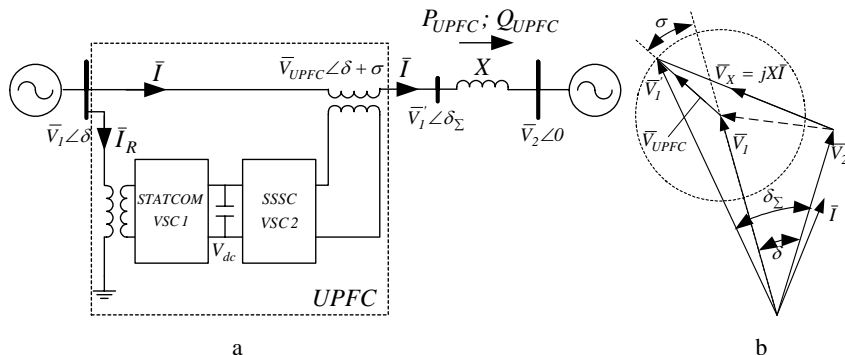


**Figure 3.20.** a. concept of the UPFC in a two machine power system; b. vector diagram clarifying principle of operation

For the system given in Figure 3.20, by performing simple mathematical manipulations the transmitted active and reactive power can be calculated as [125]

$$P_{UPFC} = \frac{V_1 \cdot V_2}{X} \sin \delta + \frac{V_{UPFC} \cdot V_2}{X} \sin(\delta + \sigma) \quad (3.32)$$

$$Q_{UPFC} = \frac{V_1 \cdot V_2}{X} - \frac{V_1 \cdot V_2}{X} \cos(\delta) - \frac{V_{UPFC} \cdot V_2}{X} \cos(\delta + \sigma) \quad (3.33)$$

As mentioned previously, the UPFC can control, independently or simultaneously, all parameters that affect power flow on a transmission line. This is illustrated in the phasor diagrams shown in Figure 3.21.

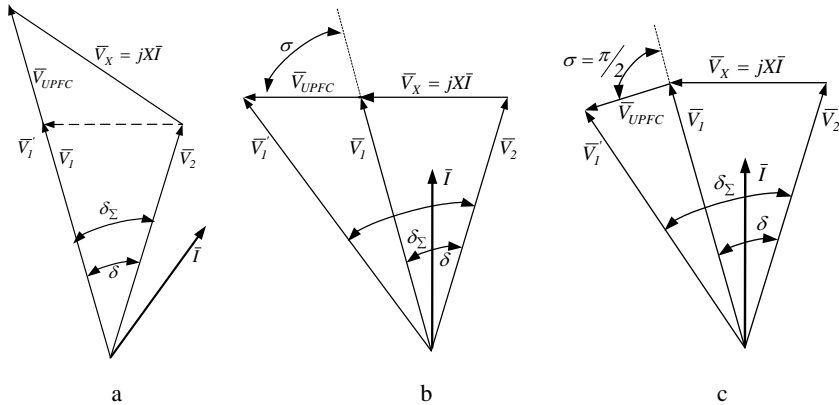


**Figure 3.21.** Phasor diagrams illustrating the general concept of: a. voltage magnitude control  $V_{UPFC}=Var$ ,  $\sigma=0$ ; b. line impedance compensation  $V_{UPFC}=Var$ ,  $\sigma=(\pi-\delta)/2$ ; c. phase angle regulation  $V_{UPFC}=Var$ ,  $\sigma=\pi/2$

Voltage regulation is shown in Figure 3.21.a. The magnitude of the sending bus voltage  $\bar{V}_1$  is increased (or decreased) by injecting a voltage  $\bar{V}_{UPFC}$ , in phase (or out of phase) with  $\bar{V}_1$ . Similar regulation can be accomplished with a transformer tap changer. Series reactive compensation is shown in Figure 3.21.b. It is obtained by injecting a voltage  $\bar{V}_{UPFC}$  but this time orthogonal to the line current  $\bar{I}$ . The effective voltage drop across the line impedance  $X$  is decreased (or increased) if the voltage  $\bar{V}_{UPFC}$  lags the current  $\bar{I}$  by  $90^\circ$  (or  $\bar{V}_{UPFC}$  leads current by  $90^\circ$ ). A desired phase shift is achieved by injecting a voltage  $\bar{V}_{UPFC}$  that shifts the phase angle of  $\bar{V}_1$  by  $\pm(\delta_\Sigma - \delta)$ .

Rotation of the series injected voltage phasor with its maximum achievable value  $V_{UPFCmax}$ , determined by the device rating, from  $0$  to  $360^\circ$  allows the real and the reactive power flow to be controlled within the boundary circle with a radius of  $V_2 V_{UPFCmax}/X$  and the centre at  $(P_{UPFC0}(\delta), Q_{UPFC0}(\delta))$  (where  $P_{UPFC0}(\delta)$ ,  $Q_{UPFC0}(\delta)$  respectively active and reactive powers transmitted at given angle  $\delta$  without combined compensation  $V_{UPFC}=0$ ). Figure 3.22 shows plots of the reactive power  $Q_{UPFC}$  demanded at the receiving bus vs. the transmitted real power  $P_{UPFC}$  as a function of the series voltage magnitude  $V_{UPFC}$  and phase angle  $\sigma$  at three different power angles  $\delta$ , i.e.,  $\delta=0^\circ$ ,  $30^\circ$ , and  $60^\circ$ . The capability of the UPFC to control real and reactive power flow independently at any transmission angle is clearly illustrated. Additionally it can be seen that the real and reactive power can be controlled between

$$P_{UPFC0}(\delta) - \frac{V_2 V_{UPFCmax}}{X} \leq P_{UPFC0}(\delta) \leq P_{UPFC0}(\delta) + \frac{V_2 V_{UPFCmax}}{X} \quad (3.34)$$

$$Q_{UPFC0}(\delta) - \frac{V_2 V_{UPFCmax}}{X} \leq Q_{UPFC0}(\delta) \leq Q_{UPFC0}(\delta) + \frac{V_2 V_{UPFCmax}}{X} \quad (3.35)$$

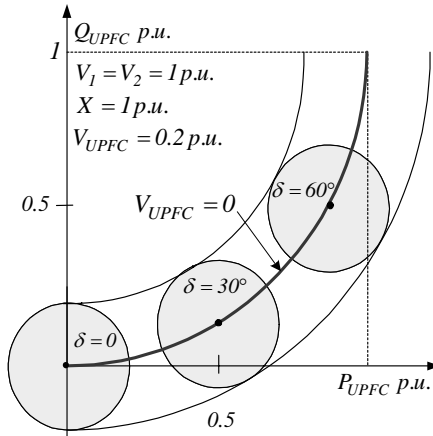


**Figure 3.22.**  $P$ - $Q$  relationship for a simple two machine system with a UPFC device at  $\delta=0^\circ$ ,  $\delta=30^\circ$ , and  $\delta=60^\circ$

In the sense of maximum influence on transmission characteristics and in consequence transient stability the UPFC controllable parameters (respectively  $V_{UPFC}$  and  $\sigma$ ) should be determined to achieve maximum impact on transmittable active power. Therefore the optimal parameters should be determined from the following equations:  $\partial P_{UPFC}/\partial V_{UPFC}=0$ ;  $\partial P_{UPFC}/\partial \sigma=0$ . Because the first equation doesn't have a solution thus the maximum impact is achieved if the  $V_{UPFC}$  parameter is set to its maximum value, determined by the device rating. However, the second dependency has a solution as follows

$$\frac{\partial P_{UPFC}}{\partial \sigma} = \frac{V_2 V_{UPFC}}{X_2} \cos(\delta + \sigma) = 0 \Rightarrow \sigma \rightarrow \left\{ -\delta \pm \frac{\pi}{2} \right\} \quad (3.36)$$

On the basis of above one can say that to achieve a maximal influence of the UPFC device on the transmitted power, the injected voltage  $\bar{V}_{UPFC}$  must be constrained to stay in quadrature with the sending end voltage  $\bar{V}_I$  (lead or lag sending end voltage). Therefore on the basis of Equation 3.32 and taking into consideration Equation 3.36 it is easy to draw the characteristics of transmitted power versus transmission angle, as in Figure 3.23. As one can see, the transmission characteristic is shifted up and down depending on the magnitude of the voltage of the UPFC. Comparison of the characteristics presented below with those achieved for STATCOM and SSSC shows clearly that UPFC device increases the transmitted active power by a fixed portion of the maximum transmitted power independently of angle  $\delta$ , however the STATCOM and SSSC can increase it only in a limited range, respectively  $\pi/2 \leq \delta \leq \pi$  and  $0 \leq \delta \leq \pi/2$ . In consequence the area representing the improvement to stability margin  $\int P_{UPFC} d\delta$

will be considerably larger for UPFC than for the previously described STATCOM and SSSC.

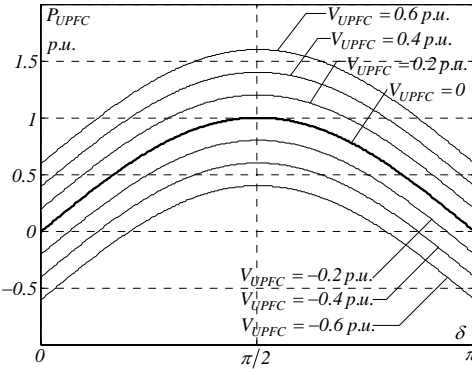


**Figure 3.23.** Basic transmission characteristics obtained for UPFC device; where  $X=1p.u.$ ,  $V_1=V_2=1p.u.$

The above presented capabilities of the UPFC to control the transmitted power can be utilized to increase the transient stability limit as well as to improve the dynamic stability. Once again let us consider the simple two generator system, introduced in Chapter 3.1 in Figure 3.7.a, but this time equipped with combined compensator. It is assumed that pre- and post-fault systems are the same; fault clearing occurs when the angle increases by 50% and with or without the combined compensation system carries the same power  $P_T$ . The Curves presented in Figure 3.24 and the data available in Table 3.3 (obtained in the same way as in Chapter 3.1) show that combined compensation can significantly increase the transient stability limit  $A_3$ . This is possible to achieve via phase angle regulation, see Equation 3.36.

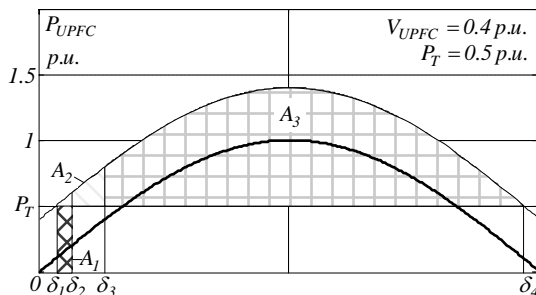


**Figure 3.24.**  $P$  vs.  $\delta$  curves to illustrate the dynamic behaviour for a two generator system with UPFC device; where  $X=1p.u.$ ,  $V_1=V_2=1p.u.$

**Table 3.3.** Parameters describing dynamic behaviour; in parentheses  $A_3$  values related to transient stability limit of the uncompensated line

Device	$\delta_1$	$\delta_2$	$\delta_3$	$\delta_4$	$A_1=A_2$	$A_3$
UPFC	0.10 p.u.	0.15 p.u.	0.33 p.u.	3.04 p.u.	0.02 p.u.	1.67 p.u. (3.2)

The combined compensation can also be useful to damp power oscillations. From the above, curves in Figure 3.25 show oscillations of the  $\delta$  angle, oscillations of the transmitted power and degree of the combined compensation. As one can see the combined compensator in the case of an accelerating generator should maximize

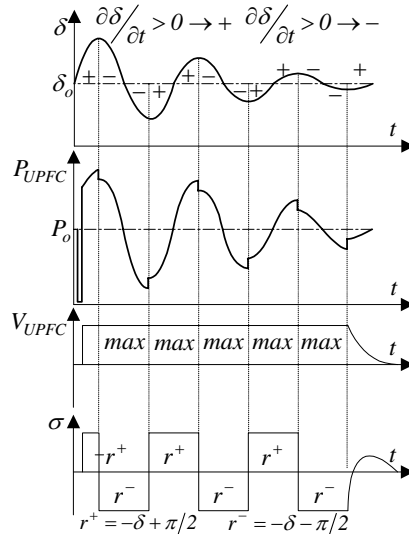


**Figure 3.25.** Power oscillations dumping by UPFC

and in the case of a decelerating generator minimize the transmittable electric power. This is possible to achieve by injecting in series with the line regulated voltage phasor with its maximum achievable rms value  $V_{UPFCmax}$ , determined by the device rating. Injected voltage for the sake of maximum influence on transmission characteristics should lead or lag the sending generator voltage  $\bar{V}_I$ , but must always be perpendicular to voltage  $\bar{V}_I$ . As one can see the oscillations for UPFC and for previously described devices are dumped in so called “bang-bang” manner, however this type of control is considered the most effective, particularly when large oscillations are encountered [10].

### 3.2.4 HVDC

The HVDC devices are the second technology suitable for flexible power flow control in AC transmission systems [36, 37]. They convert *AC* to *DC*, transport it over a *DC* line and then convert *DC* back to *AC*. Due to its controllability; a *DC* transmission has full control over transmitted power and thus ability to enhance transient and dynamic stability in associated *AC* networks. Furthermore *DC* transmission overcomes some of the problems associated with *AC* transmission:

- the distance of transmission has no influence on the power transfer in a *DC* line;
- even if converter stations require reactive power the *DC* line itself does not;

- in *DC* lines compensation to overcome the problems of line charging and stability limitations is not needed;
- only with the use of *DC* links is the asynchronous interconnection of two power systems is possible

The converters are a major part of the HVDC. They perform *AC/DC* and *DC/AC* conversion and provide the possibility to control the power flow through the HVDC link.

Two types of HVDC systems are available, conventional thyristor-based current-source converters, and the newer VSC systems [38, 39]. Conventional HVDC is a well-established technology, but it requires a source of reactive current at the end of the line. Second, the conventional converter itself is typically quite large. With recent advances in power electronics, VSC has become a new HVDC option. These converters use isolated gate bipolar thyristors (IGBTs) and allow independent control of both active and reactive current. These systems have somewhat higher losses but are more compact and also more flexible due to the reactive power capabilities and the fact that they do not require an independent *AC* source.

Since in both types of HVDC system there is a need to dimension the *AC/DC* and *DC/AC* converters on the full power exchanged between systems, which is their major disadvantage, the capital costs of the whole HVDC devices partially depend on the converter applied. On the basis of the above and additionally with regard to efficiency Silicon Controlled Rectifier (SCR) based converters are still competitive, especially for large capacities.

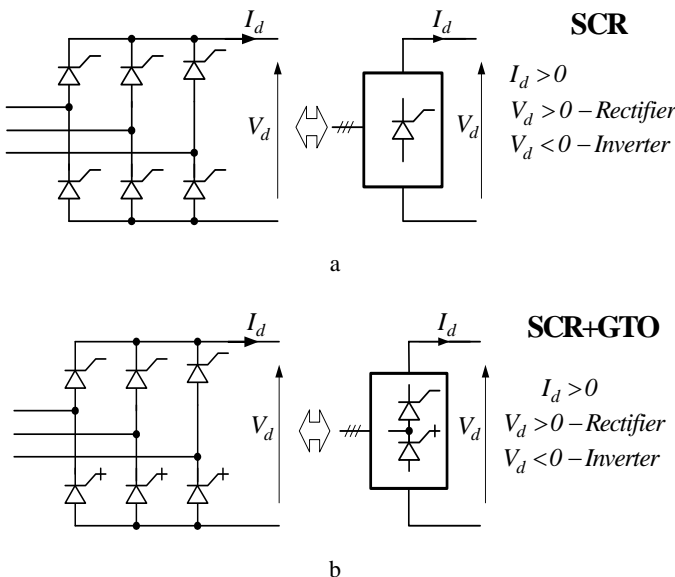


**Figure 3.26.** a. SCR based current source converter; b. SCR+GTO based current source converter

The basic module of a conventional HVDC converter is the three-phase, full-wave bridge circuit. In Figure 3.26.a such a circuit is given. Although one of the major limitations of the HVDC devices is their dependence on SCR thyristors, as mentioned above, the fact is that it is not possible to supply power to the consumers in a situation where there is a lack of the electric energy source. However, the consumers will not suffer any interruptions in delivery if the required reactive power is delivered to the converters. As a source of the required reactive power an Active Power Filter (APF) could be utilized [71, 75].

#### *Dimensioning of the Active Power Filters*

There was carried out an estimated dimensioning of the APF devices cooperating with thyristor based converters, on the assumption that at the point of common coupling  $P$  the APF has to produce sinusoidal voltage. The dimensioning was done considering the reactive power of the AC/DC converter and the reactive power of the load as well as distortion power resulting from the difference between the non-sinusoidal current components of the converter and load. Thus the APF apparent power is a sum of the earlier mentioned powers and losses in power. In Figure 3.27 APF cooperation with thyristor converters is given.

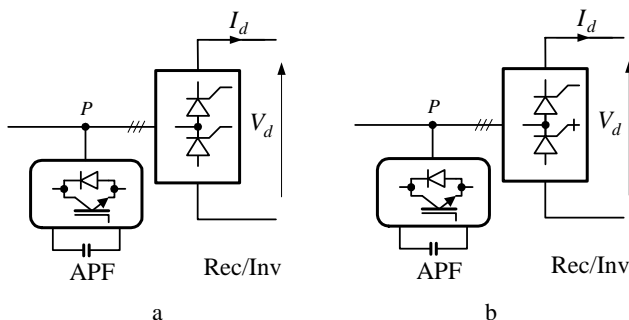


**Figure 3.27.** a. APF connected to the SCR converter; b. APF connected to the SCR+GTO converter

The below presented calculations refer to the linear resistive load and were carried out on the assumption that APF as well as 6-pulse AC/DC converter are ideal (the lossless APF produces the perfect wave shape sinusoidal voltage, in the lossless converter the DC side current  $I_d$  is constant). Working with above assumptions, for the SCR based converter the following relations are true

$$S_{APF} = \sqrt{S_{REC(SCR)}^2 - P_L^2} = 3 \cdot V_{rms} \cdot I_d \cdot \sqrt{\frac{2}{3} - \frac{6 \cdot \cos^2(\alpha)}{\pi^2}} \quad (3.37)$$

$$\frac{S_{APF}}{S_{REC(SCR)}} = \frac{S_{APF}}{S_{REC(SCR)}_{max}} = \sqrt{1 - \frac{9}{\pi^2} \cdot \cos^2(\alpha)} \quad (3.38)$$

Additionally for the SCR+GTO based converter when  $\alpha \in (\pi/2, 5\pi/6)$  the following relations are true

$$S_{APF} = \sqrt{S_{REC(SCR+GTO)}^2 - P_L^2} = 3 \cdot V_{rms} \cdot I_d \cdot \sqrt{\frac{2\alpha}{\pi} - 1 - \frac{6 \cdot \cos^2(\alpha)}{\pi^2}} \quad (3.39)$$

$$\frac{S_{APF}}{S_{REC(SCR+GTO)}} = \sqrt{1 - \frac{6}{\pi \cdot (2\alpha - \pi)} \cdot \cos^2(\alpha)} \quad (3.40)$$

$$\frac{S_{APF}}{S_{REC(SCR+GTO)_{max}}} = \sqrt{\frac{3\alpha}{\pi} - \frac{3}{2} - \frac{6 \cdot \cos^2(\alpha)}{\pi^2}} \quad (3.41)$$

and finally when  $\alpha \in (5\pi/6, \pi)$  the following dependencies are true

$$S_{APF} = \sqrt{S_{REC(SCR+GTO)}^2 - P_L^2} = 3 \cdot V_{rms} \cdot I_d \cdot \sqrt{\frac{2}{3} - \frac{6 \cdot \cos^2(\alpha)}{\pi^2}} \quad (3.42)$$

$$\frac{S_{APF}}{S_{REC(SCR+GTO)}} = \sqrt{1 - \frac{9}{\pi^2} \cdot \cos^2(\alpha)} \quad (3.43)$$

$$\frac{S_{APF}}{S_{REC(SCR+GTO)_{max}}} = \sqrt{1 - \frac{9}{\pi^2} \cdot \cos^2(\alpha)} \quad (3.44)$$

where  $S_{APF}$  – APF apparent power;  $S_{REC(SCR)}$  – SCR converter apparent power;  $S_{REC(SCR+GTO)}$  – SCR+GTO converter apparent power;  $P_L$  – DC active power emanating from the converter;  $V_{rms}$  – rms phase voltage;  $I_d$  – perfectly smoothed DC current;  $\alpha$  – SCR and SCR+GTO converters firing delay angle.

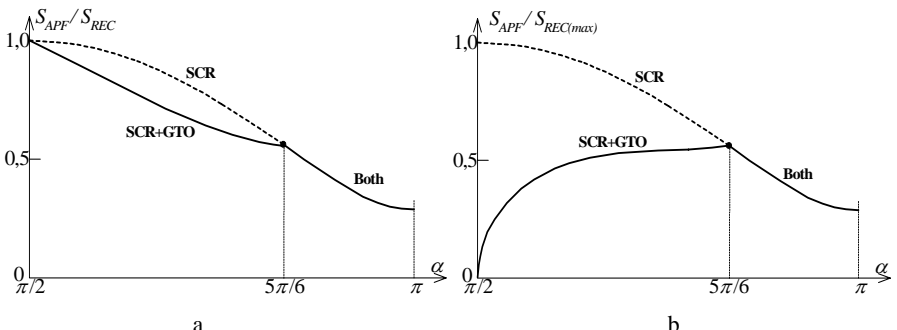


**Figure 3.28.** a. APF apparent power; b. APF maximum apparent power

Figure 3.28 illustrates the above presented relations. It is clearly evident that in the range  $5\pi/6 < \alpha < \pi$ , APF apparent powers are the same in both cases. On this basis it is possible to state that the SCR based converter equipped with an APF is a competitive solution, particularly for large firing delay angles  $\alpha$  and relatively small load reactive power (or if there is a reactive power compensator at the load side). In cases of loads with large  $\operatorname{tg}\varphi_L$  values and/or when an SCR converter's firing delay angle  $\alpha$  cannot be large (e.g., because of voltage adjustment), it is justifiable to apply the hybrid filter [137-139] instead of the APF. Hybrid filters possess one major advantage over APF, i.e., they generate capacitive reactive power [71].

#### *Provisional Experimental Results*

The capabilities of the SCR based converters equipped with APF to allow delivery of electric energy to the consumers even in the case of a lack of the electric energy source were confirmed experimentally, see Figure 3.29. The experimental results presented were obtained for the passive resistive load ca., 5kW, with the SCR rectifier supplied on its DC side by a current stabilizer.

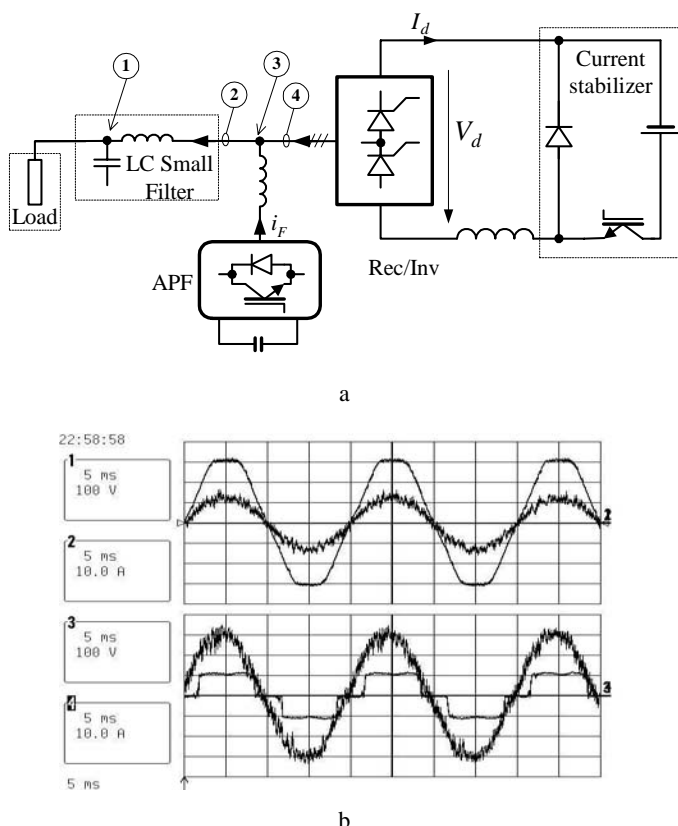


**Figure 3.29.** a. laboratory model; b. example experimental results;  $\alpha = 160^\circ$

Results of the experimental investigations completely confirm the assumed properties of this solution. The SCR rectifier equipped with an APF on its AC side allows the delivery of electric energy to consumers even when the passive resistive load is connected on the rectifier's AC side. Additionally APF isolates load from distortions produced by the rectifier and *vice versa* (secures sinusoidal load current).

In Figure 3.30 a generalized control algorithm is given. It consists of two parts. In the part dedicated to the APF, an algorithm produces signals allowing the APF to secure the stabilized sinusoidal voltage set at the point of common coupling  $P$ . In second part the gate control signals are determined, and used to delay the ignition of the converter valves and therefore to keep the DC voltage at the reference level  $V_d^*$ .

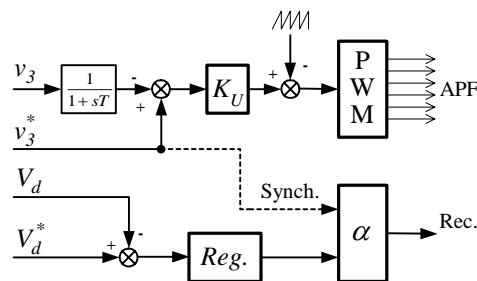


**Figure 3.30.** Simplified control algorithm

## Modern Power Electronics Systems for Transmission Control

Unified Power Flow Controllers can control active and reactive power transmitted through the transmission line. However, one of the disadvantages of this solution is the need to equip every transmission line with an independent arrangement. This feature, then, is not attractive from the economical point of view, especially in meshed systems.

The problem with power flow control in a number of separate lines can be solved by using so called Interline Power Flow Controllers [56-63]. Generally speaking the IPFC is a combination of two or more Static Synchronous Series Compensators which are coupled via a common *DC* link to facilitate bi-directional flow of active power between the *AC* terminals of the SSSCs. All the SSSC devices are controlled to provide independent series reactive compensation for the adjustment of active power flow in each line and to maintain the desired distribution of reactive power flow among the lines. However if IPFC arrangement consists only of SSSC devices, there is danger that reactive power flow control in one line will deteriorate distribution of reactive power flow in others. This happens because series connected converters cannot internally generate voltage in phase with the line current, in other words, cannot provide series active compensation (deliver active power to the transmission line) [56]. Therefore the active power needed to control reactive power in one transmission line must be provided from other lines, which leads to considerable reactive power growth. This problem can be overcome in many ways, for example, by increasing the size of the energy storage element (connecting batteries or super-capacitors), by connecting to the common *DC* element Distributed Resources and, finally, by connecting one, common for all series converters, STATCOM to provide shunt reactive compensation and supply or absorb the overall active power deficit of the SSSCs.

### 4.1 SSSC Based Interline Power Flow Controllers

The IPFC employs a number of series *DC/AC* converters, namely SSSC, each providing series compensation for a different line. However, standing alone SSSCs

are unable to control the reactive power flow and thus the proper load balancing of the line, thus in an IPFC, series VSCs are tied together at their *DC* link capacitors. Therefore converters do not only provide series reactive compensation but can also be controlled to supply active power to the common *DC* link from its own transmission line or absorb active power from the *DC* link to its own transmission line (an asynchronous tie) – series VSCs provide reactive power flow. Thus IPFC power flow control capability is the same as a UPFC device. The only difference is that the active power demand of a given converter is compensated by another series converter from another line instead of shunt converter as in UPFC.

The VSC uses forced-commutated power electronic devices (GTOs, IGBTs or IGCTs) to synthesize an injected series voltage from a *DC* voltage source. Two VSC technologies can be used:

- VSC using GTO-based square-wave converters and special interconnection transformers. Typically four three-level converters are used to build a 48-step voltage waveform. Special interconnection transformers are used to neutralize harmonics contained in the square waves generated by individual inverters;
- VSC using IGBT-based Pulse Width Modulation (PWM) converters. This type of converter uses PWM technique to synthesize a sinusoidal waveform from a *DC* voltage with a typical chopping frequency of a few kilohertz. Harmonics are cancelled by connecting filters at the AC side of the VSC

The general structure of an IPFC is shown in Figure 4.1. For simplicity the transmission system consists of two lines. Line 1 is represented by reactance  $X_1$ , sending end bus voltage  $\bar{V}_1$ , receiving end bus voltage  $\bar{V}_{21}$  and series injected voltage  $\bar{V}_{IPFC1}$ . Similarly, Line 2 is represented by  $X_2$ , and voltages  $\bar{V}_1$ ,  $\bar{V}_{22}$  and  $\bar{V}_{IPFC2}$ .

As explained above, an IPFC series converter injects controllable voltage, for given Line 1,  $\bar{V}_{IPFC1}$ . The injected series voltage can be decomposed into two components:  $\bar{V}_{IPFC1q}$ , in quadrature and  $\bar{V}_{IPFC1p}$ , in phase with the line current. The first component, produced internally by the converter provides series reactive compensation and is proportional to the reactive power  $Q_{\Sigma l}$  exchanged between series converter and line [62]

$$Q_{\Sigma l} = \text{Im}\{\bar{V}_{IPFC1}\bar{I}_l^*\} = V_{IPFC1q}I_l \quad (4.1)$$

where  $\bar{I}_l^*$  is the conjugate of  $\bar{I}_l$ .

To provide series active compensation, the series converter has to produce the second component in phase with the line current, proportional to the active power  $P_{\Sigma l}$  exchanged with the transmission line. The active power exchanged with the Line 1 is given by the following equation [62]

$$P_{\Sigma l} = \text{Re}\{\bar{V}_{IPFC1}\bar{I}_l^*\} = V_{IPFC1p}I_l \quad (4.2)$$

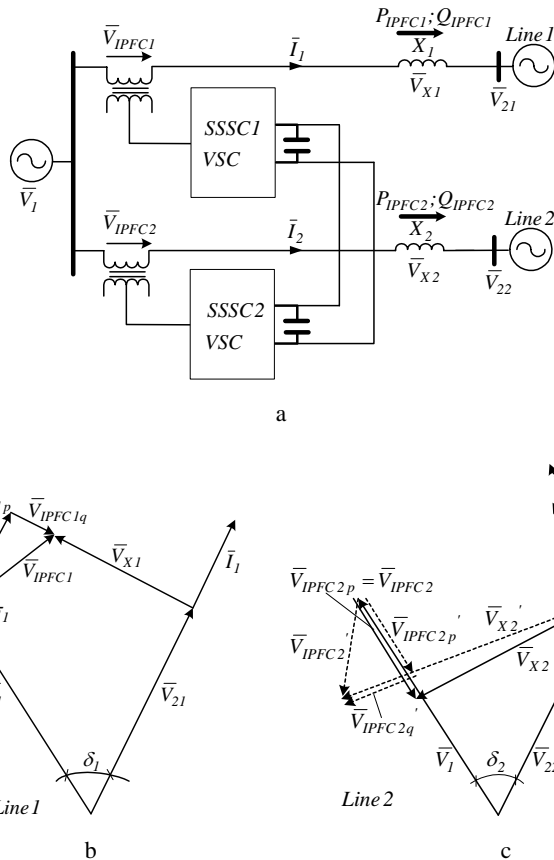


**Figure 4.1.** a. single line diagram of an IPFC with two series VSCs; b. possible vector diagram for Line 1; c. possible vector diagram for Line 2

However this power cannot be internally produced by the series converter, it has to be absorbed (or supplied) through the *DC* tie from (or to) the other transmission lines. Because to maintain a constant *DC* voltage the net active power through the *DC* link has to be zero (neglecting losses), thus the active power supplied by one of the transmission lines must be equal to that injected into the other. Therefore the operating constraint representing the active power exchange between or among the two series converters (Figure 4.1) via the common *DC* link is given by [56, 61, 62]

$$|P_{\Sigma 1}| = |P_{\Sigma 2}| \quad (4.3)$$

Phasor diagrams in Figure 4.1 mirror the situation when transmission Line 1 has to be controlled by the SSSC 1 somehow to secure only active power flow to the receiving end bus. Assuming that the series converter SSSC 2 is secondary in relation to SSSC 1 and thus has to maintain a constant *DC* voltage (has to

exchange with the *DC* tie required active power), one can see that in transmission Line 2 it is possible to both: satisfy active power demands and control, with limited degree of freedom, its own reactive power flow (degree of freedom depends on number of transmission lines participating in satisfying active power demands of their master and/or on parameters of transmission lines)

$$\left| I_1 V_{IPFCp1} \right| = \left| I_2 V_{IPFCp2} \right| = \left| I_l V_{IPFCp2} \right| \quad (4.4)$$

Let's determine the load flow equation in  $n$  ( $n=1, 2, \dots, N$ ) transmission line system equipped with an IPFC device. The following voltage phasors can be defined

$$\bar{V}_l = V_l \cos \delta_n + j V_l \sin \delta_n \quad (4.5)$$

$$\bar{V}_{2n} = V_{2n} \quad (4.6)$$

$$\bar{V}_{IPFCn} = V_{IPFCn} \cos(\delta_n + \sigma_n) + j V_{IPFCn} \sin(\delta_n + \sigma_n) \quad (4.7)$$

where  $\delta_n \angle (\bar{V}_l, \bar{V}_{2n})$ ;  $\sigma_n \angle (\bar{V}_l, \bar{V}_{IPFCn})$ .

After simple transformations, equations on active and reactive powers transmitted through  $n^{th}$  transmission line are as follows [61, 62]

$$P_{IPFCn} = \frac{V_l \cdot V_{2n}}{X_n} \sin(\delta_n) + \frac{V_{IPFCn} \cdot V_{2n}}{X_n} \sin(\delta_n + \sigma_n) \quad (4.8)$$

$$Q_{IPFCn} = \frac{V_{2n}^2}{X_n} - \frac{V_l \cdot V_{2n}}{X_n} \cos(\delta_n) - \frac{V_{IPFCn} \cdot V_{2n}}{X_n} \cos(\delta_n + \sigma_n) \quad (4.9)$$

Next, the active and reactive powers injected into the  $n^{th}$  transmission line by the SSSC voltage sources are given by, respectively [61, 62]

$$P_{\Sigma n} = \frac{V_{IPFCn} \cdot V_{2n}}{X_n} \sin(\delta_n + \sigma_n) - \frac{V_l \cdot V_{IPFCn}}{X_n} \sin(\sigma_n) \quad (4.10)$$

$$Q_{\Sigma n} = \frac{V_{IPFCn}^2}{X_n} + \frac{V_l \cdot V_{\Sigma n}}{X_n} \cos(\sigma_n) - \frac{V_{IPFCn} \cdot V_{2n}}{X_n} \cos(\delta_n + \sigma_n) \quad (4.11)$$

From Equation 4.10 it is obvious that location of an IPFC does not affect transmission characteristics, and dependency  $\partial P_{IPFCn} / \partial X_{In} / X_{2n} = 0$  (where  $X_{In} + X_{2n} = X_n$ ) does not have a solution, therefore during investigations it will be assumed that the IPFC device is positioned at the system terminals.

Considering Equations 4.8 to 4.11 for a given magnitude of voltage injected in series, the relationship between the active and reactive powers and the angle of the injected voltage is plotted in Figure 4.2.

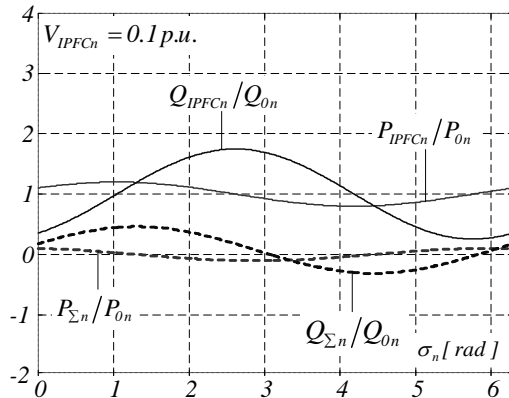


**Figure 4.2.** Changes of the active and reactive powers with the rotation of the injected series voltage;  $P_{0n} = P_{IPFCn}(V_{IPFCn} = 0) = 0.5 \text{ p.u.}$ ;  $Q_{0n} = Q_{IPFCn}(V_{IPFCn} = 0) = 0.13 \text{ p.u.}$ ;  $X_n = 1 \text{ p.u.}$ ;  $\delta_n = \pi/6$ ;  $V_I = V_{2n} = 1 \text{ p.u.}$

In the above figure it is visible that the series injected voltage phasor  $\bar{V}_{IPFCn}$  rotation with angle  $\sigma_n$  from 0 to  $360^\circ$  modulates in a sinusoidal manner both active and reactive power transmitted to the receiving end bus. Additionally in sinusoidal manner there are modulated, around zero, active power  $P_{\Sigma n}$  ( $P_{\Sigma n} > 0$  means power absorbed from and  $P_{\Sigma n} < 0$  supplied to the DC link), and around  $(V_{IPFCn}^2/(1-\cos(\delta_n))$ ) reactive power  $Q_{\Sigma n}$  produced by the series converter. To gain a better view of the relations between individual parameters describing the series voltage source in  $n^{th}$  transmission line and active and reactive powers, presented in the next page are the 3-D curves (Figure 4.3).

From these figures the observation can be made that not only the phasor of the injected voltage but also its amplitude influences active power produced by the series converter. Therefore  $\bar{V}_{IPFCn}$  voltage must be controlled in order to secure an active power balance in the DC link, keeping in mind that its maximum achievable value  $V_{IPFCn \ max}$  is determined by the device rating. Rotation of the series injected voltage phasor with its maximum achievable value  $V_{IPFCn \ max}$ , from 0 to  $360^\circ$  determines the control area within the boundary circle [62].

$$(V_{IPFCn} \cos \sigma_n)^2 + (V_{IPFCn} \sin \sigma_n)^2 = V_{IPFCn \ max}^2 \quad (4.12)$$

as it is in Figure 4.4.

Inspection of the figures shows that if the series injected voltage is controlled to keep its end on a line that is parallel to the voltage drop across the line impedance  $X_n$  (so called “voltage compensation line” [57]), then there is produced a constant real power demand  $P_{\Sigma n} = \text{const}$ , independent of  $\sigma_n$ . Therefore moving converter’s

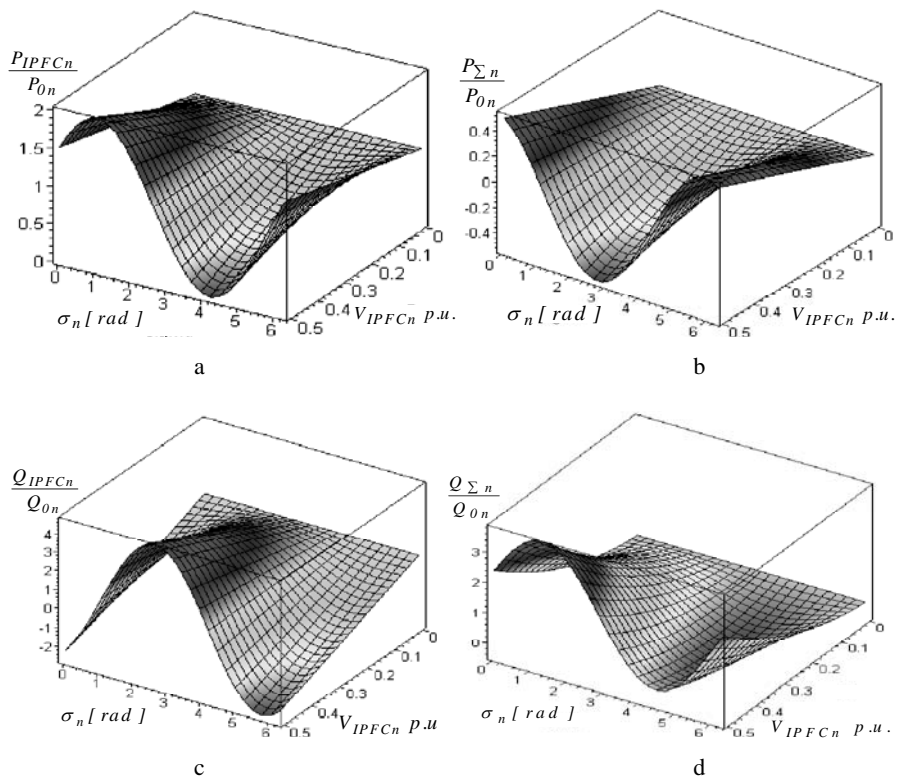


**Figure 4.3.** 3-D shapes representing changes of the active and reactive powers with the rotation of the injected series voltage: a. active power transmitted through transmission line; b. active power injected into transmission line; c. reactive power transmitted through transmission line; d. reactive power injected into transmission line;  $V_I = V_{2n} = 1p.u.$ ,  $X_n = 1p.u.$ ,  $\delta_n = \pi/6$ ;  $P_{0n} = P_{IPFCn}(V_{IPFCn} = 0) = 0.5 p.u.$   $Q_{0n} = Q_{IPFCn}(V_{IPFCn} = 0) = 0.13 p.u.$

operating point from one “voltage compensation line” to another, it is possible to change its real power demands. Considering two transmission lines equipped with IPFC, where an arbitrary series converter in line 1 is treated as a master in relation to the series converter in line 2, in order to satisfy the master converter’s active power demands, which operates along a selected “voltage compensation line”, the slave converter has to operate along a complementary “voltage compensation line” with respect to the line defining zero active power demand ( $P_{\Sigma n}=0$ ). Only then will the net active power through the DC link (neglecting losses) be zero and the DC voltage constant. From the figures the observation can be made that the complementary lines of the two converters must be in the opposite direction. This is why the IPFC device control algorithm is based on active power balance among converters to maintain the DC link voltage. If there is an  $n$  transmission line system with an IPFC device, then  $n-1$  lines can be treated as master and the  $n^{th}$  line left is made to compensate the active power demand of the other  $n-1$  lines to maintain the

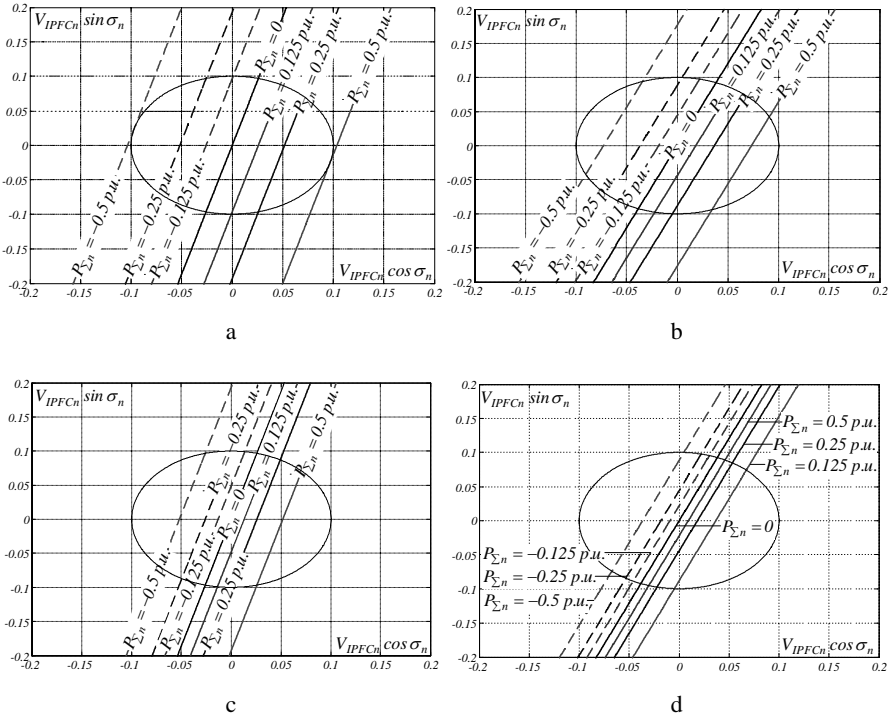


**Figure 4.4.** Variation of the series injected voltage: a.  $\delta_n = \pi/6$ ,  $X_n = 1$  p.u.; b.  $\delta_n = \pi/4$ ,  $X_n = 1$  p.u.; c.  $\delta_n = \pi/6$ ,  $X_n = 0.5$  p.u.; d.  $\delta_n = \pi/4$ ,  $X_n = 0.5$  p.u.; x axis – component in phase with the sending end voltage, y axis – component perpendicular to the sending end voltage;  $V_I = V_{2n} = 1$  p.u.;  $V_{IPFCn max} = 0.1$  p.u.

DC link voltage. The control algorithm details are described in [1].

Additionally it is possible to claim that maximum achievable real power exchanged with other transmission lines, limited by the converter's rating, strongly depends on transmission angle  $\delta_n$  and transmission line reactance  $X_n$ . This is true because in lines with relatively large  $\delta_n$  angle or low  $X_n$  impedances the line current increases and in consequence  $P_{\Sigma n}$ .

The above discussion means also that within a given control area, determined by the maximum achievable value  $V_{IPFCn max}$ , only in master transmission lines is it possible to control the reactive power flow independent of the real power flow control. In other transmission lines (slave) independent control is also possible to achieve, but only with a limited degree of freedom, while the operating point of the slave converter is shifted along a selected "voltage compensation line".

To estimate the influence of the transmission parameters on degree of freedom Figure 4.5, for three different active power demands  $P_{\Sigma n}$  and three different power angles  $\delta_n$ , shows plots of the transmitted active  $P_{IPFCn}$  power as a function of the phase angle  $\sigma_n$ . Additionally in Figure 4.5 the sinusoidal curve defines the control area, determined by transmission line parameters and  $V_{IPFCn max}$ .

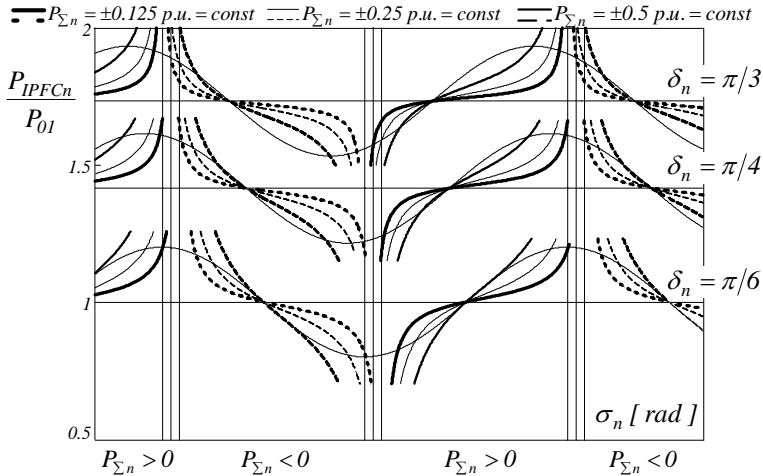


**Figure 4.5.** Changes of the transmitted active  $P_{IPFCn}$  power as a function of the phase angle  $\sigma_n$ ;  $V_I = V_{2n} = 1$  p.u.,  $X_n = 1$  p.u.,  $V_{IPFCn \max} = 0.1$  p.u.

Inspection of the curves in Figure 4.5 clearly shows that degree of freedom, limited by the sinusoidal curve, strongly depends on demanded transmission angle  $\delta_n$  (transmittable through given line active power). With decreasing  $\delta_n$  angle the line current decreases and in consequence the maximum achievable real power which the series converter can exchange with other transmission lines also decreases and simultaneously decreases the range of active and reactive power compensation.

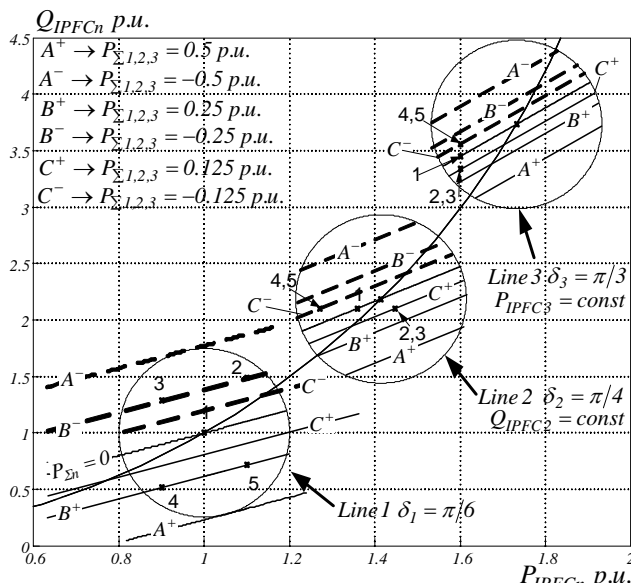


**Figure 4.6.** Behavior examples of an IPFC compensating three independent transmission lines; 1, 2, 3, 4, 5 – operating points

Additionally Figure 4.6 presents results of the theoretical investigations for an IPFC compensating three independent transmission lines. During investigations all lines were assumed identical:  $V_I=1p.u.$ , each line has equal receiving end bus voltage  $V_n=1p.u.$ , and reactance  $X_n=1p.u.$ , however different transmission angle  $\delta_n$  respectively  $\pi/6$ ,  $\pi/4$  and  $\pi/4$ . In addition the converter in Line 1 was treated as master.

Studying the results presented in Figure 4.6 one can say that while slave converters secure active power balance in the DC link there is still a relatively large range for active and reactive power compensation. For example, reactive power compensation range for the converter in transmission Line 2 at operating point 5 is about  $0.25p.u.$ , while for the uncoupled device it is about  $0.27p.u..$  Responsibility for this are the relatively large transmission angles of the slave converters in relation to the master's transmission angle (generally speaking large active powers transmitted through slave lines in relation to active powers transmitted through master lines).

In the sense of maximum influence on transmission characteristics and consequently transient stability the IPFC controllable parameters (for given line  $n$ , respectively  $V_{IPFCn}$  and  $\sigma_n$ ) should be determined to achieve maximum impact on transmittable active power. Therefore the optimal parameters should be determined from the following equations:  $\partial P_{IPFCn} / \partial V_{IPFCn} = 0$ ;  $\partial P_{IPFCn} / \partial \sigma_n = 0$ . Because the first equation doesn't have a solution the maximum impact is achieved if the  $V_{IPFCn}$  parameter is set to its maximum value,  $V_{IPFCn\ max}$ , determined by the device rating. However the second dependency has a solution as follows

$$\frac{\partial P_{IPFCn}}{\partial \sigma_n} = \frac{V_{2n} V_{IPFCn}}{X_n} \cos(\delta_n + \sigma_n) = 0 \Rightarrow \sigma_n \rightarrow \left\{ -\delta_n \pm \frac{\pi}{2} \right\} \quad (4.13)$$

On the basis of the above one can say that to achieve a maximal influence of the IPFC device on the transmitted power, the injected voltage  $\bar{V}_{IPFCn}$  must be constrained to stay in quadrature with sending end voltage  $\bar{V}_I$  (lead or lag sending end voltage). Therefore on the basis of Equation 4.8 and taking into consideration Equation 4.13 it is evident that the transmission characteristics are the same as for the UPFC device; their up or down displacement depends on exchanged active power.

The above presented capabilities of the IPFC to control the transmitted power can be utilized to increase the transient stability limit as well to improve the dynamic stability. Let us consider two, two-generator systems, but this time equipped with IPFC system.

It is assumed that pre- and post-fault systems are the same; fault clearing in every transmission line occurs when the angle increases by 50% and with or without the IPFC every line carries the same power  $P_{T1}=P_{T2}=0.5\ p.u..$  Curves presented in Figure 4.7 and the data available in the Table 4.1 (obtained in the same way as in Chapter 3.1) show that for given parameters, the series converter in the master transmission line can significantly increase the transient stability limit  $A_3$  however the second transmission line in spite of a series converter will be

unstable, after a fault occurs. This happens because to maintain *DC* link voltage the slave converter has to work at lower transmission characteristics.

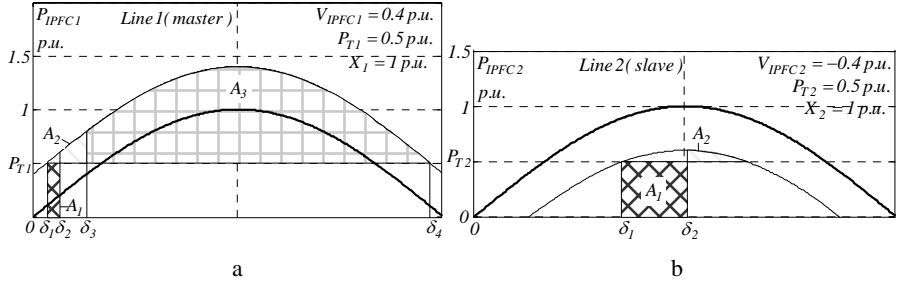


**Figure 4.7.** Basic transmission characteristics obtained for IPFC device compensating two transmission lines: a. master; b. slave

Improvement of the transient stability in the master as well as in slave transmission lines is possible to achieve choosing as the slave the line with relatively larger than its master maximum transmittable active power (line with larger transmission angle or lower reactance). Transmission lines with larger transmittable active power possesses a larger active power compensation range, see Figure 4.6. For example, in the above discussed transmission system, where both converters are controlled to get the maximum influence on transient stability Equation 4.13, on the basis of Equation 4.10, the dependency on the active power exchanged between the two series converters is as follows

$$\frac{V_{IPFC1}}{X_1} (V_{21} - V_1 \cos(\delta_1)) = \frac{V_{IPFC2}}{X_2} (V_{22} - V_1 \cos(\delta_2)) \quad (4.14)$$

Additionally considering Equation 4.8 it is possible to depict  $V_{IPFC2}$  as a function of  $P_{IPFC2}/P_{IPFC1}$  ratio:  $V_{IPFC2} = \mathfrak{J}_1/(P_{IPFC2}/P_{IPFC1})\mathfrak{J}_2 + \mathfrak{J}_3$  (where  $\mathfrak{J}_{1,2,3}$  - constants). In the sense of minimize  $|V_{IPFC2}|$  (to work at the highest possible transmission characteristic), ratio  $P_{IPFC2}/P_{IPFC1}$  should be chosen so as to maximize the denominator  $\Delta V_{IPFC2}$  in  $V_{IPFC2}$ . Calculations have shown that the equation  $\partial \Delta V_{IPFC2} / \partial (P_{IPFC2}/P_{IPFC1}) = 0$  does not have a solution and thus to minimize  $V_{IPFC2}$ , the  $P_{IPFC2}/P_{IPFC1}$  ratio should be set to its maximum achievable value, thus the following condition should be fulfilled  $P_{IPFC2} > P_{IPFC1}$ .

Assuming that transmission line 2 (slave) carries more active power in relation to its master ( $\delta_1 = \delta_2$ ,  $X_1 > X_2$ ,  $V_{21} = V_{22}$ ), thus the following relation between amplitudes of the injected series voltages is valid

$$V_{IPFC2} = \frac{X_2}{X_1} V_{IPFC1} \quad (4.15)$$

On the basis of the above one can tell that the slave converter maintains a *DC* link voltage without the need to work at low transmission characteristics and

therefore simultaneously secures the transient stability limit of its own line. The results presented in Table 4.1 seem to confirm this.

The IPFC device can also be useful to damp power oscillations. From the above, curves in Figure 4.8 show oscillations of the  $\delta_n$  angle, oscillations of the transmitted power and degree of the compensation. As one can see the IPFC in the case of an accelerating generator should maximize and in the case of a decelerating generator minimize the transmittable electric power. This is possible to achieve injecting in series with the line regulated voltage phasor its maximum achievable value  $V_{IPFCn \ max}$ , determined by the device rating. Injected voltage for the sake of maximum influence on transmission characteristics should lead or lag the sending generator voltage  $\bar{V}_I$ , but must always be perpendicular to voltage  $\bar{V}_I$ . It seems

**Table 4.1.** Parameters describing dynamic behaviour; in parentheses  $A_3$  values related to transient stability limit of the uncompensated line

Device	$\delta_I$	$\delta_2$	$\delta_3$	$\delta_4$	$A_I$	$A_3$
$V_I = V_{2I} = 1 \text{ p.u.}, X_I = 1 \text{ p.u.} \Rightarrow V_{IPFCI} = 0.4 \text{ p.u.}$						Line 1
IPFC	0.10 p.u.	0.15 p.u.	0.33 p.u.	4.04 p.u.	0.02 p.u.	1.67 p.u. (4.2)
	$V_I = V_{22} = 1 \text{ p.u.}, X_2 = 1 \text{ p.u.} \Rightarrow V_{IPFC2} = -0.4 \text{ p.u.}$					
1.12 p.u.    1.68 p.u.    -    -    0.28 p.u.    -						
$V_I = V_{22} = 1 \text{ p.u.}, X_2 = 0.5 \text{ p.u.} \Rightarrow V_{IPFC2} = -0.2 \text{ p.u.}$						Line 2
0.46 p.u.    0.70 p.u.    0.91 p.u.    2.67 p.u.    0.11 p.u.    1.42 p.u. (2.7)						

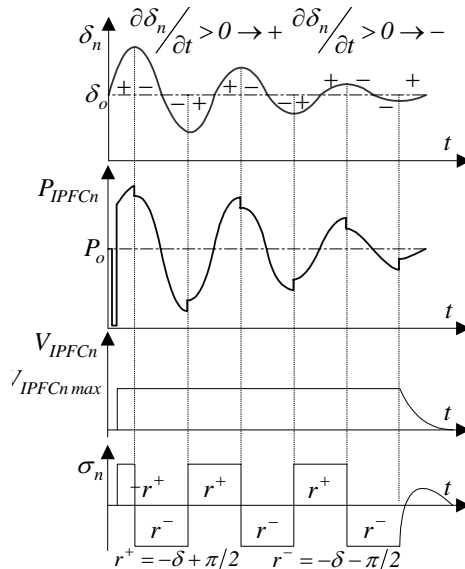


**Figure 4.8.** Power oscillations dumping by IPFC

that slave transmission lines with larger, in relation to its master, maximum transmittable active power and in consequence bigger active power compensation

range should have improved oscillation dumping capabilities. On the basis of the above discussion it is possible to draw a conclusion that from the point of view of improvement of transient and dynamic stability and distribution of the reactive power flow, the lines selected for the slave should be larger in relation to the maximum transmittable active power of the master.

Once again the oscillations should be dumped in so called “bang-bang” manner, because this type of control is considered the most effective, particularly when large oscillations are encountered [10].

## 4.2 Combined Interline Power Flow Controllers

The general form of a combined IPFC is shown in Figure 4.9 [56, 61]. It employs a number of series DC/AC converters, namely SSSC, each providing series active and reactive compensation for a different transmission line and one shunt DC/AC converter, namely STATCOM, coupled to the IPFC’s common DC link. The shunt converter provides shunt reactive compensation and supplies or absorbs the overall active power deficit of the combined SSSC’s and in this way keeps the voltage across the DC link constant. Therefore the combined IPFC device can control a total of five power system quantities including the voltage magnitude at bus and independent active and reactive power flow of the transmission lines. In other words the combined IPFC devices possess all the properties of the UPFC arrangements but extend the concepts of power flow control to multilane.

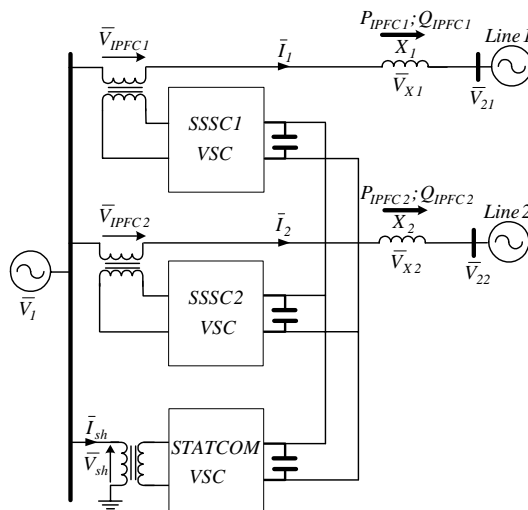


**Figure 4.9.** Single line diagram of a combined IPFC

This scheme requires then a rigorous maintenance of the overall power balance at the common DC terminal. The operating constraint representing the active power exchange among the converters via the common DC link is [62]

$$P_{sh} - \sum_{n=1}^N P_{\Sigma n} = 0 \quad (4.16)$$

where  $P_{\Sigma n}$  – active power supplied/absorbed by the series VSC in  $n^{th}$  transmission line ( $n \in 1, 2, \dots, N$ );  $P_{sh} = Re\{V_{sh}\bar{I}_{sh}^*\}$  – active power supplied/absorbed by the shunt VSC.

Additionally when the IPFC parameters are controlled in the sense of maximum influence on transmission characteristics and consequently on transient stability the above dependency can be rewritten

$$P_{sh} = \sum_{n=1}^N \frac{V_{IPFCn}}{X_n} (V_{2n} - V_I \cos(\delta_n)) \quad (4.17)$$

Taking into account an IPFC as shown in Figure 4.9 and Equation 4.16 or Equation 4.17, series VSC in every transmission line can control freely the power flow at the receiving end bus  $P_{IPFCn}, Q_{IPFCn}$ . The only limitations are series and parallel VSCs' ratings. However in the situation where parallel VSC cannot secure Equation 4.16 or Equation 4.17 because of limitations related to its rating, one or a group of the series VSCs can be designated as the primary where each of them has two degrees of control freedom: active and reactive power flow control. The remaining one or group of the series VSCs which has only one degree of control freedom can be used to compensate the active power demand of the primary VSCs and consequently to maintain the DC link voltage. However one should keep in mind that degree of freedom very much depends on the ratio  $P_{IPFCslave}/P_{IPFCmaster}$ .

As the operating points of the primary VSCs are random, *i.e.*, some of them absorb active power from the DC link while the remaining VSCs deliver at the same time, the power rating of the secondary VSCs may not necessarily be large, thus keeping the rating of the IPFC at a reasonable value which also makes its practical application feasible.

#### *Control Structure*

According to the above discussion, every series VSC in order to control power flow has to “produce” a set of amplitude and phase controllable instantaneous voltages  $v_{IPFCn}$ . Thus, series injected controllable voltage in a given transmission line forces the flow of appropriate current and consequently active and reactive power desired at the receiving end bus. Let us determine the reference current  $i_{na}^{ref}$  (for phase a) which allows the flow through the  $n^{th}$  transmission line the desired powers  $P_{IPFCna}^{ref}$  and  $Q_{IPFCna}^{ref}$ .

On the basis of known equations, one can write [61]

$$P_{IPFCna}^{ref} = V_{2na} \cdot I_{na} \cdot \cos \varphi_{na} \quad (4.18)$$

$$Q_{IPFCna}^{ref} = V_{2na} \cdot I_{na} \cdot \sin \varphi_{na} \quad (4.19)$$

where  $\varphi_{na} \angle (\bar{V}_{2na}, \bar{I}_{na})$ .

According to the above one can define two current components

$$I_{na} \cdot \cos \varphi_{na} = P_{IPFCna}^{\text{ref}} / V_{2na} \quad (4.20)$$

$$I_{na} \cdot \sin \varphi_{na} = Q_{IPFCna}^{\text{ref}} / V_{2na} \quad (4.21)$$

The first component, Equation 4.20, accounts for the instantaneous active power and the second current component, Equation 4.21, for the reactive power flow. In accordance with the above an overall control structure, showing the reference current determination, is presented in Figure 4.10 [61].

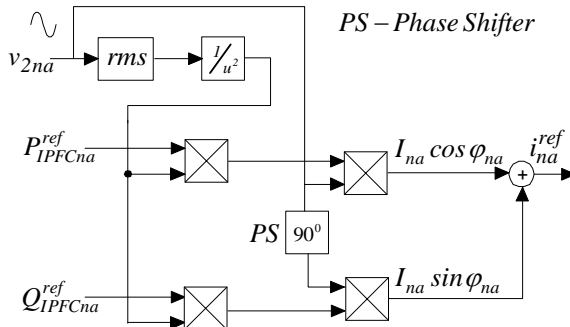


**Figure 4.10.** The reference current controller ( $n^{\text{th}}$  transmission line, phase a)

To determine the series injected voltage  $v_{IPFCna}^{\text{ref}}$  ( $n^{\text{th}}$  transmission line, phase a) which forces the flow of the reference current  $i_{na}^{\text{ref}}$  and consequently the desired active  $P_{IPFCna}^{\text{ref}}$  and reactive  $Q_{IPFCna}^{\text{ref}}$  power the circuit presented in Figure 4.11 will be useful.

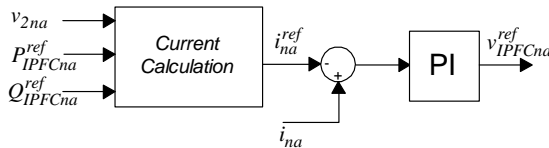


**Figure 4.11.** The series injected voltage controller ( $n^{\text{th}}$  transmission line, phase a)

An overall control design for an IPFC is proposed and shown in Figure 4.12, which for simplicity sake only shows the control design for two transmission lines where the shunt converter secures only constant DC link voltage [61]. For clarity, only the most important features are shown in this figure, while less important signal processing and limiting functions have been omitted. It should be noted that data for the receiving end bus voltage and current in every transmission line, together

with *DC* link voltage, are needed for this control design. If the receiving end bus is a local bus and the currents and voltage vectors are local signals, then, theoretically, there is not any time delay in getting these signals.

Because shunt VSC (STATCOM) secures constant *DC* link voltage, both series VSCs can almost freely (SSSC's operation limit is related only to its rating) control power at both receiving end busses. Therefore controlled voltages  $V_{IPFC_n}$  injected by both SSSCs are determined through comparison currents, as was described earlier in this section (see Figure 4.11).

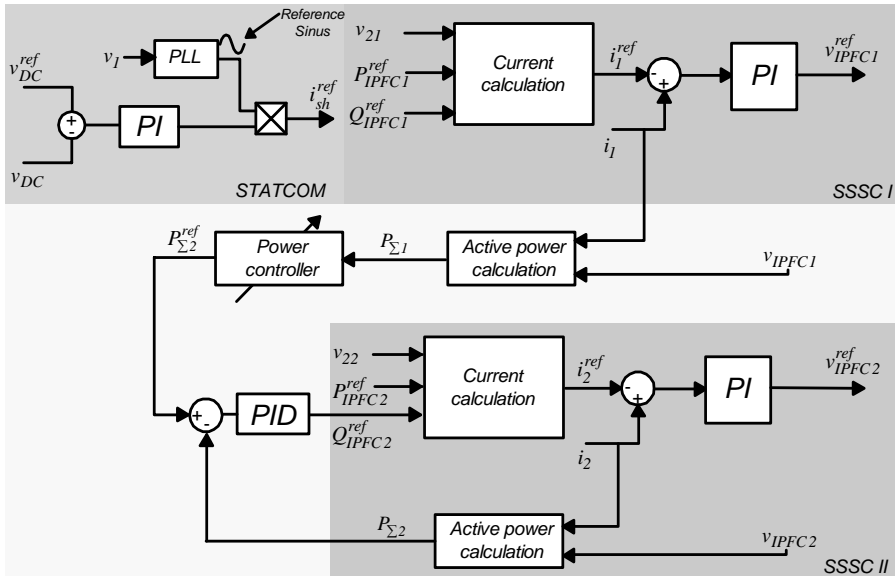


Figure 4.12. An overall control design for combined IPFC (phase a)

However it will not be possible to secure the series active compensation in a situation when the active power demand from both series VSCs exceeds the rating of the STATCOM. In this case, the reactive power flow of both transmission lines will be sub-optimized at the nearest value from the reference input along a particular reactive power compensation line.

The above problem, among others, can be solved by a so-called “power controller”. Assuming that transmission Line 2 is secondary in relation to Line 1, to secure in prime Line 1 series active compensation, the “power controller” has to equalize the active power demands of the primary VSC between STATCOM and secondary series VSC. In the simplest situation when the “power controller” transfer function is set to be “ $I$ ”, the primary VSC's active power demands will be secured exclusively by the slave VSC. But in the case of many transmission lines the “power controller” transfer function should be selected in accordance with  $P_{IPFCslave}/P_{IPFCmaster}$ . The biggest weight, *i.e.*, the biggest contribution to the active power in the *DC* link, should be given to transmission lines with the biggest  $P_{IPFCslave}/P_{IPFCmaster}$  ratio.

### Computer Simulations

In Figure 4.13, the SSSC's active and reactive power control capabilities, where a constant DC link voltage is maintained by the STATCOM (shunt connected VSC), were investigated. Simulation parameters are gathered in Table B.1 (Appendix B).

For clarity the compensating lines show SSSC's active and reactive power flow control capabilities with constant active power  $P_{\Sigma n}$  exchanged with DC link (the DC link simulation model is presented in Appendix A). Additionally the dashed circle shows SSSC's operation limit related to its power rating. As one can see SSSC allows the control of the active and reactive power delivered to the receiving end bus even without the necessity of exchanging active power through the DC link  $P_{\Sigma i}=0$ , or with constant demand for active power  $P_{\Sigma n}$ .

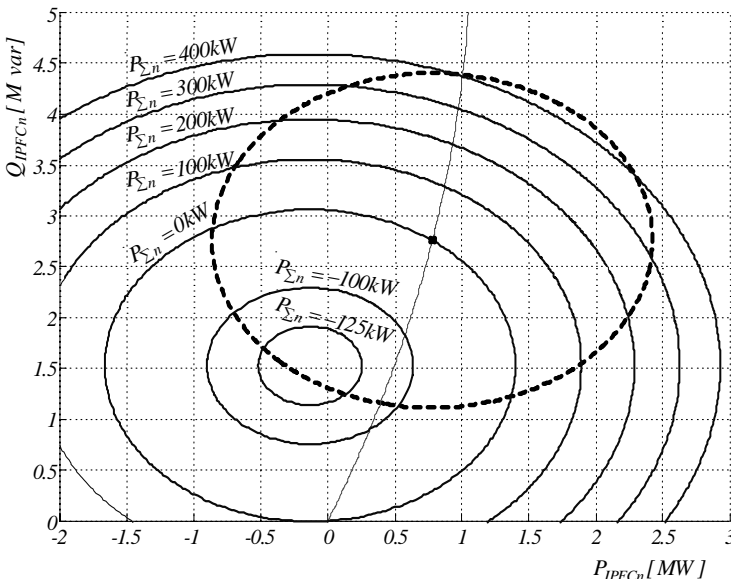
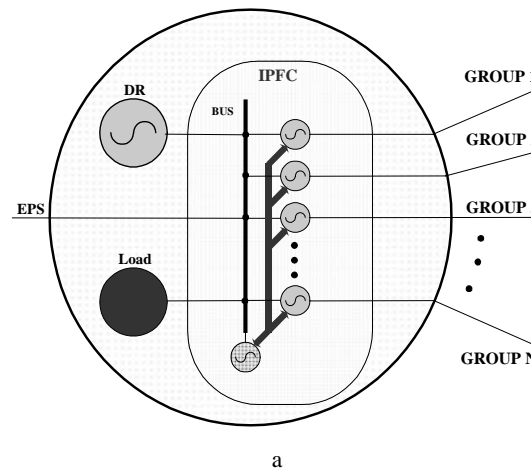


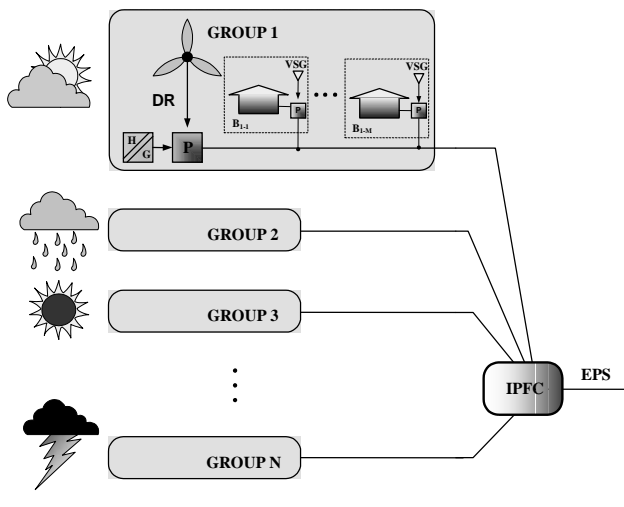
**Figure 4.13.** SSSC's power flow control capability with constant DC link voltage maintained by the STATCOM

### IPFC Feasible Applications

Figure 4.14 introduces the idea of utilization of an IPFC device to connect groups of small customers - electric energy producers in local distribution systems. Small energy sources (VSG – Voltage Source Generator) which assist electric energy supply to the individual buildings (B) are in most cases insufficient. However it can happen that because of, e.g., atmospheric conditions, one group of VSGs overproduces while another under produces energy, therefore it is advisable to connect such sources to one distribution line, common for every given group of customers/producers. For this purpose one should equip VSG sources with cheap small size residential converters (P), to deliver the AC energy with standard parameters to buildings as well as to distribution line.



a



b

**Figure 4.14.** IPFC possible applications: a. substation; b. interconnection of the distributed groups

Additionally for groups of customers/producers it is advisable to utilize the average power DRs, *e.g.*, small wind and water turbines (H), geothermal sources (G) *etc.*, at some distance from buildings because of size or accessibility. Such sources should also be connected to the distribution line through converters (P).

However because of daily and annual energy demand cycles as well as changing weather conditions a group of small costumers/producers supplied in this way is only partly EPS energy delivery independent. Therefore there could be benefits from the interconnection of the individual groups, with electric energy

flow control capability from one to another group. For this purpose, for example, an IPFC device could be utilized.

The IPFC device utilization can considerably diminish costs of delivered electric energy. This is possible if individual groups of customers establish a price to pay for exchanged electric energy lower than the price to pay for electric energy from EPS. However energy flow control between individual groups should be realized, by an IPFC device owned by a “consortium” of customers/producers, omitting the EPS.

## Probabilistic Dimensioning of the Systems for Transmission Control

Whilst high-power electronic converters, in such forms as UPFC, STATCOM and IPFC, have been used with increasing success in a FACTS, the need to economize and optimize transmission facilities at substation level is becoming more compelling.

This chapter investigates from an economic perspective the use of IPFCs, *DC/AC* converters linked by common *DC* terminals, and STATCOM, shunt converters, in an EPS. By using a probabilistic approach, it can be shown that the power rating of shunt converter used in the IPFC and also STATCOM is considerably reduced compared with that of the deterministic approach, while reliability is not compromised. Analytical predication, and experimental measurements at a *15kV* substation confirm the validity of the proposed approach.

### 5.1 Interline Power Flow Controllers – Probabilistic Dimensioning

To date, the choice of the power ratings of the shunt converter in an IPFC system have been based on the maximum active power demand of the individual series converters [56]. This deterministic approach has not taken the probabilistic nature of the electrical quantities in an EPS. In this chapter, a new probabilistic approach to assess the power ratings of an IPFC system is proposed. The approach exploits the inherent random nature of electrical quantities such as voltage and power in a distributed power system [140], resulting in considerable reduction of power rating, and hence costs, for the IPFC system, when compared with that of the deterministic approach [141, 142].

From the previous sections we know that the shunt converter provides shunt reactive compensation and supplies or absorbs the overall active power deficit of the combined SSSCs and in this way keeps the voltage across the DC link constant. Additionally when the IPFC parameters are controlled, in the sense of maximum

influence on transmission characteristics and consequently on transient stability, though without reactive compensation, the power rating of the shunt converter in IPFC system coupling  $N$  transmission lines has to be the sum of the maximum active power demand of individual lines. Thus

$$P_{sh} = \sum_{n=1}^N P_{\Sigma n}^{max} = \sum_{n=1}^N \left( \frac{V_{IPFCn} V_{2n}}{X_n} \left( I - \frac{V_1}{V_{2n}} \cos(\delta_n) \right) \right)^{max} \quad (5.1)$$

The overall power of shunt converter in IPFC system coupling  $N$  transmission lines has been determined by the maximum possible active power flowing within different lines. Such an approach is deterministic since the maximum values are readily definable. However in reality, electrical quantities such as the voltage and current in distributed power systems all manifest a degree of randomness, which can be statistically modeled by some well-known distribution density functions [140]. Using this probabilistic approach, a new power rating for the shunt converter in an IPFC system can be assessed. Since the new approach embraces the intrinsic natural random variation of the electrical quantities, a more realistic power rating than that derived by the classical deterministic approach, should be found.

It is sufficient to assume that the variables  $V_1$ ,  $V_{2n}$ ,  $\delta_n$ ,  $V_{IPFCn}$  and  $X_n$  are with known limited random distributions. By observation one can assume key variables  $V_1$ ,  $V_{2n}$  (for the  $n^{th}$  transmission line) have normal distribution with finite limits [143]. Figure 5.1.a shows the limited normal distribution  $p_{In}$  with the limit sets  $[a_{I,n}, b_{I,n}]$ , which is derived from the normal distribution with no limits. To characterize voltage  $V_1$ , the so called limited normal distributions on set  $[a_I, b_I]$  is denoted as follows [144, 145]

$$V_1 \sim N_{Ia,b} \left( \frac{a_I + b_I}{2}, \left( \frac{b_I - a_I}{2u_{\frac{p_I+1}{2}}} \right)^2 \right) \quad (5.2)$$

Similarly, for voltage  $V_{2n}$

$$V_{2n} \sim N_{2na,b} \left( \frac{a_{2n} + b_{2n}}{2}, \left( \frac{b_{2n} - a_{2n}}{2u_{\frac{p_{2n}+1}{2}}} \right)^2 \right) \quad (5.3)$$

where  $u_{p_{kn}}$  is quartile of the normal distribution  $N(0,1)$ ;  $p_{kn}$  is the probability that the limited normal distribution will be on set  $[a_{kn}, b_{kn}]$ , and  $k=1$  or  $2$ .

While normal distribution is the most usual distribution, it will be prudent to investigate the worst-case scenario, which happens when all the variables manifest uniform distributions, which are shown in Figure 5.1.b. In this case

$$V_I \sim U_{(V_{a_I}, V_{b_I})} \quad (5.4)$$

$$V_{2n} \sim U_{(V_{a_{2n}}, V_{b_{2n}})} \quad (5.5)$$

Other variables  $\delta_n$ ,  $V_{IPFCn}$  and  $X_n$  are also treated as probabilistic with uniform distributions [144, 145]

$$\delta_n \sim U_{(\delta_{a_n}, \delta_{b_n})} \quad (5.6)$$

$$V_{IPFCn} \sim U_{(V_{IPFC_{a_n}}, V_{IPFC_{b_n}})} \quad (5.7)$$

$$X_n \sim U_{(X_{a_n}, X_{b_n})} \quad (5.8)$$

where  $U$  denotes the uniform distribution.

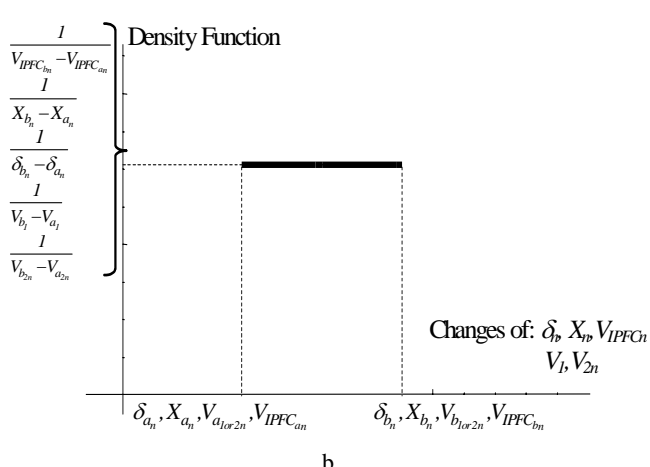
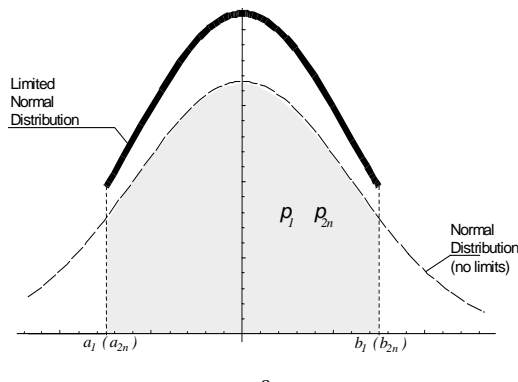


**Figure 5.1.** Typical distributions: a. normal; b. uniform

Since the integral of Equation 5.1 is very difficult to solve analytically when all variables are treated as probabilistic, a numerical approach has been used. It should be noted that very a good approximation can be obtained because distribution of the shunt converters' power rating can be found by convolution of the regular functions.

To make comparison between power ratings of the shunt converters obtained by deterministic and by probabilistic approach, it should be noted that:

- for given  $N$  transmission lines, the particular random variables have the same type of distribution;
- power in a deterministic approach is determined according to Equation 5.1;
- power in a probabilistic approach is determined according to Equation 5.9, as follows [58]

$$P_{sh}^{prob} = \max\left(\text{abs}\left(P_{sh,a}^{prob}, P_{sh,b}^{prob}\right)\right) \quad (5.9)$$

where  $P_{sh,a}^{prob}$ ,  $P_{sh,b}^{prob}$  are limits determined for maximum probability density with 99.9% level of confidence, as shown in Figure 5.2.

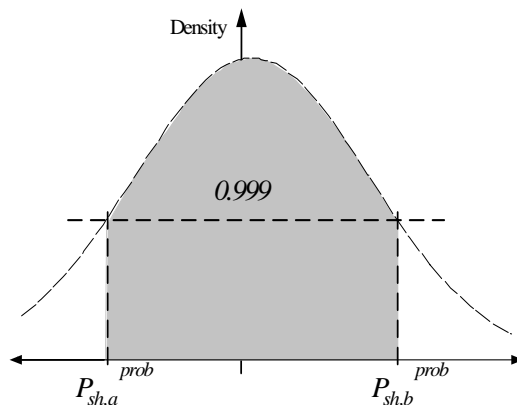


**Figure 5.2.** Method for power range determination in probabilistic approach

### 5.1.1 IPFC Theoretical Investigations

Theoretical investigations into the effects on power rating assessment due to the choice of distribution laws, and the number of converters in the IPFC system have been undertaken. Figure 5.3 depicts a series of probabilistic modeling results for an  $N$  transmission line system. These results represent the *resultant* distributions of the power rating of the system based on different distribution parameters for  $V_1$  and  $V_{2n}$ . These include normal and uniform distributions, and whether they are symmetrical or asymmetrical in relation to the nominal value. As for  $\delta_n$ ,  $X_n$  and  $V_{IPFCn}$  uniform distribution is used in all cases shown in Figure 5.3, for reasons of

worst-case condition.

Thus, angle  $\delta_n$  for all  $N$  transmission lines is given a uniform distribution with parameters

$$\delta_n \sim U_{(0.75\delta_r, 1.25\delta_r)} \quad (5.10)$$

where  $\delta_r$  is reference angle  $\delta_r = 4^\circ$ .

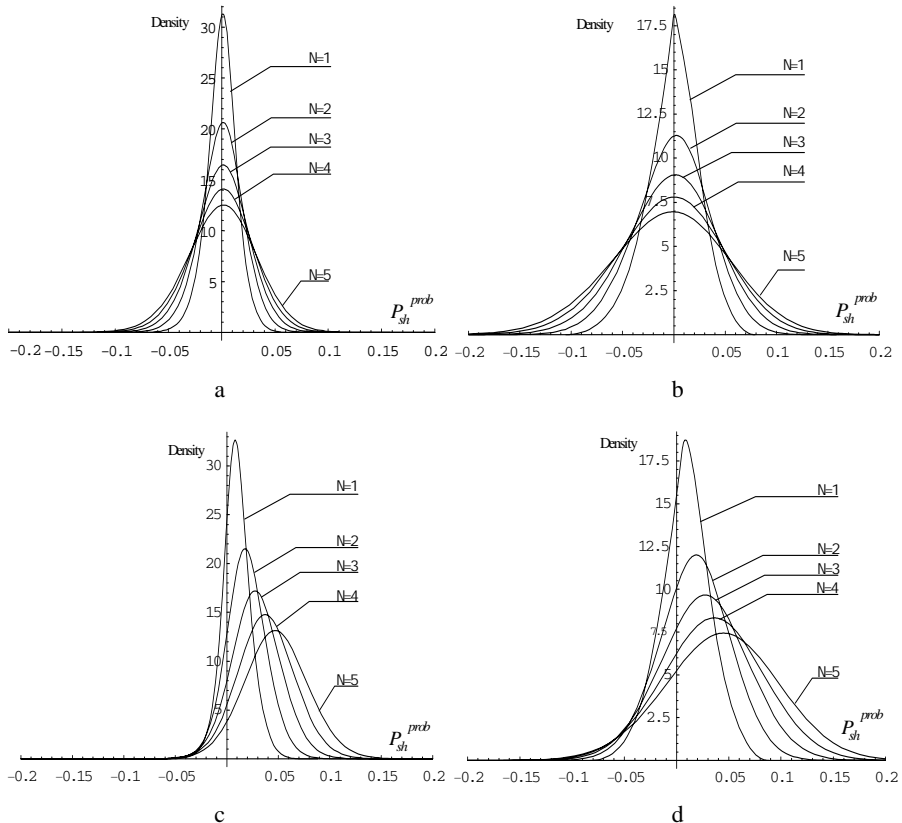


**Figure 5.3.** Resultant distributions of the shunt converter's power rating based on its respective distribution parameters: a.  $V_1 \sim N_{1a,b}(1, 0.00235)$  and  $V_{2n} \sim N_{2n,a,b}(1, 0.00235)$ ; b.  $V_1 \sim U_{(0.85V_{1nom}, 1.15V_{1nom})}$  and  $V_{2n} \sim U_{(0.85V_{2n,nom}, 1.15V_{2n,nom})}$ ; c.  $V_1 \sim N_{1a,b}(1, 0.00104)$  and  $V_{2n} \sim N_{2n,a,b}(1.075, 0.00163)$ ; d.  $V_1 \sim U_{(0.9V_{1nom}, 1.1V_{1nom})}$  and  $V_{2n} \sim U_{(0.95V_{2n,nom}, 1.2V_{2n,nom})}$

The series injected voltage  $V_{IPFCn}$ , is given a uniform distribution with parameters

$$V_{IPFCn} \sim U_{(V_{IPFCn\_min}, V_{IPFCn\_max})} \quad (5.11)$$

where  $V_{IPFCn\ min}=0$  and  $V_{IPFCn\ max}=0.1p.u.$  respectively, minimum and maximum achievable values, determined by the device rating; where sending end voltage nominal value  $V_{1nom}=V_{2n,nom}=1\ p.u.$

Reactance  $X_n$  for all  $N$  transmission lines is given a uniform distribution with parameters

$$X_n \sim U_{(0.5X_r, 1.5X_r)} \quad (5.12)$$

where  $X_r$  is reference reactance  $X_r=1\ p.u.$

Based on the results in Figure 5.3, the ratio of the power ratings of the  $N$  transmission line system due to the probabilistic and deterministic approach is shown in Table C.1 (Appendix C).

Using values from Table C.1 (Appendix C), the curve showing the variation of power saving with the number of inverters for each of the four cases is plotted in Figure 5.4. It can be seen that maximum saving occurs when the distributions are normal, as shown in the ‘a’ and ‘c’ lines; and least if the distribution is uniform, as shown in the ‘b’ and ‘d’ lines. Also, the higher the number of transmission lines, the more will be the saving. By way of example, using the new approach, a 72.1% of saving in power rating can be obtained for a 5 transmission lines system when the quantities are normally distributed.

The simulation results presented thus far are concerned with discrete events. A more comprehensive picture can be developed if the results for these discrete events are interpolated and presented in 3-D. In Figure 5.5, it shows that power savings (in percentage) are larger when both sending end and receiving end voltages are *normally* distributed. Also, power savings are biggest when set ranges are symmetrical in respect to nominal value of voltage  $V_1$ .

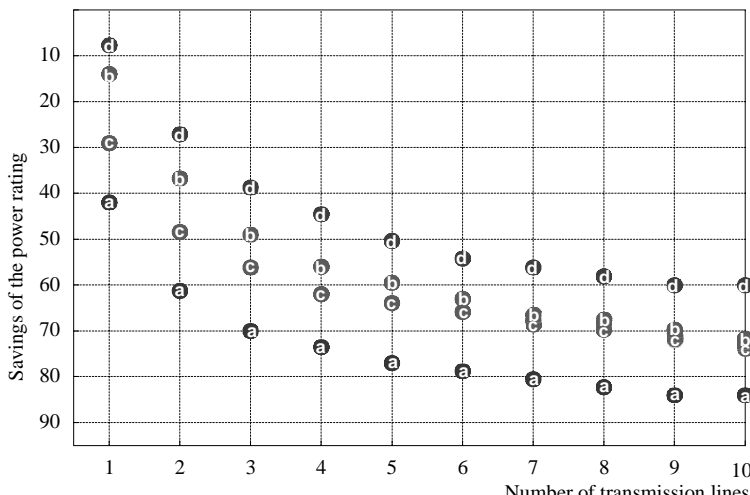


**Figure 5.4.** Savings of the parallel inverter's power rating for given number of transmission lines

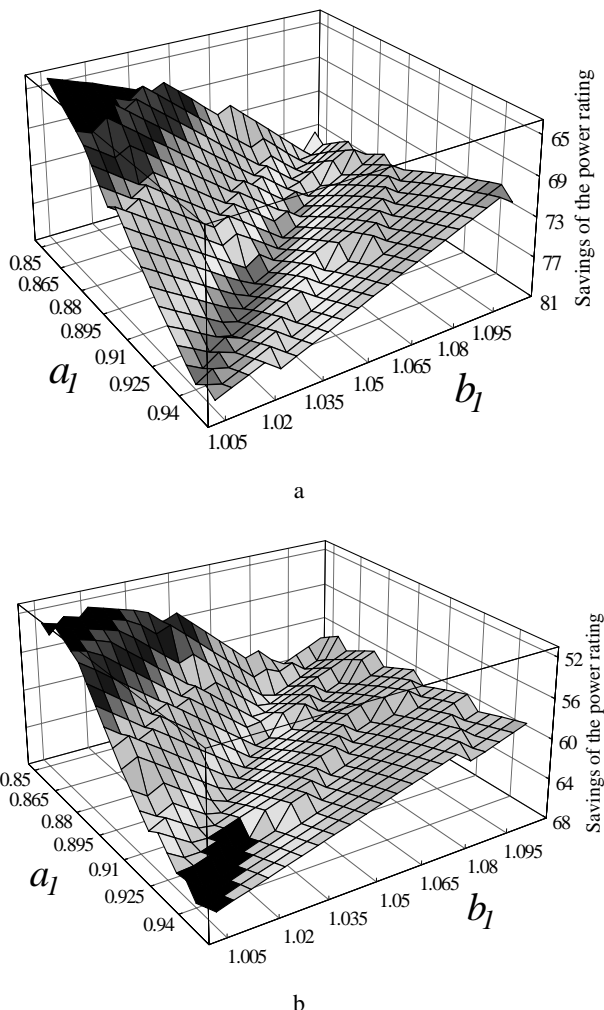


**Figure 5.5.** Shunt converter's power rating savings for different distribution of the sending end voltage  $V_I$ : a. normal distribution; b. uniform distribution;  $V_{2n} \sim N_{2n_{a,b}}(I; 0.00235)$ ,  $N=5$ , other variables are as above

Figure 5.6 shows the variation of power savings as a result of a change in the limits of the  $\delta_n$  distribution. By carefully tracing the curves, one can deduce that the biggest savings occur when angle  $\delta_n$  for  $n^{th}$  transmission line is bigger than the nominal one, which again means that there is an excess of power which could be utilized by another line.

On the basis of the above simulation results, it can be seen that considerable power savings, in the order of over 60%, for an  $N$  transmission line IPFC system are predicted when using the probabilistic approach. The next section will verify these predictions with experimental results.

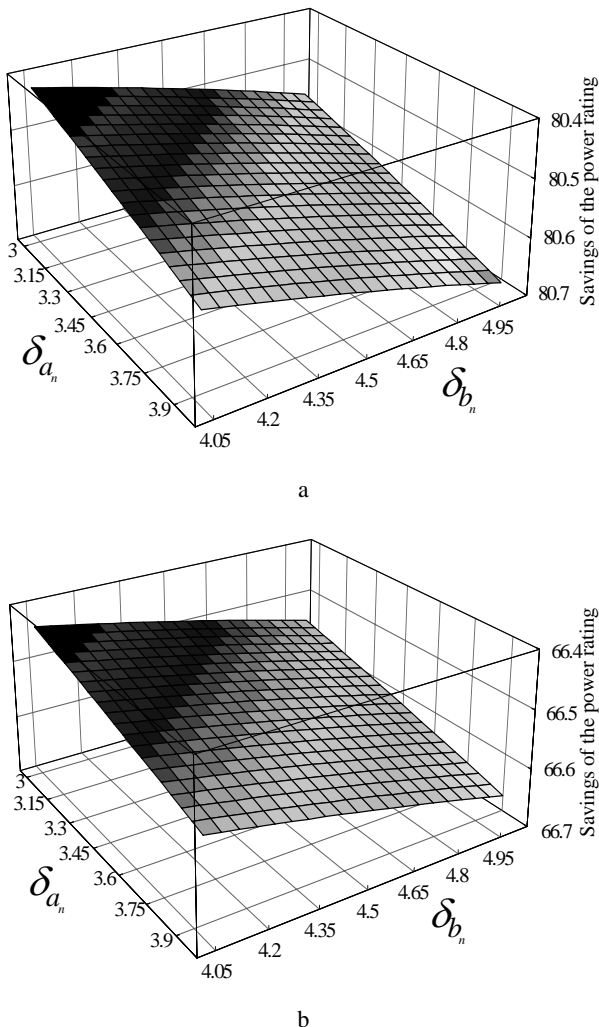


**Figure 5.6.** Parallel converter's power rating savings for uniform distribution of  $\delta_n$ : a.  $V_I \sim N_{I_{a,b}}(1;0.00235)$ ; b.  $V_I \sim U_{(0.85V_{I_{nom}}, 1.15V_{I_{nom}})}$ ;  $V_{2n} \sim N_{2n,a,b}(1;0.00235)$ ,  $N=5$ , other variables are as above

### 5.1.2 IPFC Experimental Investigations

The experimental investigations were undertaken on a system in Poland over a 4-week period. Individual transmission lines were connected at the 110kV/15kV substation of the power system. Extensive measurements at the 15kV voltage lines were undertaken, at the rate of 128 measurements per 20ms, using the modern

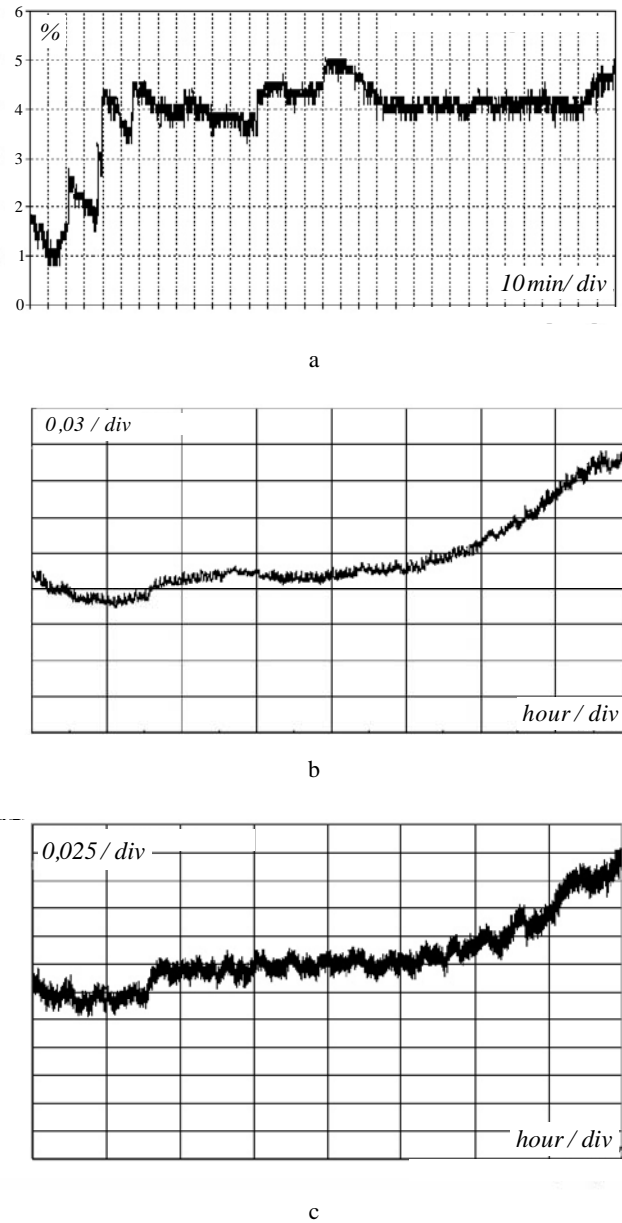


**Figure 5.7.** Measurement results in selected time periods: a. deviation from nominal voltage; b. relative active power; c. relative reactive power; voltage is related to the rated 15kV; active and reactive powers, to the transformer base rating of 16MVA

network analyzer SKYLAB HT9032. The analyzer allows high-speed measurements in accordance with the EN 50160 standard, and can perform many

tasks including averaging and harmonics analysis. The substation was feeding normal domestic electrical loads to a residential area. Thus, these measurements would contain the inherent random distributions. Figure 5.7 shows some basic electrical quantities directly from the output of the analyzer over a selected measurement cycle [143].

The basic electrical quantities measured over a 28-day period were then processed to produce the distribution density curves for some key parameters.

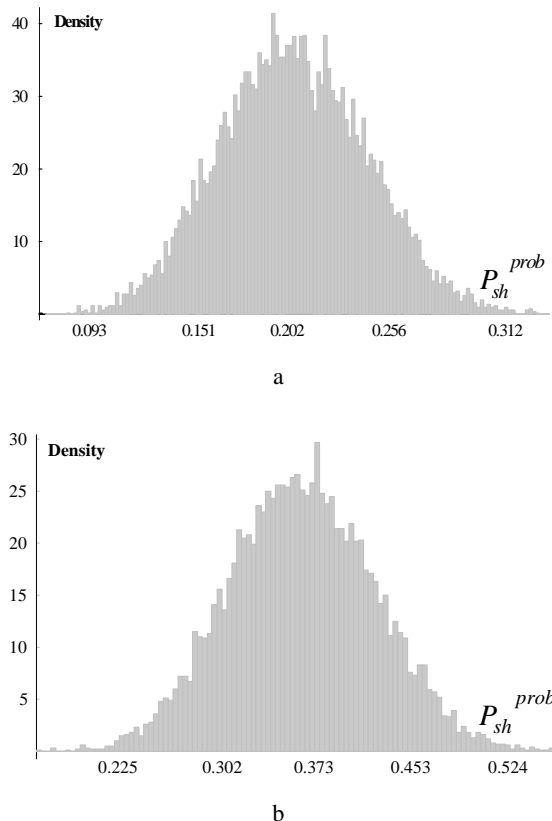


**Figure 5.8.** Resultant distributions of the shunt converter's power rating: a.  $N=5$ ; b.  $N=10$

By using numerical methods, and accounting for experimental correlations with measured quantities, the experimental results for the resultant distributions of power rating  $P_{sh}^{prob}$  of an  $N$  transmission line system were determined. Figure 5.8 shows the distributions for the case when the number of transmission lines equals five and ten respectively. The experimental results show that the distributions appear to be predominately normal rather than uniform, when compared with the theoretical predictions shown in Figure 5.3. Using Equation 5.9, the experimental results for the variation of savings with number of lines are determined as shown in Figure 5.9, with a level of confidence of 0.99.

From the curve in Figure 5.9, it can be confirmed for a one transmission line system ( $N=1$ ), IPFC behaves as “ordinary” UPFC, power savings are at a level of 7%.

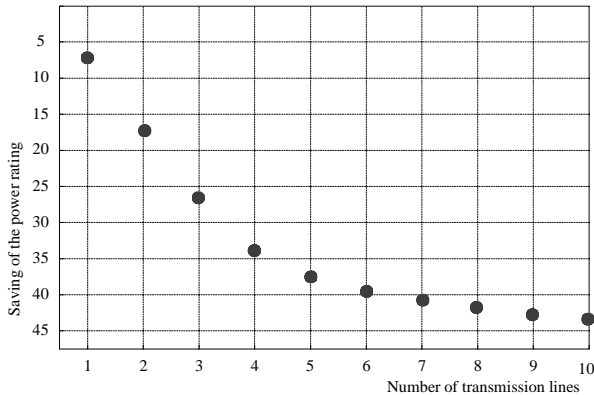


**Figure 5.9.** Experimental results for savings of power rating due to number of transmission lines

Increasing the number of transmission lines will result in an increase in power rating savings, at about 43% when  $N=10$ . It does appear that the experimental savings are less than the theoretical values. This may be due to the actual distributions being exactly of the normal type. Also, the system under test was supplied with a number of wind turbines, which invariably provide power to the system in a sporadic pattern, thus affecting the theoretical predictions. The pattern between the curves, however, is compellingly similar.

## 5.2 STATCOM – Probabilistic Dimensioning

From the EPS point of view, when losses are neglected the active power exchanged by the STATCOM with the electrical power system is zero ( $P_{st}=0$ ). Therefore the STATCOM may be treated as a source of reactive current  $\bar{I}_{st}$  perpendicular to the terminal voltage phasor  $\bar{V}_l$ . The controllable parameter may therefore be assumed its current magnitude  $I_{st}$ . Figure 5.10 shows a simplified scheme of the typical substation where STATCOM is connected to the common bus.

When the STATCOM parameters are controlled in order to protect sending end bus, coupling  $N$  transmission lines at the substation, against the burden of reactive power  $Q_l=0$ , the power rating of the STATCOM device neglecting losses  $P_{st}=0$  has to be the sum of the maximum possible reactive power demand of individual lines. Thus [146]

$$Q_{st} = \sum_{n=1}^N Q_{2n}^{max} = \sum_{n=1}^N \left( \frac{V_l V_{2n}}{X_n} \cos \delta_n - \frac{V_l^2}{X_n} \right)^{max} \quad (5.13)$$

where  $\delta_n \angle (\bar{V}_1, \bar{V}_{2n})$ ;  $n = 1 \dots N$ .

Such an approach is deterministic since the maximum values are readily definable. Using a probabilistic approach, a new power rating for STATCOM devices can be assessed. Since the new approach embraces the intrinsic natural random variation of the electrical quantities, a more realistic power rating than that derived by the classical deterministic approach should be found [146-149].

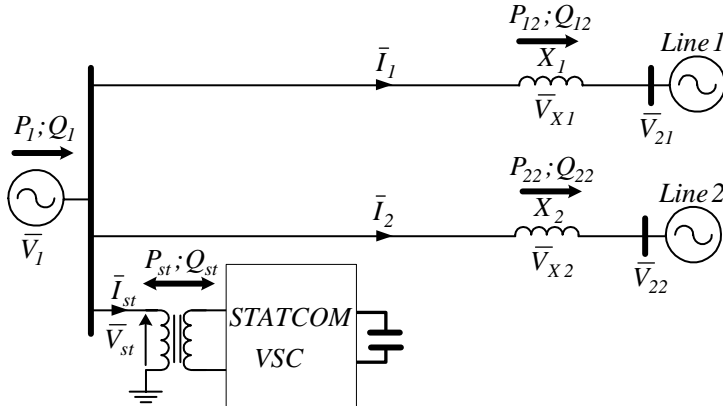


**Figure 5.10.** Substation equipped with STATCOM

As it was assumed in the previous section the key variables  $V_1$  and  $V_{2n}$  have normal distributions with finite limits, denoted respectively by Equation 5.2 and Equation 5.3. While normal distribution is the most usual distribution, it will be prudent to investigate the worst-case scenario, which happens when the above variables manifest uniform distributions defined by Equation 5.4 and Equation 5.5.

Other variables  $\delta_n$  and  $X_n$  are also treated as probabilistic with uniform distributions

$$\delta_n \sim U_{(\delta_{an}, \delta_{bn})} \quad (5.14)$$

$$X_n \sim U_{(x_{a_n}, x_{b_n})} \quad (5.15)$$

where  $U$  denotes the uniform distribution.

To make a comparison between STATCOM power rating in a deterministic and a probabilistic approach, it should be noted that:

- for given  $N$  transmission lines, the particular random variables have the same type of distribution;
- power in a deterministic approach is determined on the basis of Equation 5.13;
- power in a probabilistic approach is determined according to the Equation 5.16

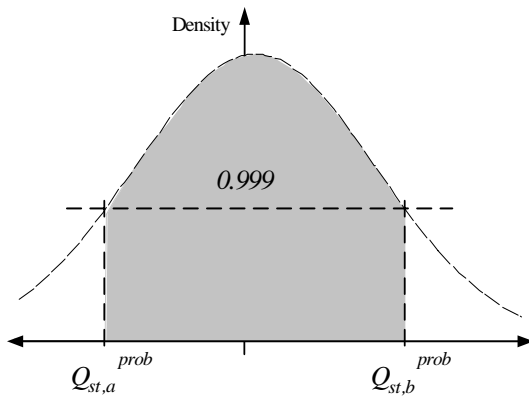


**Figure 5.11.** Method for power range determination

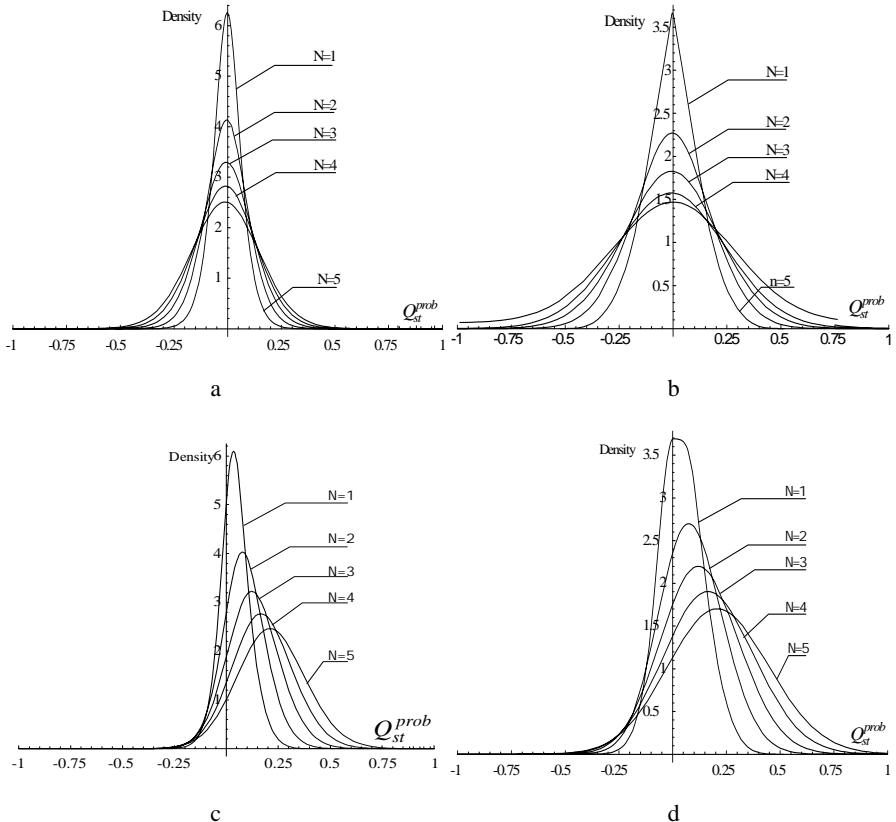


**Figure 5.12.** Resultant distributions of the STATCOM power rating:  
a.  $V_I \sim N_{1a,b}(1; 0.00235)$  and  $V_{2n} \sim N_{2n,a,b}(1; 0.00235)$ ; b.  $V_I \sim U_{(0.85V_{Inom}, 1.15V_{Inom})}$  and  $V_{2n} \sim U_{(0.85V_{2n,nom}, 1.15V_{2n,nom})}$ ; c.  $V_I \sim N_{1a,b}(1; 0.00104)$  and  $V_{2n} \sim N_{2n,a,b}(1.075; 0.00163)$ ; d.  $V_I \sim U_{(0.95V_{Inom}, 1.1V_{Inom})}$  and  $V_{2n} \sim U_{(0.95V_{2n,nom}, 1.2V_{2n,nom})}$ ; where  $V_{Inom} = V_{2n,nom} = 1$  p.u.

$$Q_{st}^{prob} = \max(\text{abs}\langle Q_{st,a}^{prob}, Q_{st,b}^{prob} \rangle) \quad (5.16)$$

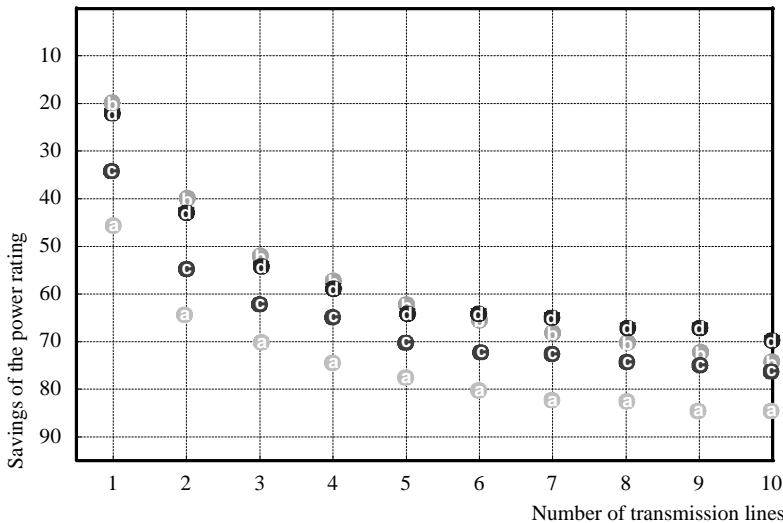
where  $Q_{st,a}^{prob}, Q_{st,b}^{prob}$  are limits determined for maximum probability density with 99.9% level of confidence, as shown in Figure 5.11.

Figure 5.12 depicts a series of probabilistic modeling results for different number  $N$  of transmission lines. These results represent the resultant distributions of the power rating of the system based on distribution parameters for  $V_1$  and  $V_{2n}$ . These include normal and uniform distributions and whether they are symmetrical or asymmetrical in relation to the nominal value. As for  $\delta_n$  and  $X_n$  uniform distribution is used. Thus, angle  $\delta_n$  and  $X_n$  for all  $N$  transmission lines is given a uniform distribution with parameters

$$\delta_n \sim U_{(0.75\delta_r, 1.25\delta_r)}, X_n \sim U_{(0.5X_r, 1.5X_r)} \quad (5.17)$$

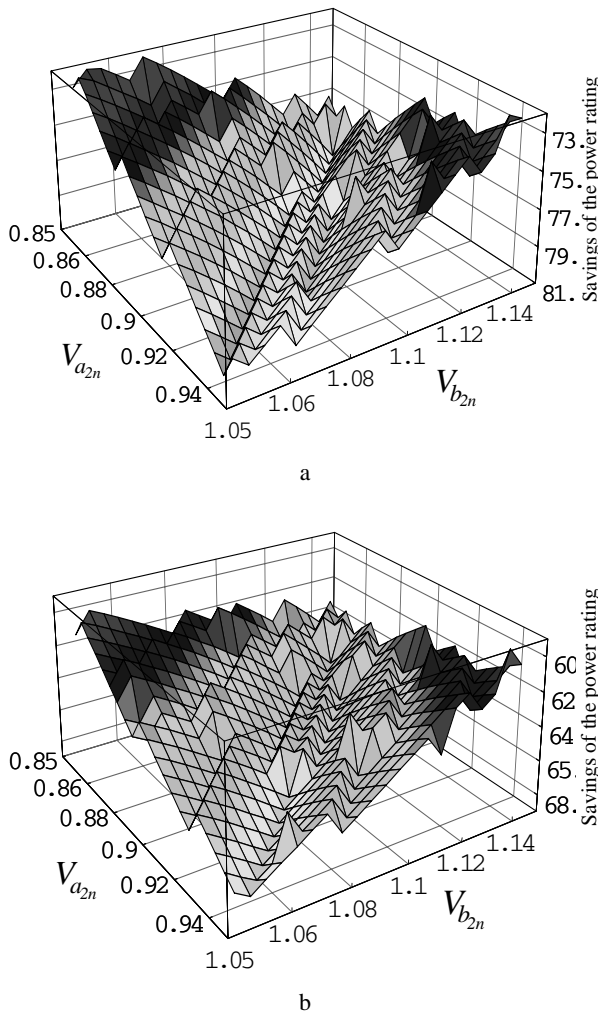
where  $\delta_r$  is reference angle  $\delta_r=4^\circ$  and  $X_r$  is reference reactance  $X_r=1$  p.u.

Based on the results in Figure 5.12, the ratio of the power ratings of the  $N$  transmission line system due to the probabilistic and deterministic approach is shown in Table C.2 (Appendix C). The curve showing the variation of power saving with the number of transmission lines for each of the four cases is plotted in Figure 5.13. It can be seen that maximum saving occurs when the distributions are symmetrical as shown in the 'a' lines.



**Figure 5.13.** Savings of the STATCOM power rating for given number of lines

The simulation results presented thus far are concerned with discrete events. A more comprehensive picture can be developed if the results for these discrete events are interpolated and presented in 3-D for  $N=5$ .



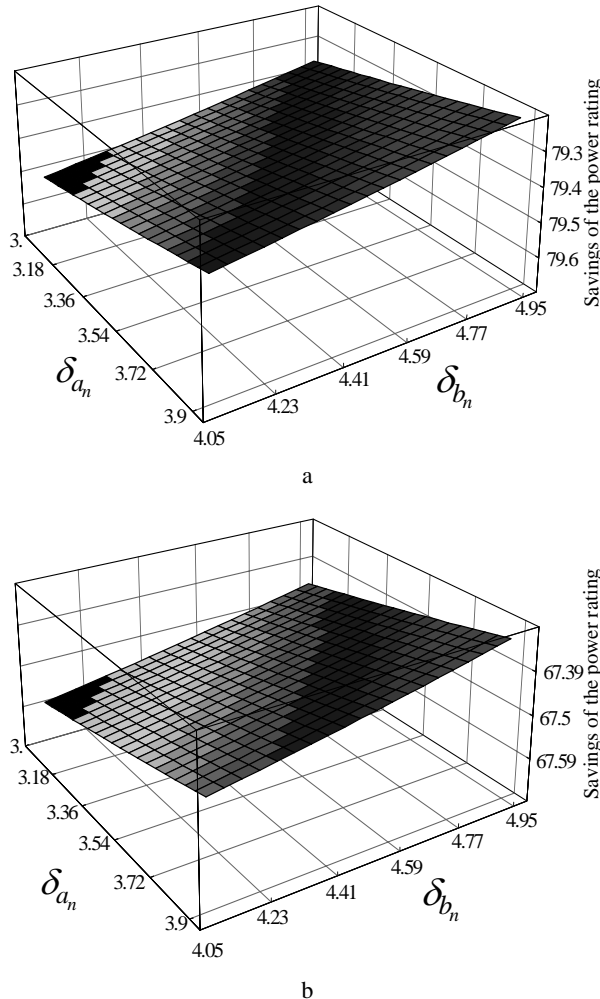
**Figure 5.14.** STATCOM power rating savings for different distribution of the receiving end voltage  $V_{2n}$ ; a. normal distribution; b. uniform distribution; where  $V_l \sim N_{l,a,b}(I; 0.00235)$

Figure 5.14 shows that power savings are larger when both sending end and receiving end voltages are symmetrical and normally distributed.

Figure 5.15 shows the variation of power savings as a result of change in limits of the  $\delta_n$  distribution. By carefully tracing the curves, one can deduce that changes of the  $\delta_n$  angle have almost no influence on STATCOM power rating savings. All this is happening because  $\delta_n$  angle only to a slight degree affects the reactive power of individual transmission lines, as a result there is almost no change in STATCOM behavior.

On the basis of the above simulation results, it can be seen that considerable

power savings, in the order of 60%, or more for a STATCOM system are predicted when using the probabilistic approach.



**Figure 5.15.** STATCOM power rating savings for uniform distribution of  $\delta_n$  and different distributions of the  $V_1$ ,  $V_{2n}$  voltages: a. normal distributions  $V_1 \sim N_{1a,b}(I;0.00235)$  and  $V_{2n} \sim N_{2n,a,b}(I;0.00235)$ ; b. uniform distributions  $V_1 \sim U_{(0.85V_{1nom},1.15V_{1nom})}$  and  $V_{2n} \sim U_{(0.85V_{2n,nom},1.15V_{2n,nom})}$

### 5.3 Summary

A new probabilistic approach to assess the power rating of an IPFC and STATCOM device has been proposed. The approach results in considerable saving

by lowering the required power ratings of the converters used in the design of the IPFC and STATCOM systems. Both analytical prediction and experimental results confirm the potential benefits the new approach will bring to bear, in terms of costs saving. Very importantly, these assessments have been achieved with a very high level of confidence, which is no less than 99.9%. Thus, the reliability of the system is not compromised by the new approach.

---

## Energy End-use Power Electronics Systems

### 6.1 Converters Suitable for Custom Power Systems

The increased severity of harmonic pollution in distributed networks has attracted attention to the development of dynamic and adjustable solutions to power quality problems. Such devices, generally known as Custom Power Systems, with capabilities to inject fully controllable currents or voltages, are based on two types of power converters: Voltage Source Converters and Current Source Converters (CSC). However the first one in comparison with CSC is becoming more dominant, since it is lighter, cheaper in initial costs, higher in efficiency and expandable to multilevel and multi-step versions, therefore it will be the basis for presentation of converters suitable for energy end-use devices. In fact, almost all CUPS that have been put into practical application have adopted the VSCs as the power circuit.

#### 6.1.1 Single Phase Converters

Figure 6.1 shows the basic topology of a full bridge converter, often called an H-bridge, with single phase output where the load is connected between the mid-points of the two phase legs [150-153]. The converter in this topology can deliver and accept both real and reactive power. Each power control device has a diode connected in

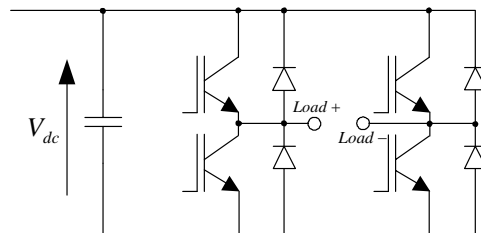


**Figure 6.1.** Topology of single phase, full bridge converter

anti-parallel to it, which provides an alternate path for the load current if the power switches are turned off. Control of the circuit is accomplished by varying the turn on time of the upper and lower IGBT of each converter leg, with the requirement of never turning on both at the same time, to avoid a short circuit of the *DC* bus.

For the single phase converter, the modulation of each of the two legs is the inverse of each other such that if the left leg has a large duty cycle for the upper switch, the right leg has a small one. The output voltage is then given by Equation 6.1 where  $m_a$  is the modulation factor. The boundaries for  $m_a$  are for linear modulation, however values greater than 1 cause overmodulation and a noticeable increase in output voltage distortion

$$v_{ac} = m_a V_{dc} \sin(\omega t) \quad 0 \leq m_a \leq 1 \quad (6.1)$$

This output voltage can be filtered using a *LC* low pass filter and, in consequence, will closely resemble the shape and frequency of the modulation signal.

### 6.1.2 Three Phase Converters

Figure 6.2 shows a three phase converter which is a one-leg extended version of the H-bridge single phase converter [150-153]. The converter provides a three phase voltage; similarly four, five, or  $n$  phase voltages can be realized by simply adding the appropriate number of phase legs.

Like the single phase converter based on the H-bridge topology, the three phase converter can deliver and accept both real and reactive power. The control strategy is similar to the control of the single phase converter, except that the reference signals for the different legs have a phase shift of  $120^\circ$  instead of  $180^\circ$  for the single phase converter. Due to this phase shift, the odd triple harmonics ( $3^{rd}$ ,  $9^{th}$ , etc.) are eliminated from the line-to-line output voltage.

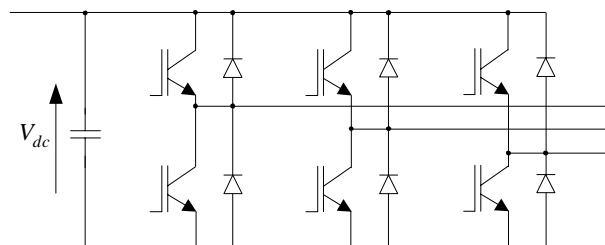


**Figure 6.2.** Topology of a three phase converter

On the basis of the above structure a back-to-back VSC with bi-directional power flow capability can also be constructed. A technical advantage of this solution is the capacitor decoupling between the two converters. This decoupling offers some protection and additionally separates control of the two converters, allowing, e.g., compensation of asymmetry.

### 6.1.3 Matrix Converters

The matrix converter should be an silicon solution with no passive components, as it is in Figure 6.3 [154-156].

Compared to two levels converters with *DC* link voltage, the output harmonic content of the matrix converter is lower, due to the fact that the output voltage is collected of three voltage levels.

Although the matrix converter possess a greater number of power switches (six more compared to the conventional back-to-back VSC), the absence of the *DC* link capacitor may increase the efficiency and the lifetime of the converter. However due to the absence of the *DC* link, there is no decoupling between converter's input

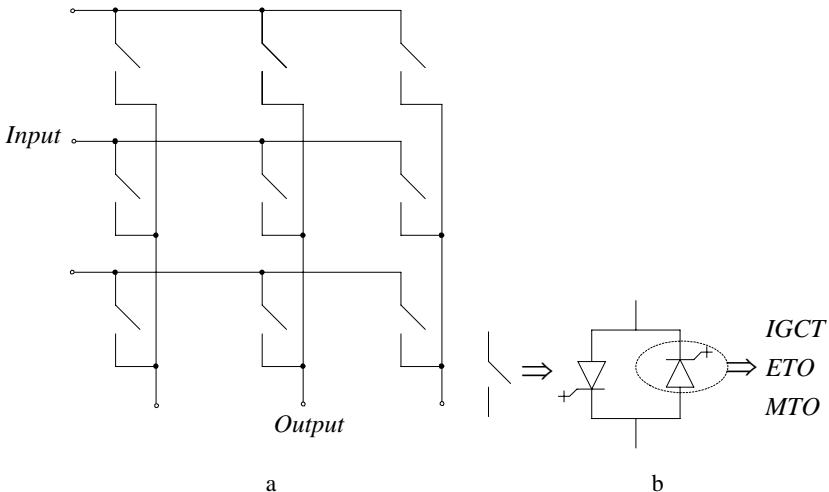


**Figure 6.3.** a. basic topology of a three phase matrix converter; b. possible realizations of the bi-directional switches

and output. In many cases this is not a problem, but in the case of unbalanced or distorted input voltages, or unbalanced load, the input current and the output voltage also become distorted.

Depending on the realization of the bi-directional switches, the switching losses of the matrix converter may be less than those of the conventional VSC, this is so because half of the switchings become natural commutations (soft switching). The lack of a true bi-directional switch is mentioned as one of the major obstacles for the propagation of the matrix converters.

The major disadvantage of the matrix converters is the intrinsic limitation of the output voltage. In linear modulation range, without over-modulation, the maximum output voltage of the matrix converter is 0.866 of the input voltage. Therefore to achieve the same output power as in the conventional back-to-back VSC, the output current of the matrix converter has to be about 1.15 times higher, giving rise to higher conducting losses [155].

### 6.1.4 Multilevel Converters

The general idea behind the multilevel converter technology is to create a sinusoidal output voltage from several small voltage steps [157-159]. There are several advantages to this approach when compared with traditional two-level converters. The smaller voltage steps lead to the production of higher quality waveforms (therefore a multilevel converter distinguishes itself by being the converter with the lowest demands on the input filters) and also reduce the  $dv/dt$  stresses [160]; the series-type connection of the semiconductors allows operation at higher voltages. Further, the switching frequency of the multilevel converter can be reduced to 25% of the switching frequency of a two level converter [160].

One clear disadvantage of multilevel power conversion is the larger number of semiconductor switches required, however lower voltage rated switches can be used and the active semiconductor cost is not significantly increased when compared with the two level case. The most commonly reported disadvantage of the multilevel converters is that the voltage steps are produced by isolated voltage sources or a bank of series capacitors. When isolated voltage sources are not available, series capacitors require voltage balance. For three level converters this problem is not very serious because the voltage balancing can be overcome by using redundant switching states, which exist due to the high number of semiconductor devices [161-163]. However for more than three level diode-clamped and flying-capacitor converters the voltage balancing problem can be solved only by adding hardware arrangements [163, 164]. Whether the voltage balancing problem is solved by hardware or software, it is necessary to measure the voltage across the capacitors in the DC link.

#### *Diode-clamped and Flying-capacitor Multilevel Converters*

Despite the more complex structure, the diode clamped multilevel converters are very similar to the conventional back-to-back VSCs [165]. Figure 6.4.a shows the three level diode-clamped structure phase leg. Even though having a larger number of switches it should be pointed out that in a three level converter the voltage rating of the transistors is half that of the transistors in a two level converter. Furthermore, the switching losses — which are reduced by the lower transistor blocking voltage and increased by the higher number of transistors — for this converter will be lower than that of a two level converter. Additionally, it should be noted that each transistor switches only during a portion of the network period, which again reduces the switching losses. For three level converters maintaining voltage balance on the capacitors can be accomplished through selection of the redundant switching states [161-163] which lead to the same output voltages, but yield different capacitor currents. For more than three levels the voltage balancing problem can be solved only adding hardware arrangements [163, 164].

The topology of the flying capacitor multilevel converter is very similar to that of the diode clamped multilevel converter, see Figure 6.4.b, where one phase of a three level flying-capacitor multilevel converter is presented. The difference between the diode clamped multilevel converter and the flying capacitor multilevel

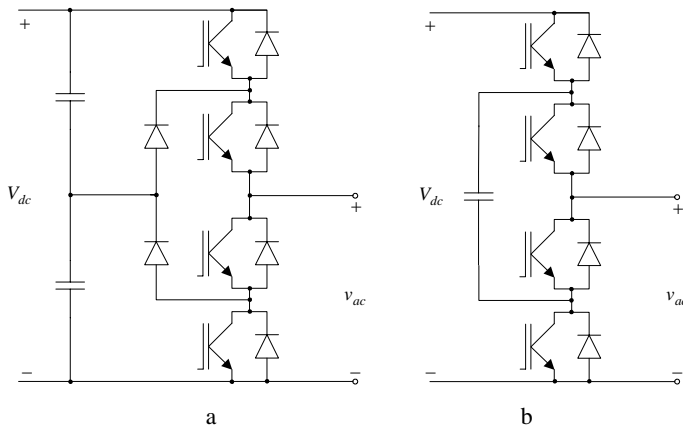


**Figure 6.4.** Three level: a. diode clamped converter phase leg; b. flying capacitor converter phase leg

converter is that two diodes per phase may be substituted by one capacitor. Therefore the general concept is that the added capacitor is charged to one half of the *DC* link voltage and may be inserted in series with the *DC* link voltage to form an additional voltage level.

#### Cascaded H-bridge Multilevel Converters

Figure 6.5 shows the single phase of a cascaded H-bridge converter, where two H-bridge cells are utilized. Generally speaking cascaded H-bridge converters consist of a number of H-bridge cells series-connected on the *AC* side and supplied by an isolated source on the *DC* side [166-168]. It should be noted that in most applications isolated sources are required for each cell in each phase. In some utilizations where cascaded H-bridge converters are used, *e.g.*, as DR/EPS interfaces, these sources may be available through batteries or photovoltaic cells, in other cases, *e.g.*,

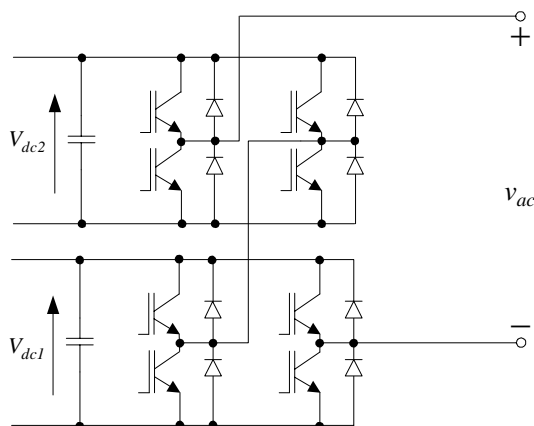


**Figure 6.5.** Five level cascaded H-bridge converter phase leg

HVDCs, transformer/rectifier sources are required. But when cascaded H-bridge converters are utilized in power quality enhancement arrangements only capacitors can be connected on the *DC* side without the need for an isolated source. The voltage balance problem whether for three or five level converters is not very serious then because it can be overcome by software using redundant switching states [163, 169].

#### Cascaded Multilevel Converters

Figure 6.6 shows a special case of the cascaded converters where the single phase three level H-bridge converters are cascaded with conventional three phase two

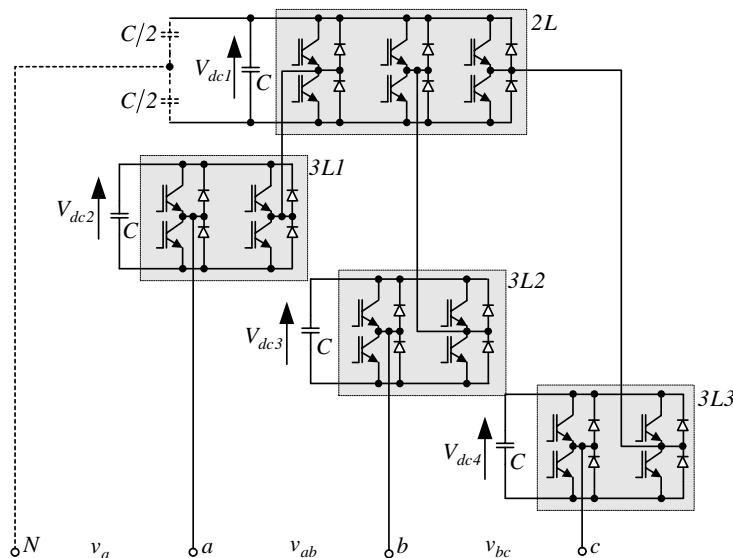


**Figure 6.6.** Cascaded multilevel converter

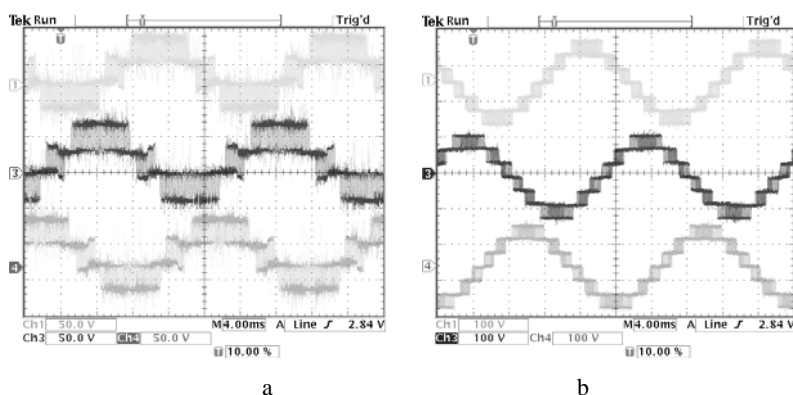


**Figure 6.7.** a. phase output voltages, *y* axis 50V/div, *x* axis 4ms/div; b. phase-to-phase output voltages, *y* axis 100V/div, *x* axis 4ms/div

level converters. This topology is referred to here as a cascaded multilevel converter and can be utilized in three- as well as four-line networks [170]. The major advantage of this topology lies in its modularity, relatively simple construction and simple way of avoiding the problems of unbalanced voltages on DC link capacitors [111].

Figure 6.7 and Figure 6.8 show the experimental results obtained for the examined converter (nominal power rating 5kVA)(when  $V_{dc1}=V_{dc2}=V_{dc3}=V_{dc4}$ ) while a multilevel carrier based PWM with set of even peak-to-peak magnitude and frequency 4 triangular carrier waves was used. As one can see, the converter produces four level phase voltages and seven level phase-to-phase quasi-sinusoidal output voltages, which are the geometrical sum of voltages on individual converters.

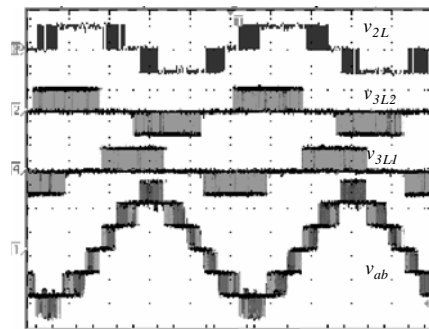


**Figure 6.8.** Experimental waveforms; y axis 50V/div, x axis 4ms/div

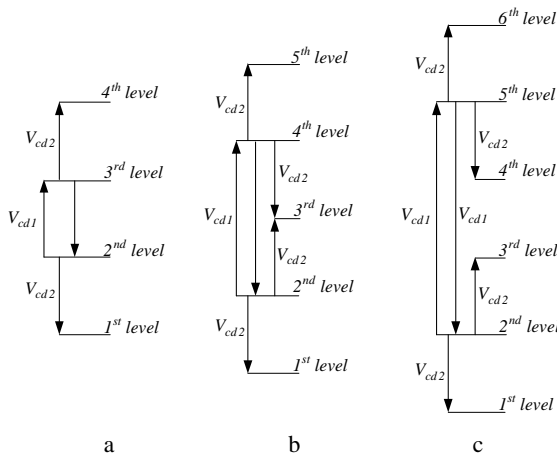


**Figure 6.9.** Method for obtaining multilevel output voltage  $v_a$ : a.  $V_{dc1}=V_{dc2}$ ; b.  $V_{dc1}=2V_{dc2}$ ; c.  $V_{dc1}=4V_{dc2}$

In the case of different DC link voltages and with a control algorithm, which makes possible both voltages addition and subtraction, the examined topology can

produce more than four levels in output phase voltage. Figure 6.9 demonstrates a method for obtaining different number of levels in the studied converter. One can see that when DC link voltages are even  $V_{dc1}=V_{dc2}=V_{dc3}=V_{dc4}$  the converter generates a 4 level phase voltage, additionally in the case when  $V_{dc1}=2V_{dc2}=2V_{dc3}=2V_{dc4}$  the converter generates a 5 level phase voltage and finally when  $V_{dc1}=4V_{dc2}=4V_{dc3}=4V_{dc4}$  and with appropriate control algorithm the converter generates 6 levels in output phase voltage.

**Table 6.1.** Coefficients characterizing examined converter

	$V_{dc1}=V_{dc2}=1p.u$				$V_{dc1}=2V_{dc2}=Ip.u$			
	0.25	0.5	0.75	1	0.25	0.5	0.75	1
$THD(v_d) (\%)$	148	55	47	30	102	45	34	22
Number of levels in $v_a$	2	4	4	4	3	3	5	5
Number of levels in $v_{ab}$	3	5	5	7	3	5	7	9

Additionally Table 6.1 displays the basic coefficients characterizing the examined cascaded multilevel converter. Studying the data in Table 6.1 and curves in Figure 6.10, one can say that the number of voltage levels is greatly improved, and

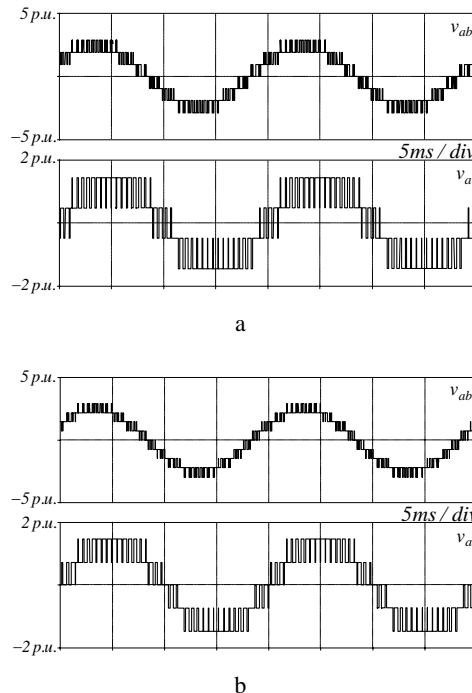


**Figure 6.10.** Converter's output voltages: a.  $V_{dc1}=V_{dc2}$ ; b.  $V_{dc1}=2V_{dc2}$ ; where modulation factor is 1

voltage closely resembles an ideal sine wave, by setting the *DC* voltages to different values. Additionally the voltage THD depends on the modulation index and can be minimized to 22%.

## 6.2 Compensating Type Custom Power Systems

In a similar way as it is with FACTS devices in transmission systems, the Custom Power Systems can be applied to the power distribution systems to improve reliability and quality of the power delivered to the end-users. There are widely varying application requirements, such as single or three phase, current or voltage based compensation, therefore selection of the CUPS for a particular application is as important a task for end-users as it is for utilities.

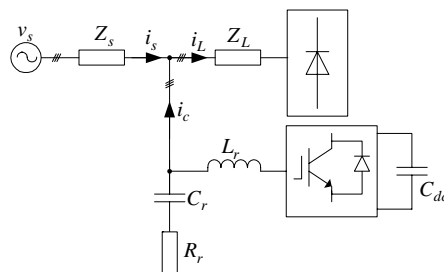


**Figure 6.11.** Principle configuration of a VSC based PAPF

There are two major compensation types; current and voltage based. Current based compensation is categorized as current harmonics filtration, reactive power compensation, and load balancing. This compensation may be needed by the individual consumers because they should pay attention to current harmonics produced by their own loads. For current harmonics filtration, the PAPF is an ideal device [70-84, 171-174]. Figure 6.11 is an example of a parallel active filter, which consists of a controllable voltage source (the VSC based PAPF is by far the most common type

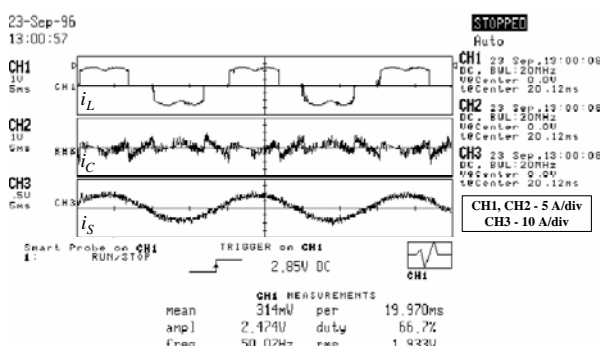


**Figure 6.12.** PAPF operation principles when performing harmonic filtering

used today, developed in two level or multi-step/multilevel configuration) [83, 93, 163, 169], a DC link capacitor  $C_{dc}$ , and output filter. It is mainly used at the load end, because current harmonics are injected by nonlinear loads. The operation of parallel APFs is based on injection of current harmonics  $i_C$  in phase with the load current  $i_L$  harmonics, thus eliminating the harmonic content of the network current  $i_S$  [172, 173, 175-186].

Figure 6.12 shows the sinusoidal phase currents when the PAPF (nominal power rating 5kVA) performs harmonic filtering of a diode rectifier. The injected  $i_C$  current cancels the current harmonics from the load, resulting in a harmonic free network current.

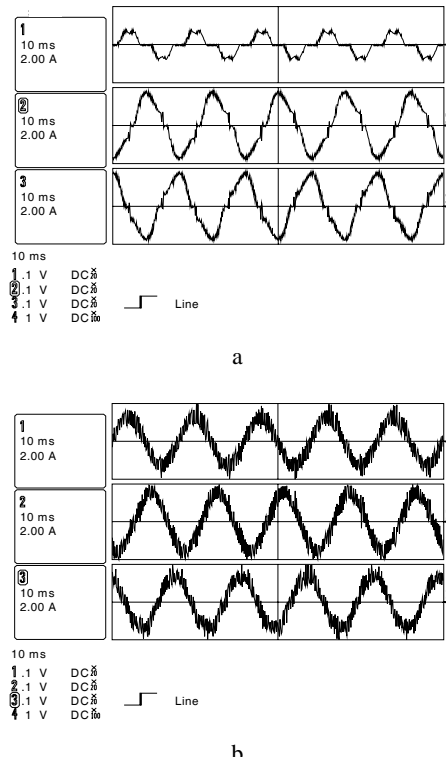


**Figure 6.13.** PAPF operation principles when performing load balancing: a. load current; b. network current

Respectively Figure 6.13 shows the sinusoidal and balanced network currents in a situation of distorted and unbalanced load. Additionally the PAPF has also the capability of damping harmonic resonance between an existing passive filter and the supply impedance [187] and can also be used as a Static Var Generator in the network for stabilizing and improving the voltage profile.

For most of above mentioned current compensation tasks, the APF technically is the right choice, however more often a hybrid of PAPF/SAPF and parallel passive filters is preferable. This happens because the solid state devices used in

the active part can be of reduced size (active part apparent power  $S$  is about 4% of the load apparent power  $S_L$ , see Figure 6.15) [137] and a major part of the hybrid filter is made of the passive shunt  $LC$  filter used to eliminate lower order harmonics.

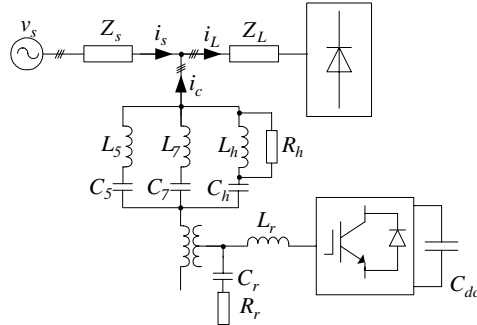


**Figure 6.14.** Principle configuration of a hybrid APF

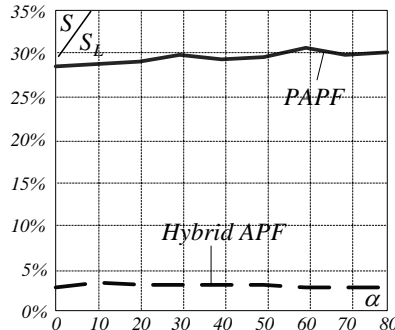


**Figure 6.15.** Apparent powers ratio for various thyristor rectifier firing angles  $\alpha$

Fig. 6.14 shows the hybrid filter, which is a combination of an active filter and passive filter [188, 189], however there are many more hybrid configurations [190-203], but for the sake of brevity, they are not discussed here.

Figure 6.16 shows the network phase currents for hybrid APF (nominal power rating 40kVA) various modes of operation; as can be noticed the examined device secures almost pure sinusoidal phase current.

Voltage based compensation is classified as voltage harmonics filtration, voltage regulation and balancing, and voltage sags and dips removal. This compensation may be required by the utilities because they should concern themselves with voltage issues, thus hopefully in the near future a CUPS with voltage compensation capabilities will be installed by utilities in power distribution systems. Voltage based compensation, in general, is carried out by using SAPF. Figure 6.17 shows the basic block of a stand alone a SAPF. It is connected before the load in series with the mains, using a matching transformer, to eliminate voltage harmonics, and to balance and regulate the terminal voltage of the load or line.

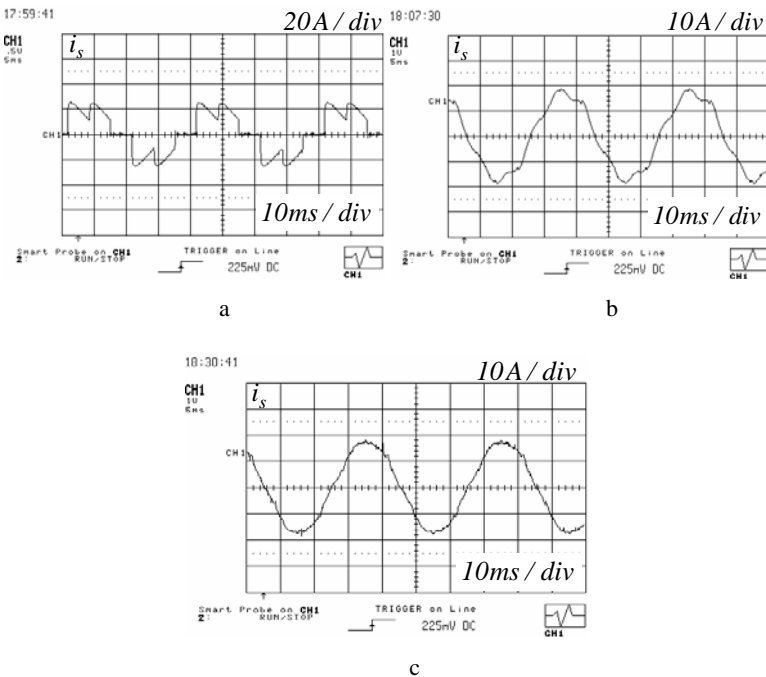


**Figure 6.16.** Hybrid APF operation principles: a. hybrid filter OFF; b. passive filter ON; c. hybrid filter ON

The SAPF also possess the capability of isolating the current harmonics in between the load and the supply [22, 71, 80]. This is achieved by the injection of harmonic voltages across the transformer line side, which affects the equivalent line impedance seen from the load. Thus the equivalent line impedance can be regarded as large for the harmonics, whereas it should ideally be zero for the fundamental frequency component [71, 80]. The voltage harmonic filtering of a SAPF (nominal power rating 5kVA) is illustrated in Figure 6.18. One can see the sinusoidal phase voltage when the SAPF performs harmonic filtering.

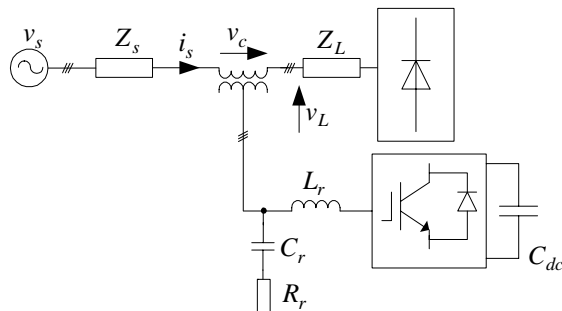


**Figure 6.17.** Principle configuration of a SAPF

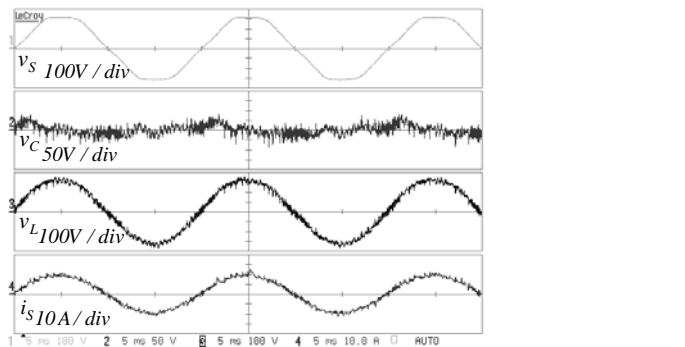


**Figure 6.18.** SAPF operation principles when performing voltage harmonic filtering

Many applications require a combination of voltage and current compensation. The optimal solution for such mixed requirements is combination of a PAPF and SAPF with a common *DC* link. This combination is referred to as the Unified Power Quality Conditioner and has the same configuration as the UPFC. However, the UPQC for distribution networks differs from the UPFC for transmission networks in terms of operation, purpose and control strategy. The conditioning functions of the UPQC are shared by the SAPF and PAPF. The SPAF performs harmonic isolation between supply and load, voltage regulation and voltage flicker/imbalance compensation. However the PAPF performs harmonic current filtering and negative sequence balancing as well as regulation of the *DC* link voltage.

Below are considered “ideal” compensating type CUPS devices, Unified Power Quality Conditioners.

### 6.2.1 Single Phase UPQC

Figure 6.19 shows selected UPQCs equipped with transformers which are suited to fulfill both voltage and current compensation [69, 99, 114]. These goals can be achieved with different connections of the *DC* link capacitor  $C$  to the network and different types of connected sources, voltage and/or current.

Inspection of the figures below shows that the full-bridge circuit requires the largest number of switches – 8 – which is undoubtedly its major disadvantage. However the source capacitance is not divided. The smallest number of power control devices is required in the half bridge UPQC device. Although there are only two bridge branches, the *DC* link capacitance consists of two independent capacitors. This disadvantage is excluded in UPQC device based on three branches. This time six switches are applied where one branch is used to split the capacitance. A “common-neutral” point is put into practice. To the disadvantages of this solution one can add the two times higher *DC* circuit voltage.

It is undisputed that one of the most important features of this solution is the possibility to take advantage of very popular three-phase Intelligent Power Modules.

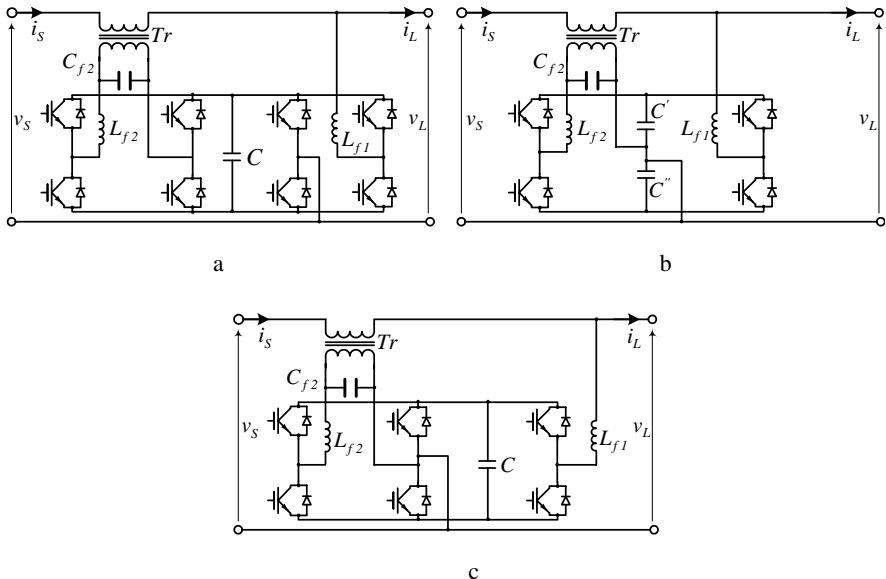


**Figure 6.19.** The UPQCs on the base of: a. full-bridge circuit; b. half-bridge circuit; c. three branches circuit

#### Transformer-less UPQC

The above described configurations require transformers as an interface between the UPQC and the network. This heavy feature is eliminated in the configuration described below [69, 114, 204, 205], see Figure 6.20. The examined device is a combination of a series voltage and parallel current sources with a common *DC* link and can be built on the foundation of three-phase Intelligent Power Modules, which is one of its major advantages. To the disadvantages of this solution one can add the need for rather large capacitance  $C_{f2}$  and the fact that the *DC* link voltage is not well matched to the required voltage of the series connected source.

The control algorithm consists of two major parts [69, 114]. The first part, where *PI* regulator plays the major role, realises the load voltage stabilization. The regulator's input signals are load voltage  $v_L$  and the reference sinusoidal wave, and then its output signal is compared to initially filtered capacitor  $C_{f2}$  current. This last activity diminishes oscillations in capacitor  $C_{f2}$  voltage.

The second part realises parallel current source control in such a way as to keep constant *DC* link voltage. The *DC* link voltage  $v_{dc}$  is compared to its reference value, and after initial filtering the error signal is inserted into the sample-hold block. Because the error signal determines the network current magnitude, thus the invariability of this signal, during one period, guarantees sinusoidal network current. For network fundamental frequency 50Hz this signal is sampled per 20ms, synchronously with network voltage 0 pass. The stored current magnitude related signal after multiplication by the reference sinusoidal course becomes the reference curve.

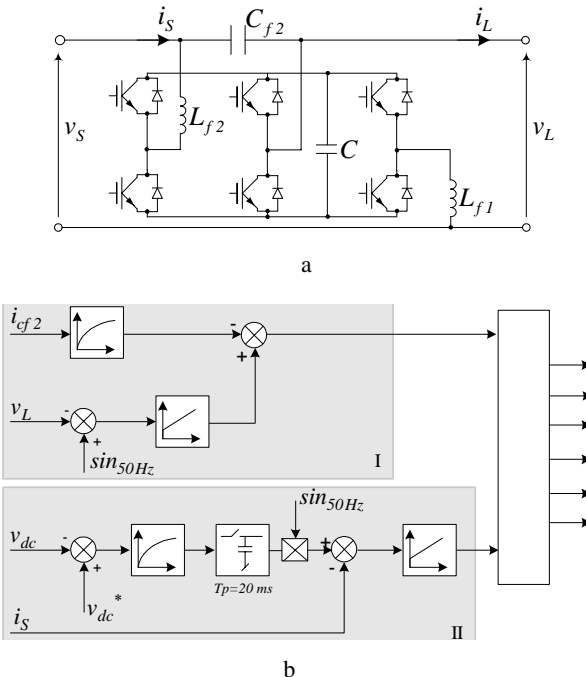


**Figure 6.20.** a. single phase transformer-less UPQC; b. its control algorithm

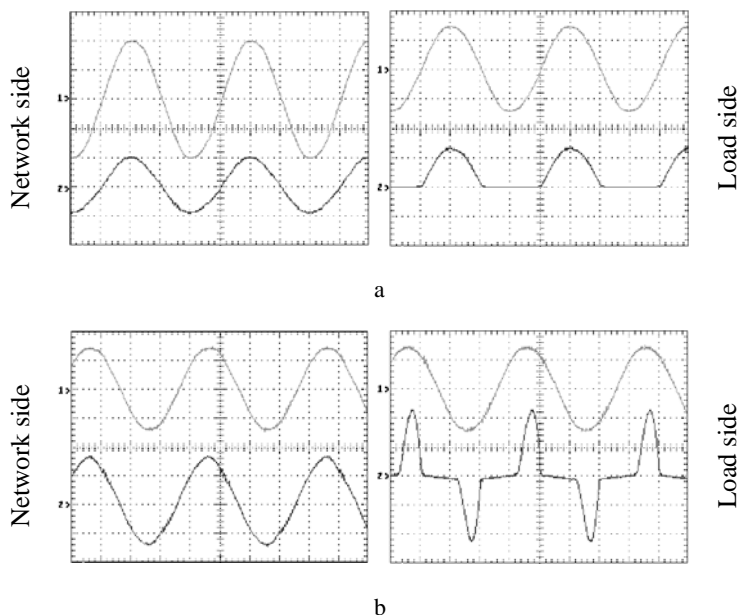


**Figure 6.21.** Experimental waveforms: a. one pulse rectifier; b. two pulse rectifier with capacitor filter; Ch1:50V/div  $\Rightarrow$  voltage; Ch2:1A/div  $\Rightarrow$  current; time 5ms/div

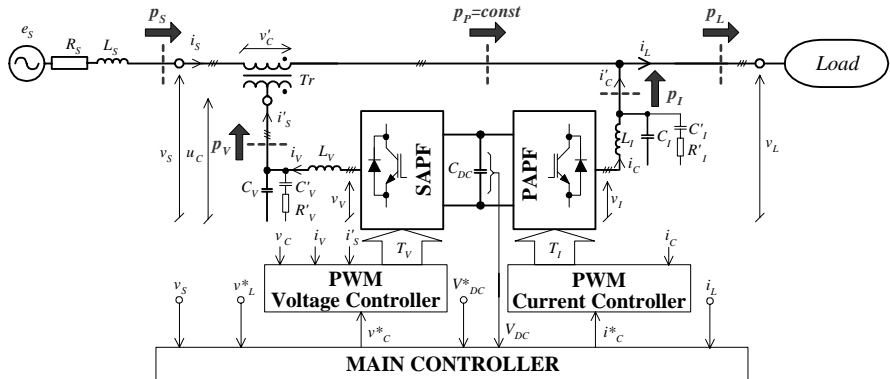
**Table 6.2.** Experimental results

	THD [%]			
	$i_S$	$v_S$	$i_L$	$v_L$
One pulse rectifier	3.6	1.8	33.1	2.1
Two pulse rectifier	3.4	1.8	80.2	2.4

To verify the properties of the proposed solution a scaled down hardware model, with parameters presented in Table B.2 (Appendix B), was developed. Study of the courses presented in Figure 6.21 and the data in Table 6.2 it is possible to say that the examined device fulfils its functions: network current becomes sinusoidal, even in the case of a strongly deformed load current; load voltage becomes stabilized in the situation of network voltage magnitude variations.

### 6.2.2 Three Phase UPQC

The 3-phase UPQC presented in Figure 6.22 consists of series and parallel active power filters, connected by a common DC circuit [92]. SAPF -  $v'_C$  voltage source - filters harmonics and stabilizes at point of measurement the load voltage  $v_L$ , during network voltage  $v_S$  changes and deformations. PAPF -  $i'_C$  current source - filters passive components in the load current  $i_L$ . Small filters,  $L_V - C_V$  as well as  $L_I - C_I$  (along with dumping circuits  $R'_V - C'_V$  as well as  $R'_I - C'_I$ ) provide filtration of the harmonics related to PWM control.

**Figure 6.22.** Scheme of the investigated UPQC

The main controller controls  $V_{DC}$  voltage and on the basis of measured instantaneous  $i_L$ ,  $v_S$  values as well as references  $V^*_{DC}$  and  $v^*_L$ , calculates the reference current  $i^*_C$  and voltage  $v^*_C$  waves. Calculations are realized in  $d-q$  coordinates, rotating with frequency  $\omega_S=2\pi/T_S$ , where:  $T_S$  - period of the network voltage. Unsettling in active power balance

$$\int_{t-T_S}^t p_V dt = - \int_{t-T_S}^t p_I dt , \quad \int_{t-T_S}^t p_S dt = \int_{t-T_S}^t p_P dt = \int_{t-T_S}^t p_L dt$$

causes  $V_{DC}$  voltage changes, thus to stabilize this voltage, in  $i_C$  current the controller forces an additional component, in phase with  $v_I$  voltage (in  $d-q$  coordinates this is most often a periodic wave). Unfortunately application of the  $d-q$  coordinates in arrangements with passive elements causes through couplings. In this case simple control in relation to one coordinate has an impact on waves in the second coordinate. To eliminate this unfavourable phenomenon, controllers have to realize the decoupling function. The manner of decoupling is explained by the model discussed in Appendix D.

### *Slow Processes in DC Circuit*

To investigate the slow dynamic processes, the simplified model introduced in Figure 6.23 suffices [92]. This model differs from the full one (introduced in Appendix D), through replacement of the SAPF and PAPF individual models and controllers, and by ideal compensating voltage and current sources. When  $d-q$  coordinates are suitably synchronized with the network voltage, the main controller by principle of operation can exclude the appearance of some current and voltage components in UPQC arrangement

$$\tilde{i}_{Sd} = 0, \tilde{i}_{Sq} = 0, \bar{i}_{Sd} = 0, \tilde{v}_{Ld} = 0, \tilde{v}_{Lq} = 0, \bar{v}_{Lq} = 0, \bar{v}_{Sq} = 0$$

where  $\bar{v}, \bar{i}$  concerns constant and  $\tilde{v}, \tilde{i}$  pulsation components of currents and voltages.

Considering the above, and in accordance with accepted symbols, instantaneous power  $p_{DC}$  delivered to the DC link, can be determined on the basis of the following dependency [92]

$$\begin{aligned} p_{DC} &= \underbrace{\bar{i}_{Sd} (\bar{v}_{Sd} + \tilde{v}_{Sd} - \bar{v}_{Ld})}_{-p_V} + \underbrace{\bar{v}_{Ld} (\bar{i}_{Sd} - \bar{i}_{Ld} - \tilde{i}_{Ld})}_{-p_I} = \\ &= \underbrace{(\bar{i}_{Sd} \bar{v}_{Sd} - \bar{v}_{Ld} \bar{i}_{Ld})}_{\Delta P_0} + \underbrace{(\bar{i}_{Sd} \tilde{v}_{Sd} - \tilde{i}_{Ld} \tilde{v}_{Ld})}_{\Delta P_\sim} \end{aligned} \quad (6.2)$$

The instantaneous active power  $p_{DC}$  can be decoupled on two components:  $\Delta P_0$  as well as  $\Delta P_\sim$ , because of their different influence on changes of  $V_{DC}$  voltage, during steady states as well as transients.

*Steady states.* During steady states, component  $\Delta P_0 = 0$ , and pulsation frequencies in periodic component  $\Delta P_\sim$  depend only on harmonics, network voltage asymmetry and load current. Let us consider that the  $\Delta P_\sim$  component is a superposition of two sinusoidal waves, with frequencies  $\tilde{\omega}_U$  and  $\tilde{\omega}_I$

$$\Delta P_\sim \approx P_L [K_{SU} \sin(\tilde{\omega}_U t) - K_{SI} \sin(\tilde{\omega}_I t + \varphi_{L/S})] \quad (6.3)$$

where  $\varphi_{L/S}$  – phase shift between waves;  $K_{SU}$ ,  $K_{SI}$  – coefficients determining influence of every sinusoidal wave on  $\Delta P_\sim$  component;  $P_L$  – average load active power.

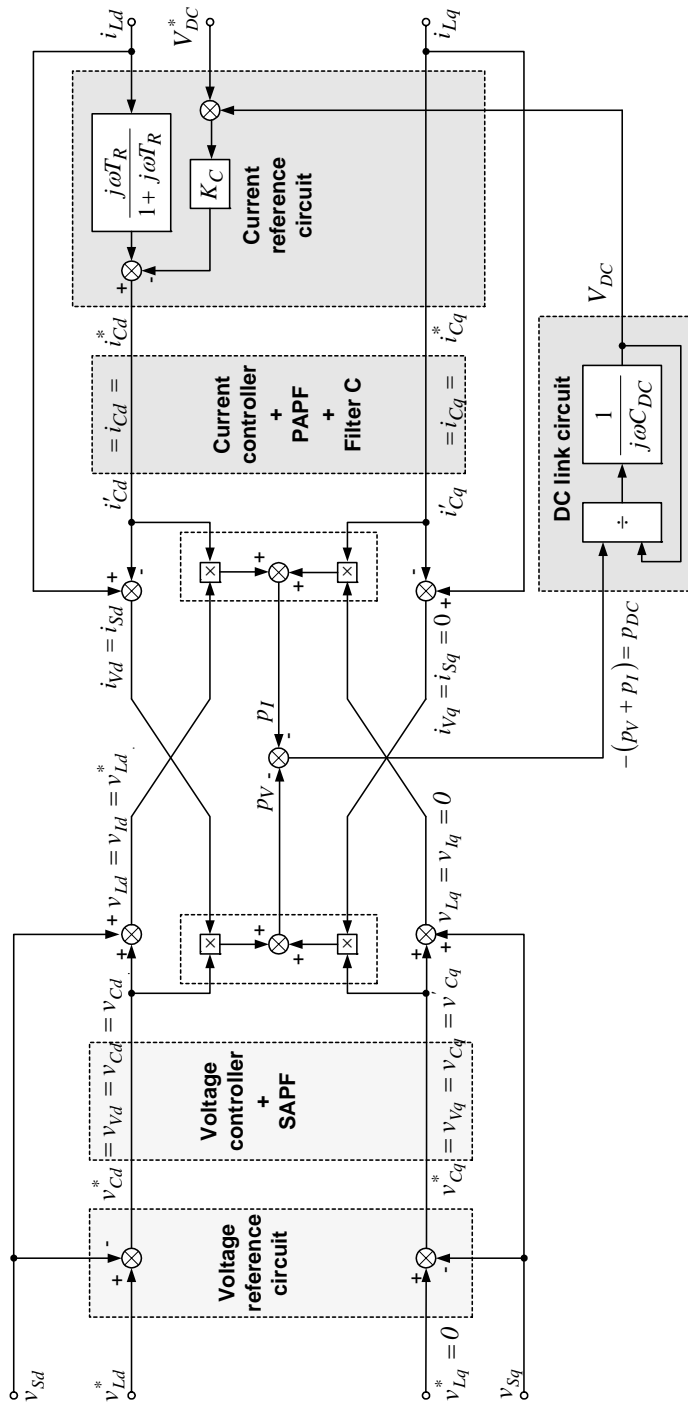


Figure 6.23. UPQC simplified model, with ideal voltage and current adding sources

In our case

$$C_{DC} \cdot V_{DC} \frac{dV_{DC}}{dt} = P_{DC} \quad (6.4)$$

and on the base of the following Equations 6.2 and 6.3 we obtain

$$\frac{C_{DC}}{2} [V_{DC(max)}^2 - V_{DC(min)}^2] \leq 2P_L \left( \frac{K_{SU}}{\tilde{\omega}_U} + \frac{K_{LI}}{\tilde{\omega}_I} \right) \quad (6.5)$$

where  $V_{DC(min)}$  – respectively minimum,  $V_{DC(max)}$  – maximum,  $C_{DC}$  capacitor voltage.

Taking into consideration that  $V_{DC}^* = (V_{DC(max)} + V_{DC(min)})/2$ , and that the  $V_{DC}$  voltage maximum error is  $\Delta V_{DC(max)} = (V_{DC(max)} - V_{DC(min)})/2$ , Equation 6.5 can be rewritten

$$C_{DC} \leq \frac{P_L}{\varepsilon_C V_{DC}^{*2}} \left( \frac{K_{SU}}{\tilde{\omega}_U} + \frac{K_{LI}}{\tilde{\omega}_I} \right) \quad (6.6)$$

where  $\varepsilon_C = \Delta V_{DC(max)} / V_{DC}^*$  -  $V_{DC}$  maximum relative error.

$K_{SU}$  and  $K_{LI}$  coefficients, see Equations 6.3, 6.5 and 6.6 should be quite the same as deformation coefficients of  $v_{Sd}$  and  $i_{Ld}$  waves

$$K_{SU} = V_{SD} / V_{SP} ; \quad K_{LI} = I_{LD} / I_{LP} \quad (6.7)$$

where

$$V_{SP}^2 = \frac{1}{2\pi} \int_0^{2\pi} (\bar{v}_{Sd}(\vartheta))^2 d\vartheta ; \quad V_{SD}^2 = \frac{1}{2\pi} \int_0^{2\pi} (\tilde{v}_{Sd}(\vartheta))^2 d\vartheta$$

$$I_{LP}^2 = \frac{1}{2\pi} \int_0^{2\pi} (\bar{i}_{Ld})^2 d\vartheta ; \quad I_{LD}^2 = \frac{1}{2\pi} \int_0^{2\pi} (\tilde{i}_{Ld}(\vartheta))^2 d\vartheta$$

$\tilde{\omega}_U$  and  $\tilde{\omega}_I$  are chosen as the lowest frequencies, in the spectrum of components  $\tilde{v}_{Sd}$  and  $\tilde{i}_{Ld}$ .

$C_{DC}$  capacitor, determined on the base of Equation 6.6, should be inflated in reference to its value required for correct operation during steady states. More exact results are given by weighed ratios, considering the full spectra of  $v_{Sd}$  and  $i_{Ld}$  courses, although in practice their determination is not required. Mostly  $C_{DC}$  capacitor is determined by the transient states, during load active power step changes and/or network voltage amplitude variations.

*Transient states.* Let us consider that in a UPQC load an active power step change  $\Delta P_L$  occurred (e.g. additional load was turned on). For constant voltage  $v_{Ld} = \bar{v}_{Ld} = const$  and with higher harmonic omission, this change is identified as

load current increase  $\Delta \bar{i}_{Ld} = \Delta P_L / v_{Ld}$ . When the reference current circuit is applied, as it is in Figure 6.23, changes in compensating current  $i_{Cd}$  are following wave

$$\Delta \bar{i}_{Cd} = \frac{\Delta P_L}{v_{Ld}} e^{-\frac{t}{T_R}} + K_C \cdot \Delta V_{DC} \quad (6.8)$$

where  $K_C$  - gain of the  $V_{DC}$  voltage  $P$  regulator.

Because  $i_{Ld} = i_{Sd} + i_{Cd}$ , thus changes of compensating currents, see Equation 6.8, create also the network current changes

$$\Delta \bar{i}_{Sd} = \frac{\Delta P_L}{v_{Ld}} \left( I - e^{-\frac{t}{T_R}} \right) - K_C \cdot \Delta V_{DC} \quad (6.9)$$

Simultaneously with this change, considering Equations 6.2 and 6.9, also component  $\Delta P_+$  in instantaneous power  $p_{DC}$ , changes

$$\Delta P_+ = \Delta P_L \cdot (\mu_v - 1) - \mu_v \cdot \Delta P \cdot e^{-\frac{t}{T_R}} - K'_C \cdot \Delta V_{DC} \quad (6.10)$$

where  $\mu_v = v_{Sd} / v_{Ld}$ ;  $K'_C = v_{Ld} \cdot \mu_v \cdot K_C$ .

On the basis of Equation 6.4 which defines DC link capacitor voltage balance (linearized around  $V_{DC}^*$ ), and considering Equation 6.10 as well as assuming without loss of generality  $\mu_v=1$ , we have

$$\Delta V_{DC} = -\frac{\Delta P_L}{K'_C} \cdot \frac{T_R}{(T_R - T_C)} \cdot \left( e^{-\frac{t}{T_R}} - e^{-\frac{t}{T_C}} \right) \quad (6.11)$$

where  $T_C = C_{DC} V_{DC}^* / K'_C$ .

On the base of Equation 6.11 one can say, that voltage  $\Delta V_{DC} = V_{DC} - V_{DC}^*$  changes are function with one extreme, which occurs after time  $t_{sup} = T_C T_R \ln T_R / T_C / (T_R - T_C)$ .

Putting  $t_{sup}$  to Equation 6.11 we have

$$|\Delta V_{DC(max)}| < \frac{|\Delta P_L| \cdot T_R}{C_{DC} \cdot V_{DC}^* + K'_C \cdot T_R} \quad (6.12)$$

Equation 6.12 in a practical and simple way permits the evaluation of the influence of the main controller's  $T_R$  and  $K_C$  coefficients, reference  $V_{DC}^*$  voltage,  $C_{DC}$  capacitor and load power  $\Delta P_L$  step changes, (on  $V_{DC}$  voltage maximum deviations  $\Delta V_{DC(max)}$ ).  $\Delta V_{DC(max)}$  changes, as the function of  $\Delta P_L$  increases,

calculated on the basis of Equation 6.12 as well as experimental data, are compared in the following section.

$C_{DC}$  capacitor, determined on the basis of equation

$$C_{DC} < \frac{T_R}{V_{DC}^*} \cdot \frac{|\Delta P| - K'_C \cdot |\Delta V_{DC(max)}|}{|\Delta V_{DC(max)}|}. \quad (6.13)$$

guarantees that  $V_{DC}$  voltage will not exceed the acceptable range of changes. A theoretically possible negative  $C_{DC}$  value is the result of linearization of Equation 6.3. In practice however, from the point of view of the required small  $\Delta V_{DC(max)}$  deviations as well as  $K'_C$  limited value, determined with regard to sensor ratio, such a negative value is not possible. Finally,  $C_{DC}$  capacitor should be selected taking into consideration the worst cases, as the largest value from two calculated on the basis of Equation 6.6 as well as 6.13.

### Experimental Results

In Figure 6.24, one can see the laboratory setup to investigate the UPQC device. In the arrangement, a simple main controller (Figure 6.23) with type  $P$  regulator for voltage  $V_{DC}$  control was applied. The selected parameters and adjustments of the laboratory model are introduced in Table B.3 (Appendix B). Further, presented are the results which occurred during steady states and transients and those showing UPQC power flow control capabilities.

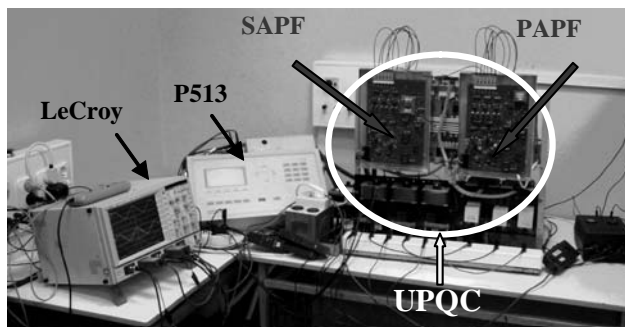
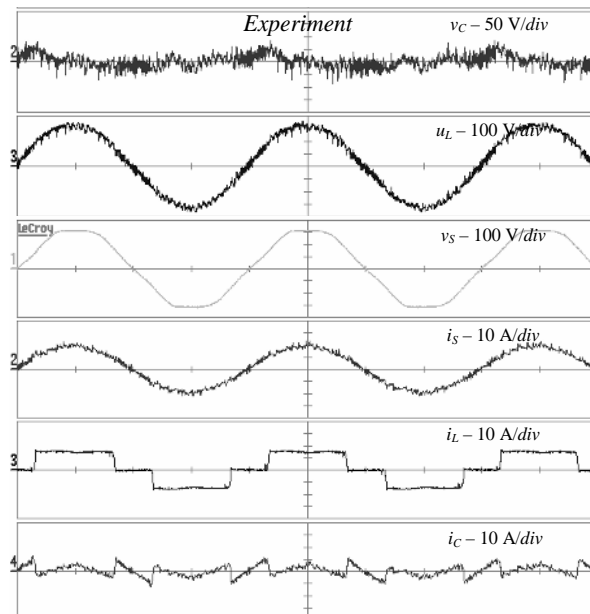


Figure 6.24. Experimental model to the UPQC

*Steady state results.* In Figure 6.25, the exemplary experimental current and voltage courses, illustrating UPQC steady state filtration capabilities, were introduced.

The experimental courses concern the case of an arrangement loaded with controlled 7kW, 6-pulse rectifier ( $\alpha=0^\circ$ ,  $THD(I_L) \approx 28\%$ ) and supplied with deformed network voltage, distortion coefficient  $THD(V_S) \approx 9\%$ . In this case both, network current  $i_S$  as well as load voltage  $v_L$  are practically sinusoidal.

UPQC filtration properties depend only to a small degree on load power (Figure 6.26). For small loads the  $THD(I_S)$  coefficient increases because of enlarged



**Figure 6.25.** Experimental courses in respect to network voltage and load current harmonics filtration

participation of harmonics, with frequencies related to the PWM triangular carrier in PAPF controller. On the other hand, in the case of large loads the  $THD(V_L)$  coefficient increases because of voltage drop on impedance of the adding transformer. This voltage drop is caused by the uncompensated load current harmonics.

Load changes mainly infect the PAPF and SAPF nominal powers (Figure 6.27). In the general case PAPF nominal power depends on distortion power, reactive

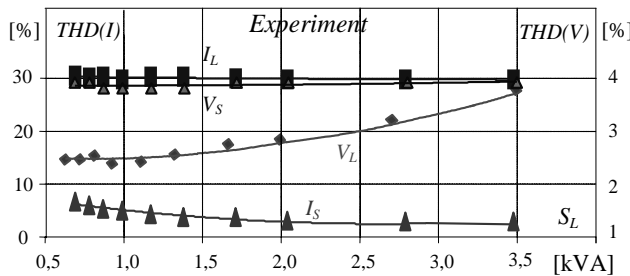


**Figure 6.26.** Current and voltage THD coefficients as a function of load apparent power ( $\alpha=0^\circ$ )

power and load asymmetry power, additionally SAPF nominal power depends on active components of the load current, deformations and asymmetry of the network voltage. Experimental dependencies, introduced in Figure 6.27, concern the case

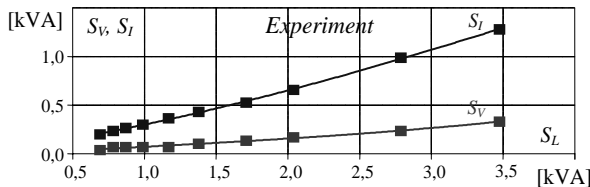


**Figure 6.27.** SAPF ( $S_V$ ) and PAPF ( $S_I$ ) nominal powers as a function of load apparent power ( $\alpha=0^\circ$ )

when the UPQC is loaded with a *6-pulse* rectifier and supplied with sinusoidal ( $THD(V_S) \approx 4\%$ ), symmetrical, nominal voltage.

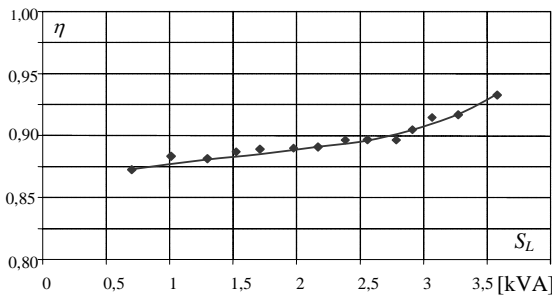


**Figure 6.28.** UPQC efficiency as a function of load apparent power ( $\alpha=0^\circ$ )

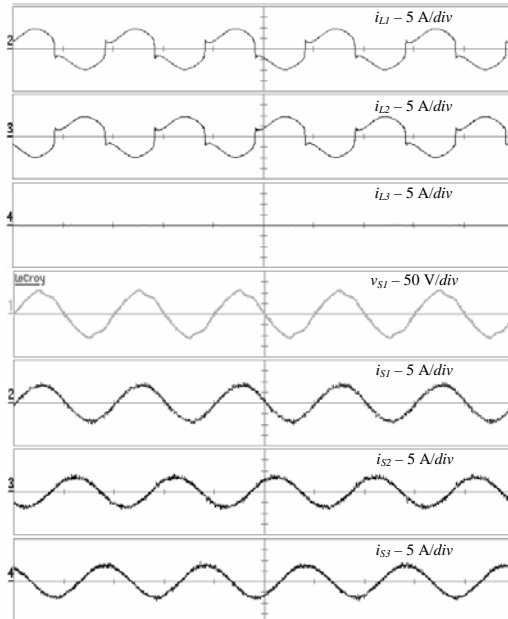


**Figure 6.29.** Experimental courses in situation of symmetric supply and non-linear and asymmetric load

The nominal powers, albeit to a small degree, depend on SAPF and PAPF efficiency. With increasing load power, participation of losses in nominal power decreases. The same dependency concerns, in an obvious way, the efficiency of the whole UPQC (Figure 6.28).

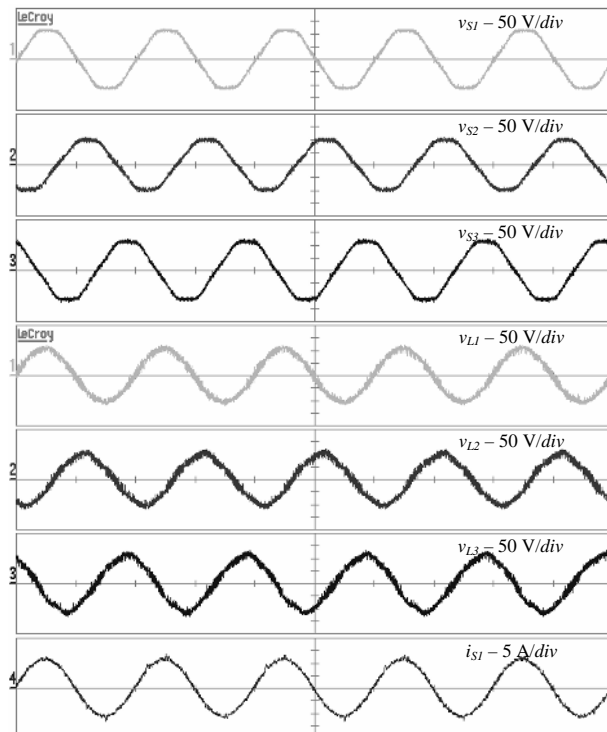


**Figure 6.30.** Experimental courses in situation of asymmetric supply and symmetric resistive load

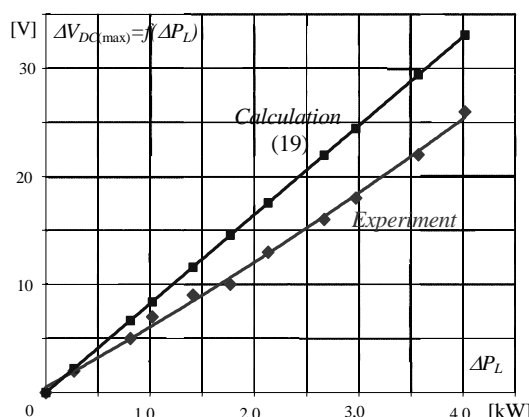


**Figure 6.31.**  $\Delta V_{DC(max)}$  voltage deviations as a function of  $\Delta P_L$  increases

Steady states in the experimental investigations contained also an estimation of UPQC potential for load current as well as network voltage symmetrization. Investigations were carried out in the case of lowered network (supply) voltage. As the asymmetric load two, 2-pulse rectifiers, 1.1kVA each, were used. The asymmetric network (supply) voltage was obtained with the assistance of three independent autotransformers. Exemplary current and voltage courses are introduced in Figure 6.29 and Figure 6.30.

*Transient state results.* Experimental verification of Equation 6.13 was the major aim of the investigations reported in this section. During theoretical calculations the following values were considered:  $T_R=10ms$  and  $K_C=1V/V$ , nominal network voltage  $V_S=220V$ , the reference DC link voltage  $V_{DC}^*=610V$ . In

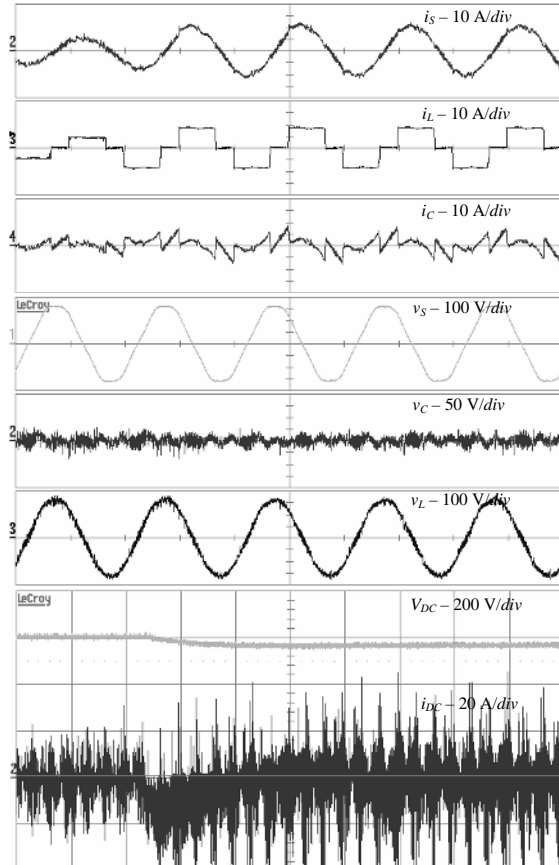


**Figure 6.32.** Experimental courses in the case of harmonics filtration and load step changes  $\Delta P_L$ , from 4kW to 8kW

the laboratory model the  $V_{DC}$  voltage sensor ratio was  $\mu_u=0.052$ . Allowing the maximum DC link voltage deviation  $\Delta V_{DC(max)}=30V$  and load active power step ( $\Delta t=0$ ) changes  $\Delta P_L < \Delta P_{L(max)}=4kW$ , calculated  $C_{DC}$  capacitance totalled  $1850\mu F$ .

In the laboratory model, from a practical point of view, the value  $C_{DC}=1650\mu F$  was applied. The results of calculations and experimental investigations, presented in Figure 6.31 and Figure 6.32, were obtained for this smaller capacitor.

*Additional functions – power flow control.* UPQC can be successfully used for power flow control [25, 92]. Considering the problem cognitively, a power flow controller can generally be represented as a Synchronous Voltage Source (SVS), with frequency dependent on the network voltage frequency. An SVS should have the possibility of controlling its voltage: amplitude, in range  $0 \leq V_C \leq V_{Cmax}$ , and angle  $\gamma$

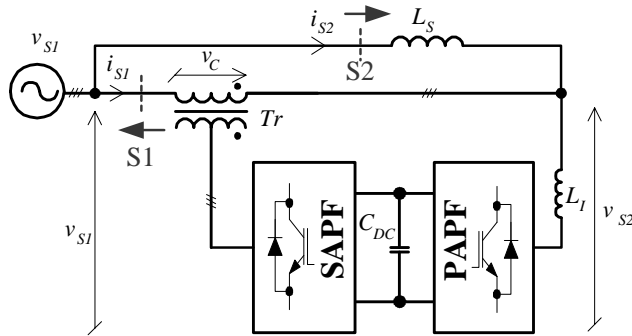


**Figure 6.33.** Connection scheme for investigation of UPQC capabilities of power flow control

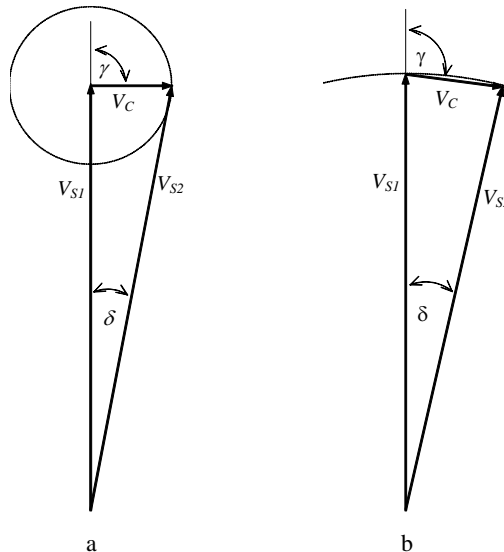


**Figure 6.34.** Vector diagrams for verification power flow control methods: a. 1<sup>st</sup> method; b. 2<sup>nd</sup> method

in the limits:  $0 \leq \gamma \leq 2\pi$ . Figure 6.33 presents a connection scheme for the investigation of UPQC power flow control capabilities. In UPQC, a SAPF

exchanges with the transmission line active power (series active compensation) and reactive power (series reactive compensation), because of which it is possible to control power flow. However, active power exchange, which mostly affects reactive power in the transmission line, is related to active power consumption from the DC link. Therefore the major role of PAPF is to stabilize the  $V_{DC}$  voltage.

A UPQC, behaving as power flow controller, can be controlled in accordance with two rules, presented in Figure 6.34. The vector diagram in Figure 6.34.a introduces a situation when added voltage has constant amplitude  $V_C=const$ , and in this case only angle  $\gamma$  is changed in the range  $(0 \div 2\pi)$ . Such a technique of control causes, however, variable voltage load  $V_{S2}$ . If voltage  $V_{S2}$  has to be stabilized, UPQC should be controlled in accordance with the rule introduced in Figure 6.34.b. In this case, amplitude of the  $V_C$  adding voltage as well as  $\delta$  angle are changed.

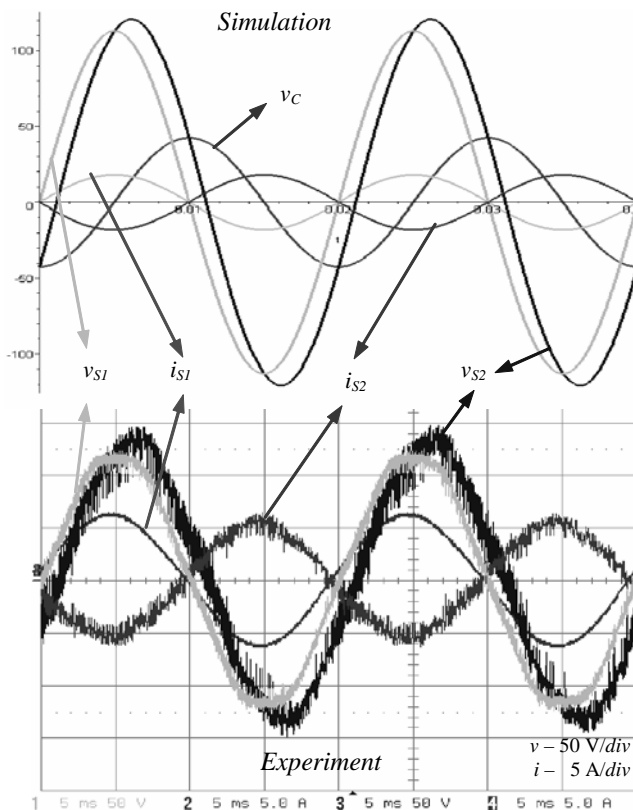


**Figure 6.35.** Simulation and experiment for 1<sup>st</sup> method as in Figure 6.34.a

In Figure 6.35 simulation and experimental voltage and current courses for a UPQC working in accordance with the rule from Figure 6.34.a, were introduced. As one can see, experimental and simulation results agree, however such control causes changes in  $V_{S2}$  load voltage. The characteristics of the changes in active and

reactive power as a function of variable  $\gamma$  angle are presented in Figure 6.36. As one can see, the characteristics confirm the UPQC power flow control capabilities.

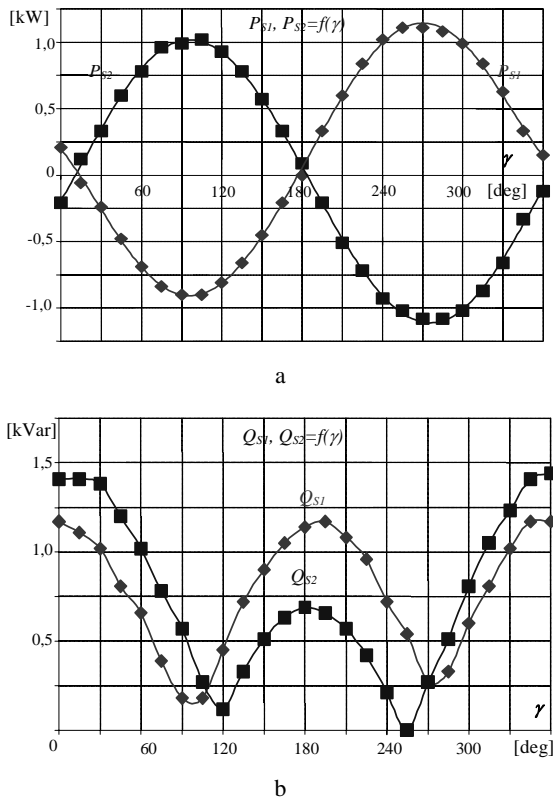


**Figure 6.36.** a. active power; b. reactive power; measured at  $S1$  and  $S2$  points for 1<sup>st</sup> method

In Figure 6.37 simulation and experimental voltage and current courses, for a UPQC arrangement working in accordance with the rule from Figure 6.34.b, were introduced. As one can see the experimental and simulation results are the same. Characteristics of the changes of active and reactive power as a function of variable  $\delta$  angle are presented in Figure 6.38. The second method of control is equivalent to the situation when SAPF exchanges with the transmission line mainly the reactive power (series reactive compensation). In consequence, predominantly in the transmission line, the active power is changed, and the range of reactive power control is smaller than in first case.

Summarizing, the results of both analyses (theoretical and experimental) confirm good compensating proprieties as well as multi-functionality of the UPQC. The investigated arrangement simultaneously permits the fulfilment of the following functions: voltage and current harmonics filtration, network voltage and load current symmetrization as well as network voltage stabilization and power flow control.

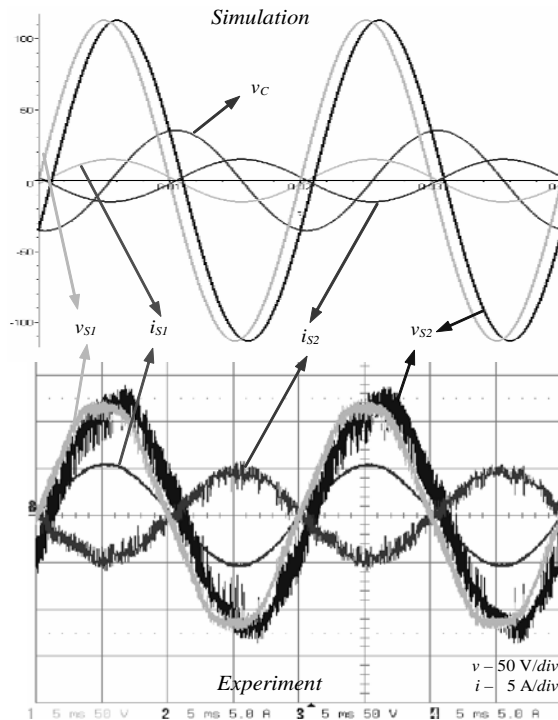


**Figure 6.37.** Simulation and experiment for 2<sup>nd</sup> method as in Figure 6.34.b

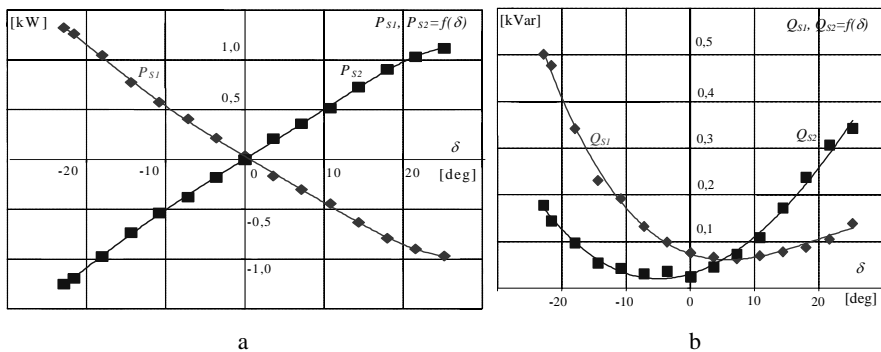


**Figure 6.38.** a. active power; b. reactive power; measured at S1 and S2 points for 2<sup>nd</sup> method

### 6.3 Voltage Source Custom Power Systems

In the professional literature there are described many different ways to “isolate” a network from disturbances introduced by nonlinear loads and *vice versa*. For example to filter out higher harmonics from currents, produced by the nonlinear loads, PAPF could be used [70-84]. In these devices there is a need to extract

compensating components from the measured currents. Therefore the filtration quality is as good as well this is possible to extract compensating components and to shape them.

VAPF [99-118] and SVAPF [109, 115, 119] present a different way for power quality improvement. Generally in VAPF there is no need to measure load or network currents, or to extract any compensating components, the PQ improvement is possible because the parallel connected VSC acts as a sinusoidal voltage source with fundamental frequency ( $50Hz$ ). A quite similar way for power quality improvement is represented by the SVAPF device which additionally possesses the extra current source; therefore it is possible to overcome some limitations of the VAPF devices, which will be described later in this chapter. Because on the whole VAPF and SVAPF have to “produce” fundamental frequency sinusoidal voltage, multilevel converters could be the perfect solution for both arrangements.

### 6.3.1 Voltage Active Power Filter

The basic equivalent circuit of a VAPF is presented in Figure 6.39 [99, 104]. In this solution the sine wave voltage source  $v_S$  is connected in parallel with the load. Next, the series inductance  $X_S$  connects the network voltage  $v_S$  to the rest of the arrangement. the general function of the voltage source  $v_V$  is the removal of the distortions produced by the load from the network, as well as removal of the load from the distortions generated by the network. The separation is possible because stabilized and sinusoidal  $v_V$  voltage, shifted with angle  $\gamma_0$  with regard to

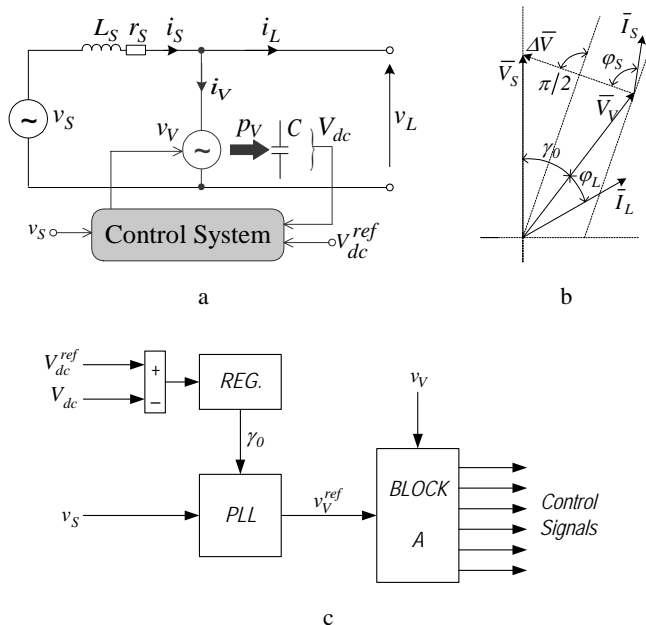


**Figure 6.39.** VAPF: a. one line scheme; b. vector diagram; c. simplified control algorithm

the network voltage  $v_S$ , secures sinusoidal and almost in phase with voltage  $v_S$  network current  $i_S$  ( $v_V$  voltage source absorbs in the natural way current harmonics produced by the load) and also stabilized and sinusoidal load voltage.

In the simplified control algorithm, *PLL* generates signal  $v_V^{ref}$  whose frequency is equal to that of the network and whose phase is shifted in relation to  $v_S$  with angle  $\gamma_0$  proportional to the load active power  $P_L$ . Block *A* stabilizes load voltage at the reference value by means of a closed-loop control error between the  $v_V$  and the reference voltage  $v_V^{ref}$ . To keep total DC link voltage on constant value regulator *REG* was implemented.

*Harmonics separation.* The VAPF equivalent circuits for different conditions are presented in Figure 6.40 [110]. In those circuits  $X_{Sh}$  represents the series reactance for higher harmonics and  $v_{Vh}$  represents VSC output voltage in conditions of distorted network voltage  $v_{Sh}$ . Additionally  $i_{Sh}$  and  $i_{Lh}$  represent respectively network and load current higher harmonics.

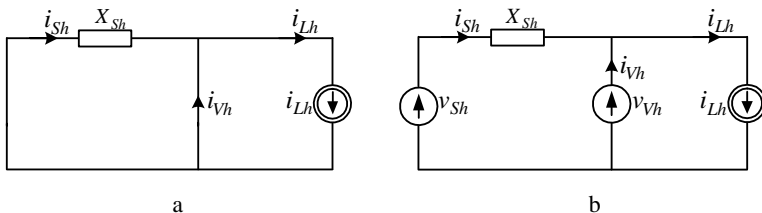


**Figure 6.40.** VAPF equivalent circuits for higher harmonics in the case of: a. sinusoidal network voltage; b. distorted network voltage

Inspection of the Figure 6.40a clearly shows that neglecting both sinusoidal sources:  $v_S$  and  $v_V$ ; and because  $X_{Sh} > 0$ , the load current is given by  $i_{Lh} = i_{Vh}$ . Therefore, the compensation characteristics to load can be written as

$$\frac{i_{Sh}}{i_{Lh}} \rightarrow 0 \quad (6.14)$$

On the basis of above one can conclude that the VAPF under consideration has the effect of “separating” the network from the non-linear loads.

In the case of distorted network voltage (see Figure 6.40.b), when VSC – except sinusoidal with fundamental frequency – produces also higher harmonics components just to meet the condition  $v_{Sh} = v_{Vh}$ , then the load current is given by  $i_{Lh} = i_{Vh}$  and the VAPF acts as early “separation” of the network from the non-linear loads, see Equation 6.14.

*Reactive power compensation.* In case when  $V_V$  and  $V_S$  amplitudes are the same ( $V_V = V_S = V$ ) and neglecting  $r_s$ , the angle between network voltage  $\bar{V}_S$  and current  $\bar{I}_S$  is  $\gamma_0/2$ , and in consequence the input power factor  $PF_S$  is not unity. On the basis of the above the input power factor can be defined [104, 115]

$$PF_S = \sin\left(\frac{\gamma_0}{2} + \varphi_S\right) \underset{r_s \rightarrow 0}{\approx} \cos(\gamma_0/2) = \cos\left(\frac{1}{2} \arcsin \frac{P_L}{P_{max}}\right) \quad (6.15)$$

where  $P_{max} = V^2 / (\omega L_S)$ .

Figure 6.41 presents the relation between the input power factor  $PF_S$  and the load active power  $P_L$  for different  $P_{max}$  (in relation to the reference power  $P_{U(max)}$ ). Examining the curves below one can see that in decreasing  $P_L$ , input power factor  $PF_S$  increases. Additionally, only in the case of very slight loads is it possible to reach  $PF_S$  near unity.

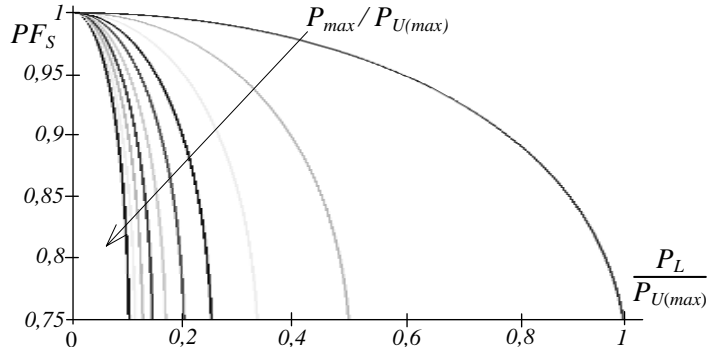


**Figure 6.41.** Relation between  $PF_S$  and  $P_L$ ; where:  $P_{max}/P_{U(max)}=1/10, 2/10, \dots, 1$

Power factor improvement can be reached, for example, by increasing  $V_V$  voltage amplitude above the network voltage  $V_S$  and shifting angle  $\gamma_0$  to a new value  $\gamma'_0$  just to keep the following rule true,  $P_S = P_L = \text{const}$  (*Case 1*). On the basis of the above and the assumption  $r_s \rightarrow 0$  one can define the following [115]

$$V'_{V rms} = V_{S rms} \sqrt{1 + \sin^2 \gamma'_0} ; \gamma'_0 = \arcsin \left( \sin \gamma_0 / \sqrt{1 + \sin^2 \gamma_0} \right) \quad (6.16)$$

Another case is also possible, *i.e.*, when maintaining unity the input power factor load active power is variable (*Case 2*). Then voltage produced by the VAPF

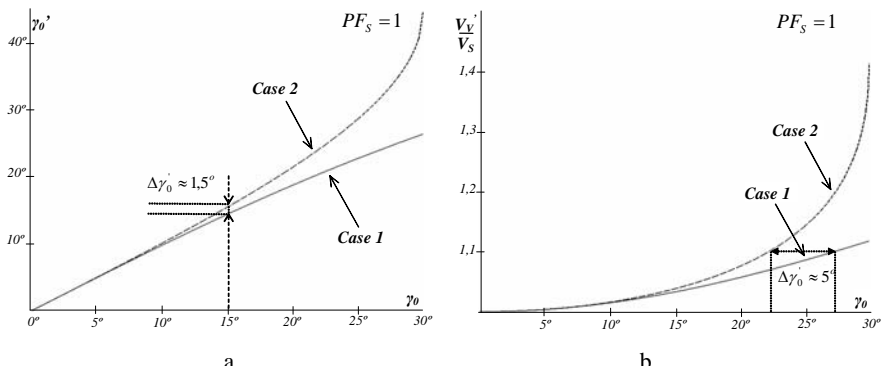


**Figure 6.42.** Changes of the: a. angle  $\gamma'_0$ ; b. voltage  $V_V$

could be defined by equations [115]

$$V'_{V_{rms}} = V_{S_{rms}} \left/ \cos\left(\frac{\arcsin(2 \sin \gamma_0)}{2}\right)\right.; \gamma'_0 = \frac{\arcsin(2 \sin \gamma_0)}{2} \quad (6.17)$$

Examining the above dependencies and curves in Figure 6.42 one can claim that for low  $\gamma_0$  angles both cases are pretty much the same. Increasing  $\gamma_0$  value above  $15^\circ$ ,  $\gamma'_0$  in Case 1 is evidently lower, and in consequence  $V_V$  voltage and reactive power exchanged between VAPF and the supply network are lower.

However there are some difficulties implementing the above equations in practice. For the most desirable Case 1, it is possible to reach  $PF_S=1$  and  $P_L=const$  if in the control algorithm orthogonal voltage  $\bar{V}_{Vq}$  is added to the reference voltage  $\bar{V}_V^{ref}$ , as it is in Figure 6.43.

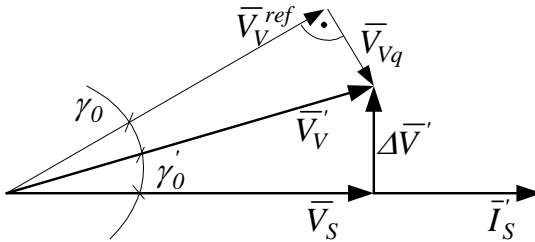


**Figure 6.43.** Input power factor correction

#### Slow Processes in DC Circuit

During steady states (neglecting losses in the VAPF) angle  $\gamma_0$  corresponds to the real power supplied by the network [104]. In this case instantaneous power exchanged by the VAPF varies in accordance with the dependency

$$p_V(t) = Q_V \sin(2\omega t + 2\gamma_0) \quad (6.18)$$

Thus the variable component of the energy accumulated on  $C$  capacitor is expressed by the equation

$$\tilde{A}E = \int p_V(t) dt = -\frac{Q_V}{2\omega} \cos(2\omega t + 2\gamma_0) \quad (6.19)$$

On the basis of the above we obtain the following equation

$$|\Delta E_{max}| = C \cdot (V_{dc(max)}^2 - V_{dc(min)}^2) / 2 = Q_V / \omega \quad (6.20)$$

where  $\Delta E_{max}$  – peak-to-peak changes of energy accumulated on  $C$  capacitor;  $V_{dc(max)}$ ,  $V_{dc(min)}$  – respectively maximum and minimum values of  $V_{dc}$  voltage.

Taking into consideration that the reference *DC* circuit voltage is

$$V_{dc}^{ref} = \left( V_{dc(max)} + V_{dc(min)} \right) / 2 \quad (6.21)$$

Equation 6.20 can be expressed as

$$|\Delta E_{max}| = Q_V / \omega = 2 \cdot C \cdot \varepsilon_{V_{dc}} \cdot V_{dc}^{ref^2} \quad (6.22)$$

$$\text{where } \varepsilon_{V_{dc}} = \Delta V_{dc} / V_{dc}^{ref}; \Delta V_{dc} = \left( V_{dc(max)} - V_{dc(min)} \right) / 2.$$

Assuming that VAPF is connected to the linear load with  $\cos(\varphi_L)$  power factor and considering that during steady states  $P=P_S=P_L$ , VAPF reactive power demands can be calculated

$$Q_V = P_{max} \left( 1 + S - \sqrt{1 - \chi^2} + \chi \cdot \operatorname{tg}(\varphi_L) \right) \quad (6.23)$$

$$\text{where } P_{max} = V_S \cdot V_V / X_S, S = V_V - V_S / V_S, \chi = P / P_{max}.$$

Thus the *DC* circuit capacitor, determined on the base of equation

$$C \geq P_{max} \frac{\left( 1 + S - \sqrt{1 - \chi^2} + \chi \cdot \operatorname{tg}(\varphi_L) \right)}{2 \cdot \omega \cdot \varepsilon_{V_{dc}} \cdot V_{dc}^{ref^2}} \quad (6.24)$$

$$\text{where } V_{dc}^{ref} \geq \left[ \sqrt{2} \cdot (I + S) \cdot V_S \right] / (I - 2 \cdot \varepsilon_{V_{dc}});$$

guarantees, that  $V_{dc}$  voltage will not exceed the acceptable range of changes. In practice, from the point of view of transient states as well as non-linear loads, one should choose  $C$  larger than the one resulting from Equation 6.24.

#### VAPF Stability Analysis

The following equations describe VAPF device [109, 118]

$$L_S di_S / dt + r_S i_S = v_S - v_V, i_V = i_S - i_L, p_V = v_V i_V, CV_{dc} dV_{dc} / dt = p_V \quad (6.25)$$

Assuming that VAPF is connected to the linear  $R_L-L_L$  load and considering that  $v_L = v_V$  one can write

$$L_L di_L / dt + R_L i_L = v_L \quad (6.26)$$

Because  $V_{dc}$  voltage fluctuations cause changes of the  $\gamma_0$  angle once per  $T=N\pi/\omega$  ( $N=1, 2, \dots$ ) inching, thus in every  $k^{th}$  period the VAPF generates voltage

$$v_{V(k)} = v_{V(k)}^{ref} = V \sin(\omega t - \gamma_0(k)) \quad (6.27)$$

with amplitude  $V$ , and angle

$$\gamma_{0(k)} = K_D (\varepsilon_{(k)} - \varepsilon_{(k-1)}) + K_P \varepsilon_{(k)} + K_I \sum_{i=0}^k \varepsilon_{(i)}, \quad \varepsilon_{(k)} = \varepsilon(kT) = \int \delta(t - kT) \varepsilon(t) dt \quad (6.28)$$

where  $\varepsilon = V_{dc}^{ref} - V_{dc}$  - DC capacitor voltage error;  $K_D$ ,  $K_P$ ,  $K_I$  - PID regulator coefficients.

On the basis of Equations 6.25 to 6.28, assuming that  $v_S = V \sin(\omega t)$  and  $v_V = V \sin(\omega t - \gamma_0)$ , the linearized equivalent impulse model can be defined by the following dependencies

$$\Delta I_{S(k)} = (A_S)^N \Delta I_{S(k-1)} + \Delta \gamma_{0(k)} B_S [(-1)^N - (A_S)^N] \quad (6.29a)$$

$$\Delta I_{L(k)} = (A_L)^N \Delta I_{L(k-1)} - \Delta \gamma_{0(k)} B_L [(-1)^N - (A_L)^N] \quad (6.29b)$$

$$\begin{aligned} \Delta E_{(k)} = & \Delta I_{S(k-1)} C_S [I - (-A_S)^N] - \Delta I_{L(k-1)} C_L [I - (-A_L)^N] + \\ & + \Delta \gamma_{0(k)} \{N \cdot D - B_S C_S [I - (-A_S)^N] - B_L C_L [I - (-A_L)^N]\} \end{aligned} \quad (6.29c)$$

where  $C_S = V \frac{\sin \varphi_S \sin(\varphi_S - \gamma_0)}{\omega}$ ,  $A_S = e^{-\frac{\pi}{tg \varphi_S}}$ ,  $C_L = V \frac{\sin \varphi_L \sin(\varphi_L - \gamma_0)}{\omega}$ ,  
 $A_L = e^{-\frac{\pi}{tg \varphi_L}}$ ,  $B_S = V \frac{\cos(\varphi_S + \gamma_0)}{Z_S}$ ,  $B_L = V \frac{\cos(\varphi_L + \gamma_0)}{Z_L}$ ,  $D = V^2 \frac{\pi \sin(\varphi_S - \gamma_0)}{2 \omega Z_S}$ ;

and on the basis of above the equivalent circuit diagram is presented in Figure 6.44 [109, 113, 118].

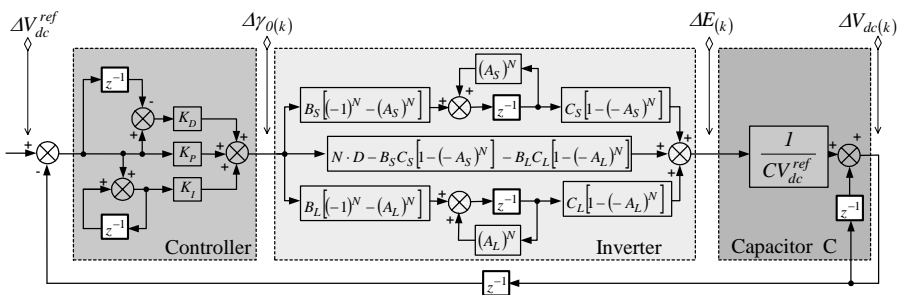


**Figure 6.44.** VAPF-the equivalent impulse diagram

Because in practice  $L_S$  inductor's magnification factor  $D_R$  is considerable ( $D_R \geq 12$ ), the following can be accepted  $A_S \approx 1$ ,  $\cos \varphi_S \approx 0$  and  $\sin \varphi_S \approx 1$  (for example if  $\varphi_S = 85^\circ$  then  $A_S \approx 0.76$ ,  $\sin \varphi_S > 0.996$  and  $\cos \varphi_S < 0.088$ ) and  $B_S$ ,  $C_S$ ,  $D$  coefficients are as follows

$$B_S \approx -V \frac{\sin \gamma_0}{\omega L_S}, \quad C_S \approx V \frac{\cos \gamma_0}{\omega}, \quad D \approx V^2 \frac{\pi \cos \gamma_0}{2\omega^2 L_S} \quad (6.30)$$

Additionally, when analyzing loads with  $\varphi_L < 45^\circ$ , the coefficient  $A_L < 0.044 \approx 0$  and remaining coefficients are

$$D \approx P_{max} \frac{\pi \sqrt{\ell^2 - 1}}{\omega \ell}, \quad B_S C_S \approx -D \frac{2}{\pi \ell}, \quad B_L C_L \approx P_{max} \frac{2 \operatorname{tg} \varphi_L}{\omega \ell} \left( \frac{\operatorname{tg} \varphi_L}{1 + \operatorname{tg}^2 \varphi_L} - \frac{\sqrt{\ell^2 - 1}}{\ell^2} \right) \quad (6.31)$$

where  $\ell = P_{max}/P_L$  - load factor.

Furthermore, assuming that VAPF is connected to the resistive load, then product  $B_L C_L = 0$  and the simplified equivalent impulse diagram of the VAPF with proportional regulator is presented in Figure 6.45.

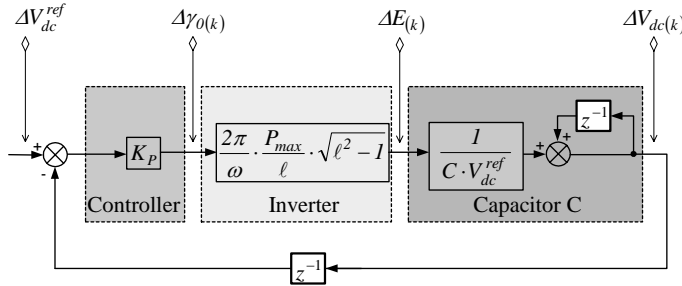


**Figure 6.45.** VAPF – the simplified equivalent impulse diagram

On the basis of the above the closed system transfer function is as follows

$$G_{VAPF}(z) = \frac{z \cdot K_p \frac{2\pi}{\omega} \frac{P_{max}}{\ell} \sqrt{\ell^2 - 1} \frac{I}{C \cdot V_{dc(0)}}}{z - \left( 1 - K_p \frac{2\pi}{\omega} \frac{P_{max}}{\ell} \sqrt{\ell^2 - 1} \frac{I}{C \cdot V_{dc(0)}} \right)} \quad (6.32)$$

Depending on the above, the  $K_p$  coefficient determined on the base of the following equation

$$K_p \leq \omega \cdot \ell \cdot C \cdot V_{dc(0)} / \left( \pi \cdot P_{max} \cdot \sqrt{\ell^2 - 1} \right) \quad (6.33)$$

guarantees that VAPF will be stable.

#### *Single Phase VAPF – Experimental Results*

To verify properties of the VAPF device a down scaled hardware model, presented in Figure 6.46, with parameters collected in Table B.4 (Appendix B), was

developed. In this circuit, a two level PWM modulation VSC as  $v_V$  voltage source was implemented with a  $\Gamma$  passive filter on its output.

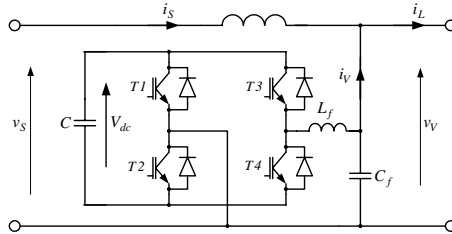


**Figure 6.46.** Single phase VAPF

Additionally Figure 6.47 presents a control diagram [104, 110, 115]. To regulate the *DC* circuit voltage a *PI* controller was implemented which uses error between the reference  $V_{dc}^{ref}$  and the actual *DC* voltage  $V_{dc}$  as a feedback signal. Next the control algorithm generates a signal  $v'_V$  whose frequency is equal to that of the network and whose phase is shifted in relation to  $v_s$  with angle  $\gamma_0$  proportional to the load active power  $P_L$ . The reference load voltage is secured by means of a closed-loop control error between the  $v_V$  and the reference voltage  $v'_V$ .

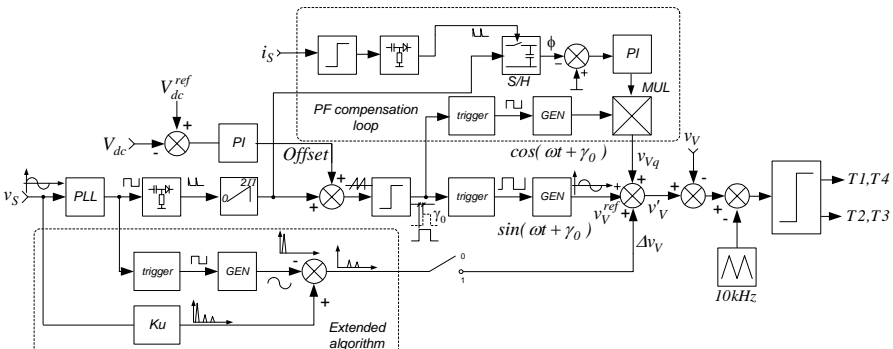


**Figure 6.47.** Control diagram

In the case of distorted network voltage  $v_s$ , to avoid network current distortion, there is a need to use an extended algorithm. The extended part has to extract from the distorted network voltage the unneeded components and add to the already shifted basic component (at frequency 50Hz) of the network voltage. Unfortunately this solution leads to distorted load voltage.

In the figures below experimental waveforms obtained for two different load types, linear (resistive-inductive) and non-linear (two pulse rectifier with capacitor filter), are presented. Figure 6.48 illustrates VAPF behaviour in the case of linear (resistive) load. It can be seen that the device under consideration only to a slight degree changes network current and its influence can be additionally diminished through an extended control algorithm (because of distorted network voltage).

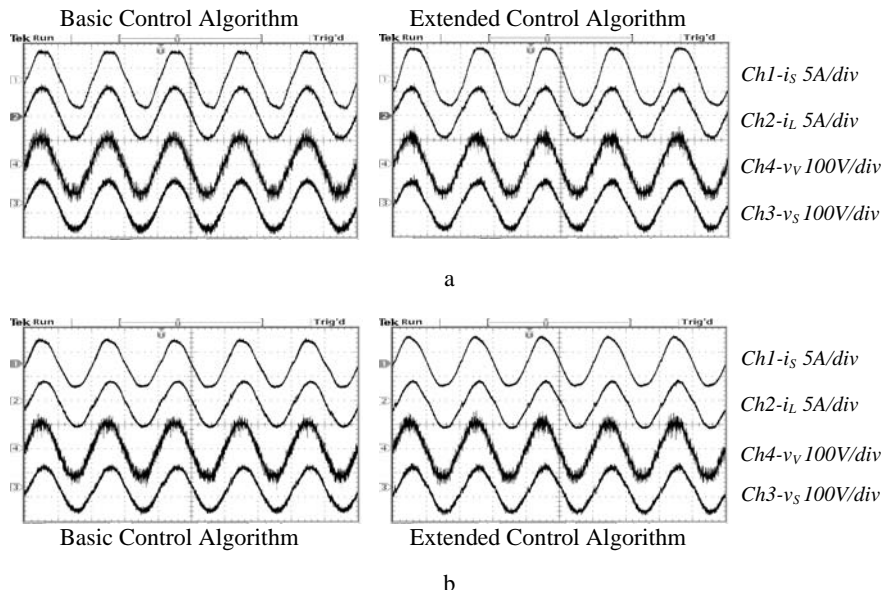


**Figure 6.48.** Experimental waveforms ( $\Delta t=10ms/div$ ) for linear load: a.  $P_L=0.4kW$ ; b.  $P_L=1kW$

Figure 6.49 and Figure 6.50 demonstrate the harmonics separation capability. As one can see, the load current contains a large amount of harmonics due to a two pulse rectifier with capacitor filter; however the network current is sinusoidal. Because of distorted network voltage the extended control algorithm can additionally improve the shape of the network current.

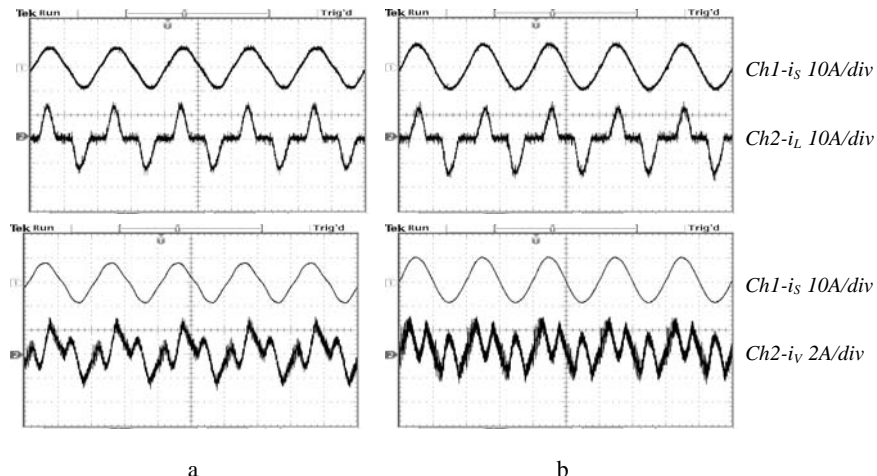


**Figure 6.49.** Experimental waveforms ( $\Delta t=10ms/div$ ) for non-linear load  $P_L=1kW$ : a. basic control algorithm; b. extended control algorithm

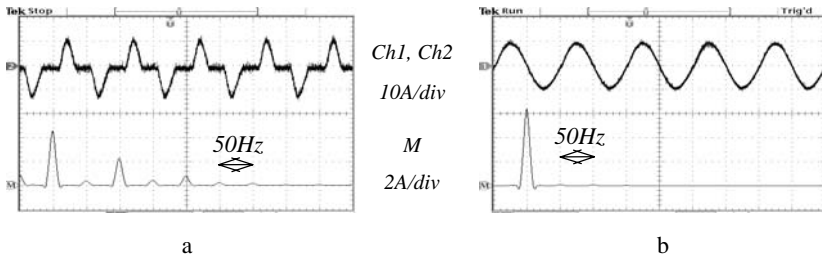


**Figure 6.50.** Experimental waveforms ( $\Delta t=10ms/div$ ) and spectrum for non-linear load  $P_L=1kW$  (extended control algorithm): a. load current; b. network current

Additionally Table 6.3 collects THD coefficients at characteristic points of the VAPF device.

**Table 6.3.** THD coefficient; in parentheses, values obtained for extended control algorithm

Load		THD [%]			
		$i_S$	$v_S$	$i_L$	$v_V=v_L$
Linear	0.4kW	13.7 (9.9)	3.6 (6.1)	2.8 (6.3)	4.5 (7.7)
	1kW	7.9 (5.9)	5.6 (9.2)	4.4 (5.9)	9.1 (15.6)
Non-linear	0.4kW	11.2 (3.5)	5.1 (6.1)	60.0 (60.8)	8.0 (8.6)
	1kW	7.7 (3.5)	5.2 (6.6)	44.0 (45.0)	8.6 (8. 8)

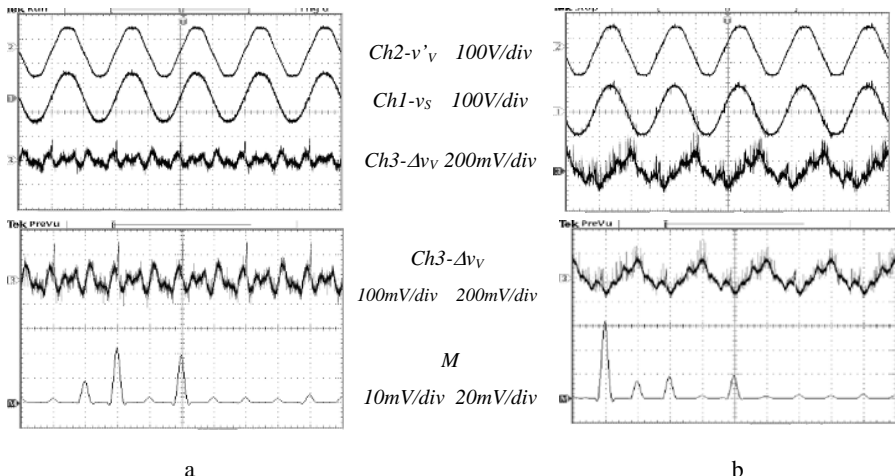


**Figure 6.51.** Experimental waveforms ( $\Delta t=10ms/div$ ) and spectrum in case of network voltage magnitude variations; non-linear load  $P_L=1kW$  (extended control algorithm): a. nominal network voltage; b. reduced network voltage

Figure 6.51 demonstrates arrangement capabilities in the case of the network voltage magnitude variations. It can be observed that in the situation of nominal amplitude, the extended part generates only signal  $\Delta v_V$  proportional to the network voltage higher harmonics, however in the case of variable amplitude (3% under nominal value) the algorithm additionally generates a basic frequency component and thus secures stabilized load voltage.

For the linear load  $P_L=1kW$  angle between network voltage  $\bar{V}_S$  and current  $\bar{I}_S$  is  $\varphi_S=9^\circ$  the input power factor  $PF_S$  is 0.98. However activating the power factor compensation loop and thus increasing  $V_V$  voltage amplitude 1.3% above  $V_S$  voltage amplitude, increases this value to unity, see Figure 6.52.

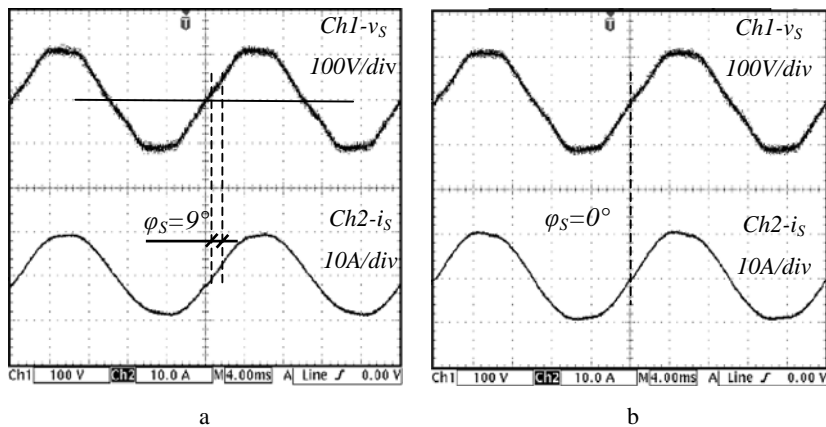


**Figure 6.52.** VAPF – input power factor correction ( $\Delta t=4ms/div$ ): a. without PFS coorection; b. with PFS coorection

*Dynamic properties verification.* Transient results obtained by generating a step change in the linear load, are shown in Figure 6.53. From calculations made for the experimental arrangement:  $\ell = 5$ ,  $\omega = 3141/s$ ,  $P_{max} = 2kW$ ,  $C = 2 \cdot 10^{-3}F$ ,  $V_{dc}^{ref} = 180V$ ,

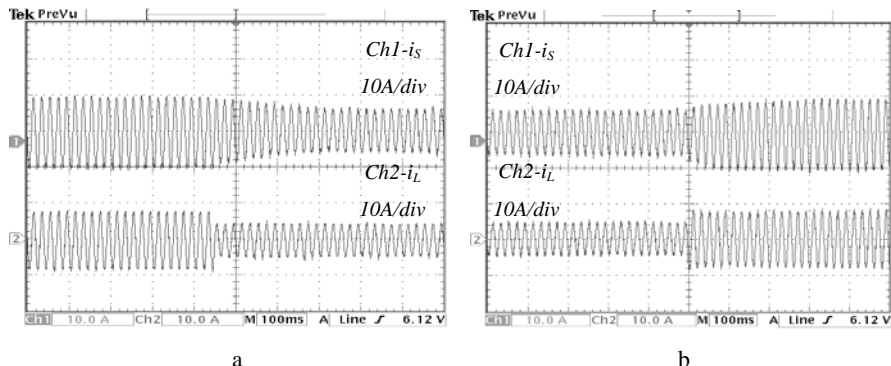


**Figure 6.53.** VAPF – behaviour during linear load changes ( $\Delta t=100ms/div$ ): a. decreased load; b. increased load

on the basis of Equation 6.53 it occurred that  $K_P \leq 0.018$ , however in practice  $K_P=0.01$  was accepted. Experimental results confirm that a previously presented stability analysis methodology is suitable for VAPF device.

### Three Phase Multilevel VAPF – Experimental Results

To verify properties of the three phase VAPF device a down scaled hardware model with parameters collected in Table B.5 (Appendix B), was developed. In this circuit, a four level cascaded multilevel converter (see Figure 6.6) as  $v_V$  voltage source was implemented. During the study  $DC$  voltages were even,  $V_{dc1}=V_{dc2}=V_{dc3}=V_{dc4}$ , and on the converter's output a  $\Gamma$  passive filter was implemented.

This time the control algorithm can be divided into two major parts. The first one generates signal  $v'_V$  shifted in relation to  $v_V$  with angle  $\gamma'_o$  proportional to the load active power  $P_L$ , as it was for a single phase device. Thus during steady state the total  $V_{dc}$  voltage is constant, and in consequence the average active power exchanged between VAPF and network is zero (on the assumption that commutation losses are diminished) [104, 111, 112, 115].

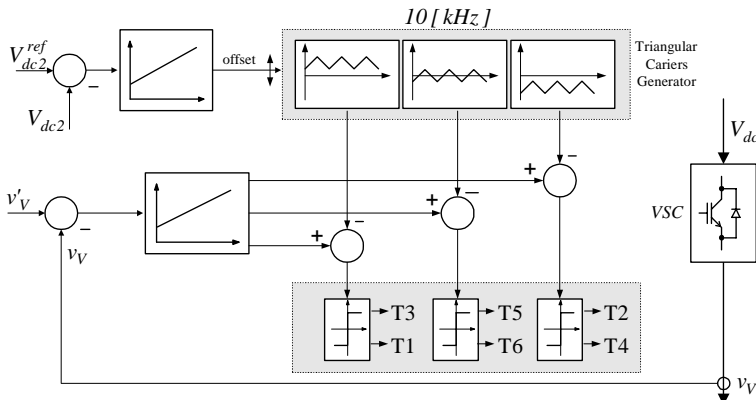
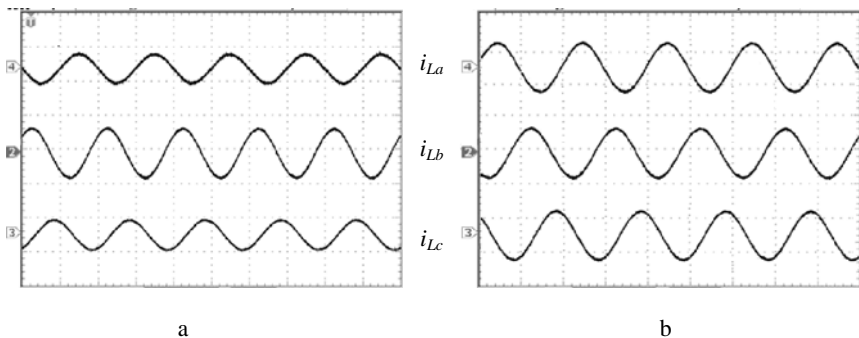


**Figure 6.54.** Algorithm for balancing  $DC$  voltages (phase a)

As stated earlier,  $\gamma'_o$  angle changes have an impact on the real power absorbed or supplied by the VAPF, thus it is possible to regulate the total  $DC$  voltage. However to avoid the problem of unbalanced voltages on the selected capacitors ( $V_{dc2}$ ,  $V_{dc3}$  and  $V_{dc4}$ ) the control algorithm has to be equipped with an additional second part, see Figure 6.54. The second part secures constant and balanced voltages  $V_{dc2}$ ,  $V_{dc3}$  and  $V_{dc4}$  as a result of a variable switching strategy of the transistors. A changeable switching strategy can be achieved adding a suitable constant component to the triangular carriers (this does not cause changes on the converter's output voltages and currents). The required constant component can be obtained from comparison of the reference voltage, in phase  $a$  that will be  $V_{dc2}^{ref}$ , with the actual measured value  $V_{dc2}$ . The constant component obtained in this manner shifts the triangular waves and in this way changes the switching strategy which finally leads to equalization of the  $DC$  voltages. Additionally in [163, 169], the appropriate

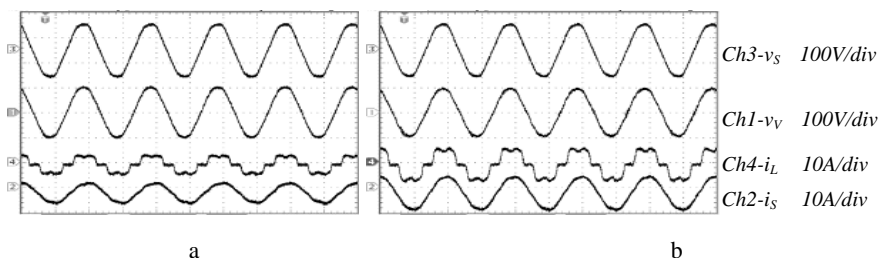
methods to avoid problems of unbalanced *DC* voltages for other types of multilevel converters are introduced.

In the figures below experimental waveforms obtained for two different load types, linear (*R-L* load) and non-linear (6-pulse rectifier with *R-L* load), are presented.



**Figure 6.55.** Experimental current waveforms ( $\Delta t=10\text{ ms/div}, 10\text{ A/div}$ ) for linear unbalanced load: a. load side; b. network side

Figure 6.55 demonstrates the arrangement's capability for balancing the network in conditions of unbalanced loads. Because VAPF produces sinusoidal balanced voltages, network currents are, therefore, also balanced. This condition is satisfied whether the load currents are balanced or not, because the network currents are determined only by the network voltages, the  $v_V$  voltage as well as  $X_S$  reactance. However in conditions of unbalanced loads,  $i_V$  currents are also unbalanced which results in a 100Hz component in *DC* voltages.

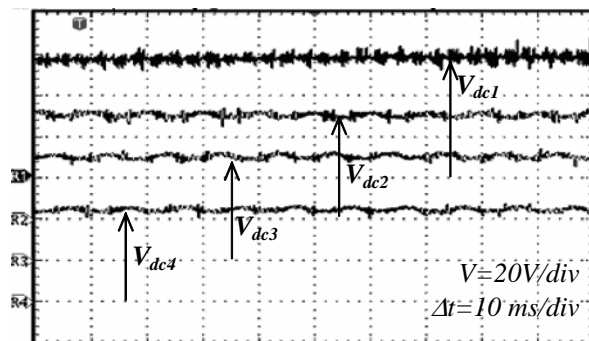


**Figure 6.56.** Experimental waveforms ( $\Delta t=10\text{ ms/div}$ ) for non-linear balanced load: a.  $P_L=0.8\text{kW}$ ; b.  $P_L=1.2\text{kW}$

Figure 6.56 demonstrates the harmonics separation capability. As one can see the load current contains a large amount of harmonics due to the six pulse rectifier with resistive-inductive load; however the network current is almost sinusoidal. Additionally Table 6.4 presents the THD coefficients at characteristic points of the of the VAPF device.

**Table 6.4.** THD coefficients

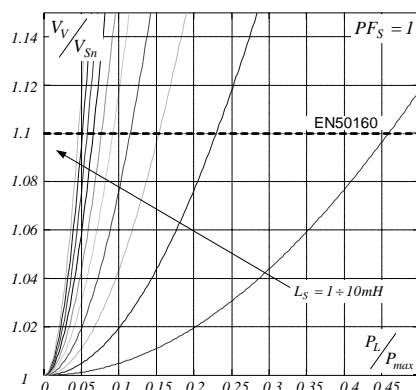
		THD [%]			
		$i_S$	$v_S$	$i_L$	$v_V=v_L$
Non-linear load	$P_L=0.8[kW]$	3.3	3.3	25.3	2.9
	$P_L=1.2[kW]$	2.6	3.5	24.2	3.7

**Figure 6.57.** DC voltages

Furthermore Figure 6.57 demonstrates, in the case of the non-linear balanced load, DC voltages.

### 6.3.2 Symmetrical Voltage Active Power Filter

As stated earlier in this chapter the VAPF among various properties (see Table 6.5) secures unity input power factor  $PF_S$  by increasing  $V_V$  voltage amplitude above network voltage  $V_s$ . However the major limitation of this method is the maximum-acceptable (defined by the international standards) amplitude of the load voltage.

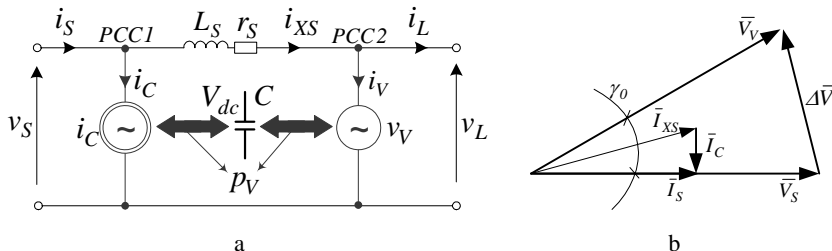
**Figure 6.58.**  $P_L$  possible changes to secure  $PF_S=I$

**Table 6.5.** VAPF – basic properties

Feature	Estimation	Remarks
Input power factor	Unity	Only when voltage $v_V$ is higher than $v_S$ . Range of unity depends on maximum acceptable load voltage amplitude
Network current harmonics separation	Very good	Natural absorption of harmonics generated by the load. Sinusoidal network current only in situation of sinusoidal network voltage $v_S$
Load voltage amplitude stabilization	Not advisable	In the case of network voltage sags and dips considerable growth of input reactive power
Sinusoidal load voltage	Depends on $v_S$	Advisable only in the case of sinusoidal network voltage $v_S$ . In the case of distorted network voltage, network current will be also distorted
Dynamic properties	Fair	Control of energy accumulated on DC capacitor depends on DC voltage control loop

Figure 6.58 shows that for a given series reactance, for the sake of maximum  $V_L$  amplitude, achieving unity input power factor is possible only in a limited range of load changes. Additionally, possible load changes, from the point of view of  $PF_S=1$ , are smaller for higher series reactance values.

A quite similar method of power quality improvement is represented by the SVAPF device, which in comparison with VAPF additionally possesses the extra parallel current source  $i_C$ , as in Figure 6.59 [104, 110, 115, 119]. The suggested structure overcomes the above mentioned limitations of the VAPF devices and secures: constant and unity input power factor (without necessity to increase  $v_V$  voltage above network voltage  $v_S$ ); sinusoidal network current (with no dependency on network voltage shape); stabilized and sinusoidal load voltage (without danger of reactive over-currents during network voltage sags, dips etc.) and improvement of the dynamic properties.

**Figure 6.59.** SVAPF: a. one line scheme; b. vector diagram

The principle of operation of the  $i_C$  current source during steady states (with the following assumptions: voltages  $v_V$  and  $v_S$  have even amplitudes, additionally network voltage is sinusoidal) is explained by the vector diagram in Figure 6.59.

In SVAPF the load is connected in parallel with a controlled sinusoidal voltage source  $v_V$ , which always produces a sinusoidal waveform with amplitude equal to the nominal amplitude of the network voltage  $V_{Sn}$  and angle  $\gamma_0$  just sufficient to allow to flow all the required power thru series inductance  $L_S$  to the load. Because of sinusoidal and stabilized  $v_V$  voltage, it is possible to “isolate” load from all disturbances produced by the network, such as, network voltage dips, sags, or harmonics, as well as to “isolate” the network from disturbances produced by the load, such as, current harmonics, or reactive power. To secure unity input power factor  $PF_S$  the arrangement possess parallel current source  $i_C$  (during steady states the current source exchanges with the network only reactive power; during transients, e.g., source voltage sags, dips etc., there is also exchanged some active power, to improve dynamic properties). Applying sophisticated controls the current source can additionally operate as an active filter and filtrate harmonics in current  $i_{XS}$ , caused by distortions in the network voltage; therefore it is possible to secure sinusoidal load voltage and network current in the case of distorted network voltage.

**Table 6.6.** SVAPF – basic properties

Feature	Estimation	Remarks
Input power factor	Unity	No need to increase amplitude of $V_V$ voltage. Secured by additional parallel current source
Network current harmonics separation	Very good	Natural absorption of the harmonics generated by the load
Load voltage amplitude stabilization	Always when needed	No danger of excessive growth of the input reactive power
Sinusoidal load voltage	Always	No relation to $V_S$ voltage shape
Dynamic properties	Good	Control of energy accumulated on <i>DC</i> capacitor depends on <i>DC</i> voltage control loop and active power supplied by the current source to the common <i>DC</i> link capacitor

One of the most important features of the SVAPF is improvement of the dynamic properties. This is possible because both parallel current and voltage sources possess common a *DC* capacitor, through which it is possible to exchange active power  $p_V$ . Thus, control of the energy accumulated on the *DC* capacitor depends not only on the *DC* voltage control loop as is the case in VAPF but also on the active power supplied by the current source to the common *DC* link capacitor. Selected features of the SVAPF are listed in Table 6.6.

**SVAPF – structure.** The SVAPF presented in Figure 6.60 is built on the basis of one three-phase Intelligent Power Module. Transistors  $T3-T6$  realize voltage source  $v_V$ , however transistors  $T1-T4$  realize current source  $i_C$ . As one can see, transistors  $T3$  and  $T4$  (switched with frequency  $1p.u.$ ) realize the algorithm for both voltage source as well as current source. Therefore to increase precision in shaping the output current produced by the source  $i_C$ , transistors  $T1$  and  $T2$  are switched with a frequency about three times lower ( $0.3p.u.$ ) than the transistors realizing the voltage source [119]. Because both sources possess a common *DC* element (capacitor  $C$ ), with appropriate controls it is, therefore, possible to exchange some active power and hence to improve dynamic properties.

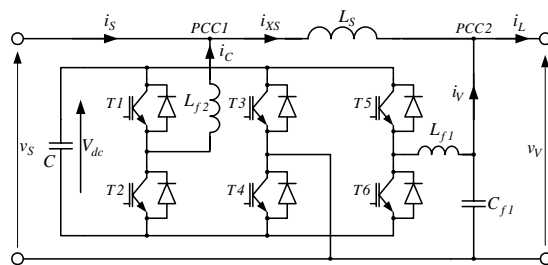


Figure 6.60. Single phase SVAPF

To decrease the component related to commutation, source  $v_V$  on its exit possess a small passive *LC* filter, simultaneously the current source is connected to the network through inductance  $L_{f2}$ .

**SVAPF – control algorithm.** The controller (see Figure 6.61 [119]) consists of three major parts. The first one, at the bottom, determines voltage  $v_V$  with amplitude equal to the nominal amplitude of the network voltage  $V_{Sn}$  and with angle  $\gamma_0$ . Thus angle  $\gamma_0$  is determined on the basis of the energy balance on the *DC* capacitor. When angle  $\gamma_0$  is determined properly, voltage  $V_{dc}$  is constant, and thus consequently the average active power exchanged between voltage source and network is zero (on the assumption that commutation losses are diminished). The second part, at the top, determines the current  $i_C^{ref}$ , which is calculated as the difference between  $i_{XS}$  current (measured on series inductance) and the basic ( $50Hz$ ) active component of the network current  $i_S^{active}$ . The amplitude of the component  $i_S^{active}$  is determined from the *DC* capacitor energy balance rule. In this way the current source acts as an active filter and secures not only unity input power factor but also sinusoidal network current in the case of distorted network voltage. The third part, in the middle, controls the energy flow between parallel current and voltage sources and in this way improves dynamic properties. This is possible because during rapid load changes the *PID* controller, in which the *Derivate* unit is located, determines the additional component. In this situation the control of the energy accumulated on the *DC* capacitor depends not only on the *DC* voltage control loop but also on the active power supplied by the current source.

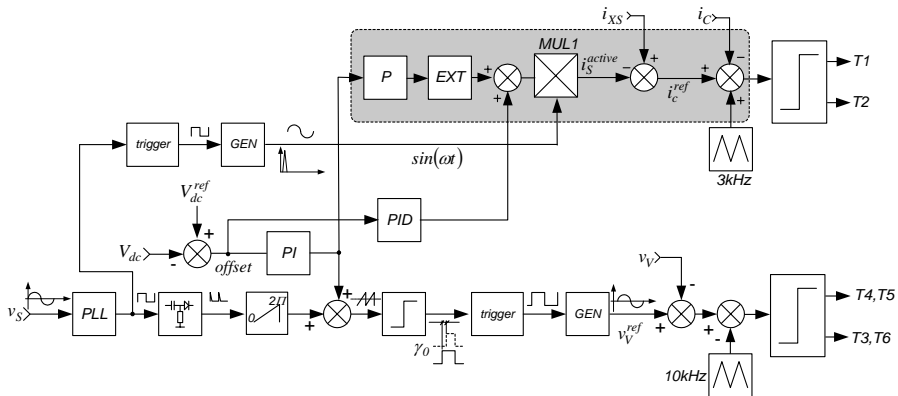
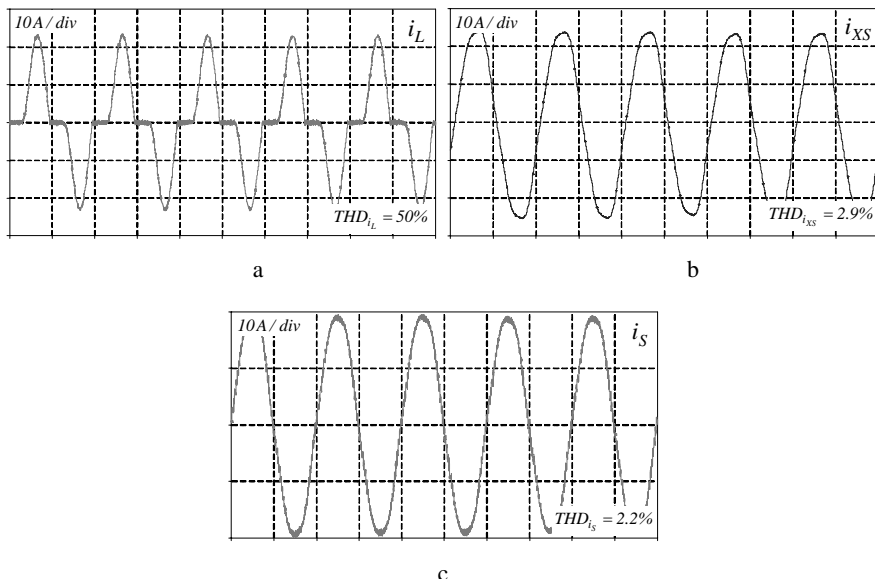


Figure 6.61. Control algorithm

### Single Phase SVAPF – Simulation Results

All simulation investigations were conducted with the parameters presented in Table B.6 (Appendix B), for a non-linear load which was a two pulse rectifier with capacitor filter. Examining the curves in Figure 6.62 one can tell that the load current contains a large amount of harmonics due to the two pulse rectifier with capacitor filter; however the parallel voltage source  $v_V$  secures almost sinusoidal  $i_{xs}$  current ( $THD=2.9\%$ ). Furthermore distortions in  $i_{xs}$ , related to network voltage distortions, can be diminished by the parallel current source  $i_C$ , which also secures unity input power factor.



**Figure 6.62.** SVAPF operation principles,  $P_L=1kW$  ( $\Delta t=10ms/div$ ): a. network current; b. impedance current; c. load current

Additionally observing the results in Figure 6.63 one can see that in both cases, *i.e.*, distorted network voltage below and above its nominal value, the arrangement secures sinusoidal and stabilized load voltage.

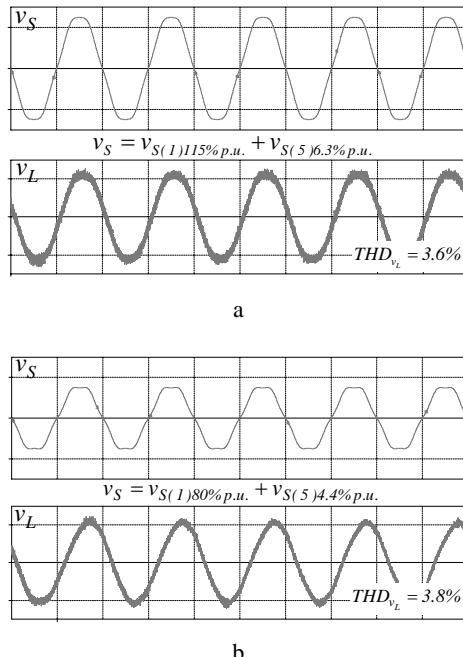


**Figure 6.63.** SVAPF operation principles,  $P_L=1kW$  ( $\Delta t=10ms/div$ ,  $100V/div$ ): a. overvoltage in network voltage; b. undervoltage in network voltage

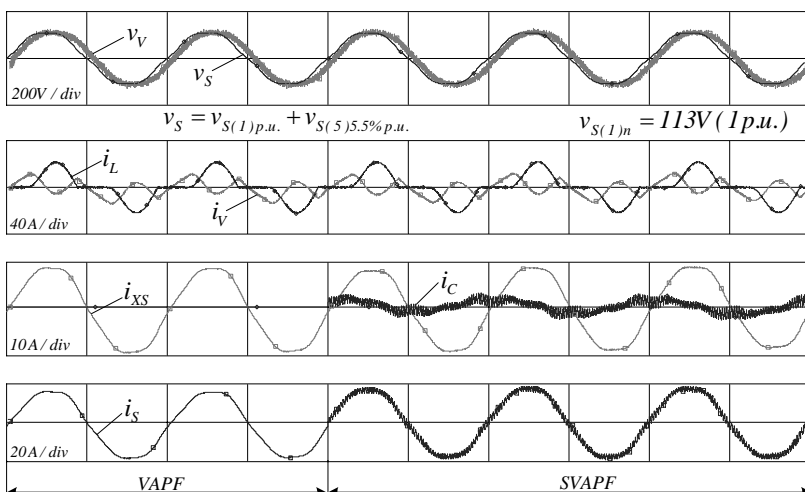


**Figure 6.64.** VAPF and SVAPF operation principles,  $P_L=0.5kW$  ( $\Delta t=10ms/div$ )

Further, observing Figure 6.64 one can claim that if only the  $v_V$  source is turned on (VAPF), it is possible to secure sinusoidal load voltage. Unfortunately network current is not in phase with voltage and, because of distorted network voltage ( $5^{\text{th}}$  harmonic), is also not sinusoidal. Turning on the parallel source  $i_C$  (SVAPF) it is possible to secure both unity input power factor and sinusoidal network current. This is so because  $i_C$  current is perpendicular (capacitive) to the network voltage and possess a higher harmonics component proportional to distortions in the network voltage.

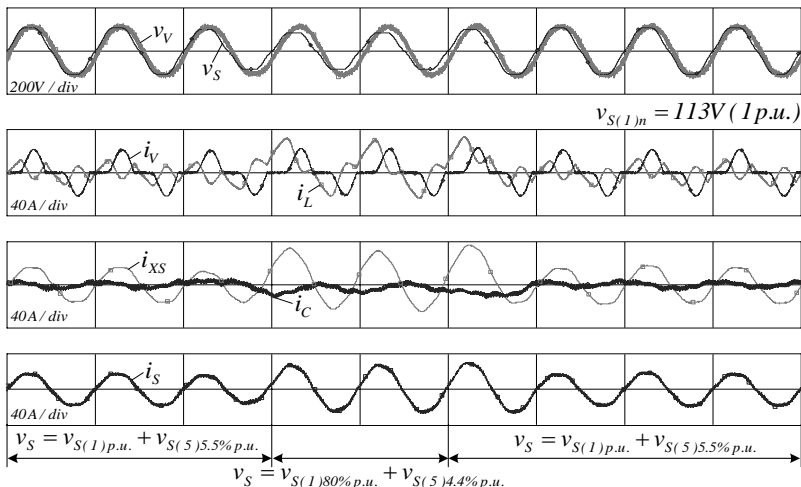


**Figure 6.65.** SVAPF – network voltage sag,  $P_L=0.5\text{kW}$  ( $\Delta t=20\text{ms/div}$ )

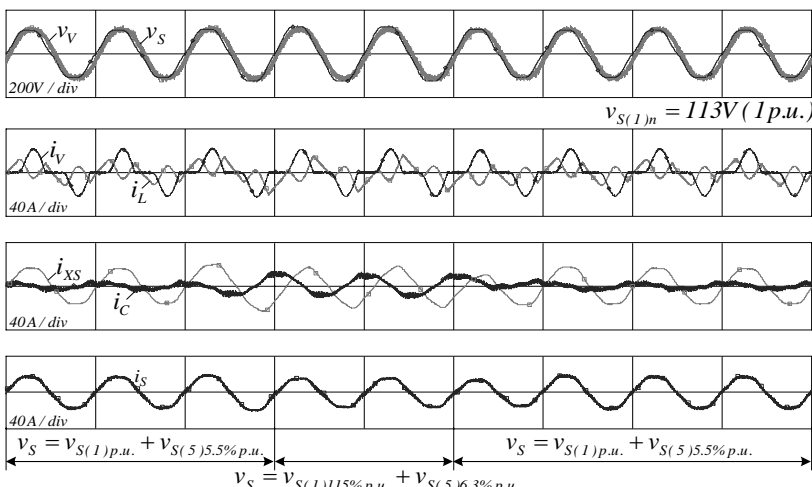


**Figure 6.66.** SVAPF – network voltage overvoltage,  $P_L=0.5\text{kW}$  ( $\Delta t=20\text{ms/div}$ )

Following this two types of network voltage  $v_S$  disturbances were considered. Analysed first was 40ms and 20% voltage sag, see Figure 6.65, and then 40ms and 15% overvoltage, see Figure 6.66.

To visualize, in selected conditions, active power values as well as their flow directions, Figure 6.67 was developed. During nominal network voltage (see Figure 6.64 and Figure 6.67a) in the idealized form all power goes directly to the load, nothing is converted, and theoretically there are no losses. In the case when

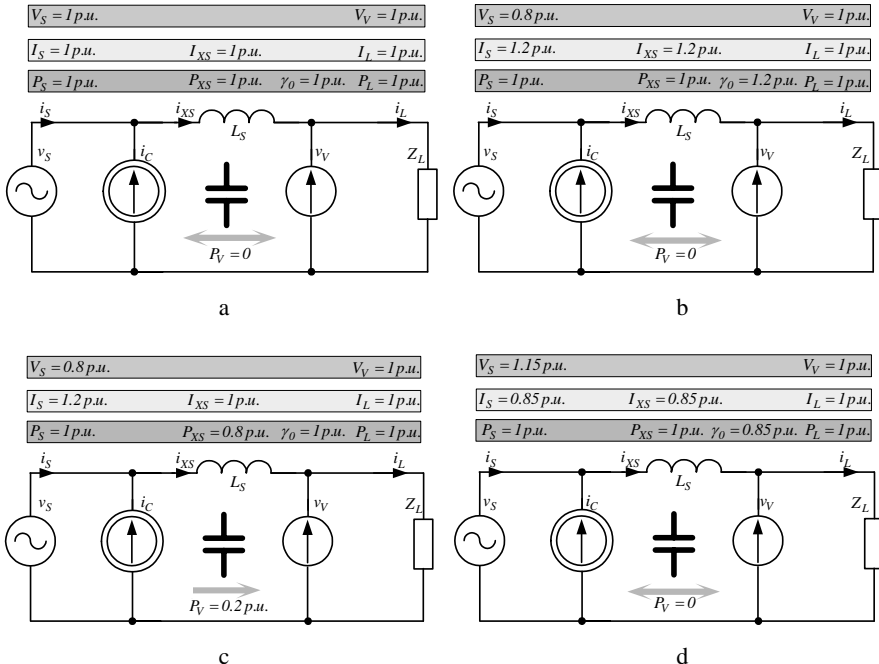


**Figure 6.67.** SVAPF – behavior in selected conditions: a. “normal” operation; b. network voltage sag; c. network voltage overvoltage

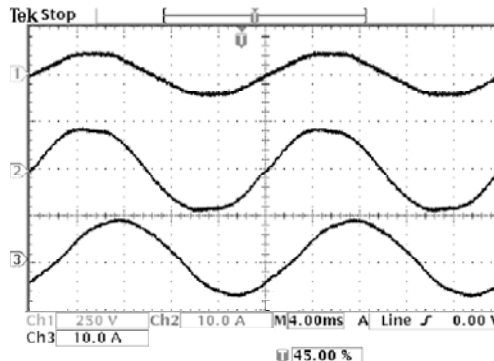
load has reactive and harmonic part, such reactive and harmonic currents are supported by the voltage source  $v_V$  and additionally current source  $i_C$  secures unity input power factor and sinusoidal network current (in the case of distorted network voltage). Figure 6.65 and Figure 6.67.b explain the situation when network voltage sag occurs. Since the load voltage must remain stable, the voltage source  $v_V$  must “add 20% to the network voltage”. The required active power is simply taken from the network via the series reactance, by increasing  $\gamma_0$  angle. Another scenario is possible, keeping  $\gamma_0$  constant, all the required active power can be taken from the network by the current source  $i_C$  via the DC link to the  $v_V$  source, see Figure 6.67.c.

Figure 6.66 and Figure 6.67.d show the situation of network overvoltage. This time the  $v_V$  source must “absorb 15% of the network voltage” to make the balance. This time decreasing  $\gamma_0$  angle it is possible to decrease by 15% the power passed via the series reactance and in this way secure the balance. What is significant in

the analysed arrangement is that in every single situation it is possible to secure constant power delivered to the load.

#### *Single Phase SVAPF – Preliminary Experimental Results*

To verify the SVAPF properties a scaled down hardware model, with parameters presented in Table B.7 (Appendix B), was developed. Figure 6.68 presents experimental waveforms obtained for the linear load and the reactive power compensation capabilities are evident.



**Figure 6.68.** Experimental waveforms ( $\Delta t=4\text{ms/div}$ ) for linear load  $P_L \approx 1\text{kW}$ ; Ch1 - network voltage  $v_S$  (250V/div); Ch2 - network current  $i_S$  (10A/div); Ch3 - load current  $i_L$  (10A/div)

#### *Interline VAPF and SVAPF Arrangements*

The Interline VAPF employs a number of parallel DC/AC converters, each providing power quality improvement for a different line [116, 117]. Because the parallel VSCs are tied together at their DC link capacitors, one of them can also be controlled to supply active power to the common DC link from its own line or absorb active power from the DC link to its own line (an asynchronous tie).

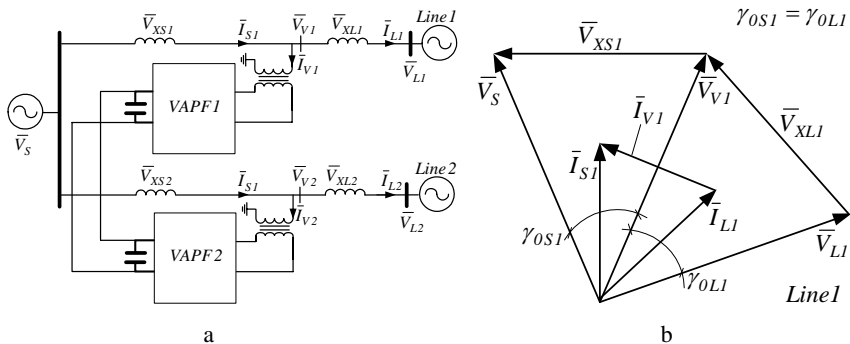


**Figure 6.69.** a. Interline VAPF; b. vector diagram

The general structure of an Interline VAPF is shown in Figure 6.69. For simplicity the system consists of two lines. Line 1 is represented by the sending end bus voltage  $\bar{V}_S$ , receiving end bus voltage  $\bar{V}_{L1}$  and voltage  $\bar{V}_{V1}$ . Similarly, Line 2 is represented by voltages  $\bar{V}_S$ ,  $\bar{V}_{L2}$  and  $V_{V2}$ . For clarity all voltages are assumed to be constant with fixed identical amplitudes  $V$  and fixed angles  $\gamma_{0S1} + \gamma_{0L1} = \gamma_{0S2} + \gamma_{0L2}$ . Additionally, reactances of the lines are the same  $X$  and only linear loads are considered.

In changing the angles of the voltages  $\bar{V}_{V1}$  (Line 1) and  $\bar{V}_{V2}$  (Line 2), the Interline VAPF under consideration allows control of the real power exchange between Lines. When for given Line 1 voltage  $\bar{V}_{V1}$  is controlled in order to secure  $\gamma_{0S1} = \gamma_{0L1}$ , there is no active power absorbed from or supplied to the DC link (Figure 6.69). However if there is a need to send some power from Line 1 to Line 2, angles between voltages should be as follows  $\gamma_{0S1} > \gamma_{0L1}$  (Line 1),  $\gamma_{0S2} < \gamma_{0L2}$  (Line 2) as shown in Figure 6.70, and vice versa exchanging active power from Line 2 to Line 1, angles must be as follows  $\gamma_{0S1} < \gamma_{0L1}$  and  $\gamma_{0S2} > \gamma_{0L2}$ .

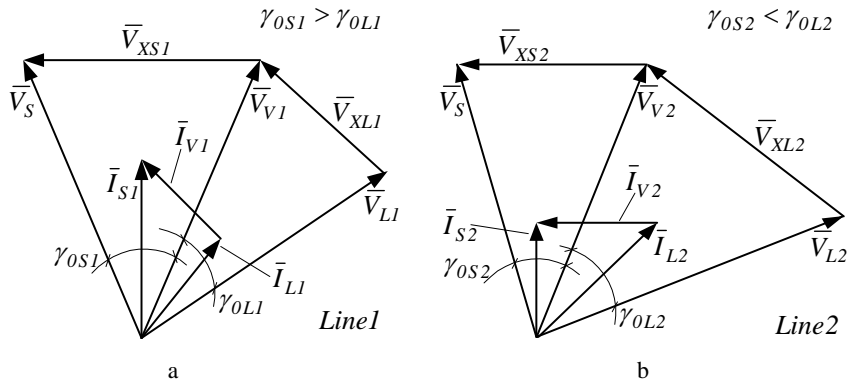


**Figure 6.70.** Possible vector diagrams for: a. Line 1; b. Line 2

The active power exchanged with the Line 1 is given by the following equation [117]

$$P_{V1} = \operatorname{Re}\left\{\bar{V}_{V1} \cdot \bar{I}_{V1}^*\right\} = \frac{V^2}{X} (\sin(\gamma_{0S1}) - \sin(\gamma_{0L1})) \quad (6.34)$$

However as explained earlier this power has to be absorbed (or supplied) through the DC tie from (or to) the other Lines. Because to maintain a constant DC voltage the net active power through the DC link has to be zero (neglecting losses) thus the active power supplied by one of the Lines must be equal to that injected into the other. Therefore the operating constraint representing the active power exchange between or among the two series converters via the common DC link is given by

$$|P_{V1}| = |P_{V2}| \quad (6.35)$$

The load flow equations in given Line 1 equipped with an Interline VAPF device are as follows [116, 117]

$$P_{SI} = \operatorname{Re}\{\bar{V}_S \cdot \bar{I}_{SI}^*\} = \frac{V^2}{X} \sin(\gamma_{OSI}) \quad Q_{SI} = \operatorname{Im}\{\bar{V}_S \cdot \bar{I}_{SI}^*\} = \frac{V^2}{X} - \frac{V^2}{X} \cos(\gamma_{OSI}) \quad (6.36)$$

$$P_{LI} = \operatorname{Re}\{\bar{V}_{LI} \cdot \bar{I}_{LI}^*\} = \frac{V^2}{X} \sin(\gamma_{OLI}) \quad Q_{LI} = \operatorname{Im}\{\bar{V}_{LI} \cdot \bar{I}_{LI}^*\} = \frac{V^2}{X} \cos(\gamma_{OLI}) - \frac{V^2}{X} \quad (6.37)$$

$$Q_{VI} = \operatorname{Im}\{\bar{V}_{VI} \cdot \bar{I}_{VI}^*\} = \frac{V^2}{X} (\cos(\gamma_{OSI}) + \cos(\gamma_{OLI}) - 2) \quad (6.38)$$

Considering Equations 6.34-6.38 the relationships between the active and reactive powers and angle of the  $\bar{V}_{VI}$  voltage are plotted in Figure 6.71 (all values are determined in relation to maximum active and reactive powers transmitted through given Line).

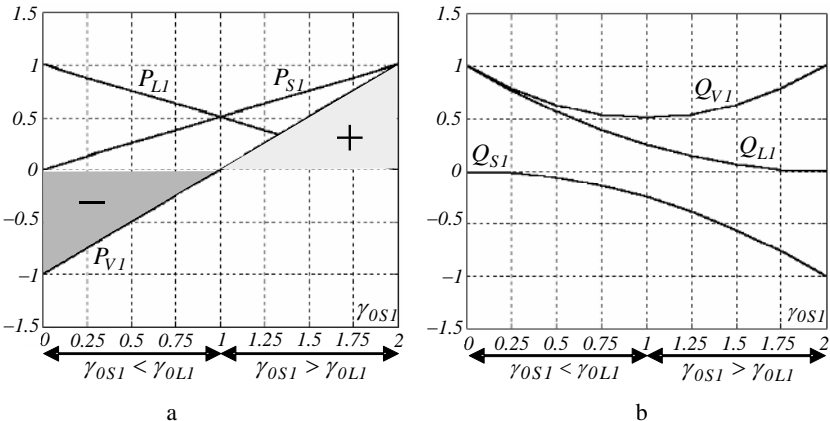


**Figure 6.71.** Changes of the individual powers with the angular rotation of the  $\bar{V}_{VI}$  voltage:  
a. active powers; b. reactive powers;  $V=0.25\text{p.u.}$ ,  $X=0.25\text{p.u.}$ ,  $\gamma_{OLI}=4\text{deg}=1\text{p.u.}$ , Line 1

In Figure 6.71,  $P_{VI}>0$  means power absorbed from (Line 2 supplies power to Line 1) and  $P_{VI}<0$  supplied to (Line 1 supplies power to Line 2) the DC link.

Implementation of the proposed solution gives the opportunity to exchange active power between different Lines, and to isolate the sending-end from distortions introduced by the receiving-end and *vice versa*.

The arrangement presented can be additionally improved by connecting in parallel with the given Line current source. In this way Interline SVAPF owns all the properties of the SVAPF devices and, additionally, allows the exchange of active power between different Lines. This solution may also be attractive from an economical point of view. Comparing the current source apparent power  $S_{CI(SVAPF)}$

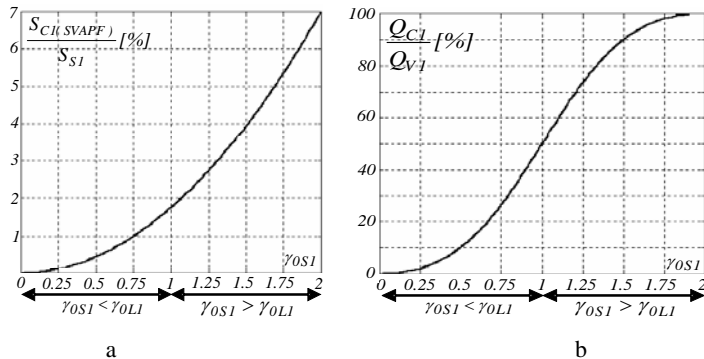


**Figure 6.72.** Energetic properties of the parallel current source: a. apparent powers relation; b. reactive powers relation;  $V=0.25\text{p.u.}$ ,  $X=0.25\text{p.u.}$ ,  $\gamma_{0LI}=4\text{deg}=1\text{p.u.}$ , Line 1

with apparent power flowing through Line 1 ( $S_{SI}$ ) see Figure 6.72, it is possible to claim that the current source power amounts to only 7% of the maximum apparent power transmitted through a given Line (in an operating region). Similar relations exist for reactive power of the parallel voltage source  $v_V$  ( $Q_{VI}$ ).

## 6.4 Compensating and Voltage Source Custom Power Systems – Comparison of Properties

### VAPF – Energetic Properties

Taking a more precise view of the energetic capabilities, on the basis of the vector graph in Figure 6.39 (Chapter 6.3.1), one can determine the following dependencies

$$\bar{V}_S = V = V_m / \sqrt{2}, \quad \bar{V}_V = \bar{V}_L = V \cdot e^{-j\gamma_0}, \quad \Delta \bar{V} = 2 \cdot V \cdot \sin \frac{\gamma_0}{2} \cdot e^{j(\pi - \gamma_0)/2} \quad (6.39)$$

$$\bar{I}_S = \frac{2 \cdot V}{\sqrt{\omega^2 L_S^2 + r_S^2}} \cdot \sin \frac{\gamma_0}{2} \cdot e^{j(\pi - \gamma_0 - 2\varphi_S)/2}, \quad \bar{I}_L = \frac{V}{\sqrt{\omega^2 L_L^2 + R_L^2}} \cdot e^{-j(\gamma_0 + \varphi_L)} \quad (6.40)$$

where  $\varphi_S = \arctg \omega L_S / r_S$ ;  $\varphi_L = \arctg \omega L_L / R_L$ ;  $V_m$  – voltage amplitude.

On the basis of the above, respectively, active, reactive and distortion powers of the voltage source  $v_V$  are as follows

$$\begin{aligned} P_V &= V^2 \left[ \frac{\sin \varphi_S \cdot \sin \gamma_0 - \cos \varphi_S \cdot (1 - \cos \gamma_0)}{|Z_S|} - \frac{\cos \varphi_L}{|Z_L|} \right] \approx \\ &\approx V^2 \left( \frac{\sin \gamma_0}{\omega L_S} - \frac{\cos \varphi_L}{|Z_L|} \right) \end{aligned} \quad (6.41)$$

$$\begin{aligned} Q_V &= -V^2 \left[ \frac{\sin \varphi_S \cdot (1 - \cos \gamma_0) + \cos \varphi_S \cdot \sin \gamma_0}{|Z_S|} + \frac{\sin \varphi_L}{|Z_L|} \right] \approx \\ &\approx -V^2 \left( \frac{1 - \cos \gamma_0}{\omega L_S} + \frac{\sin \varphi_L}{|Z_L|} \right) \end{aligned} \quad (6.42)$$

$$D_V = V \cdot \sqrt{\sum_{k=2}^{\infty} I_{L(k)}^2} = \sqrt{\sum_{k=2}^{\infty} (V \cdot I_{L(k)})^2} = \sqrt{\sum_{k=2}^{\infty} D_{L(k)}^2} \quad (6.43)$$

where  $Z_L$ ,  $Z_S$  – respectively, load and network impedances;  $I_{L(k)}$ ,  $D_{L(k)}$  – respectively,  $k^{\text{th}}$  harmonic in load current (rms value) and distortion power of the load related to  $k^{\text{th}}$  harmonic.

Considering the Equations 6.42 and 6.43, on the assumption that VAPF is a perfect compensator, which means  $D_V = D_L$  and  $Q_V = Q_L$ , and the fact that during steady states  $P_V = 0$ , the apparent power of the voltage source  $v_V$  in VAPF can be defined by the following equation

$$\begin{aligned} S_{V(\text{VAPF})} &\underset{r_s \rightarrow 0}{\approx} P_L \sqrt{\left( \frac{P_{\max}}{P_L} - \sqrt{\left( \frac{P_{\max}}{P_L} \right)^2 - 1} + \tan \varphi_L \right)^2 + \left( \frac{\text{THD}(I_L)}{\cos \varphi_L} \right)^2} \rightarrow \\ &\xrightarrow{\frac{P_L}{P_{\max}} \ll 1} \sqrt{Q_L^2 + D_L^2} \end{aligned} \quad (6.44)$$

where  $P_L = (V^2 / |Z_L|) \cdot \cos \varphi_L$  - active power of the load;  $Q_L = (V^2 / |Z_L|) \cdot \sin \varphi_L$  - reactive power of the load;  $P_{\max} = V^2 / (\omega L_S)$  – maximum transmittable, through inductance  $L_S$ , active power;  $\text{THD}(I_L)$  – total harmonic distortion coefficient of the load current,  $I_{L(1)} = |I_L|$  - rms value of the 1<sup>st</sup> harmonic in load current.

### *PAPF – Energetic Properties*

In the situation where PAPF filters out higher harmonics in the load current (and is treated as the perfect compensator) as well as reactive power  $Q_L$  produced by the load, the voltage produced by the ideal voltage source in PAPF – which forces inductance  $L_r$  compensating current to flow through the parallel coupling (see Figure 6.11, Chapter 6.2) – is as follows

$$V_{V(\text{PAPF})} = \sqrt{(V + \Delta V)^2 + V_h^2} = \sqrt{(V + \omega L_r \cdot (P_L/V) \cdot \tan \varphi_L)^2 + \sum_{k=2}^{\infty} (k \cdot \omega L_r \cdot I_{L(k)})^2} \quad (6.45)$$

where  $\Delta V$  – voltage drop on the coupling inductance  $L_r$  caused by the component in the compensating current, responsible for load reactive power  $Q_L$  compensation;  $V_h$  – voltage drop on the coupling inductance  $L_r$  caused by the component in

compensating current responsible for compensation of higher harmonics in load current  $I_{L(k)}$ .

Considered as a non-linear load, the *6-pulse* controlled rectifier, voltage  $V_h$  could be defined as follows

$$V_h = \sqrt{\sum_{k=2}^{\infty} (k \cdot \omega L_r \cdot I_{L(k)}/k)^2} = \omega L_r \cdot \frac{P_L}{V \cdot \cos \varphi_L} \cdot \sqrt{N} \quad (6.46)$$

where  $I_{L(k)} = I_{L(1)}/k$ ;  $N$  – number of the filtered out higher harmonics.

Considering the above one can write the following equations

$$V_{V(PAPF)} = V \sqrt{\left(1 + \frac{P_L}{P'_{max}} \cdot \operatorname{tg} \varphi_L\right)^2 + \left(\frac{P_L}{P'_{max}} \frac{I}{\cos \varphi_L}\right)^2 \cdot N} \quad (6.47)$$

$$I_{V(PAPF)} = \frac{P_L}{V \cdot \cos \varphi_L} \cdot \sqrt{\sin^2 \varphi_L + \operatorname{THD}^2(I_L)} \quad (6.48)$$

where  $P'_{max} = V^2 / \omega L_r$  - maximum transmittable, through coupling inductance  $L_r$  active power.

After some transformations, the apparent power of the voltage source in PAPF can be defined by the following equation

$$S_{V(PAPF)} = \frac{P_L}{\cos \varphi_L} \sqrt{\left[\left(1 + \frac{P_L}{P'_{max}} \cdot \operatorname{tg} \varphi_L\right)^2 + \left(\frac{P_L}{P'_{max}} \cdot \frac{I}{\cos \varphi_L}\right)^2 \cdot N\right]} \cdot \sqrt{\sin^2 \varphi_L + \operatorname{THD}^2(I_L)} \xrightarrow[\frac{P_L \ll I}{P'_{max}}} \sqrt{Q_L^2 + D_L^2} \quad (6.49)$$

### *Energetic Properties Comparison*

On the basis of Equations 6.44 and 6.49 the relation between VAPF and PAPF voltage source apparent powers can be defined by the following equation

$$\frac{S_{V(VAPF)}}{S_{V(PAPF)}} = \frac{\varepsilon' \cdot \cos \varphi_L \cdot \sqrt{\cos^2 \varphi_L \cdot \left(\varepsilon - \sqrt{\varepsilon^2 - 1} + \operatorname{tg} \varphi_L\right)^2 + \operatorname{THD}^2(I_L)}}{\sqrt{\left[\cos^2 \varphi_L \cdot (\varepsilon' + \operatorname{tg} \varphi_L)^2 + N\right] \cdot \left[\sin^2 \varphi_L + \operatorname{THD}^2(I_L)\right]}} \xrightarrow[\frac{P'_{max} \gg I}{P_L}; \frac{P_{max} \gg I}{P_L}]{} 1 \quad (6.50)$$

where  $\varepsilon = P_{max} / P_L$  (for VAPF),  $\varepsilon' = P'_{max} / P_L$  (for PAPF).

Figure 6.73 shows theoretical curves obtained on the basis of Equation 6.50 for different  $\varphi_L$  and  $\operatorname{THD}(I_L)$ . As one can see, the apparent power of the voltage source

in VAPF in comparison with the apparent power of the voltage source in PAPF is smaller for greater deformations in the load current and for greater  $\varphi_L$  values. This is so because VAPF by principle of operation has to generate reactive power, thus in the case of small  $\varphi_L$  and large loads (small value of the  $\varepsilon = P_{max}/P_L$  coefficient) reactive power generated by the VAPF can be considerably larger than the reactive power of the load.

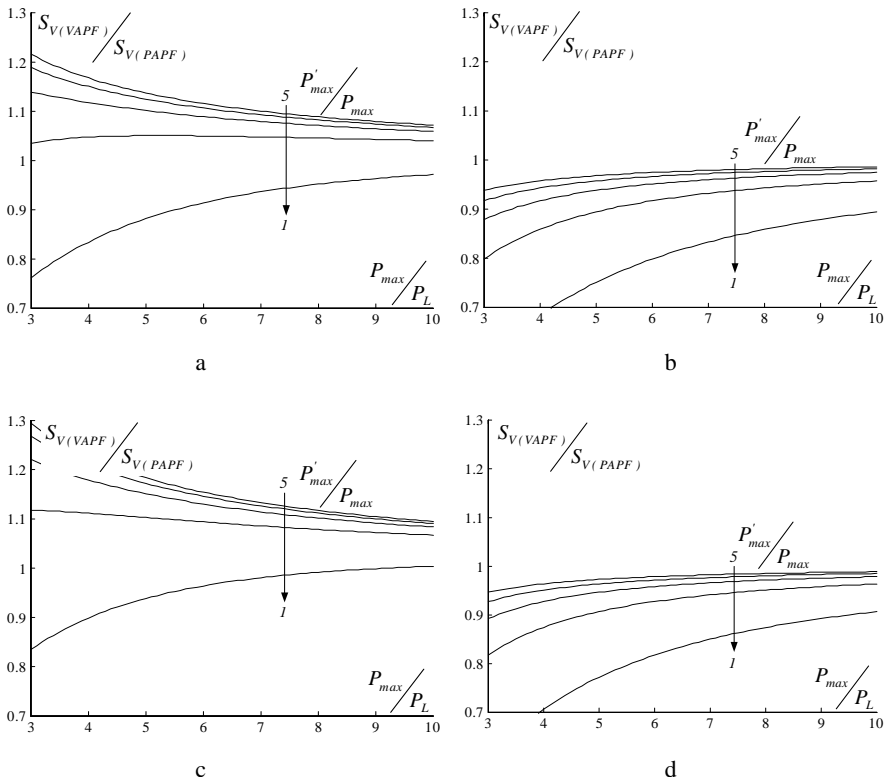


**Figure 6.73.** Energetic properties comparison: a.  $\varphi_L=30^\circ$ ,  $THD(I_L)=0\%$ ; b.  $\varphi_L=30^\circ$ ,  $THD(I_L)=80\%$ ; c.  $\varphi_L=25^\circ$ ,  $THD(I_L)=0\%$ ; d.  $\varphi_L=25^\circ$ ,  $THD(I_L)=80\%$

Additionally, deformations in load current, characterized by the number of compensated harmonics  $N$  as well as  $THD(I_L)$ , have very significant influence on energetic properties of the two arrangements. In VAPF filtration of the load current higher harmonics does not require any changes in voltage  $v_V$ , quite contrary to the case with PAPFs, where the component in compensating current responsible for higher harmonics filtration (which flows through coupling inductance  $L_r$ ) is determined by the additional component in voltage  $v_{V(PAPF)}$ , which leads to considerable growth of its effective value. On this basis, it is possible to conclude that VAPF is particularly desirable for loads with large harmonic content, e.g., for rectifiers with capacitive load.

## Conclusions

### 7.1 Summary of Results

The major objective of this thesis was to present the possibilities, detailed features, as well as selected solutions and applications of the power electronics arrangements useful in improving quality of delivery of the electrical energy in Electric Power Systems. In the course of completing the objective of this thesis, there have been found new and practical algorithms, arrangements and procedures that can effectively address the utilization of the power electronics systems in EPS. The investigation of power electronics arrangements to enhance the quality of delivery has provided results which can be summarized as follow:

- TSSC and SVC increase the transmitted active power by a fixed percentage of that transmitted by the uncompensated line. The SSSC and STATCOM can increase it by a fixed portion of the maximum transmitted power independent of  $\delta$  in the following range respectively  $0 \leq \delta \leq \pi/2$  and  $\pi/2 \leq \delta \leq \pi$ ;
- location of an SSSC and TSSC does not affect a transmission characteristics in the line where they are installed. To maximize STATCOM and SVC impact on transmitted power they should be located at the middle point of the line;
- in the sense of improvement of the transient and dynamic stability the SSSC and TSSC controllable parameters (respectively  $V_{sssc}$  and  $k$ ) should be set to their maximum values to achieve maximum impact on transmission characteristics;
- in the sense of improvement of the transient stability and dynamic stability the STATCOM and SVC controllable parameters (respectively  $I_c$  and  $B$ ) should be set to their maximum values to achieve maximum impact on transmission characteristics;
- UPFC devices increase the transmitted active power by a fixed portion of the maximum transmitted power independently of  $\delta$ ;

- when the UPFC device is positioned at the system terminals, this location does not affect transmission characteristics. However if a UPFC is positioned at any other place than system terminal the optimal UPFC location is middle of the line;
- in the sense of maximum influence on transmission characteristics and, in consequence, on transient and dynamic stability, the UPFC and IPFC controllable parameters respectively  $\bar{V}_{UPFC}$  and  $\bar{V}_{IPFCn}$  must be constrained to stay in quadrature with sending end voltage  $\bar{V}_l$  (lead or lag sending end voltage);
- location of an IPFC does not affect a transmission characteristics in line where is installed;
- transmission lines with larger transmittable active power possess larger active power compensation range, therefore from the point of view of improvement of transient and dynamic stability and distribution of the reactive power flow, lines selected as slaves should be those with transmittable active power larger in relation to the maximum of their masters;
- direct control strategy based on current control has been studied and the effectiveness of the proposed controller has been demonstrated via digital simulation studies. The proposed approach secures very good dynamic properties, tracking the reference inputs and showing very quick responses. Additionally the coupling effect is only shown in transients and does not exist in steady states;
- a new probabilistic approach to assess the power rating of IPFC and STATCOM devices has been proposed. The approach results in considerable saving by lowering the required power ratings of the converters used in the design of IPFC and STATCOM systems. Both theoretical prediction and experimental results confer on the potential benefits the new approach will bring to bear, in terms of cost saving. Very importantly, these assessments have been achieved with a very high level of confidence, which is no less than 99.9%. Thus, the reliability of the system is not compromised with the new approach;
- the HVDC devices, built on the basis of SCR thyristors equipped with an APF on its AC side (APF produces sinusoidal voltage), allow the delivery of electric energy to consumers even when a passive resistive load is connected. Additionally APF isolates a load from the distortions produced by an HVDC device and vice versa (securing sinusoidal load current);
- HVDC devices, built on the basis of SCR thyristors equipped with an APF particularly for large firing delay angles  $\alpha$  and relatively small load reactive power (or if there is a reactive power compensator at the load side), are a competitive solution. In cases of loads with large  $\operatorname{tg}\varphi_L$  and/or when firing delay angle  $\alpha$  cannot be large (e.g., because of voltage adjustment), it is justifiable to apply the hybrid filter, instead of the APF;
- a model of the UPQC device has been proposed. The model, created with the minimum number of simplifying assumptions, permits entirely independent control in relation to both  $p$ - $q$  coordinates and is particularly

useful in stability investigations, and selection of regulator parameters as well as values of passive elements. On this basis, a method of analytic determination of the *DC* link capacitor coupling for both parallel and series arrangements, was worked out and verified experimentally;

- the results of both theoretical and experimental analyses confirm the good filtration proprieties as well as multi-functionality of the UPQC device. The arrangement under consideration simultaneously permits the fulfilling of the following functions: voltage and current harmonics filtration, network voltage and load current symmetrization, as well as network voltage stabilization and power flow control;
- on the basis of the theoretical and experimental investigations one can say that VAPF possess: i) very good current and voltage harmonics separation proprieties for any kind of non-linear loads; ii) reactive power compensation capability; iii) load voltage stabilization potential; iv) capability for balancing the network in conditions of unbalanced loads; v) very good energetic properties – apparent power of the voltage source in VAPF in comparison with apparent power of the voltage source in PAPF is smaller for greater deformations in the load current; vi) ability to use simple network inductance matched only with regard to basic frequency;
- on the basis of the theoretical and preliminary experimental investigations one can say that SVAPF possess properties of the VAPF device and additionally secures: i) sinusoidal load voltage with no dependency to network voltage shape; ii) reactive power compensation without need to increase load voltage; iii) stabilized load voltage with no danger of excessive growth of the input reactive power

## 7.2 Future Work

As Distributed Resources hardware becomes more reliable and economically feasible, there is a trend to connect DR units to the existing utilities to serve different purposes and offer more possibilities to end-users, such as:

- improving availability and reliability of electric power;
- peak load shaving;
- energy cost savings;
- selling power back to utilities or other users;
- reactive power compensation;
- mitigation of harmonics and voltage sag

However, a wide range of system issues arise when DR units attempt to connect to the EPS. Major issues regarding the connection of DRs include protection, power quality, and system operation. These issues are barriers that limit the penetration of DRs into the EPS. Future electric power systems should be versatile and flexible so electric energy can be freely generated, transmitted, distributed, and consumed.

The overall general aim of future investigations is to lower or eliminate these technological barriers by addressing the connection issues between DRs/EPS. The main objectives will be to investigate the impact of the DRs on EPS, and the reciprocal impact and effects of EPS events on the operation of DRs.

The investigations will have three main scientific objectives that concern acquiring understanding of the integration and connection between the DR and EPS. These are:

- an in-depth investigation into the impact of the DRs on EPS, and the effects of EPS events on the operation of DR units;
- an in-depth investigation into various DRs/EPS connection issues due to various distributed sources, such as fuel cells and the renewables;
- an in-depth investigation into advanced coordinated control of DRs within the EPS

These scientific objectives will provide the underpinnings that are vital for the exploitation and advancement of the DR technology. There are three main technological objectives involved in acquiring capabilities of integrating the DR and EPS as follows.

*Definition of DR/EPS connection interfaces.* At present distribution system voltage regulation design is based on relatively predictable daily and seasonal changes in load patterns. Without DRs, power flow is mostly unidirectional, and monotonically decreasing in real power magnitude with increasing distance from the substation. The addition of DRs units to the EPS can radically shift power flow patterns, which lead to complex and unpredictable load flow dynamics. This will make it difficult to maintain adequate voltage regulation, among other things. It is therefore essential to formulate new definitions for the DRs/EPS connection interface by developing some specific requirements from the point of view of a system's voltage regulation, transient response and fault behaviors; reclosing; anti-islanding; power systems dynamics and stability. In particular, recommendations regarding voltage regulation improvement as well as DRs interaction with Load Tap Changers (LTC) and Step Voltage Regulators (SVR) controls will be defined. To reflect the increased use of new equipment in the DRs, recommendations will also be given regarding design of the power electronics based DRs to meet power quality requirements (*e.g.*, current distortions below acceptable limits, negligible impact on flicker, no DC current injection, effective grounding, negligible impact of the unbalanced voltage on PWM inverter-based DRs). Moreover, recommendations regarding protection and reliability will be proposed (*e.g.*, minimal impact on fault currents, reclosing with negligible impact on the EPS, DRs with minimal impact on local dynamics).

*Design and build of a DRs/EPS interface.* This concerns the design and build of the interface that possesses all the quality of delivery requirements. Industrial and domestic applications require the DRs/EPS connection interface to generate high-quality electrical power, possibly close to the perfect sinusoid. This requires the invention of new power electronics topologies and hardware to provide solutions for low harmonic content and minimum EMI. It is proposed that while existing

matrix and multilevel converter techniques are used as the baseline, novel topologies and controls must be developed to address specific system requirements within a DR, and characteristics of the DR sources these converters use. Matrix converter techniques offer the ability to convert directly from AC to AC without the intermediate *DC* stage. The particular advantage of this approach is the elimination of the *DC* link capacitor. Because of high generator output frequency integral pulse operation may be possible, leading to a significant reduction in losses. Multilevel converters offer, among other significant advantages, reduced harmonic distortion

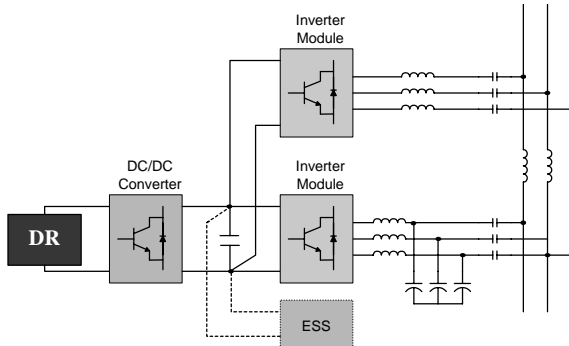


**Figure 7.1.** Proposed DR/EPS connection interfaces

and EMI. Other advantages inherent in the topology are reduced switching losses and the possibility of using lower rate power devices. Lower device ratings imply faster switching speeds and lower on-state losses. Special attention will be paid to cascaded multilevel converters, with several separate *DC* sources. This arrangement should be the perfect DRs/EPS interface, because several batteries, fuel cells, solar cells, wind turbines, and micro-turbines can be connected through a multilevel converter to feed a load or the *AC* grid without voltage balancing problems.

A DRs/EPS connection system can consist solely of a parallel current connected to the EPS sinusoidal voltage source. As an alternative, proprieties of “double converter” systems will be studied. The interface depicted in Figure 7.1, has an additional parallel current source that makes possible reactive power compensation, voltage dips and sags compensation, effective power systems dynamics and stability issues improvement, especially with additional energy sources. It can also, with appropriate control algorithm, behave as an active power filter. Proposed interface system, with potential for many other possible functionalities, will find wide utilization in future EPS, especially in low and medium voltage networks.

Apart from the above research, two additional interfaces will be investigated. The interface depicted in Figure 7.2.a consists of two sources, current connected in parallel and voltage connected in series. In this manner it is possible not only to “deliver” energy to the EPS, because of parallel current source, but also to provide among other things local energy management as well as energy efficiency

improvement. The interface in Figure 7.2.b can also provide energy management for a number of independent transmission lines. Additionally it is possible to increase the degree of supply security, because underloaded transmission lines

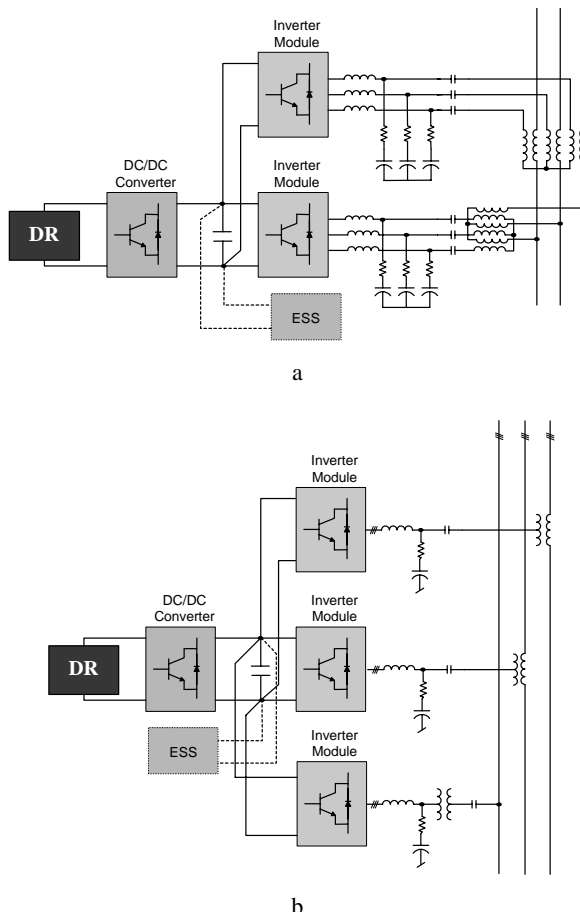


**Figure 7.2.** DRs/EPS connection interfaces: a. single-terminal; b. multi-terminal

provide help, in the form of real power transfer, for the overloaded lines. The above proposed interface systems, with their potential for many other possible functionalities, can find wide utilization in low-, medium- and high-voltage networks.

Multi-terminal *DC* systems, see Figure 7.3, which are expected to increase the scope of application of the *DC* transmission will be investigated as the DRs/EPS connection interface (especially for wind power installations). The benefit of such an approach arises from the fact that with a *DC* distributed system, conditioning can be applied at a central level of the *AC* distribution system, close to the *DC* system connection points.

The central unit connected to the EPS at the DRs connection point, could contribute to the frequency control by regulation of the active power, and to the voltage control by regulation of the reactive power. In this respect, DRs with central power electronic units can act more like a regular power plant.

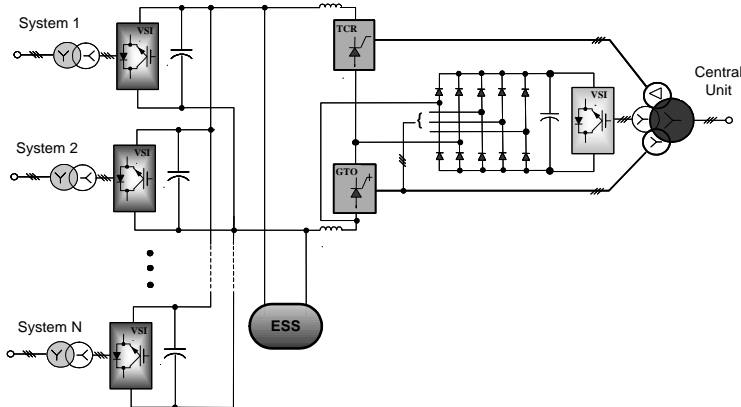


**Figure 7.3.** Multi-terminal DC system

Additionally the development of DRs/EPS connection interfaces equipped with storage technologies will be an object of future investigations [206]. Special attention will be paid to the batteries of super-capacitors, see Figure 7.4 and Figure 7.5. [207].

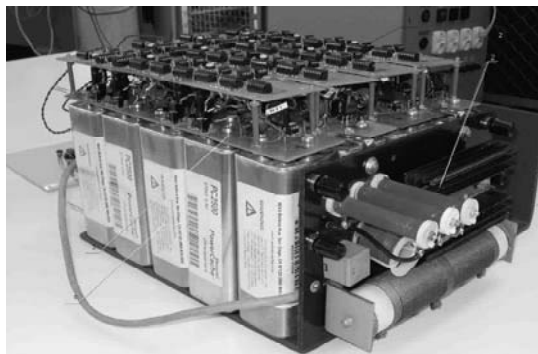


**Figure 7.4.** Battery of super-capacitors with active balancing arrangements

The above mentioned DRs/EPS connection interfaces, equipped with modern power electronics arrangements (*e.g.*, multilevel converters) and ESS provide significant opportunities in the control of distributed power systems. These topologies are attractive for controlling the frequency, voltage output (including phase angle), real and reactive power flow at a DC/AC interface, system dynamic behavior and for reducing power quality problems, such as voltage harmonics, voltage imbalance, or sag.

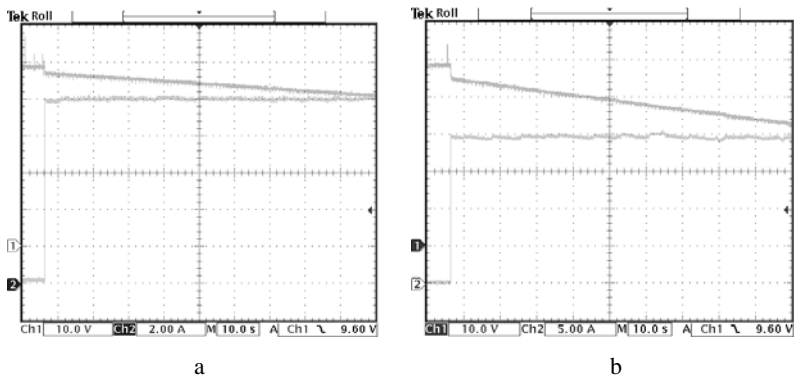


**Figure 7.5.** Experimental results: a. load current 10A (2A/div); b. load current 20A (5A/div); Ch1-battery voltage (10V/div), Ch2-load current( $\Delta t=10\text{s}/\text{div}$ )

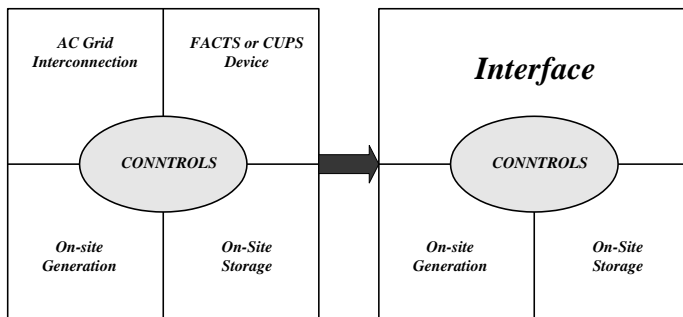


**Figure 7.6.** The new power delivery concept

Because of this a new power delivery concept has arisen and will be investigated. This concept comes from the assumption that in the near future more DRs will be equipped with modern power electronics interfaces, “wind” with Multi-Terminal DC systems, etc. Therefore, the duties of the FACTS or CUPS arrangements will be intercepted by DRs with modern interfaces, as this is in Figure 7.6.

*Development of Coordinated Control System (CCS) in DRs.* To enable future EPS systems to absorb high penetration of DRs, the connection interface must incorporate a CCS that makes the overall distribution network act proactively and collectively with LTC, SVR, load changes and other environment distributions. The dispersed nature of the CCS within the future DRs/EPS means that modern communications and real time control technologies should be employed. The CCS would be based on a collection of local controllers connected together via the Internet. These local controllers would be used to monitor and log the power quality output from the DRs. The monitoring aspects would include the following:

- acquisition of voltage and current traces, and their processing into meaningful parameters such as rms power, power factor angle, phase and harmonic distortion *etc.* The processing would be done at source;

- acquisition and storage of data for later post-analysis. This would be done at high sample rate *e.g.*,  $1kHz$  or higher;
- detection of abnormal conditions and alert reporting of these conditions;
- general condition monitoring of DRs components such as switching transistor temperatures, battery/fuel levels *etc.*

The collected information would be available as a web service to operators and web-based data analysis server agents. Web based technologies would be employed to make the data as transparent as possible both to humans and machines. The control system would be networked on a high speed, low latency network. The latency is important as it determines the response time of the whole coordinated control system. With embedded real-time control capability now readily available on internet or intranet, it is proposed that sub-second response times over wide geographical areas be targeted, which would mean that a network of DRs could respond rapidly to load variation in the EPS (or grid) by increasing supply, or switching in power factor correction capacitors. A networked CCS would also have a role in anti-islanding by phase locking an islanded system to that of the grid. The local controllers would use a global clock system, such as the Global Position System (GPS) together with the internet communication system to phase lock the output of a DR should it become disconnected. The phase information together with current grid voltage would ensure that when the islanded system is ready to be reconnected the voltages and phases would match allowing a much faster re-connection. Another key functionality for the CCS is concerned with the conflicting requirements from voltage regulation and anti-islanding, which would be made more complex in future DRs/EPS systems. It is known that it is difficult to compromise between island avoidance and ensuring the system is not vulnerable to voltage collapse. It is also important for the DRs units to avoid disruption from EPS voltage regulation performance.

All the above will benefit manufacturers of such technologies and assist in the further development in this field, and will enable faster growth and penetration for distributed generation network, resulting in fast growth of use of clean power based on renewable sources.

---

## Appendices

### Appendix A. The DC Link Modelling

To simulate the *DC* link, an average state space model has been utilized. In this model the  $n^{th}$  converter outputs, instantaneous voltages as well as currents, are defined as

$$\bar{v}_{IPFCna,b,c} = \bar{d}_{na,b,c} \cdot v_{DC} \quad (\text{A.1})$$

$$\bar{i}_{na,b,c} = \bar{d}_{na,b,c} \cdot i_{DC} \quad (\text{A.2})$$

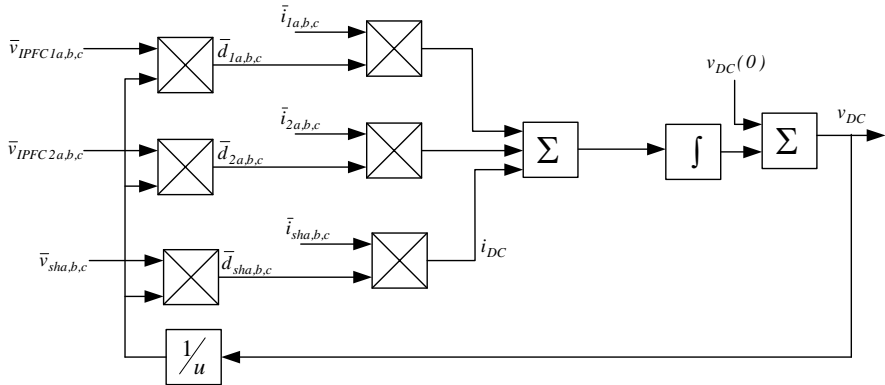
where  $\bar{v}_{IPFCna,b,c}$  vector of the converter's output phase voltages (instantaneous);  $v_{DC}$  measured *DC* link voltage;  $i_{DC}$  *DC* link current;  $\bar{i}_{na,b,c}$  vector of the converter's phase currents (instantaneous);  $\bar{d}_{na,b,c}^T = [d_{na} \ d_{nb} \ d_{nc}]$  duty cycles vector.

Since converter output voltages and *DC* link voltage are known (measured) it is possible to determine the duty cycles and then, using converter output currents, the *DC* link current. The final equation on the influence of the three converters (two series and one parallel) on the voltage in the *DC* link can be defined as

$$v_{DC} = \frac{1}{C} \int \left( \begin{array}{l} d_{1a} \cdot i_{1a} + d_{1b} \cdot i_{1b} + d_{1c} \cdot i_{1c} + \\ d_{2a} \cdot i_{2a} + d_{12} \cdot i_{2b} + d_{2c} \cdot i_{2c} + \\ d_{sha} \cdot i_{sha} + d_{shb} \cdot i_{shb} + d_{shc} \cdot i_{shc} \end{array} \right) dt + V_{DC}(0) \quad (\text{A.3})$$

where  $V_{DC}(0)$  - *DC* link voltage for  $t=0s$ .

Additionally Equation (A.3) is presented in Figure A.1.

**Figure A.1.** DC link simulation model

## Appendix B. Parameters of the Investigated Arrangements

**Table B.1.** Parameters of the transmission lines

line-line voltage (rms)	26	kV
line distance	15	km
line inductance	1.03*3	mH/km
line resistance	0.85*3	$\Omega$ /km
power angle	10	Degree
maximum $V_{\Sigma h}$ (rms)	1.5	kV
DC link capacitor	1000	$\mu$ F
DC link voltage	5	kV

**Table B.2.** Single phase UPQC – selected parameters and adjustments

network voltage	50	V
DC link reference voltage	300	V
filter inductance $L_{f1}$	2	mH
filter inductance $L_{f2}$	2	mH
filter capacitance $C_{f2}$	20	$\mu$ F
DC link capacitance $C$	3000	$\mu$ F
switching frequency	20	kHz

**Table B.3.** Three phase UPQC – selected parameters and adjustments

nominal network voltage	3×220	V
admissible range of changes in network voltage	60÷340	V
stabilized load voltage	3×60÷240	V
<i>DC</i> link capacitor	1650	μF
the reference <i>DC</i> link voltage	610	V
maximum network current	20	A
the main controller, HPF's time constant $T_R$	10	ms
$U_{DC}$ voltage regulator, $K_C$ gain (with assumption of sensor ratio 0,052 V/V)	1	V/V
PWM frequency in PAPF controller	4	kHz
PWM frequency in SAPF controller	12	kHz

**Table B.4.** Single phase VAPF – selected parameters

network voltage	80	V
the reference <i>DC</i> link voltage	180	V
series inductance $L_S$	10.4	mH
filter inductance $L_f$	0.3	mH
filter capacitance $C_f$	24	μF
<i>DC</i> link capacitance $C$	2000	μF
PWM frequency	10	kHz

**Table B.5.** Three phase VAPF – selected parameters

network voltage	80	V
the reference <i>DC</i> link voltage	70	V
series inductance $L_S$	5.4	mH
filter inductance $L_f$	0.3	mH
Filter capacitance $C_f$	18	μF
<i>DC</i> link capacitance $C$	2200	μF
PWM frequency	10	kHz

**Table B.6.** Single phase SVAPF – elected simulation parameters

network voltage	80	V
the reference <i>DC</i> link voltage	180	V
series inductance $L_S$	10	mH
filter inductance $L_{f1}$	0.3	mH
filter inductance $L_{f2}$	3.5	mH
filter capacitance $C_{f1}$	24	μF
<i>DC</i> link capacitance $C$	2000	μF
PWM frequency	3 and 10	kHz

**Table B.7.** Single phase SVAPF – selected experimental parameters

network voltage	80	V
the reference DC link voltage	180	V
series inductance $L_S$	10	mH
filter inductance $L_{f1}$	0.3	mH
filter inductance $L_{f2}$	3.5	mH
filter capacitance $C_{f1}$	24	$\mu$ F
DC link capacitance $C$	2000	$\mu$ F
PWM frequency	3 and 10	kHz

## Appendix C. Results of the Probabilistic Investigations

**Table C.1.** Comparison of IPFC power ratings for probabilistic and deterministic approaches

	$N$	$\mu_n \times 10^{-4}$	$\sigma_n^2 \times 10^{-5}$	$P_{sh}^{prob}$	$P_{sh}$	$P_{sh}^{prob} / P_{sh}$ [%]
Fig.5.3.a	1	0.084	21.25	0.061	0.105	57.9
	2	0.169	42.51	0.081	0.210	38.7
	3	0.254	63.77	0.094	0.315	29.9
	4	0.339	85.03	0.111	0.421	26.4
	5	0.425	106.29	0.120	0.526	22.9
Fig.5.3.b	1	-10.18	66.55	0.090	0.105	85.99
	2	-20.37	133.08	0.133	0.210	63.22
	3	-30.55	199.62	0.161	0.315	50.97
	4	-40.74	266.16	0.185	0.421	43.96
	5	-50.93	332.70	0.213	0.526	40.46
Fig.5.3.c	1	95.75	19.12	0.062	0.088	70.93
	2	191.50	38.24	0.091	0.176	51.55
	3	287.26	57.36	0.116	0.264	43.80
	4	383.01	76.49	0.134	0.353	37.99
	5	478.77	95.61	0.159	0.441	36.05
Fig.5.3.d	1	86.89	58.00	0.081	0.088	92.04
	2	173.79	116.00	0.128	0.176	72.72
	3	260.68	174.01	0.162	0.264	61.36
	4	347.58	232.58	0.195	0.353	55.24
	5	434.47	290.02	0.219	0.441	49.65

**Table C.2.** Comparison of STATCOM power rating for probabilistic and deterministic approaches

	$N$	$\mu_n \times 10^{-4}$	$\sigma_n^2 \times 10^{-3}$	$Q_{st}^{prob}$	$Q_{st}$	$Q_{st}^{prob} / Q_{st} [\%]$
Fig.5.12.a	1	-24.84	5.27	0.28	0.52	54.3
	2	-49.69	10.54	0.38	1.04	35.5
	3	-74.53	15.82	0.48	1.56	30.5
	4	-99.38	21.09	0.55	2.09	26.5
	5	-124.22	26.37	0.59	2.61	22.6
Fig.5.12.b	1	-24.05	16.35	0.41	0.52	80.1
	2	-48.11	32.07	0.63	1.04	60.3
	3	-72.17	49.06	0.75	1.56	48.4
	4	-96.23	65.41	0.88	2.09	42.4
	5	-120.29	81.77	1.00	2.61	38.5
Fig.5.12.c	1	43.74	5.43	0.33	0.52	64.6
	2	87.49	10.87	0.46	1.04	44.8
	3	131.24	16.31	0.61	1.56	38.8
	4	174.99	21.75	0.73	2.09	34.9
	5	218.73	27.19	0.80	2.61	30.9
Fig.5.12.d	1	43.74	11.00	0.41	0.52	78.5
	2	87.49	22.01	0.61	1.04	58.7
	3	131.24	33.01	0.76	1.56	48.8
	4	174.99	44.02	0.89	2.09	42.8
	5	218.73	55.02	1.01	2.61	38.8

## Appendix D. The UPQC Device Modelling

Models of the individual circuits as well as UPQC full *3-phase* model were elaborated in *d-q* coordinates with regard to the following assumptions:

- all circuits in UPQC are symmetrical;
- PWM controllers in SAPF and PAPF do not come into range of over-modulation;
- frequency of the triangular carrier in PWM modulator is so large that in case of  $L_V - C_V$  as well as  $L_I - C_I$  filters its influence is negligible;
- $V_{DC}$  voltage pulsations and changes are controlled and do not cause deformations in shape in closed-loop adding (compensating) currents and voltages;
- the ratio  $Tr$  of the adding transformer is set to be *1:1* and additionally the influence of its main impedance is skipped

Block diagrams of the models are introduced below, linked undeniably with their mathematical representations.

*Supply line model.* This model, presented in Figure D.1.a as the block diagram, considers  $L_S$  inductance and supply network resistance  $R_S$  as well as loss resistance  $R_{Tr}$  and the dispersion inductance  $L_{Tr}$  in an adding transformer  $Tr$ . One should notice that in practice short circuit impedance in the transformer very often exceeds network short circuit impedance. Therefore a simplified model of the supply line, presented in Figure D.1.b and further applied in this paper, is sufficiently adequate. Voltage  $v_S$  at the point of measurement, is practically the same as source voltage  $e_S$ . Despite this, in the measurement of the arrangement (Figure D.2) additional correction of the measured voltage  $v_S$ , taking into consideration the voltage drop on the transformer, is advisable. Because of such correction, transformer parameters as well as current (concerning mostly frequency  $\omega_S$ )  $i_S = i'_C + i_L \approx i_C + i_L$  knowledge is needed. Harmonics in current  $i_L$  will be compensated by the PAPF.

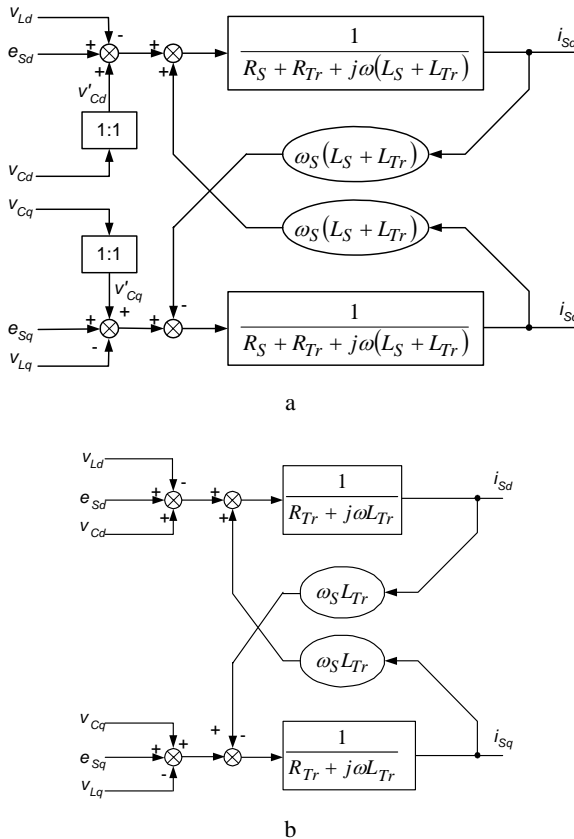


**Figure D.1.** Block diagram of the supply line: a. considering network impedance; b. simplified

*SAPF model with PWM controller.* The major task of SAPF is to compensate for deformations in the network voltage, including also higher harmonics. Therefore high dynamics and accuracy in voltage  $v_C$  formation is required. It is possible to

achieve this in the case of the utilization of  $L_V - C_V$  output filter with the help of: 1) state spaces regulator; 2) voltage regulator with internal coupling in regard of  $C_V$  capacitor current. In the model presented in Figure D.3 there was an assumption also of a second regulator, taking into consideration temporary tendencies of changes in output voltage ( $C_V \cdot dv_C/dt$ ).

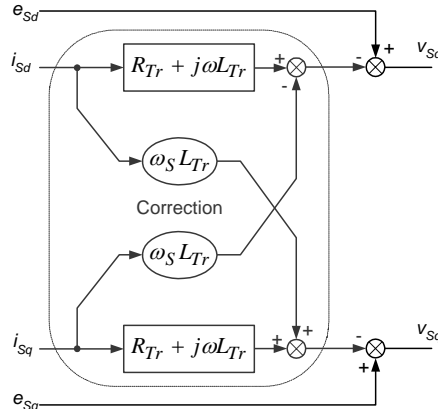


**Figure D.2.** Block diagram of the network voltage measure arrangement; without and with correction of influence of the transformer

The scheme presented in Figure D.3 shows also the manner of realization of the double decoupling of the state spaces. In the decoupling circuit there are used instantaneous measurements of  $C_V$  capacitor current as well as choke current in the  $L_V - C_V$  filter. There is no need for exact identification of the capacitor capacity. In the case when the state spaces regulator is applied it is much easier to get the double decoupling measuring current in the output filter.

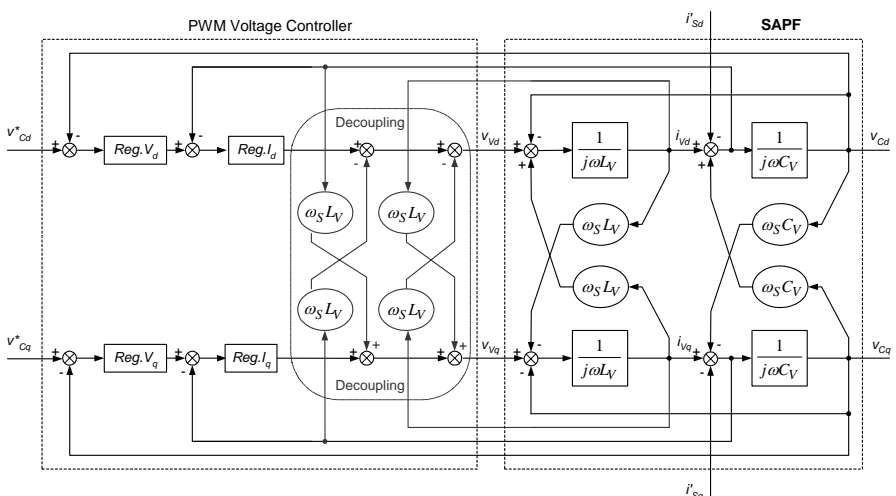


**Figure D.3.** SAPF block diagram, with PWM controller and output filter

*PAPF model with PWM controller.* In PAPF, questions concerning the compensating  $i_C$  current shaping are much the same as questions concerning  $v_C$  voltage shaping in an SAPF. The output filters  $L_I - C_I$  are also employed in PAPF. Such filters are required because of disturbances and consequences of uncompensated  $di_L/dt$  outgrowths. If such filters are installed, it is advisable for the regulator to realize also the state spaces double decoupling. The double decoupling manner in PAPF is analogous to that described in the previous section, as it is in Figure D.4. The PAPF block diagram differs from the SAPF diagram because of the lack of circuit for  $C_I$  capacitance voltage control (load voltage  $v_L$ ).

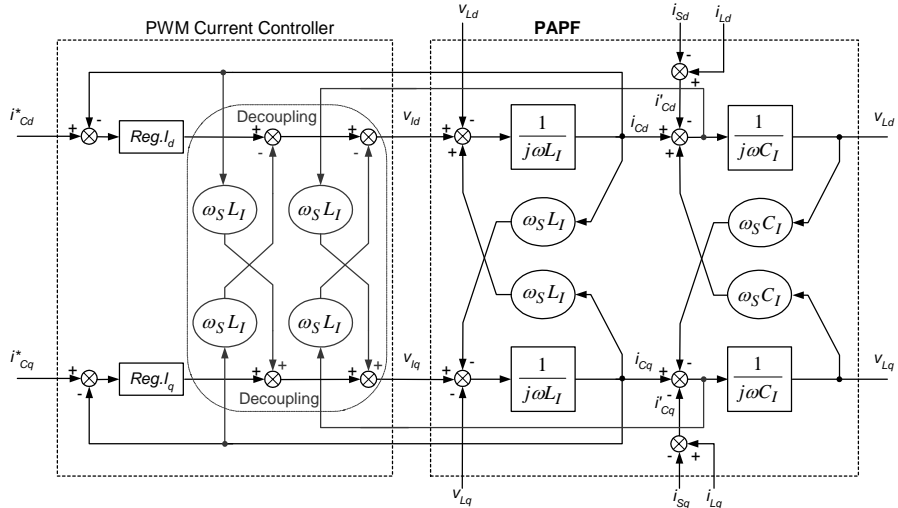


**Figure D.4.** PAPF block diagram, with PWM controller and output filter

*DC circuit model.* The Figure D.5, presented in the DC circuit block diagram, results from the balance of instantaneous powers. Each deviation from zero, in sum of the instantaneous  $p_V$  and  $p_I$  active powers, causes changes of the instantaneous  $V_{DC}$  voltage, in accordance with dependency

$$C_{DC} \cdot V_{DC} \frac{dV_{DC}}{dt} = p_{DC} = -(p_V + p_I) = p_S - p_V \quad (\text{D.1})$$

From Equation D.1 it follows in an obvious way that the sum of the instantaneous powers  $p_V + p_I$  has to change periodically in a steady state.

Model (Figure D.5) omits power losses in SAPF and PAPF, profitably slowing  $V_{DC}$  voltage changes. Accepting such simplification, it is also possible to omit  $LC$  filters as well as transformer losses. In this case instantaneous power in the DC link can be expressed by the following dependency

$$p_V + p_I = \underbrace{i_{Sd}v_{Cd} + i_{Sq}v_{Cq}}_{p_V} + \underbrace{i_{Cd}v_{Ld} + i_{Cq}v_{Lq}}_{p_I} \quad (\text{D.2})$$

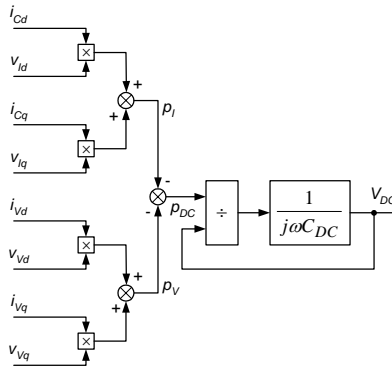


Figure D.5. DC circuit block diagram

*Load model.* In Figure D.6, load block diagrams were introduced. The voltage model in particularly should be used in the case when the UPQC employs a diode rectifier with capacitive filter or is used to power flow control between two network sources. From the other side, a current model should be used in the situation when, e.g., a thyristor rectifier with smoothing choke is used as a load.

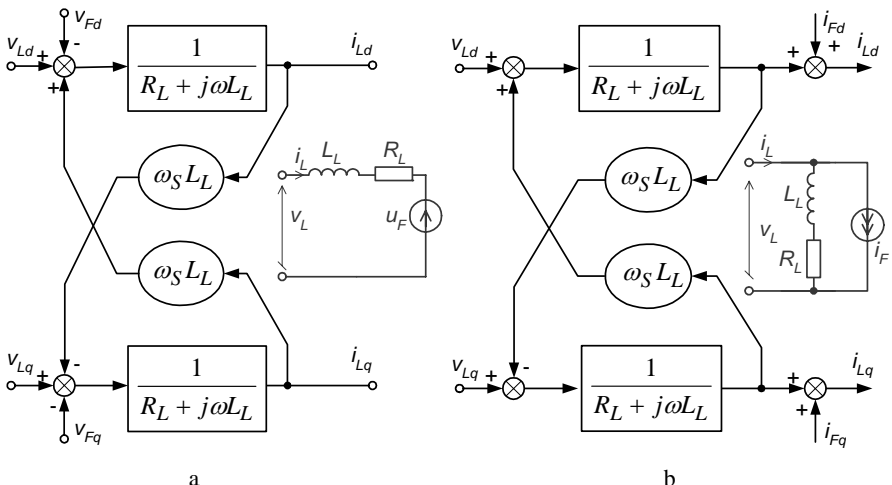


Figure D.6. Loads block diagrams: a. voltage; b. current

*The main controller model.* In the main controller introduced in Figure D.7, the reference courses of the adding voltages and currents ( $v^*_c$  and  $i^*_c$ ) are determined in two independent circuits. In the first circuit (Figure D.7.a) the input signals are: set courses of load voltage  $v_L^*$  and measured  $v_S$  network voltages. The first circuit does not take part in  $V_{DC}$  voltage stabilization or in compensation/filtering, which is undesirable in load current  $i_L$  components. This is the domain of the second circuit in the main controller (Figure D.7.b).

To stabilize  $V_{DC}$  voltage, from the compensating courses extracted in the second circuit by the  $F_L(j\omega)$  filters the reference active components  $i^{*}_{Dd}$  and  $i^{*}_{Dq}$  in PAPF's output current are subtracted. These components are determined on the basis of instantaneous power theory in accordance with the following dependencies

$$i^{*}_{Cd} = \Delta p_{DC}^* \frac{v_{Ld}}{v_{Ld}^2 + v_{Lq}^2}, \quad i^{*}_{Cq} = \Delta p_{DC}^* \frac{v_{Lq}}{v_{Ld}^2 + v_{Lq}^2} \quad (D.3)$$

where  $\Delta p_{DC}^*$  - voltage regulator exit signals, they cause faster or slower  $C_{DC}$  capacitor charging/discharging, in dependency on value and sign of  $\Delta V_{DC} = V_{DC}^* - V_{DC}$  error signal.

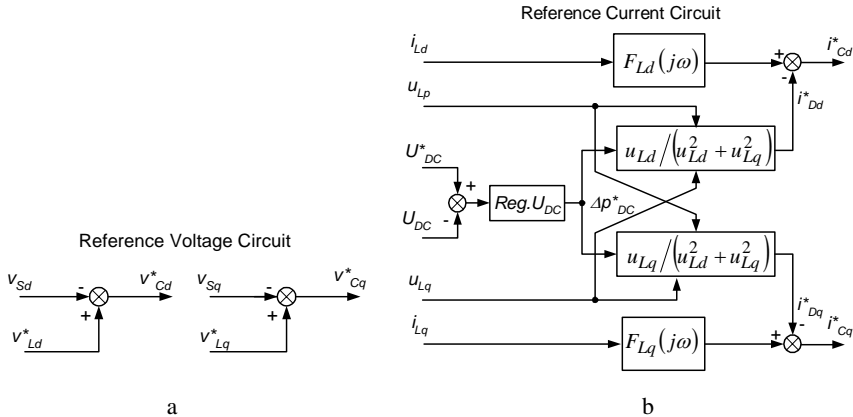


**Figure D.7.** UPQC main controller – block diagram: a. reference voltage circuit; b. reference current circuit

*UPQC complete model.* This model concerns the UPQC which simultaneously fulfils the following functions: network voltage stabilization, symmetrization and harmonics compensation, as well as load current passive components

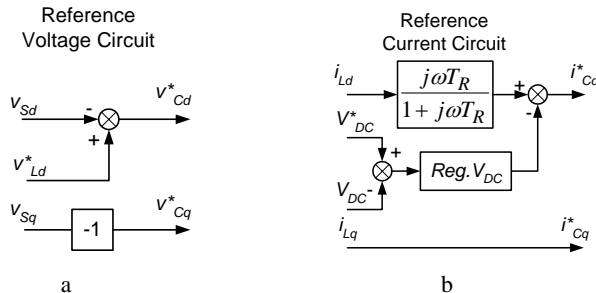


**Figure D.8.** UPQC simple main controller – block diagram: a. reference voltage circuit; b. reference current circuit

compensation. In this case and when  $d-q$  rotating coordinates are suitably synchronized with the network voltage, the main controller become a very simple arrangement (Figure D.8), containing only one High Pass Filter – HPS (*e.g.*, differential module with  $T_R$  constant in limits 10-20 ms), suitable adders as well as  $V_{DC}$  voltage regulator - usually *PI* or inertia *P*. Therefore such a simple main controller was considered, introduced in Figure D.9, the UPQC full block diagram.

A complete model was elaborated for UPQC filtration/compensation proprieties analysis, often met in practice in conditions of: small network impedance (Figure D.1.b) and large internal impedance of the non-linear current type load (Figure D.6.b). On the basis of the above, in the UPQC model, supply network parameters  $R_S$  and  $L_S$  as well as current type load parameters  $R_L$  and  $L_L$  were skipped. Additionally, all regulators in SAPF and PAPF, PWM controllers were accepted as type *P* (proportional). In an obvious way, in this model, there could also be implemented different types of regulators. However one should note that type *P* regulators permit sufficiently exact shape of the non-sinusoidal adding voltages and currents ( $v_C$  and  $i_C$ ) and do not introduce additional dynamic errors during the following of the reference compensating courses.

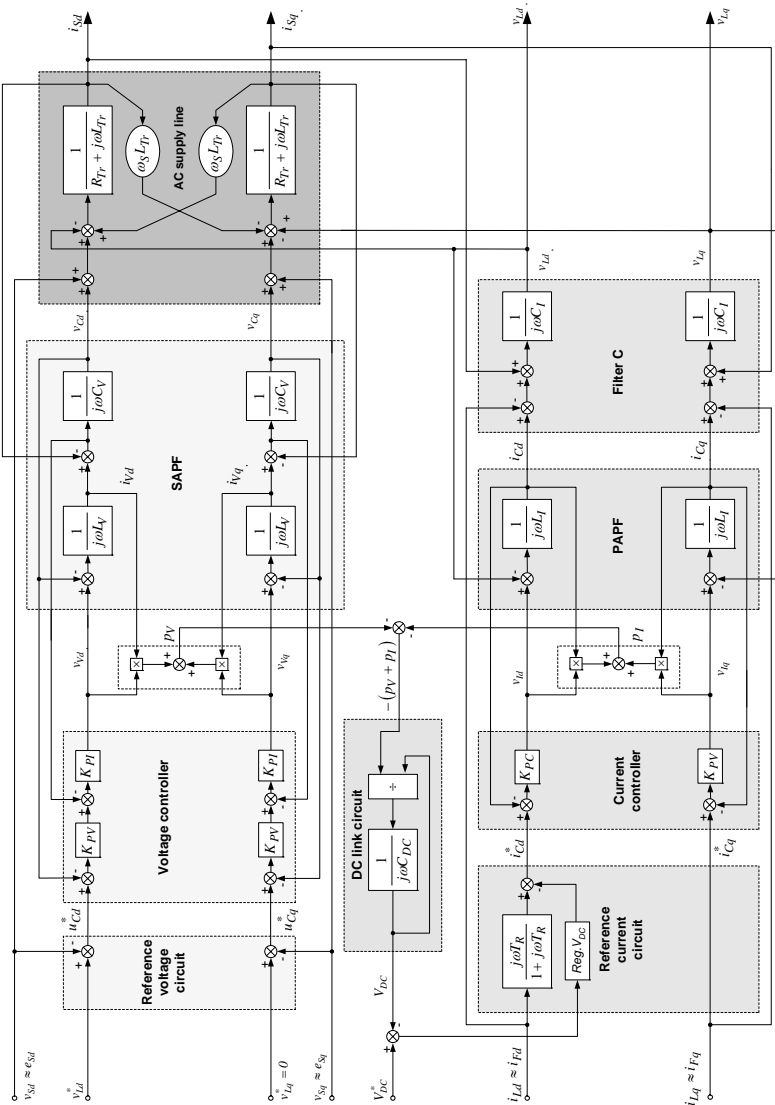


Figure D.9. UPQC complete block diagram, influence of supply network impedance omission

---

## **Acronyms and Symbols**

### **Acronym Description**

AC	Alternating Current
APF	Active Power Filter
ASD	Adjustable Speed Drives
AVF	Automatic Voltage Regulator
CCS	Coordinated Control System
CEER	Council of European Energy Regulators
CIGRE	International Council on Large Electric Systems
CSC	Current Source Converters
CUPS	Custom Power System
DC	Direct Current
DR	Distributed Resources
DSTATCOM	Distribution Static Synchronous Compensators
DVR	Dynamic Voltage Restorer
EMI	Electromagnetic Interference
EPS	Electrical Power System
ESS	Energy Storage System
ETO	Emitter Turn-Off Thyristor
EURELECTRIC	Union of the Electricity Industry
FACTS	Flexible Alternating Current Transmission System
GPS	Global Position System
GTO	Gate Turn Off
HV	High Voltage
HVDC	High Voltage Direct Current

IEC	International Electrotechnical Commission
IEEE	Institute of Electrical and Electronic Engineers
IGBT	Insulated Gate Bipolar Transistor
IGCT	Integrated Gate Commutated Thyristor
IPFC	Interline Power Flow Controller
LTC	Load Tap Changers
LV	Low Voltage
MTO	MOS Turn-Off Thyristor
MV	Medium Voltage
PAPF	Parallel Active Power Filter
PQ	Power Quality
PSS	Power System Stabilizer
PWM	Pulse Width Modulation
RPL	Reactive Power Loss Sensitivity Factors
SAPF	Series Active Power Filter
SCR	Silicon Controlled Rectifier
SSSC	Static Synchronous Series Compensator
STATCOM	Static Synchronous Compensators
SVAPF	Symmetrical Voltage Active Power Filter
SVC	Static Var Compensators
SVR	Step Voltage Regulators
SVS	Synchronous Voltage Source
TCBR	Thyristor Controlled Braking Resistor
TCPAR	Thyristor Controlled Phase Angle Regulator
TCSC	Thyristor Controlled Series Compensators
TS	Transient Stability
TSSC	Thyristor Switched Series Capacitor
UPFC	Unified Power Flow Controllers
UPQC	Unified Power Quality Conditioner
UPS	Uninterrupted Power Supply
VAPF	Voltage Active Power Filter
VSC	Voltage Source Converter
VSG	Voltage Source Generator

## Symbol Description

$a, b, c$	phase order
$d$	instantaneous duty cycle

$f$	frequency in general
$i$	instantaneous current in general
$I$	steady state current in general
$L$	reactance in general
$p$	instantaneous active power in general
$P$	steady state active power in general
$q$	instantaneous reactive power in general
$Q$	steady state reactive power in general
$R$	resistance in general
$s$	instantaneous apparent power in general
$S$	steady state apparent power in general
$t$	time in general
$THD$	total harmonic distortion factor
$v$	instantaneous voltage in general
$v_i$	instantaneous voltage for phase $i$
$V$	steady state voltage in general
$V_i$	steady state voltage for phase $i$
$X$	reactance in general
$Z$	impedance in general

## Greek Symbols

$\alpha$	converter control angle
$\omega$	angular frequency in general

---

## References

- [1] Hingorani N, Gyugyi L, (2000) Understanding FACTS: concepts and technology of flexible ac transmission systems. IEEE, New York
- [2] Ghosh A, Ledwich G, (2002) Power quality enhancement using custom power devices. Kluwer Academic Publishers, Boston
- [3] Dugan R, McGranaghan M, Beaty W, (1996) Electrical power systems quality. McGraw-Hill, New York, 1996
- [4] Arrillaga J, Watson N, Chan S, (2000) Power system quality assessment. Wiley & Sons, Chichester, England
- [5] CIGRE Working Group 14.31, (1999) Custom power - state of the art.
- [6] Gyugyi L, (2000) Converter-based FACTS technology: electric power transmission in the 21st century. International Power Electronics Conference, vol.1:15-26
- [7] Mohan N, Undeland T, Robbins W, (1995) Power electronics, converters, applications, and design. 2<sup>nd</sup> edition, John Wiley & Sons, New York
- [8] Hingorani N, (1998) Power electronics in electric utilities: role of power electronics in future power systems. Proceedings of the IEEE, vol.76, no.4:481-482
- [9] Edris A, (2000) FACTS technology development: an update. IEEE Power Engineering Review, vol.20, no.3:4-9
- [10] Song Y, Johns A, (1999) Flexible ac transmission systems (FACTS). IEE Power and Energy series 30, TJ International Ltd, Padstow, Cornwall, London
- [11] Hingorani N, (1993) Flexible ac transmission systems. IEEE spectrum, vol.30, no.4:41-48
- [12] IEEE/CIGRE, (1995) FACTS overview. Special issue 95-TP-108, IEEE Service Center, Piscataway, New York
- [13] Hingorani N, (1995) Introducing custom power. IEEE spectrum, vol.32, no.6:41-48
- [14] Akagi H, (1996) New trends in active filters for power conditioning. IEEE Transactions on Industry Applications, vol.32, no.6:1312-1322

- [15] Akagi H, (1994) Trends in active power line conditioners. IEEE Transactions on Power Electronics, vol.9, no.3:263-268
- [16] Renz B, (1999) AEP unified power flow controller performance. IEEE Transactions on Power Delivery, vol.14, no.4:1374-1381
- [17] Gyugyi L, Schauder S, Williams S, Rietmann T, Torgerson D, Edris A, (1995) The unified power flow controller: a new approach to power transmission control. IEEE Transactions on Power Delivery, vol.10:1085-1097
- [18] Schauder C, Gyugyi L, Lund M, Hamai D, Rietman T, Torgerson D, *et al.*, (1998) Operation of the unified power flow controller (UPFC) under practical constraints. IEEE Transactions on Power Delivery, vol.13:630-639
- [19] Strzelecki R, (2002) Active arrangements for energy conditioning - a new fashion or quality ?. (in Polish), Modern Supplying Arrangements in Power Systems Conference:1.14-9.14
- [20] Strzelecki R, (2002) Active arrangements for energy conditioning - APC. (in Polish), Przegląd Elektrotechniczny - Journal, no.2:196-202
- [21] Akagi H, Fujita H, (1995) A new power line conditioner for harmonic compensation in power systems. IEEE Transactions on Power Delivery, vol.10, no.3:1570-1575
- [22] Akagi H, (1995) New trends in active filters. EPE Conference:17-26
- [23] Jeon S, Cho G, (1997) A series-parallel compensated uninterruptible power supply with sinusoidal input current and sinusoidal output voltage. IEEE-PESC Conference:297-303
- [24] Fujita H, Akagi H, (1998) Unified power quality conditioner: the integration of series and shunt active filter. IEEE Transactions on Power Electronics, vol.13, no.2:315-322
- [25] Aredes M, Heumann K, Watanabe E, (1998) An universal active power line conditioner. IEEE Transactions on Power Delivery, vol.13, no.2:1453-1460
- [26] Strzelecki R, Kukluk J, Rusiński J, (1999) Active power line conditioners based on symmetrical topologies. IEEE-ISIE Conference, vol.2:825-830
- [27] Ghosh A, Ledwich G, (2001) A unified power quality conditioner (UPQC) for simultaneous voltage and current compensation. Electric Power Systems Research, vol.59:55-63
- [28] Malabika Basu M, Das S, Dubey G, (2002) Performance study of UPQC-Q for load compensation and voltage sag mitigation. IEEE-IECON Conference:698-702
- [29] Meckien G, Strzelecki R, (2002) Single phase active power line conditioners-without transformers. EPE-PEMC Conference
- [30] da Silva S, (2002) A three-phase line-interactive UPS system implementation with series-parallel active power-line conditioning capabilities. IEEE Transactions on Industry Applications, vol.38, no.6:1581-1590
- [31] Watanabe E, Aredes M, (2002) Power quality considerations on shunt/series current and voltage conditioners. Conference on Harmonics and Quality of Power, vol.2:595-600

- [32] Strzelecki R, (2003) New concepts of the conditioning and power flow control in the ac distribution systems. Modern Feed Equipments in Electrical Power Systems Conference:65-72
- [33] McHattie R, (1998) Dynamic voltage restorer: the customer's perspective. IEE Colloquium on Dynamic Voltage Restorers, Digest No. 98/189
- [34] Kundur P, (1994) Power system stability and control. McGraw-Hill, New York
- [35] Machowski J, Bialek J, Bumby J, (1997) Power system dynamics and stability. John Wiley & Sons, Chichester, New York
- [36] Hingorani N, (1996) High-voltage dc transmission: a power electronics workhorse. IEEE spectrum, vol.33, no.4:63-72
- [37] Arrillaga J, (1999) HVDC transmission. IEE Publications, London
- [38] McMurray W, (1987) Feasibility of GTO thyristors in a HVDC transmission system. EPRI EL-5332, project 2443-5, final report
- [39] Asplund G, Eriksson K, Svensson K, (1998) HVDC light - dc transmission based on voltage sourced converters. ABB Review, no.1:4-9
- [40] Mori S, Matsuno K, Hasegawa T, Ohnishi S, Takeda M, Seto M, *et al.*, (1993) Development of a large static var generator using self-commutated inverters for improving power system stability. IEEE Transactions on Power Systems, vol.8, no.1:371-377
- [41] Hirakawa M, Somiya H, Mino Y, Baba K, Murakami S, Watanabe Y, (1996) Application of self-commutated inverters to substation reactive power control. CIGRE paper 23-205, Paris session
- [42] Schauder C, Gernhardt M, Stacey E, Lemak T, Gyugyi L, Cease T, *et al.*, (1996) TVA STATCOM project: design, installation, and commissioning. CIGRE paper 14-106, Paris session
- [43] Schauder C, (1999) STATCOM for compensation of large electric arc furnace installations. IEEE-PES summer power meeting:1109-1112
- [44] Schauder C, Gernhardt M, Stacey E, Lemak T, Gyugyi L, Cease T, *et al.*, (1995) A development of a  $\pm 100$  Mvar static condenser for voltage control of transmission systems. IEEE Transactions on Power Delivery, vol.10, no.3:1486-1493
- [45] Reed G, Paserba J, Croasdaile T, Takeda M, Morishima N, Hamasaki Y, *et al.*, (2001) STATCOM application at VELCO Essex substation. IEEE-PES T&D Conference and Exposition:1133-1138
- [46] Schauder C, Stacey E, Lund M, Gyugyi L, Kovalsky L, Keri A, *et al.*, (1998) AEP UPFC project: installation, commissioning and operation of the  $\pm 160$  MVA STATCOM (phase 1). IEEE Transactions on Power Delivery, vol.13, no.4:1530-1535
- [47] Renz B, Keri A, Mehraban A, Kessinger J, Schauder C, Gyugyi L, *et al.*, (1998) World's first unified power flow controller on the AEP system. CIGRE paper 14-107, Paris session
- [48] IEEE special publication no. 87TH1087-5-PWR, (1987 ) Application of static var systems for system dynamic performance

- [49] Ekanayake J, Jenkins N, (1996) A three-level advanced static var compensator. IEEE Transactions on Power Delivery, vol.11, no.1:540-545
- [50] IEEE Special Stability Controls Working Group, (1995) Static var compensator: models for power flow and dynamic performance simulation. IEEE Transactions on Power Systems, vol.9, no.1:229-240
- [51] Gyugyi L, (1988) Power electronics in electric utilities: static var compensators. IEE proceedings, vol.76, no.4:483-494
- [52] Piwko R, Wegner C, Damsky B, Furumasu B, Eden J, (1994) The slat thyristor controlled series capacitor project-design, installation, commissioning, and system testing. CIGRE paper 14-104, Paris session
- [53] Chistl N, Hedin R, Sadek K, Lutzlerberger P, Krause P, McKenna S, *et al.*, (1992) Advanced series compensation (ASC) with thyristor controlled impedance. CIGRE paper 14/37/38-05, Paris session
- [54] Keri A, Ware B, Byron R, Chamia M, Halvarsson P, Angquist L, (1992) Improving transmission system performance using controlled series capacitors. CIGRE paper 14/37/38-07, Paris session
- [55] Gama C, (1999) Brazilian north-south interconnection - control application and operative experience with thyristor controlled series compensation (TCSC). IEEE-PES summer power meeting:1103-1108
- [56] Gyugyi L, Kalyan K, Schauder C, (1998) The interline power flow controller concept: a new approach to power flow management in transmission systems. IEEE Transactions on Power Delivery, vol.14, no.3:1115-1122
- [57] Strzelecki R, Benysek G, Bojarski J, (2001) Interline power flow controller. (in Polish), SENE Conference, vol.2:591-596
- [58] Strzelecki R, Benysek G, Fedyczak Z, Bojarski J, (2002) Interline power flow controller-probabilistic approach. IEEE-PESC Conference, vol.2:1037-1042
- [59] Strzelecki R, Smereczyński P, Benysek G, (2004) Static properties of the interline power flow controllers. Technicna Elektrodinamika - Journal, no.1:63-69
- [60] Strzelecki R, Benysek G, (2002) Interline power flow controller - new concept of the connection in multilane transmission systems. Technicna Elektrodinamika – Journal, no.4:6366
- [61] Strzelecki R, Smereczyński P, Benysek G, (2005) Interline Power Flow Controller - properties and control strategy in dynamic states. CPE Conference
- [62] Strzelecki R, Smereczyński P, Benysek G, (2004) Interline power flow controllers - energetic properties. EPE-PEMC Conference
- [63] Strzelecki R, Benysek G, (2003) Dimensioning of the interline power flow controllers. EPQU Conference:391-398
- [64] Kurowski T, Benysek G, Kempski A, Smoleński R, (2000) About proper cooperation of the electric drives and static converters. (in Polish), Institute of Drives and Electrical Measurements, Wrocław University of Technology Press, vol.48:326-334

- [65] Strzelecki R, Kempski A, Smoleński R, Benysek G, (2003) Common mode voltage cancellation in systems containing 3-phase adding transformer with PWM excitation. EPE Conference
- [66] Kempski A, Strzelecki R, Smoleński R, Benysek G, (2003) Suppression of conducted EMI in four-quadrant ac drive system. IEEE-PESC Conference:1121-1126
- [67] Thomsen P, (1999) Application and control of CUPS in the distribution grid. Institute of Energy Technology, Aalborg University, vol.3:2-11
- [68] Strzelecki R, Benysek G, (2004) Conceptions and properties of the arrangements in distributed electrical power systems. MITEL Conference:241-248
- [69] Strzelecki R, Jarnut M, Benysek G, (2003) Active electrical energy conditioners for individual customers. PES Conference, Warsaw University of Technology Press, vol.1: 27-34
- [70] Malesani L, Rossetto L, Tenti P, (1986) Active filter for reactive power and harmonic compensation. IEEE Power Electronic Council annual meeting:321-330
- [71] Strzelecki R, Supronowicz H, (1999) Harmonic filtration in ac power systems. (in Polish), 2<sup>nd</sup> edition, Adam Marszałek Publishing House
- [72] Gyugyi L, Strycula E, (1976) Active ac power filter. IEEE-IAS annual meeting:529-535
- [73] Peng F, Akagi H, Nabae A, (1986) A study of active power filters using quad-series voltage-source PWM converters for harmonic compensation. IEEE Transactions on Industry Applications, vol.22, no.3:460-465
- [74] Moran L, Fernandez L, Dixon J, (1997) A simple and low-cost control strategy for active power filters connected in cascade. IEEE Transactions on Industrial Electronics, vol.44, no.5:402-408
- [75] El-Habrouk M, Darwish M, Mehta P, (2000) Active power filters: a review. IEE Proceedings-Electric Power Applications, vol.147, no.5:403-413
- [76] Aburto V, Schneider M, Moran L, Dixon J, (1997) An active power filter implemented with a three-level NPC voltage-source inverter. IEEE-PESC Conference:1121-1126
- [77] Strzelecki R, Sozański K, (2001) Active filters in supplying networks and drives. (in Polish), Modern Supplying Arrangements in Power Systems Conference:17.1-17.12
- [78] Akagi H, Fujita H, Wada K, (1999) A shunt active filter based on voltage detection for harmonic termination of a radial power distribution line. IEEE Transactions on Industry Applications, vol.35, no.3:638-645
- [79] Peng F, (1998) Application issues of active power filters. IEEE Industry Application Magazine, vol.4, no.5:21-30
- [80] Strzelecki R, Supronowicz H, (2000) Power factor in ac supply systems and improvements methods. (in Polish), Publishing House of the Warsaw University of Technology

- [81] Greczko E, Benysek G, Kot E, (2001) Properties of the active filters constructed on the base of the multilevel converters. (in Russian), Technicna Elektrodinamika – Journal, no.3:13-18
- [82] Greczko E, Benysek G, Branicki R, Smoleński R, (1999) Passive and active filters utilization in ac voltage stabilizers. (in Russian), Technicna Elektrodinamika – Journal:89-92
- [83] Kot E, Baranowski A, Benysek G, (2000) Comparative analysis of the parallel active filters on base of the multilevel inverters. EDPE Conference: 38-43
- [84] Singh B, Al-Haddad K, Chandra A, (1999) A review of active filters for power quality improvement. IEEE Transactions on Industrial Electronics, vol.46, no.5:960-971
- [85] Peng F, Lai J, (1996) Application considerations and compensation characteristics of shunt active and series active filters in power systems. Conference on Harmonics and Quality Power:12-20
- [86] Aredes M, Heumann K, (1996) A unified power flow controller with active filtering capabilities. EPE-PEMC Conference, vol.3:139-144
- [87] Strzelecki R, Kukluk J, Supronowicz H, Tunia H, (1999) A universal symmetrical topologies for active power line conditioners. EPE Conference
- [88] Elnady A, Goauda A, Salama M, (2001) Unified power quality conditioner with a novel control algorithm based on wavelet transform. Canadian Conference on Electrical and Computer Engineering, vol.2:1041-1045
- [89] Pengcheng Zhu, (2003) A novel control scheme in 2-phase unified power quality conditioner. IEEE-IECON Conference, vol.2:1617-1622
- [90] Peng F, McKleever J, Adams D, (1997) A power line conditioner using cascade multilevel inverters for distribution systems. IEEE Industrial Application Society annual meeting:1316-1321
- [91] Tolbert L, Peng F, (1999) A multilevel converter-based universal power conditioner. IEEE-PESC Conference, vol.1:393-399
- [92] Strzelecki R, Benysek G, Rusiński J, Dębicki H, (2005) Modeling and experimental investigation of the small UPQC systems. CPE Conference
- [93] Rusiński J, Benysek G, Kot E, (2000) Multilevel series-parallel active power filter - parameters and topologies comparison. SRE Symposium, vol.1:283-287
- [94] Gyugyi L, (1992) Unified power flow control concept for flexible ac transmission systems. IEE Proceedings, vol.139, no. 3:323-331
- [95] Fujita H, Watanabe Y, Akagi H, (1999) Control and analysis of a unified power flow controller. IEEE Transactions on Power Electronics, vol.14, no.6:1021-1027
- [96] Strzelecki R, Benysek G, Noculak A, (2003) Utilization of the power electronics arrangements in electrical power system. (in Polish), Przegląd Elektrotechniczny - Journal, no.2:41-48
- [97] Strzelecki R, Benysek G, (2005) Power electronics based flexible electrical energy flow arrangements. Gdynia Maritime University Press:148-157

- [98] Chen Y, Wolanski Z, Oil B, (2000) Unified power flow controller (UPFC) based on chopper stabilized diode-clamped multilevel converters. IEEE Transactions on Power Electronics, vol.15, no.2:258-267
- [99] Strzelecki R, Benysek G, Rusiński J, Jarnut M, Meckien G, (2003) Active power filter - new control system and topology. AES Conference:99-106
- [100] Moran L, (1995) Line conditioning system with simple strategy and fast dynamic response. IEE - Generation, Transmission, Distribution Conference, vol.142, no.2:128-134
- [101] Moran L, Ziodas P, Joos G, (1989) Analysis and design of a novel 3-phase solid-state power factor compensator and harmonic suppressor system. IEEE Transaction on Industry Applications, vol.25:609-619
- [102] Liang Y, Nwankpa C, (2000) A power-line conditioner based on flying-capacitor multilevel voltage-source converter with phase-shift SPWM. IEEE Transactions on Industry Applications, vol.36, no.4:965-971
- [103] Jarnut M, Benysek G, Strzelecki R, (2004) Transformer-less 1-phase active power line conditioners. Technicna Elektrodinamika - Journal, no.7:93-99
- [104] Strzelecki R, Benysek G, Jarnut M, Kot E, (2004) Voltage source power line conditioners. (in Polish), Jakość i Użytowanie Energii Elektrycznej - Journal, vol.10:13-24
- [105] Strzelecki R, Jarnut M, Benysek G, (2004) Static and dynamic properties of the 1-phase voltage source active power filter. Rzeszów University of Technology Press, no.214:141-152
- [106] Strzelecki R, Benysek G, Sozański K, Jarnut M, Rusiński J, (2005) Voltage power line conditioner - voltage restoring mode. EPE Conference
- [107] Strzelecki R, Jarnut M, Benysek G, (2004) Modified voltage source active power filter. EPE-PEMC Conference
- [108] Strzelecki R, Jarnut M, Benysek G, (2004) Voltage power line conditioner VPLC - input power factor correction solutions. BEC Conference:339-342
- [109] Strzelecki R, Jarnut M, Benysek G, (2004) Voltage source conditioners property. Uees Conference:767-772
- [110] Strzelecki R, Supronowicz H, Jarnut M, Benysek G, (2003) 1-Phase active power line conditioner. EPE Conference
- [111] Strzelecki R, Jarnut M, Kot E, Kempski A, Benysek G, (2003) Multilevel voltage source power quality conditioner. IEEE-PESC Conference:1043-1048
- [112] Strzelecki R, Benysek G, Jarnut M, Kot E, (2003) Controlled voltage sources in electrical energy conditioning arrangements. PES-WZEE Conference, Warsaw University of Technology Press, vol.2:287-294
- [113] Strzelecki R, Dębicki H, Benysek G, Jarnut M, (2003) Control in simple scheme of the network voltage conditioner. PPEE Symposium, vol.18:91-94
- [114] Strzelecki R, Tunia H, Jarnut M, Meckien G, Benysek G, (2003) Transformer-less 1-phase active power line conditioners. IEEE-PESC Conference:321-326

- [115] Strzelecki R, Jarnut M, Kot E, Benysek G, (2003) Voltage source power line conditioners. CPE Conference:152-161
- [116] Strzelecki R, Benysek G, Jarnut M, Rusiński J, (2002) New concept of the parallel active power filtering. BEC Conference:381-384
- [117] Strzelecki R, Rusiński J, Benysek G, (2002) Voltage source power quality conditioner. EPNC Symposium:179-182
- [118] Strzelecki R, Benysek G, Jarnut M, Dębicki H, (2003) Static and dynamic properties of the VPLC active filters with additional voltage source. (in Polish), SENE Conference:569-574
- [119] Strzelecki R, Jarnut M, Benysek G, (2005) Symmetrical power line conditioner - basic properties. CPE Conference
- [120] Strzelecki R, Benysek G, Dębicki H, (2004) The universal multifunctional interline arrangements. (in Polish), Przegląd Elektrotechniczny - Journal, no.3:226-232
- [121] IEEE standard 100-1996, (1997) Dictionary of electrical and electronics terms. 6<sup>th</sup> edition, New York
- [122] IEC 61000-4-30, (2003) Electromagnetic compatibility (EMC) - Part 4-30: Testing and measurement techniques - power quality measurement methods
- [123] EURELECTRIC, (2002) Power quality in European electricity supply networks. 1<sup>st</sup> edition, Brussels
- [124] CEER working group on quality of electricity supply, (2001) Quality of electricity supply: initial benchmarking on actual levels, standards and regulatory strategies
- [125] Strzelecki R, Benysek G, Jarnut M, Rusiński J, Meckien G, (2002) Active electrical energy conditioning arrangements – a new perspective. MITEL Conference:19-30
- [126] Han B, Back S, Kim H, Karady G, (2002) Dynamic characteristic analysis of SSSC bases on multi-bridge inverter. IEEE Transactions on Power Delivery, vol.17, no.2:623-629
- [127] CIGRE Working Group 14.19, (1998) Static synchronous compensator
- [128] Hatzidiadouli C, Chalkiadakis F, (1997) A 12-pulse static synchronous compensator for the distribution system employing the 3-Level GTO-inverter. IEEE Transactions on Power Delivery, vol.12, no.4:1830-1835
- [129] Kot E, Benysek G, Strzelecki R, (2004) Multilevel STATCOM based on cascade topology. Technicna Elektrodinamika - Journal, no.7:86-92
- [130] Greczko E, Benysek G, (1999) Square modulation in three-phase voltage converters. (in Polish), PPEE Symposium:417-422
- [131] Greczko E, Benysek G, Kot E, (1999) Comparison of the square and conventional sinusoidal pulse width modulations. (in Polish), SENE Conference, vol.1:205-210
- [132] Herbig A, (2000) On load flow control in electric power systems. Ph.D. dissertation, Royal Institute of Technology, Stockholm
- [133] Chun L, Qirong J, Jianxin X, (2000) Investigation of voltage regulation stability of static synchronous compensator in power system. IEEE Power Engineering Society, winter meeting, vol.4:2642-2647

- [134] Hochgraf C, Lasseter R, Divan D, Lipo T, (1994) Comparison of multilevel inverters for static var compensation. IEEE Industry Applications annual meeting:921-928
- [135] Yang Z, Shen C, Zhang L, Crow M, (2001) Integration of a STATCOM and battery energy storage. IEEE Transactions on Power System, vol.16, no.2:254-260
- [136] Yang Z, (2000) Integration of battery energy storage with flexible ac transmission system devices. Ph. D. dissertation, University of Missouri
- [137] Benysek G, (1998) Analysis of the hybrid compensators for higher harmonics filtration in ac supplying networks. Ph.D. dissertation, Technical University of Zielona Góra
- [138] Strzelecki R, Benysek G, Goncarova M, (1995) Structures and properties of the hybrid compensators. (in Polish), EPN Conference:136-145
- [139] Bhattachary, S, Cheng P, Divan D, (1997) Hybrid solutions for improving passive filter performance in high power applications. IEEE Transactions on Industry Applications, vol.33, no.3:732-747
- [140] Popczyk J, (1991) Probabilistic models in electrical systems. (in Polish), WNT, Warszawa
- [141] Benysek G, Strzelecki R, (2004) STATCOM and interline power flow controllers dimensioning in the distributed electric power system. Technicna Elektrodinamika - Journal, no.1:104-111
- [142] Strzelecki R, Benysek G, (2004) Probabilistic method for power flow controllers dimensioning. Electric Power Quality and Supply Reliability Conference:149-156
- [143] Benysek G, (2003) Measurements in medium voltage networks to IPFC arrangements dimensioning. (in Polish), Pomiary Automatyka Kontrola - Journal, no.2-3:29-32
- [144] Krzyśko M, (1996) Mathematical statistics. (in Polish), Publishing house of the Adam Mickiewicz University, Poznań
- [145] Bartoszewicz J, (1989) Lectures from mathematical statistics. (in Polish), PWN, Warszawa
- [146] Strzelecki R, Bojarski J, Benysek G, (2002) Probabilistic method for parallel filter's power selection in interline power flow controller. EPE-PEMC Conference
- [147] Benysek G, (2003) STATCOM dimensioning in the distributed electric power system. EPQU Conference:377-381
- [148] Strzelecki R, Bojarski J, Benysek G, (2002) Probabilistic method for parallel filter's power selection in interline power flow controller. PMAPS Conference, vol.2:997-1002
- [149] Strzelecki R, Supronowicz H, Benysek G, Bojarski J, Klytta M, (2002) Selection of the parallel active filter's power rating when it is applied in distribution systems. EPE-PEMC Conference
- [150] Bird B, King K, Pedder D, (1993) An introduction to power electronics. 2<sup>nd</sup> edition, John Wiley & Sons, New York

- [151] Bose B, (1992) Modern power electronics, evolution, technology, and applications. IEEE Press, Piscataway, New York
- [152] Hart D, (1997) Introduction to power electronics. Prentice-Hall, Upper Saddle River, New York
- [153] Lander C, (1993) Power Electronics. McGraw Hill
- [154] Schuster A, (1998) A matrix converter without reactive clamp elements for an induction motor drive system. IEEE-PESC Conference, vol.1:714-720
- [155] Wheeler P, Grant D, (1993) A low loss matrix converter for ac variable-speed drives. EPE Conference, vol.5:27-32
- [156] Siyoung Kim, Seung-Ki Sul, Lipo T, (1998) AC to ac power conversion based on matrix converter topology with unidirectional switches. IEEE-APEC Conference and Exposition, vol.2:15-19
- [157] Lai J, Peng F, (1996) Multilevel converters - a new breed of power converters. IEEE Transactions on Industry Applications, vol.32, no.3:509-517
- [158] Nabae A, Takahashi I, Akagi H, (1981) A new neutral-point-clamped PWM inverter. IEEE Transactions on Industry Applications, vol.17, no.5:518-523
- [159] Bhagwat P, Stefanovic V, (1983) Generalized structure of a multilevel PWM inverter. IEEE Transactions on Industry Applications, vol.19, no.6:1057-1069
- [160] Brumsickle W, Divan D, Lipo T, (1998) Reduced switching stress in high-voltage IGBT inverters via a three-level structure. IEEE-APEC Conference:544-550
- [161] Sun-Kyoung Lim, Jun-Ha Kim, Kwanghee Nam, (1999) A dc-link voltage balancing algorithm for 3-level converter using the zero sequence current. IEEE-PESC Conference, vol.2:1083-1088
- [162] Greczko E, Benysek G, Kot E, (2001) The dc link voltage balancing in multilevel active power filters. (in Russian) Technicna Elektrodinamika – Journal, no.3:1922
- [163] Strzelecki R, Benysek G, Rusiński J, Kot E, (2001) Analysis of dc link capacitor voltage balance in multilevel active power filters. EPE Conference
- [164] Summer M, Newton C, (1998) Arrangements for balancing the capacitors in a five level diode clamped inverter. EPE-PEMC Conference:131-136
- [165] Greczko E, Benysek G, Kot E, (2002) The multilevel converters with multilevel carrier based PWM – properties assessment. (in Russian), Technicna Elektrodinamika - Journal, no.7:37-42
- [166] Corzine K, (1997) Topology and control of cascaded multi-level converters. Ph.D. dissertation, University of Missouri
- [167] Corzine K, Sudhoff S, Whitcomb C, (1999) Performance characteristics of a cascaded two level converter. IEEE Transactions on Energy Conversion:433-439
- [168] Peng F, McKeever J, Adams D, (1997) Cascade multilevel inverters for utility applications. IEEE-IECON Conference:437-442
- [169] Kot E, Benysek G, (2001) Analysis of dc link capacitor voltage balance in cascade parallel active power filters. PEDC Conference:120-126

- [170] Lipo T, Menjrekar M, (1999) Hybrid topology for multi-level power conversion. U.S. Patent 6,005,788
- [171] Grady W, Samotyj M, Noyola A, (1990) Survey of active power line conditioning methodologies. IEEE Transactions on Power Delivery, vol.5, no.3:1536-1542
- [172] Benysek G, Greczko E, (2002) Control of the active filters using extended Kalman filters. (in Russian), Technicna Elektrodinamika – Journal, no.7:52-55
- [173] Rusiński J, Kot E, Benysek G, (2001) Active power filter's behavior in non-periodic conditions. EPQU Conference:279-284
- [174] Greczko E, Benysek G, Smoleński R, (1999) Reduction of the negative influence of ac/ac converters on supplying network. (in Polish), PPEE Symposium:316-321
- [175] Furuhashi T, Okuma S, Uchikawa Y, (1990) A study on the theory of instantaneous reactive power. IEEE Transaction on Industrial Electronics, vol.37:86-90
- [176] Bhattacharya S, Veltman A, Divan D, Lorenz R, (1995) Flux based active filter controller. IEEE-IAS annual meeting:2483-2491
- [177] Bhattacharya S, Divan D, (1995) Synchronous frame based controller implementation for a hybrid series active filter system. IEEE-IAS annual meeting:2531-2540
- [178] Jeong S, Woo M, (1995) DSP based active power filter with predictive current control. IEEE-IECON Conference:645-650
- [179] Peng F, Lai J, (1996) Generalized instantaneous reactive power theory for three-phase power system. IEEE Transactions on Instrumentation and Measurement, vol.45:293-297
- [180] Akagi H, Kanazawa Y, Nabae A, (1983) Generalized theory of the instantaneous reactive power in three-phase circuits. IPEC Conference:1375-1386
- [181] Zhou L, Smedley K, (2000) Unified constant-frequency integration control of single phase active power filter. IEEE-APEC Conference
- [182] Kaźmierkowski MP, Krishnan R, Blaabjerg F, (2002) Control in power converters. Selected Problems. Academic Press
- [183] Ghosh A, Jindal A, Joshi A, (2003) Inverter control using output feedback for power compensating devices. TENCON Conference, vol.1:48-52
- [184] Jin T, Li L, Smedley K, (2004) A universal vector controller for three-phase PFC, APF, STATCOM, and grid-connected inverter. IEEE-APEC Conference, vol.1:594-600
- [185] Karimi-Ghartemani M, (2004) A signal processing system for extraction of harmonics and reactive current of single-phase systems. IEEE Transactions on Power Delivery, vol.19, no.3:979-986
- [186] Donghua Chen, Shaojun Xie, (2004) Review of the control strategies applied to active power filters. IEEE-DRPT Conference, vol.2:666-670

- [187] L  e T, Pereira M, Renz K, Vaupel G, (1994) Active damping of resonances in power systems. IEEE Transactions on Power Delivery, vol.9, no.2:1001-1008
- [188] Kowalski M, Strzelecki R, (1994) The hybrid filter of network current harmonics with the compensation of the reactive component. EPE-PEMC Conference:219-224
- [189] Fr  ckowiak L, Strzelecki R, (1997) Hybrid filter operation during nonlinear current pulsation. COMPEL - Journal, vol.16, no.1:38-48
- [190] Sevcenko V, Kurowski T, Bure I, Benysek G, (2002) Optimized hybrid filter utilized in high ac voltage networks. (in Russian), Elektricestvo – Journal, no.7:15-22
- [191] Strzelecki R, Benysek G, Fr  ckowiak L,   yborski J, (1995) Section hybrid filter for thyristor stand to regenerative braking of internal combustion engines for locomotives. EPE Conference:1886-1891
- [192] Balbo N, Penzo R, Sella D, Malesani L, Mattavelli P, Zuccato A, (1994) Simplified hybrid active filters for harmonic compensation in low voltage industrial applications. IEEE-PES International Conference on Harmonics in Power Systems:263-269
- [193] Peng F, Akagi H, Nabae A, (1993) Compensation characteristics of the combined system of shunt passive and series active filters. IEEE Transactions on Industry Applications, vol.29, no.1:144-152
- [194] Peng F, Akagi H, Nabae A, (1990) A new approach to harmonic compensation in power systems - a combined system of shunt passive and series active filters. IEEE Transactions on Industry Applications, vol.26, no.6:983-990
- [195] Fujita H, Akagi H, (1990) A practical approach to harmonic compensation in power systems - series connection of passive and active filters. IEEE-IAS annual meeting:1107-1112
- [196] Strzelecki R, Benysek G, Fr  ckowiak L, (1996) Dynamic properties of hybrid filters in regenerative braking thyristor systems. IEEE-ISIE Conference:596-601
- [197] Strzelecki R, Fr  ckowiak L, Benysek G, Rusi  ski J, (1999) Power flow in typical series-parallel hybrid filters topologies. EPE Conference
- [198] Strzelecki R, Fr  ckowiak L, Rusi  ski J, Benysek G, (1998) Influence of the nonlinear load current pulsation on hybrid filter behavior. EPE-PEMC Conference, vol.6:31-36
- [199] Kurowski T, Benysek G, Smo  enski R, (1998) Energetic properties of the optimized large power current hybrid filter. (in Polish), EPN Conference, vol.1:227-235
- [200] Strzelecki R, Soza  nski K, Benysek G, (1997) Hybrid filter controlled by the signal processor – results of the experimental investigations. (in Polish), EPN Conference, vol.2:265-274
- [201] Strzelecki R, Fr  ckowiak L, Benysek G, (1997) Hybrid filtration in conditions of asymmetric nonlinear load current pulsation. EPE Conference, vol.1:1453-1458

- [202] Benysek G, (1999) Influence of the asymmetrical load on hybrid filter behavior. SENE Conference, vol.1:59-64
- [203] Strzelecki R, Strzelecka N, Benysek G, (2006) A modified control algorithm for hybrid filter. Technicna Elektrodinamika – Journal, no.8:54-60
- [204] Meckien G, Mućko J, Strzelecki R, (2003) Single phase, transformer-less electrical energy conditioner. (in Polish) Przegląd Elektrotechniczny - Journal, no.2:121-123
- [205] Meckien G, Strzelecki R, Klytta M, (1999) Single-phase ALPC controllers. PEDC Conference:48-58
- [206] Kolluri S, (2002) Application of distributed super-conducting magnetic energy storage systems (D-SMES) in the energy system to improve voltage stability. IEEE-PES winter power meeting:838-841
- [207] Strzelecki R, Benysek G, Jarnut M, (2006) Super-capacitor storage arrangement with ac voltage stabilizer. (in Polish) Przegląd Elektrotechniczny – Journal, vol.7, no.8:129-132

---

## **About the Author**

Grzegorz Benysek was born in Sulechów, Poland, on June 17, 1968. He received his undergraduate education at the Technical University of Zielona Góra (M.Sc. degree in 1994). The Ph.D. degree was confirmed upon him also by the Technical University of Zielona Góra in 1998. From 1994 to 1998 he was a Lecturer and since 1998 an Assistant Professor at the Institute of Electrical Engineering, University of Zielona Góra.

His major research interest include analysis and control of power electronics circuits, control methods and properties investigations of the filtration systems as: active power filters, hybrid filters, series-parallel filters and FACTS Systems. His researches are also going in direction of utilization of the renewable energy sources in FACTS technologies. Dr Benysek is an author or coauthor of over 60 papers in these fields.

---

# Index

- Active Power Filter (APF), 48, 148  
Adjustable Speed Drive (ASD), 3  
Automatic Voltage Regulator (AVR),  
    10
- Converter, 22, 34, 41, 46, 53, 62, 64,  
    71, 74, 77, 139  
    matrix, 91, 151  
    multilevel, 92, 151, 153  
        cascaded, 94  
        cascaded H-bridge, 93  
        diode-clamped, 92  
        flying-capacitor, 92  
    single phase, 89  
    slave, 61  
    three phase, 90
- Coordinated Control System (CCS),  
    154
- Council of European Energy  
    Regulators (CEER) standard, 14
- Current  
    deterioration, 6  
    injection, 25  
    stabilizer, 50
- Current Source Converter (CSC), 89
- Custom Power System (CUPS), 3, 6,  
    14, 89, 99  
    compensating type, 6, 97, 142
- Decelerating energy, 24,  
Deterministic approach, 71, 74, 76,  
    82,
- Distributed Resources (DR), 1, 53,  
    149
- Distribution, 2, 9,  
    system, 2, 5, 152
- Distribution density function, 72, 80
- Electrical and Electronic Engineers  
    (IEEE) standards, 11
- Electrical Power System (EPS), 2, 6,  
    9, 23, 69, 81, 147, 149
- Electromagnetic Interference (EMI),  
    5, 150
- Energy Storage System (ESS), 25
- Equal-area criterion, 23
- Flexible Alternating Current  
    Transmission System (FACTS), 3,  
    7, 10, 14, 17, 31, 41, 71, 97  
    benefits, 4  
    combined, 10, 25, 40  
    series, 10, 25  
    shunt, 10, 25, 33, 37
- Gate Turn Off (GTO), 4, 26, 34, 41,  
    47, 54
- Generation, 2, 9
- Global Position System (GPS), 155
- High Voltage Direct Current  
    (HVDC), 4, 7, 17, 21, 26, 46, 94,  
    148

- Insulated Gate Bipolar Transistor (IGBT), 4, 26, 34, 41, 42, 47, 54, 90
- Integrated Gate Commutated Thyristor (IGCT), 4, 26, 41, 54
- Interline Power Flow Controller (IPFC), 5, 7, 11, 26, 53, 58, 60, 65, 68, 70, 74, 77, 81, 148, 160  
combined, 64  
control, 66  
probabilistic dimensioning, 71, 86
- International Electrotechnical Commission (IEC) standards, 12
- Load Tap Changer (LTC), 150, 154
- Normal distribution, 72, 85
- Parallel Active Power Filter (PAPF), 6, 14, 16, 97, 101, 104, 110, 161  
energetic properties, 143
- Phase Angle Regulator, 20
- Power  
active, 3, 7, 19, 23, 28, 36, 41, 56, 61, 63, 67, 89, 120, 125, 129, 133, 138  
flow, 20, 22, 25, 27, 43, 53, 65, 68  
injection, 20, 55  
instantaneous, 66, 105, 106, 108  
controller, 67  
flow control, 17, 20, 41, 43, 46, 53  
reactive, 3, 5, 7, 9, 10, 17, 28, 34, 39, 41, 48, 56, 81, 89, 119, 121, 132, 139, 141, 144, 149  
flow, 43, 53, 56, 59, 65, 68  
injection, 20, 25, 56
- Power Quality (PQ), 2, 6, 9, 11, 14, 16  
deterioration, 3  
issues, 13  
standard, 5  
supply reliability, 3, 5, 14  
voltage quality, 3, 14
- Power System Stabilizer (PSS), 10
- Probabilistic approach, 71, 74, 76, 82, 86
- Pulse Width Modulation (PWM), 26, 34, 42, 54, 110, 150, 161  
multilevel carrier, 95
- Quality of delivery, 2, 6, 9
- Reactive Power Loss Sensitivity Factor (RPL), 33
- Series Active Power Filter (SAPF), 6, 14, 16, 98, 104, 110, 161
- Silicon Controlled Rectifier (SCR), 47, 148
- Static Synchronous Compensator (STATCOM), 4, 7, 10, 20, 26, 33, 44, 53, 64, 67, 71, 81, 84, 147, 161  
probabilistic dimensioning, 81, 86
- Static Synchronous Series Compensator (SSSC), 5, 7, 10, 20, 26, 41, 44, 53, 55, 64, 67, 147
- Static Var Compensator (SVC), 5, 10, 20, 33, 37, 147
- Step Voltage Regulator (SVR), 150, 154
- Super-capacitors, 53, 153
- Symmetrical Voltage Active Power Filter (SVAPF), 6, 16, 118, 131, 149  
basic properties, 133  
interline, 139  
single phase, 134
- Synchronous Voltage Source (SVS), 114
- Thyristor Controlled Braking Resistor (TCBR), 4
- Thyristor Controlled Phase Angle Regulator (TCPAR), 4
- Thyristor Controlled Series Compensator (TCSC), 5, 11
- Thyristor Switched Series Capacitor (TSSC), 5, 10, 29, 147
- Transmission, 2, 3, 9  
control, 17, 53, 71

- system, 2, 9, 18, 24, 54  
    limitations, 2, 9, 11  
    losses, 4, 9, 18  
    stability, 4, 11  
        dynamic, 9, 18, 20, 23, 36,  
            39, 46  
        transient, 9, 18, 20, 23, 30,  
            36, 39, 45, 61, 65
- Unified Power Flow Controllers  
(UPFC), 4, 6, 11, 20, 26, 40, 53,  
61, 71, 81, 101, 148
- Unified Power Quality Conditioner  
(UPQC), 6, 7, 16, 148  
    single phase, 101, 103  
    three phase, 104, 107, 109, 112  
        efficiency, 111  
        model, 106, 161
- Uniform distribution, 72, 82, 84
- Uninterrupted Power Supply (UPS),  
3, 5
- Union of the Electricity Industry  
(EURELECTRIC) standards, 12
- Voltage  
    compensation line, 59  
    dips, 5, 12, 14  
    injection, 43, 46, 57  
        series, 20, 25, 41, 43, 54, 57,  
            65, 75  
    receiving end, 4, 19, 54  
    regulation, 6, 36, 43  
    sag, 5, 14  
    sending end, 4, 19, 44, 54, 76
- Voltage Active Power Filters  
(VAPF), 6, 16, 118, 120, 137, 149  
    energetic properties, 142, 144  
    impulse diagram, 123  
    interline, 139  
    single phase, 124  
    three phase, 129
- Voltage Source Converter (VSC), 4,  
6, 14, 26, 34, 41, 47, 54, 65, 67,  
89, 97, 119